



UNIVERSITY OF NAPLES FEDERICO II

DEPARTMENT OF PHARMACY

PhD COURSE IN

“PHARMACEUTICAL SCIENCE”

CYCLE XXXIII

**Taurisolo[®], a novel nutraceutical formulation based on grape
pomace polyphenols, as a tool for the management of oxidative
stress- and atherosclerosis-related diseases**

Supervisor: Prof. Gian Carlo Tenore

Candidate: Giuseppe Annunziata

Table of content

Section	Page
Summary	4
1. Introduction	5-52
1.1 Oxidative stress, the iceberg underwater side	6-9
1.1.1 Reactive oxygen species	6
1.1.2 Biological activities of ROS	7
1.1.3 Endogenous antioxidant defences	8-9
1.2 Cardiovascular risk and cardiovascular diseases	10-27
1.2.1 Atherosclerosis	13-17
1.2.2 The role of TMAO as a novel prognostic biomarker for CVD	17-27
1.2.2.1 The relationship between gut microbiota, TMAO and CVR	20-21
1.2.2.2 Analytic methods for circulating TMAO quantification	22-27
1.3 Other diseases related to oxidative stress and/or atherosclerotic processes	28-32
1.3.1 Aged brain-associated cognitive impairment	28-29
1.3.2 Age-related macular degeneration	29-31
1.3.3 Endothelial dysfunction	31-32
1.4 Nutraceutical, the health-promoting effect from nature	33-52
1.4.1 The use of agri-food by-products as sources of bioactive compounds	34-35
1.4.2 The antioxidant and cardio-protective activity of polyphenols	35-52
1.4.2.1 Chemistry and food sources of polyphenols	36-43
1.4.2.2 Bioavailability of polyphenols	44-46
1.4.2.3 Metabolic fate of polyphenols – Adsorption, Distribution, Metabolism, Excretion (ADME)	46-48
1.4.2.4 Nutraceutical properties of polyphenols – focus on the antioxidant and anti-inflammatory activities	48-52
2. Taurisolo® nutraceutical formulation	53-61
2.1 Productive process. The use of microencapsulation as a strategy to enhance the polyphenol bioaccessibility and bioavailability	53-58
2.2 Chemical profile	58-59
2.3 Pharmacokinetic	59-61
3. Antioxidant activity of Taurisolo®	62-81
4. Anti-atherosclerotic activity of Taurisolo®	82-93

5. The effects of Taurisolo® on oxidative stress- and atherosclerosis-related diseases	94-148
5.1 CVD	94-102
5.1.1 Endothelial dysfunction	102-123
5.2 Neurodegenerative disorders	124-130
5.3 Ageing-related chronic diseases	131-148
5.3.1 Age-related macular degeneration	131-139
5.3.2 Age-related muscle decline	140-148
6. Conclusion and future perspectives	149-150
7. References	151-192
<i>Appendix A – Detailed materials and methods of in vitro studies and instrumental analyses</i>	193-204
<i>Appendix B – Detailed materials and methods of animal-based studies</i>	205-211
<i>Appendix C – Detailed study populations and methods of RCTs</i>	212-221

Summary

The present PhD thesis summarises evidence from all the studies performed during the three-year PhD Course in Pharmaceutical Science, at the *NutraPharmaLabs* of the Department of Pharmacy, University of Naples Federico II, having as main goal the evaluation of the nutraceutical potential of Taurisolo[®], a novel nutraceutical formulation based on grape pomace polyphenolic extract. In particular, the present PhD project has been conducted in cooperation with both industrial (MBMed Company, Turin, Italy) and foreign University (University of Balearic Islands, Palma del Mallorca, Spain) partners. The entire project was planned with a dual view:

- design and formulate a novel nutraceutical product starting from re-use of *agri-food by-products*, following all the steps required by the nutraceutical industry, including preventive characterisation of the chemical profile, evaluation of bioaccessibility and bioavailability of bioactive compounds, optimisation of the productive processes and their translation in large-scale, marketing techniques
- evaluation of the biological activities, following a pharmacological approach including pre-clinical and clinical studies.

More specifically, results herein presented refer to all the studies performed in our Labs and in collaboration with other Departments and Research Institutes. They include *in vitro* studies, animal-based studies and randomised clinical trials conducted on both healthy and pathological subjects.

Further studies are still ongoing with the aim to clarify the main putative mechanisms of action for the cardioprotective role played by Taurisolo[®] or to provide novel insight regarding the observed clinical results.

In summary, data so far collected allow concluding that Taurisolo[®] is a useful and valid polyphenol-based formulation with promising nutraceutical properties in reduction of risk factors related to both development and progression of cardiovascular diseases, in particular atherosclerosis.

1. Introduction

Oxidative stress (OxS) is nowadays universally considered as one of the leading causes of chronic and degenerative diseases, among which cardiovascular disease (CVD) are the most representative. Therapeutical approaches aimed to contrast the OxS, thus, have been licensed by both research and physicians as effective strategies for prevention and management of such diseases. In this context, Nutraceutical plays a key role, since the health-promoting effect of food-derived bioactive compounds administered in concentrated forms is well-established and -accepted. Among these, polyphenols emerge as the most effective and studied, probably due to their ubiquitous presence in plant kingdom. During the last decades, indeed, a very large number of authors studied about polyphenols, spacing in various field of application, from the food chemistry to the pharmacology, from the pharmaceutical technique to the clinical. This allowed obtaining a very solid and remarkable body of evidence of the efficacy of polyphenol-based nutraceuticals.

Our research group has been engaged for years in the study of Nutraceutical, by conceiving this relatively novel field likewise its name suggests: exactly between NUTRition and pharmACEUTICAL. In this sense, the present PhD project was planned with the scope to develop a novel nutraceutical formulation, following all the necessary steps from its production to the evaluation of its effects on human health. In this thesis I will describe all these phases that characterised my research during the three-year PhD projects, following a step-by-step approach. In particular, after a general overview about the main topics on which our research has been based, I present our results starting from a basic chemical analysis and formulation of our studied product. Then, I describe all the results obtained from *in vitro*, *ex-vivo*, animal-based studies and clinical trials, focusing on both antioxidant and anti-atherosclerotic potential of our product. All these studies have been conducted with multidisciplinary collaborations with various National and International Universities, giving the opportunity to enlarge the expertise of our research group.

This thesis wants to be not only a mere report of the research activities of a PhD student, but a proof-of-concept for the health-promoting potential of Nutraceutical obtained from a multi-stages research approach, maybe providing a novel point of view on this research field.

1.1 Oxidative stress, the iceberg underwater side

In 1936, Hans Selye proposed the concept of “*stress*” defining it as a “non-specific response of the body to any demand” (Selye, 1976, 1936; Sies et al., 2017). The term “*oxidative stress*”, instead, was introduced in 1970 to describe the treatment of erythrocytes with H₂O₂ (Paniker et al., 1970). However, the concept of OxS, as we understand it, was formulated in 1985 as “*a disturbance in the pro-oxidant/antioxidant balance in favour of the former*” (Sies et al., 2017). According to this definition, thus, OxS refers to an unbalance between production and elimination of oxidants, mainly free radicals, in favour of their generation, leading to alterations of redox signalling and control (Sies et al., 2017). Among the main oxidant agents there are reactive oxygen species (ROS) (including •OH, O₂•⁻, HO₂•, and ROO•) and reactive nitrogen species (RNS) (including NO• and •ONOO) (Berlett and Stadtman, 1997). Physiologically, ROS/RNS serve as signalling molecules involved in important biological processes, including cell proliferation, programmed cell death and gene expression (Dowling and Simmons, 2009; Scherz-Shouval and Elazar, 2011), as discussed below in this section. However, the chronic and progressive accumulation of both ROS and RNS damages biological macromolecules, such as sugar, lipids, proteins and nucleic acids, leading to both pathophysiological alterations and accelerating ageing, finally culminating in development of several diseases (Luo et al., 2020), including cardiovascular diseases, cancer, diabetes and neurodegenerative disorders (Acharya et al., 2010; Castro and Freeman, 2001). Notably, when the increase of ROS/RNS is within certain limits, the organism is able to counteract the OxS activating antioxidant defence systems, including specific enzymes that act as free radical scavengers (Truong et al., 2018). Nevertheless, whether OxS exceeds and endogenous antioxidant defence are not able to contrast it, the use of exogenous molecules in form of antioxidant supplements may represent a useful tool for prevention and management of OxS-related diseases.

1.1.1 Reactive oxygen species

Free radicals (namely ROS) are produced as *by-products* as a result of mitochondrial respiration, metabolism or by specific enzymes. Several environmental factors (i.e. UV radiation, cigarette smoking, excessive alcohol consumption) promote ROS production, resulting in development of OxS-related pathological conditions, including CVD (Dubois-Deruy et al., 2020). O₂ is recognised as the starting point for ROS formation, due to its ability to the superoxide anion (•O₂⁻) by capturing an electron. These anions are the most abundant in cells and are responsible for production of other ROS, including hydroxyl and hydroperoxyl radicals, hydrogen peroxide. This latter, in presence of ferrous ions, can be involved in Fenton reaction forming hypochlorous acid by the action of myeloperoxidases (MPO). Finally, hydrogen peroxide is enzymatically detoxified in water by the action of glutathione peroxidase (GPx), catalase (CAT) and peroxiredoxins (Prx), while hypochlorous acid interact with hydrogen peroxide forming singlet oxygen (¹O₂) (Dubois-Deruy et al., 2020). Moreover, superoxide anions interact with nitric oxide (NO) forming

peroxynitrite that, in turn, can be converted in peroxynitrous acid *via* protonation (Dubois-Deruy et al., 2020).

1.1.2 Biological effects of ROS

Free radicals (namely ROS) are directly involved in several mechanisms and pathways at cellular level (Burton and Jauniaux, 2011), including:

- activation of redox-sensitive transcription factors activation (i.e. AP-1, p53, NF- κ B) involved in regulation of pro-inflammatory, cell differentiation and apoptosis gene expression
- activation of protein kinases, such as mitogen-activated protein kinases (MAPK), ROS-induced activation of extracellular regulated kinases (ERK1/2), stress-activated protein kinase-c-Jun amino terminal kinases (SAPK-JNK), that promote various cell functions, including survival, proliferation and apoptosis
- activation of Ca²⁺ ion channels in endoplasmic reticulum, resulting in increased release of calcium that, in turn, activates Ca²⁺-sensitive processes. The increased [Ca²⁺]_i affects mitochondrial function, resulting in further ROS production. Also, increased [Ca²⁺]_i and oxidation of thiol groups on protein in the inner mitochondrial membrane promote the opening of the membrane permeability transition, resulting in collapses of both mitochondrial membrane potential and ATP synthesis. This process causes reduced ATP production, loss of ionic homeostasis and cellular necrosis.

Also, when produced in excessive amount, ROS tend to attack biomolecules (lipid, protein and nucleic acids), causing their oxidation (Burton and Jauniaux, 2011). In particular, ROS are responsible for:

- lipid peroxidation in biological membranes containing polyunsaturated fatty acids. Oxygen, indeed, react with a carbon-centred radical, C•, forming a peroxy radical (–C–O–O•), that in turn abstracts hydrogen from an adjacent fatty acid, so propagating the reaction
- protein modification secondary to oxidative damage at aminoacidic level. Direct oxidation of the side chains, indeed, results in carbonyl group (aldehydes and ketones) formation. Also, abstraction of hydrogen ions from the thiol group of cysteine causes the formation of disulfide bonds, with consequent abnormal protein folding, that affects protein function and promotes protein aggregation and cell death
- DNA oxidation caused by attacks on the sugar moieties (causing strand breakages) or histone proteins (causing cross-linkages that interfere with chromatin folding, DNA repair and transcription, resulting in mutations or aberrant gene expression). Due to the presence

in the same site of ROS production (mitochondria), the lack of histone protection, and the existence of minimal repair mechanisms, mitochondrial DNA is particularly vulnerable to ROS attack.

1.1.3 Endogenous antioxidant defences

Physiologically, both enzymatic and non-enzymatic endogenous defences help the human body to contrast the OxS. Non-enzymatic ones include ascorbate (vitamin C) and α -tocopherol (vitamin E) that act synergistically and in concert (vitamin C promotes regeneration of reduced vitamin E). Also, thiol compounds (i.e. thioredoxin) contribute to detoxification of hydrogen peroxide, but it needs to be reconverted in reduced form by thioredoxin reductase (Burton and Jauniaux, 2011). Another thiol with antioxidant properties is glutathione, that acts as cofactor of GPx, as chelator of transition metals and plays a role in regeneration of ascorbate and α -tocopherol. The reduced glutathione (GSH)/oxidated glutathione (GSSG) ratio is recognised as a valid marker of OxS, and more specifically of lipid peroxidation (Dubois-Deruy et al., 2020). Proteins such as ceruloplasmin and transferrin are able to inhibit the Fenton reaction (and the consequent $\text{OH}\cdot$ production) *via* sequestering free iron ions (Burton and Jauniaux, 2011).

Enzymatic antioxidant defences are represented by specific enzyme, such as:

- Superoxide dismutase (SOD) – it is a metalloproteins catalysing the transformation of superoxide anion into hydrogen peroxide. There are three isoforms with different subcellular localization (SOD1 in cytosol, SOD2 in mitochondria, SOD3 in extracellular compartments). For their activity they require different cofactors and dimerization: SOD1 dimer and the SOD3 tetramer require a copper (Cu) and to zinc (Zn) (Cu-ZnSOD), while the SOD2 tetramer requires manganese (Mn) (MnSOD)
- CAT – it is a tetrameric heme protein detoxifying hydrogen peroxide into water. Its function is dependent on hydrogen peroxide concentration: in case of high H_2O_2 concentrations the most important activity is catalytic detoxification; on the contrary, in case of low H_2O_2 concentrations, peroxidase activity is the main function
- GPx – it is a cytosolic, nuclear and mitochondrial tetrameric selenoproteins that acts detoxifying hydrogen peroxide in water and the eliminating peroxide residues from lipids through the reducing capacities of GSH/GSSG. This reaction system can proceed only if GSSG is continuously reduced to GSH (by the activity of glutathione reductase)
- Prx – it is an enzyme able to reduce the peroxide functions of several molecules, including hydrogen peroxide and peroxyxynitrite. In humans have been identified six different isoforms with different subcellular locations (Dubois-Deruy et al., 2020).

The involvement of OxS in both development and progression of several chronic and degenerative diseases will be extensively discussed in following sections focusing, in particular, on CVD.

1.2 Cardiovascular risk and cardiovascular diseases

Cardiovascular diseases are multifactorial diseases with a complex pathophysiology comprising various phenomena, including functional and morphological alterations of cardiovascular structures (heart and blood vessels), such as blood vessel remodelling, occurring at different body districts. According to the World Health Organization (WHO), CVD are the leading causes of death in the World (Benjamin et al., 2017). From 1990 to 2010 the incidence of CVD raised by one third, and 2015 one in three deaths are to cardiovascular events (Lozano et al., 2012).

The main disorders included into the global definition of CVD are coronary artery diseases (CAD), stroke, hypertension, heart failure, congenital heart disease (CHD), vascular diseases, for which various risk factors have been identified, including obesity, diabetes, cigarette smoking, a sedentary and unhealthy lifestyle, and genetic predisposition (Benjamin et al., 2017). Interestingly, ageing represents another risk factor for development and progression of CVD is played by ageing, due to the accumulation of oxidative damage. In particular, studies evidenced an age-related loss of the heart tolerance to the OxS due to a reduction of both concentration and activity of antioxidant enzymes (i.e. GPx and SOD) (Abete et al., 1999). It appears clear, thus, the central role played by OxS in cardiovascular risk (CVR).

Notably, when present in low concentrations, ROS exert physiological roles in cardiovascular tissues (Dubois-Deruy et al., 2020), suggesting the so-called hormesis concept. More specifically, ROS are physiologically involved in a specific cellular function, named redox signalling, consisting of reversible oxidation/reduction modification of cellular signalling components that regulate gene expression, excitation-contraction coupling, or cell growth, migration, differentiation, and death (Burgoyne et al., 2012; Sack et al., 2017). A number cellular components take part in the redox signalling and are involved in various functions, including excitation-contraction coupling, antioxidant enzyme activity, vasodilation and vascular tone, as schematically reported in **Figure 1.2**¹.

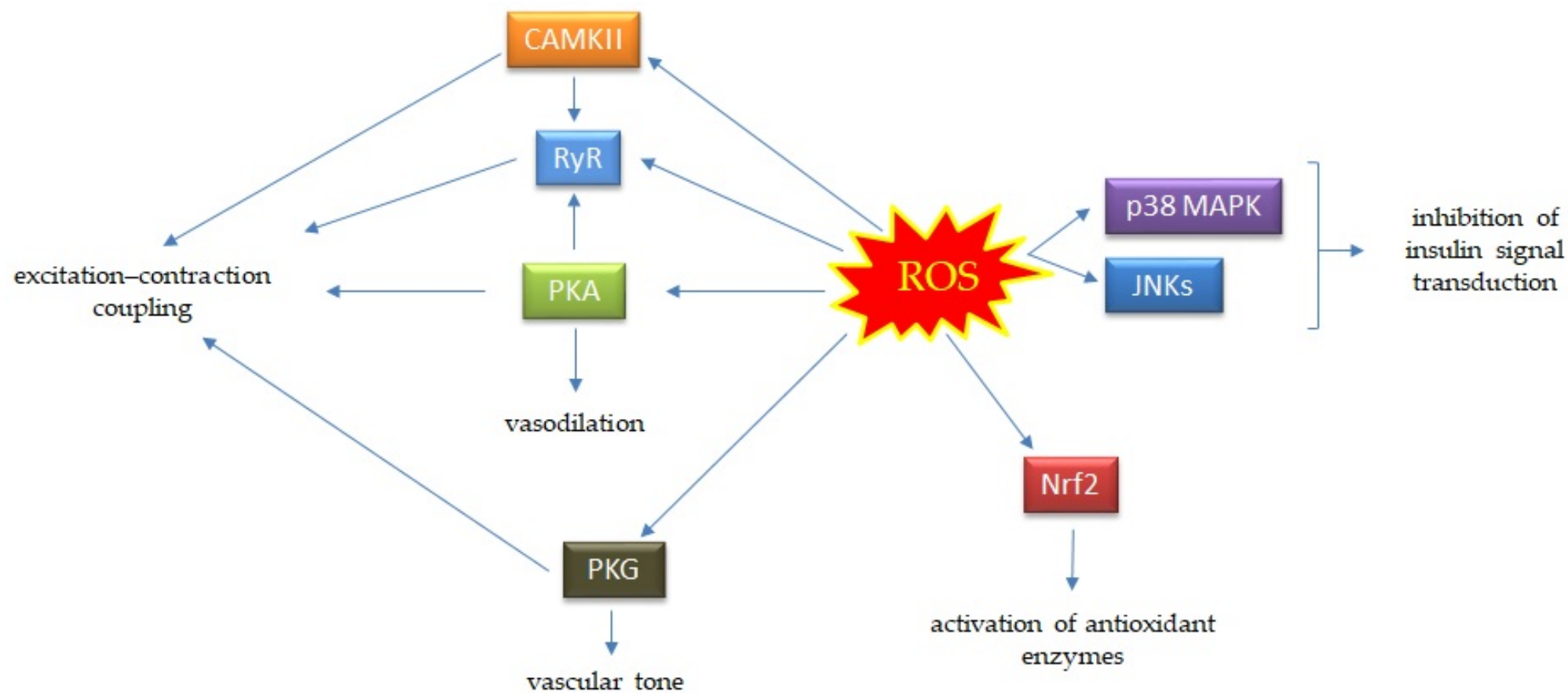


Figure 1.2¹. Physiological roles played by ROS in cardiovascular tissues. Abbreviations: CAMKII, Ca/calmodulin-dependent kinase II; RyR, ruanodine receptor; PKA, cAMP-induced protein kinase A; PKG, protein kinase G; Nrf2, nuclear factor erythroid 2-related factor 2; p38 MAPK, p38 mitogen-activated protein kinase; JNKs, c-Jun N-terminal kinase.

Despite the physiological effects exerted when OxS is relatively limited, increased production of ROS is responsible for a wide range of complications that increase the CVR. A number of studies, indeed, reported increased ROS production in several CVDs, such as myocardial fibrosis, cardiac hypertrophy, heart failure, myocardial infarction, as previously reviewed (Dubois-Deruy et al., 2020). As aforementioned, ROS cause oxidation of biomolecules, such as lipids, proteins and nucleic acids, resulting in modifications of cellular and subcellular structures. With reference to cardiovascular tissues, ROS-induced oxidation of sarcoplasmic reticulum Ca^{2+} -ATPase (SERCA) and contractile proteins (i.e. tropomyosin and actin) causes contractile dysfunctions (Lancel et al., 2010; Steinberg, 2013).

A key role in modulation of OxS in CVD is played by NADPH oxidases (NOX), a family of enzymatic complexes involved in ROS production *via* catalysing the production of superoxide anions by dioxygen using NADPH or NADH as electron donors. NOX family comprises seven members (NOX 1-7) found in neutrophils, inner ear, thyroid, pulmonary epithelium and colon. Isoforms 1, 2, 4 and 5 are particularly expressed in cardiovascular tissues. More specifically, NOX 1, 4 and are expressed in human aortic smooth muscle cells, while NOX 2 and 4 in other cardiac cells (such as cardiomyocytes, fibroblasts, endothelial cells, or smooth muscle cells) (Dubois-Deruy et al., 2020). Cardiac NOX are activated by AngII, endothelin-1, growth factors, cytokines or mechanical force-induced stress (Dubois-Deruy et al., 2020), and its activity has been found increased in patients with metabolic syndrome as well as plasma levels of oxidized low-density lipoprotein (oxLDL) and nitrotyrosine (Fortuño et al., 2006). Animal based studies reported increased NOX-dependent production of superoxide anion in left ventricle after three weeks of aorta binding (Li et al., 2002). Interestingly, it has been described the ability of NOX 2-derived ROS to activate apoptosis by ASK-1/p38MAPK and the CAMKII pro-apoptotic pathway after myocardial infarction or AngII stimulation (Erickson et al., 2008).

As reported in section 1.1.1 (Reactive oxygen species), mitochondria are the principal site of ROS production (about 90%). Oxidative damages at mitochondrial level result in mitochondrial dysfunction that, in turn, contributes to CVD development (Bhatti et al., 2017). In particular, increased mitochondrial production of ROS causes alterations at mitochondrial DNA (mtDNA) and reduced expression of genes encoding for respiratory complexes I, III and IV. Similarly, ROS produced in this cellular organelle are responsible for oxidation of proteins from complexes I and II. Overall, these oxidative damages result in reduced mitochondrial respiration that, in turn, is associated with further increases in OxS and ROS production, culminating with the activation of many protein kinases and transcription factors involved in hypertrophic signalling (Dubois-Deruy et al., 2020). Dysfunctions of the various the mitochondrial respiratory chain complexes have been observed in the non-infarcted zone of the myocardium in *in vivo* models of myocardial infarction, associated with a decrease in mitochondrial respiration (Bugger and Pfeil, 2020). Evidence reported the involvement of mitochondrial ROS production in diabetes-related

cardiovascular complications. In mice fed with a high-fat high-sucrose diet it was observed the development of mitochondrial OxS, mitochondrial dysfunction, and cardiac hypertrophy (Jeong et al., 2016; Sverdlov et al., 2016). Similarly, increased production of mitochondrial ROS was observed in diabetic patients (Anderson et al., 2009) and in right atrial cardiomyocytes from obese patients (Niemann et al., 2011).

1.2.1 Atherosclerosis

Atherosclerosis is a chronic, multifactorial disease involving medium- and large-calibre arteries. It is characterised by typical lesions at intimal level resulting in a progressive arterial lumen narrowing. Such lesions are generally distributed within single or multiple arterial districts; they develop during the first decades of life, but the clinical symptomatology occurs when the normal arterial flux is severely impaired. Clinical manifestations are ischemic and result in the onset of different disorders on the bases of the arterial district involved (Mancini et al., 2011; Marzocchi and Magnani, 1986; Menotti, 1987; Puato et al., 2002).

An accurate analysis of the atherosclerosis epidemiology is difficult, since it is an asymptomatic condition. However, epidemiological studies estimated that about 75% of acute myocardial infarction cases occur from plaque rupture, suggesting the strong relationship between atherosclerosis and incidence of cardiovascular diseases. Interestingly, gender differences have been reported in relation to the atherosclerosis prevalence. In particular, the risk increase in men over 45 years and in women beyond age 50 years. It is supposed that this gender difference is due to the protective role played by female sex hormones, that is lost after menopause onset (Pahwa and Jialal, 2020).

The etiology of atherosclerosis is multifactorial and still not clear. However, several risk factors have been identified, including hypercholesterolemia, hypertension, diabetes, cigarette smoking, overweight/obesity, sedentary lifestyle and unhealthy dietary patterns. Overall, these factors increase the risk of development and progression of atherosclerotic disease mainly through their impact on both LDL-cholesterol and inflammation (Pahwa and Jialal, 2020).

As mentioned above, arterial lesions are the main features of atherosclerotic disease and leading causes of clinical manifestations. According to the American Heart Association, atherosclerotic lesions are differently classified into six classes (I-VI) on the basis of both progression degree and disease severity. More specifically:

- lesions I and II are considered as *early lesions*. They are characterised by accumulation (class I) or layering (class II) of macrophages, foam cells, smooth muscle cells (SMCs) and T lymphocytes. Only a small portion of early lesions progresses to the advanced stage

- lesions III are considered as *intermediate lesions*. Also defined as *pro-atheroma*, these lesions are characterised by extracellular lipid stores that may alter the intimal SMCs organization
- lesions IV-VI are considered as *advanced lesions*. Lesions IV (atheroma) present a dense extracellular lipid storage within the intima, resulting in formation of a *lipid core*, where calcium particles may be present. A layer of macrophages, SMCs, lymphocytes and mast cells is localised between the lipid core and the endothelium, where they can cause plaque rupture. Also, neoangiogenesis processes may occur, resulting in formation of numerous blood vessels on the plaque external surface. Lesions V (fibro-atheroma) are formed by increased fibrous connective tissue that alters the intima structure, causing a lumen narrowing. Both the lipid core and the plaque may present calcifications; neoangiogenesis is higher than lesions IV. Lesions VI are considered as the last stage of atherosclerotic progression and the severest one. They are more susceptible to rupture, causing thrombosis. For this reason they are responsible for morbidity and mortality (Mancini et al., 2011; Marzocchi and Magnani, 1986; Menotti, 1987; Puato et al., 2002).

Advanced lesions develop as result of chronic and proliferative mechanisms, including increased number of SMCs, macrophages and lymphocytes into the intima, secretion of extracellular matrix and accumulation of lipids in SMCs and macrophages, resulting in foam cells formations. These mechanisms are at the base of different pathogenesis theories proposed, such as (i) response to endothelial damage and role of (ii) lipoproteins, (iii) SMCs, (iv) growth factors and (v) inflammation (Puato et al., 2002).

- i. Response to endothelial damage – mechanic, chemical, toxic, viral and immunological stimuli are responsible for modifications of the intrinsic permeability and adhesion features of the endothelium, causing a physical damage that results in development of the atherosclerotic lesion. In response to this damage, firstly lipoproteins accumulate into the vessel wall and endothelial cells begin to express adhesive glycoprotein (i.e. selectin), Intercellular Adhesion Molecule (ICAM) and Vascular cell adhesion protein (VCAM). Subsequently, circulating monocytes and lymphocytes adhere to the endothelial surface and penetrate into the sub-endothelial region. Monocytes transform into macrophages and accumulate lipids, resulting in foam cells formation. In the site where macrophages penetrate, mechanisms of platelet activation and aggregation are induced. Activated platelets release the Platelet Derived Growth Factor (PDGF), a mitogen factor that stimulates SMCs migration and proliferation in the tunica media, resulting in further production and secretion of connective matrix and growth factors.

- ii. Role of lipoproteins – according to this pathogenesis hypothesis, lipoproteins, in particular low-density lipoproteins (LDL) play a crucial role in development and progression of atherosclerotic plaque. Such lipoproteins are physiologically metabolised by macrophages; on the contrary, when in excess, they are transported across the endothelial barrier and accumulate in monocytes-macrophages and SMCs originating foam cells. During this transport, LDL undergo various modifications, including oxidation and glycation, processes favoured by high serum levels of cholesterol or glucose, respectively. LDL oxidation occur in two steps. Firstly, they are slightly oxidised and act as chemotactic factor for monocytes promoting their penetration across the endothelial barrier. Then, when monocytes are transformed in macrophages, LDL are further oxidised (becoming named oxLDL), presenting modifications to the protein portion. oxLDL, thus, are not recognised by the LDL receptor, but have high affinity with the scavenger receptor of macrophages. In endothelial cells, oxLDL activate the nuclear factor kappa-light-chain-enhancer of activated B cells (NF- κ B) and promote its nuclear translocation, resulting in up-regulation of specific genes associated to atherosclerosis, including genes encoding for adhesion molecules and cytokines. Also, oxLDL are able to stimulate the platelet aggregation, thus promoting the release of PDGF.
- iii. Role of SMCs – vascular SMCs express two different phenotypes: contractile (or quiescent) and synthetic (active). In contrast to the contractile phenotype, the synthetic one expresses genes encoding for growth factors and cytokines, and is able to migrate, proliferate and secrete matrix. During the atherosclerotic process, contractile phenotype SMCs convert to synthetic, giving lesions the ability to counteract atherogen stimuli. When damaged, SMCs release Fibroblast Growth Factor (FGF) that stimulates neighbouring SMCs and endothelial cells.
- iv. Role of growth factors – the main growth factors involved in atherosclerotic process derive from platelet, endothelial cells, macrophages and SMCs. As described above, PDGF is produced and secreted by platelet; it is a mitogen factor activating migration and proliferation of SMCs in tunica media. The basic Fibroblast Growth Factor (bFGF) is produced by SMCs and promotes the angiogenesis. Another SMC-derived growth factor is the Transforming Growth Factor beta (TGF β), that increase the synthetic activity of SMCs, promoting their extracellular matrix production. The Vascular Endothelial Growth Factor (VEGF) is specific for endothelial cells and promotes the angiogenesis in synergy with bFGF. Moreover, other molecules are involved in pathogenesis of atherosclerosis, including Insulin-like Growth Factor-I (IGF-I), Tumor Necrosis Factor α

(TNF α), angiogenin, Heparin-Binding Epidermal Growth Factor-like Growth Factor (HB-EGF), promoting proliferation, migration and angiogenesis.

- v. Role of inflammation – it is well-established that the endothelial damage causes a chronic inflammatory response. This is confirmed by the presence of immune cells in the atherosclerotic lesion, such as monocytes-macrophages and T-lymphocytes. In this context, a central role is played by chemokines, a family of cytokines. Two groups of chemokines are directly involved in the atherosclerotic process: Interferon-inducible Protein 10 (IP-10) and Monocyte Chemoattractant Protein-1 and -4 (MCP-1 and -4), that exert a chemotactic action specific for activated T-lymphocytes and monocytes, respectively. The inflammatory cascade is triggered by oxLDL that promote activation and adhesion of monocytes *via* induction of various molecules, including P-selectin, MCP-1, Monocyte Colony Stimulating Factor (M-CSF) and Growth-Regulated Oncogene (GRO)-chemokine (Puato et al., 2002).

Generally, atherosclerosis remains clinically silent during various years, and pathological manifestations occur when lesions become advanced, causing arterial lumen narrowing, thus the flux is severely impaired. The clinical picture will be different on the basis of the arterial district involved in the atherosclerotic process:

- heart: angina pectoris, acute myocardial infarction, arrhythmia, sudden cardiac death
- kidney: renovascular hypertension, renal infarction
- lower limbs: claudicatio intermittens, gangrene
- brain: stroke, cerebral infarction with transient signs (CITS), transient ischemic attack (TIA), dementia
- mesenteric circulation: angina abdominis, intestinal infarction
- aorta: aneurysm, Leriche syndrome (Puato et al., 2002).

A number of anamnestic criteria and techniques have been licensed for diagnosis of atherosclerosis, as reported in **Table 1.2.1**¹. Anamnesis and physical examination aim to evaluate family history, risk profile, clinical pictures suggesting atherosclerosis and the presence of other predisposing diseases (i.e. diabetes, hypertension) (Puato et al., 2002).

Table 1.2.1¹. Techniques for diagnosis of atherosclerosis

<i>Blood parameters</i>	Glucose, cholesterol (total, LDL-c, HDL-c), triglycerides, Lp(a), homocysteine, C-reactive protein
<i>Non-invasive instrumental diagnostics</i>	ECG (at rest and under exercise), Doppler velocimetry, cardiac ultrasound, computerized axial tomography (CAT) and CT angiography, Nuclear magnetic resonance (NMR) and NMR-angiography, scintigraphy, radiography
<i>Invasive diagnostics</i>	Arteriography, angioscopy, intra-arterial ultrasound

Epidemiological studies suggest that correction of the risk factors is the first-line intervention for prevention of the atherosclerosis-related pathological consequences. On the other hand, surgery is the best approach to reverse or remove the atherosclerotic lesion. However, pharmacological approaches have been licensed. They include the use of fibrinolytic drugs and tissue plasminogen activators. Also, studies reported beneficial effects on the atherosclerotic plaques after treatments with anti-hypertensive (calcium channel blockers, ACE-inhibitors, beta-blockers) alone or in association with cholesterol lowering therapy (statins) and antioxidants (Puato et al., 2002).

The strong relationship between atherosclerosis and OxS is historically-known and well established. In an holistic view, thus, using therapeutic strategies with the scope to counteract the OxS is a desirable approach. However, no specific antioxidant treatments have been licensed for prevention of cardiovascular complications (Pignatelli et al., 2018). Also, it should be take into account that the conventional anti-atherosclerosis pharmacological approaches only aimed to target the traditional risk factors (Zhu et al., 2020), resulting in a permanence of the CVR (Fihn et al., 2012; Fruchart et al., 2008). This underlines the need to individuate novel targeted therapeutic strategies for management of atherosclerotic patients. In this sense, the use of antioxidant-based nutraceutical products (generally characterised by no side-effects neither drug interactions) might be a useful tool.

1.2.2 The role of TMAO as a novel prognostic biomarker for CVR

A very large body of evidence, during the decades, established that several factors contributed to increasing CVR, including smoking, obesity, hypercholesterolemia, and hyperglycaemia, and numerous

studies have been performed in order to clarify the exact role of these risk factors and the main molecular mechanisms underlying this increased risk. Not recently, however, several findings have added a new piece to the complex puzzle of the CVR, suggesting the existence of a novel prognostic biomarker for CVR, trimethylamine *N*-oxide (TMAO). TMAO is an amine oxide with structural formula $(\text{CH}_3)_3\text{NO}$ (Subramaniam and Fletcher, 2018; Ufnal et al., 2015) that is currently recognised as a novel risk factor for CVD, including atherosclerosis (Randrianarisoa et al., 2016), heart failure (Tang et al., 2014), stroke (Haghikia et al., 2018; Liang et al., 2019; Nie et al., 2018; Wu et al., 2018), and other major adverse cardiovascular events (Koeth et al., 2013; Lever et al., 2014; Li et al., 2017; Mente et al., 2015; Tang et al., 2013; Trøseid et al., 2015; Z. Wang et al., 2011). Observational studies reported a direct relationship between high serum levels of TMAO and increased risk of infarct relapse (Li et al., 2017), rehospitalisation (Suzuki et al., 2019) and mortality (Li et al., 2017; Suzuki et al., 2019) in patients with CVD. Moreover, TMAO has been positively correlated with levels of inflammatory and endothelial dysfunction biomarkers in patients with T2DM and chronic kidney disease (Al-Obaide et al., 2017). Overall, this evidence suggests that TMAO plays a crucial role in increasing CVR (Janeiro et al., 2018). Interestingly, TMAO has been suggested by several authors as “a prognostic biomarker for CVD beyond the traditional risk factors” (Dong et al., 2018; Li et al., 2017; Senthong et al., 2016; Tang et al., 2014), suggesting the importance to evaluate its levels for management of CVD. Preclinical studies revealed a mechanistic association between TMAO and CVD, in particular exerting a pro-atherosclerotic effect; furthermore, a meta-analysis demonstrated that TMAO serum levels are positively and dose-dependently associated with cardiovascular events and mortality (Schiattarella et al., 2017). Interestingly, TMAO seems to be related to the CVR independently of other risk factors, especially in patients with acute coronary syndrome (Li et al., 2017). According to several studies, TMAO seems to be involved in various pathways related to the CVR; in particular, evidence reported that TMAO is able to increase recruitment of leukocyte, expression of pro-inflammatory cytokine and adhesion molecules, resulting in enhanced vascular inflammation (Janeiro et al., 2018). Moreover, TMAO is also responsible for the accumulation of cholesterol in peripheral endothelial cells (Seldin et al., 2016), platelet aggregation and adhesion induced by both ADP and thrombin (Zhu et al., 2016).

In the last ten years, studies investigating TMAO significantly increased, as shown in **Figure 1.2.2**, reflecting the growing interest of scientific research in elucidating the main mechanisms involving TMAO in CVR.

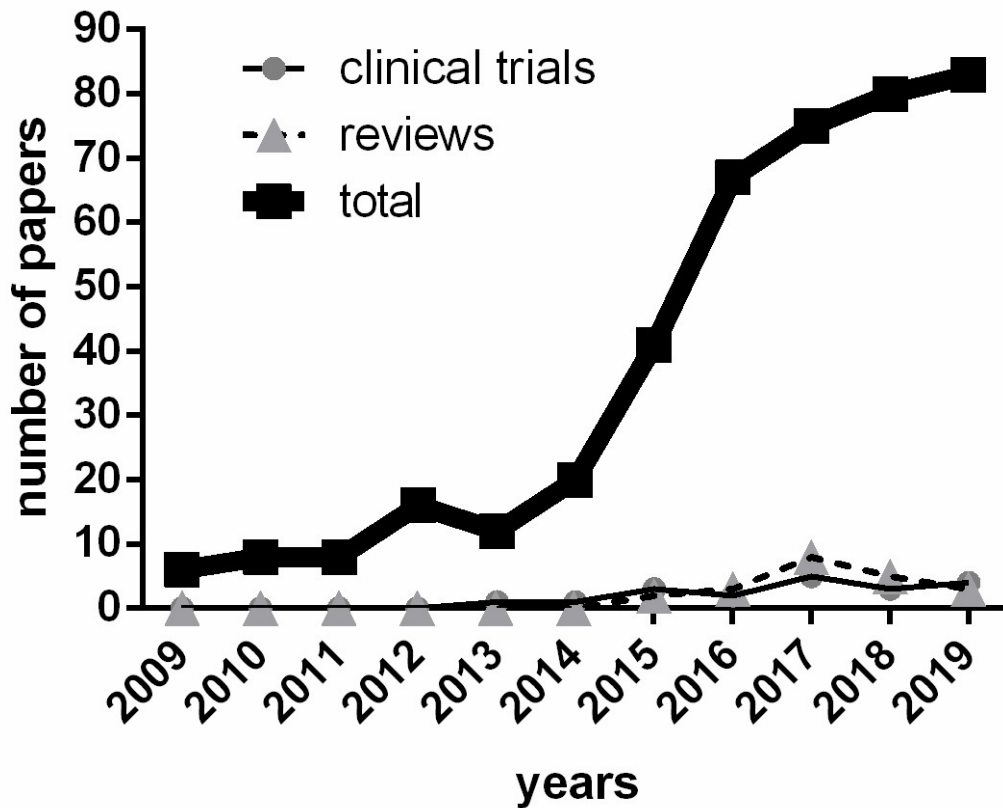


Figure 1.2.2¹. The number of papers on TMAO per year. Papers have been selected typing the words “trimethylamine N-oxide” and “TMAO” in titles.

In a very large number of studies, high serum or urinary levels of TMAO have been associated with a plethora of CVD, acting by specific mechanisms, that will be extensively discussed above. Interestingly, evidence also reported high TMAO levels in patients with high-CVR pathologies, such as obesity, metabolic syndrome (MetS) (Barrea et al., 2018) and vitamin D deficiency (Barrea et al., 2019d), with the existence of an interesting gender-specific relationship (Barrea et al., 2019b); thus, it is plausible to speculate that TMAO might be also involved in metabolic-endocrine disorders in which coexists a high CVR, representing, once again, a novel interpretation. More specifically, it we reported a direct association between TMAO and both visceral Adiposity Index (VAI) and Fatty Liver Index (FLI), that are recognized as a gender-specific indicator of adipose dysfunction and a predictor of non-alcoholic fatty liver disease (NAFLD), respectively (Barrea et al., 2018). Also, it is extensively described in literature that TMAO is a highly oxidant and reactive molecule, closely associated to OxS-related diseases (Pignatelli et al., 2018). In particular, evidence reported that TMAO is able to (i) promote ROS generation and nitrogen oxide reduction (Chen et al., 2019; George et al., 2012), resulting in increasing OxS and (ii) down-regulate Il-10, resulting in increasing inflammation (Chen et al., 2019). These mechanisms suggest the role played by TMAO in onset of cardiovascular alterations, such as endothelial dysfunction (Zhu et al., 2020). Notably, both the pro-oxidant and pro-inflammatory effects have

been indicated as key mechanism for the observed reduction in circulating endothelial progenitor cells in stable angina patients (Chou et al., 2019). However, the main interest in clinical implication of TMAO levels is related to its role as pro-atherogenic factor, playing a central role in both development and progression of atherosclerosis through different mechanisms (including foam cell formation, endothelial dysfunction, plaque instability and platelet activation) (Zhu et al., 2020), as schematically represented in **Figure 1.2.2ⁱⁱ**.

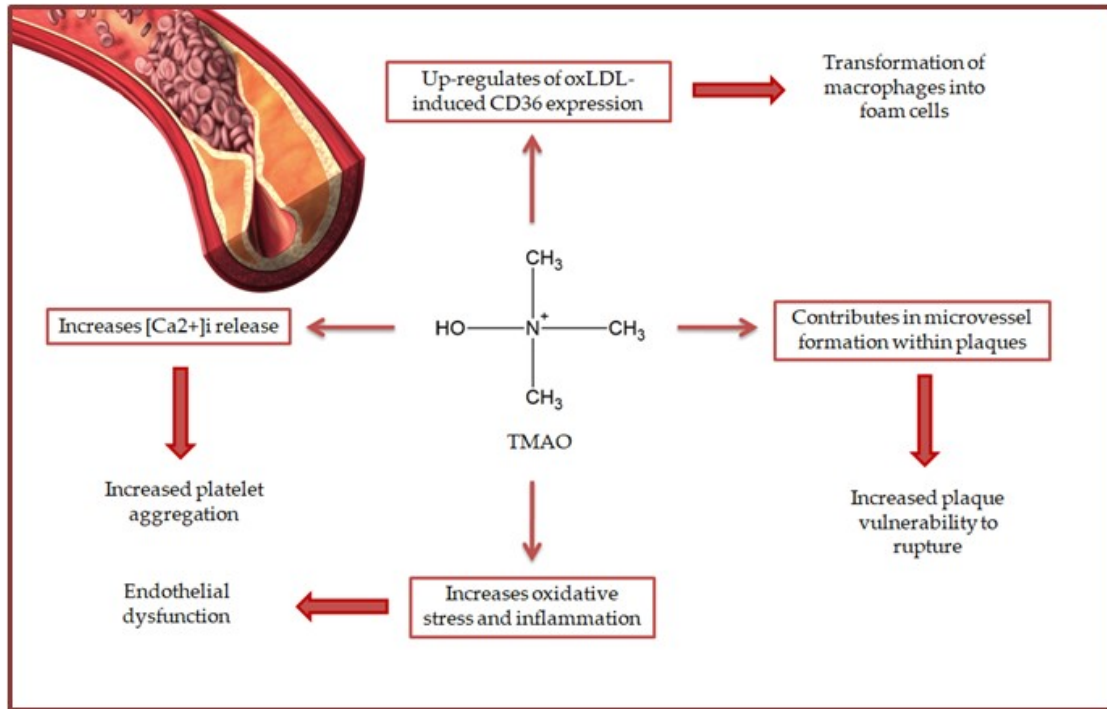


Figure 1.2.2ⁱⁱ. The role of TMAO in atherosclerosis development and progression [source: **Article in press**]

Interestingly, studies reported the ability of TMAO to up-regulate the expression of oxLDL-induced scavenger receptor CD36 in macrophages (Geng et al., 2018; Mohammadi et al., 2016), promoting the transformation of macrophages into foam cells (Koeth et al., 2013; Z. Wang et al., 2011), and suggesting the role played by TMAO in early stages of atherosclerotic plaque formation. Also, it was reported the close involvement of TMAO in plaque instability (Zhu et al., 2020) *via* favouring the formation of microvessels within the plaque (Virmani et al., 2005). Furthermore, TMAO positively correlates with the percentage of intermediate CD14⁺⁺CD16⁺ monocytes (Haghikia et al., 2018), a subset promoting both (i) plaque rupture through matrix metalloproteinase overproduction (Newby, 2008) and (ii) angiogenesis (Jaipersad et al., 2014). Finally, evidence suggests that TMAO is involved in increasing platelet aggregation *via* triggering the [Ca²⁺]_i release (Zhu et al., 2016). Overall, this evidence clarifies the role played by TMAO in atherosclerotic risk and suggests this compound as a potential target for management of atherosclerosis.

1.2.2.1 The relationship between gut microbiota, TMAO and CVR

Gut microbiota, thus, is directly involved in the synthesis of TMAO. In the colon, indeed, bacteria metabolise diet-derived compounds, mainly choline, phosphatidylcholin, L-carnitine, and betaine (contained in several foods, including eggs, red meat and fish), producing trimethylamine (TMA), by the activity of specific TMA lyase, carnitine oxygenase and betaine reductase (Ascher and Reinhardt, 2018; Nam, 2019). Through the portal circulation, TMA reaches the liver where is oxidised by flavin mono-oxygenases 3 (FMO3) to TMAO (**Figure 1.2.2.1¹**). After the hepatic oxidization, circulating TMAO is mainly excreted through urine, breath, and sweat (Ayesh et al., 1993; Smith et al., 1994; Zhang et al., 1999), while the remaining part is further metabolised by microbiota to TMA (Fennema et al., 2016; Kwan and Barrett, 1983). Diet, thus, plays a pivotal role in modulation of the TMAO serum levels; in particular, high and prolonged consumption of foods rich in TMA precursors seems to be responsible for increased serum levels of TMAO (Velasquez et al., 2016).

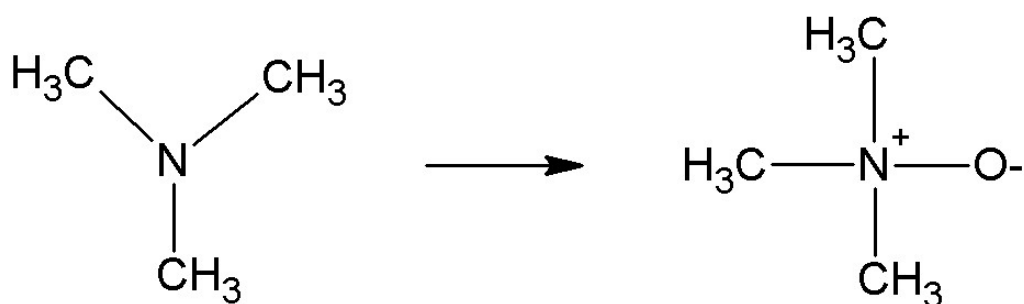


Figure 1.2.2.1¹. TMA to TMAO conversion occurring in the liver by FMO3 [source: **Article in press**]

There is evidence, however, that in addition to an unhealthy diet, microbiota *per se* contributes to increasing the circulating levels of TMAO (Tang et al., 2013). In this sense, studies in animals fed high-carnitine diet showed that antibiotic treatment intended to decimate the commensal microbiota resulted in reduced serum levels of TMAO and abolished cardiovascular consequences, including atherosclerotic lesions, the content of cholesterol in macrophages and foam cell formation (Koeth et al., 2013; Z. Wang et al., 2011). Furthermore, the atherosclerotic risk increased or decreased after microbial transplantation with TMA-producing strains or non-TMA producing strains, respectively (Gregory et al., 2015).

Interestingly, specific bacterial strains have been indicated as more responsible than others to produce TMA. In particular, studies demonstrated the existence of a direct relationship between TMAO serum levels and the abundance of *Tenericutes* and *Desulfovibrio* (Nam, 2019). Further studies reported that bacteria belonging to the *Clostridiaceae* or *Lachnospiraceae* families and *Ruminococcus*, *Allobaculum* and *Candidatus arthromitus* genera are also implicated, and their abundance results in an increased risk of atherosclerosis and arterial thrombosis *via* increased TMAO serum levels (Z. Wang et al., 2015; Zhu et al., 2016). In line with this evidence, studies investigating human microbiota identified TMA-producing bacterial species, mainly

belonging to *Firmicutes* and *Proteobacteria* phyla (Romano et al., 2015). It is possible to speculate that the strain-specific ability of such bacteria to produce TMA is mainly due to the fact that some of them predominantly express enzymes involved in the metabolism of TMA precursors, including lyases (*Clostridia* and *Eubacteria*) and carnitine oxygenases (*Proteobacteria*) (Rath et al., 2017; Z. Wang et al., 2011). Notably, a gender-specific diversity has been found, suggesting that in male mice, *Clostridiaceae* play a major role in the microbiota-TMAO relationship, while in the female it is due to *Ruminococci* (Z. Wang et al., 2015).

1.2.2.2 Analytic methods for circulating TMAO quantification

An extensive literature widely described several methods developed for the determination of TMAO levels in various biological fluids (i.e. serum and urine), including nuclear magnetic resonance spectroscopy (NMR) (Lam et al., 2014; Murphy et al., 2000; Podadera et al., 2005), gas chromatography (GC) (Mills et al., 1999; Zhang et al., 1995), high-performance liquid chromatography (HPLC) (Cháfer-Pericás et al., 2004) and mass spectrometry (MS) (Hsu et al., 2007; Mamer et al., 1999; Zhao et al., 2015). Among these, MS and NMR are the most effective (Albert and Tang, 2018; Cheng et al., 2017). However, these two methods have pros and cons, as reported in **Table 1.2.2.2¹**.

Table 1.2.2.2^I. Pros and cons of nuclear magnetic resonance spectroscopy and mass spectrometry methods for identification and quantification of TMAO levels

Method	Description	Pros	Cons	Reference
NMR	The compound identification and quantification is based on chemical shifts in resonance frequency when it is undergone electromagnetic field	Samples are minimally processed	Low sensitivity, expensive, useful for identification of the most representative compounds in a sample	(Cheng et al., 2017; Deidda et al., 2015; Tenori et al., 2013)
MS	Compounds are identified on the base of their unique mass/charge (m/z) ratio	High sensitivity, can be routinely used, can be performed in “targeted” or “untargeted” fashion	Complex sample preparation (requiring compound extraction from the matrix)	(Albert and Tang, 2018; Cheng et al., 2017)

In 2019 our research group developed and validated a novel LC/MS-based method for detection and quantification of TMAO serum levels without using marked/isotopic internal standard (Annunziata et al., 2019b). Materials and methods used are detailed in **Appendix A**. For the method validation we evaluated:

- *precision and accuracy* – the intra-day and inter-day accuracy (% bias) and precision (% C.V.) were determined at the concentrations of 0.033, 0.333, 0.667, 3.333, 6.667, 13.333, and 26.667 μM (**Table 1.2.2.2^I**, **Figure 1.2.2.2^I**). As expected, the higher % C.V. was measured at lower concentration tested (0.0025 ppm) with intraday and inter-day % C.V. of 12.12 and 8.25%, respectively. The same was for the accuracy, where the lower values of % bias were obtained at the lower concentration tested, with % bias of -5.82% (intra-day) and of -1.41% (inter-day). Generally, we have found that % C.V. values ranged from 12.12 to 3.92% and from 8.25 to 1.07% for intraday and inter-day precision, respectively; the % bias ranged from -5.52 to 0.5% for the estimation of intraday accuracy and from -1.42 to 3.08% for the evaluation of inter-day accuracy. TMAO recoveries from serum ranged from 99 to 97% depending on the three different standard dilutions used (**Table 1.2.2.2^{II}**, **Figure 1.2.2.2^{II}**)

- *linearity and sensitivity* – linearity studies were conducted by the preparation of calibration curves on a wide range of analytical standard concentrations (seven dilutions ranging from 0.033 to 26.667 μ M). All the analyses were conducted in triplicate, the ratio of standards concentrations versus peak area ratio (analyte peak area/internal standard peak area) was plotted with a correlation coefficient of R^2 0.999. Our results have indicated the LOD is 2 ng/mL while LOQ is of 6 ng/mL.

Table 1.2.2.2¹. Intra-day and inter-day precision and accuracy of the LC/MS method [source: (Annunziata et al., 2019b)]

TMAO concentration tested (μM)	Intra-day precision (% C.V. $n=6$)	Intra-day accuracy (% bias $n=6$)	Inter-day precision (% C.V. $n=6$)	Inter-day accuracy (% bias $n=6$)
0.033	8.25	-5.52	12.12	- 1.42
0.333	8.12	-3.52	10.5	1.02
0.667	1.78	0.89	7.20	1.42
3.333	1.54	2.6	4.89	0.85
6.667	1.10	0.62	5.20	0.79
13.333	1.52	0.66	3.95	0.65
26.667	2.75	0.45	4.68	-0.69

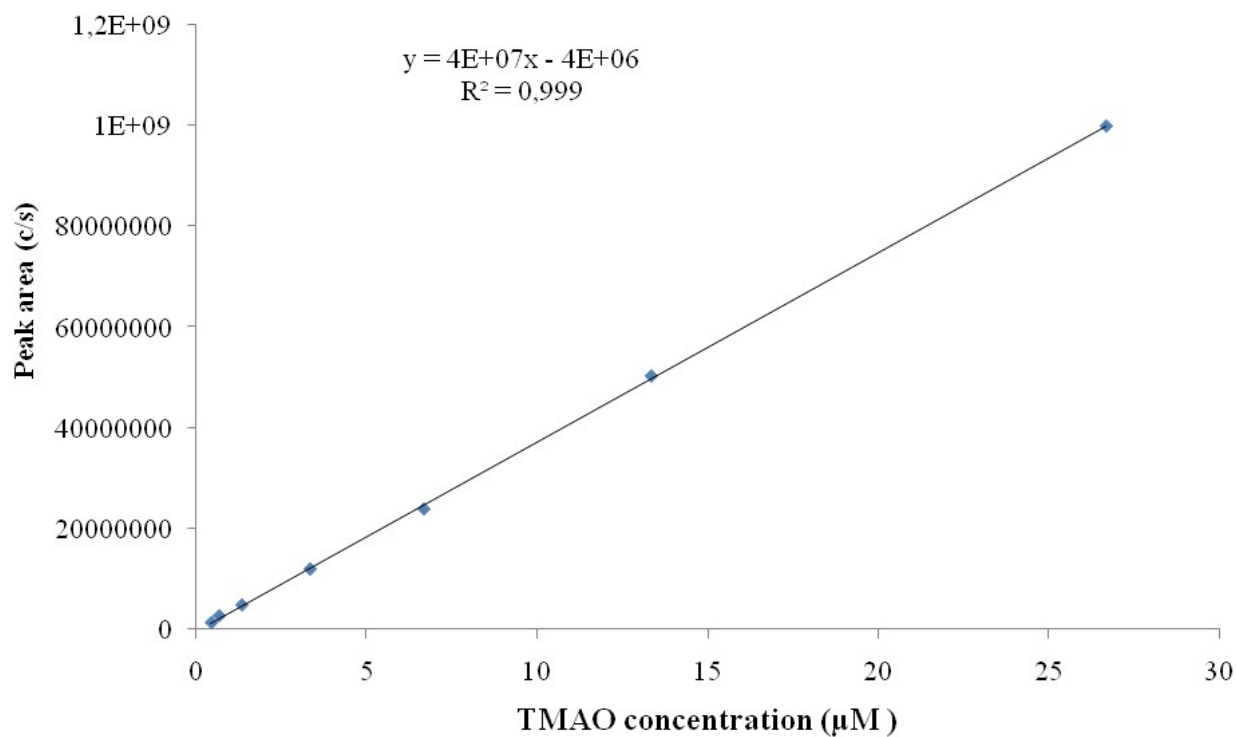


Figure 1.2.2.2¹. Calibration curve of TMAO over the concentration range of 0.033–26.667 μM [source: (Annunziata et al., 2019b)]

Table 1.2.2.2ⁱⁱ. Recovery of TMAO in pooled patient serum ($n=3$) [source: (Annunziata et al., 2019b)]

Baseline TMAO concentration in pooled t0 patients' serum	Spiked concentration (μM)	Measured	% recovery
5.347 \pm 0.003	0.333	5.679 \pm 0.360	99.99
	3.333	8.532 \pm 0.063	98.30
	13.333	18.121 \pm 1.083	97.01

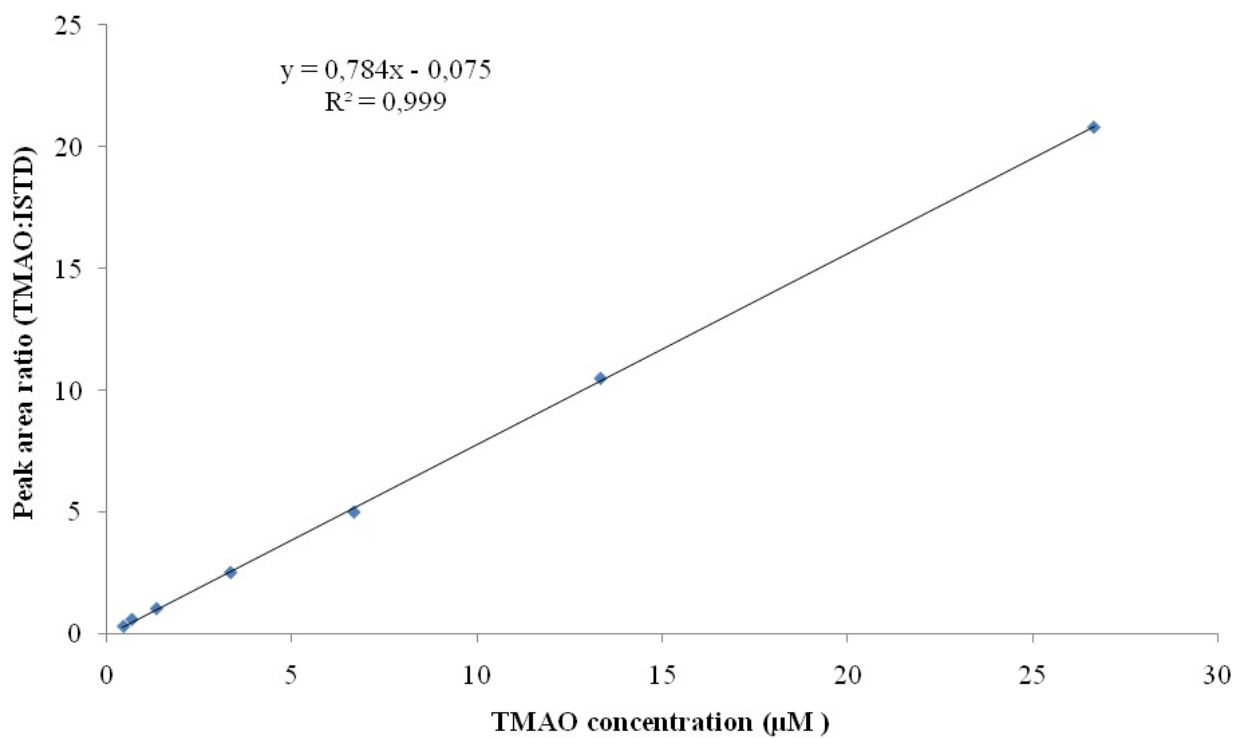


Figure 1.2.2.2ⁱⁱ. Linearity for TMAO over the concentration range of 0.033–26.667 μM . All the analysis are run in duplicate [source: (Annunziata et al., 2019b)]

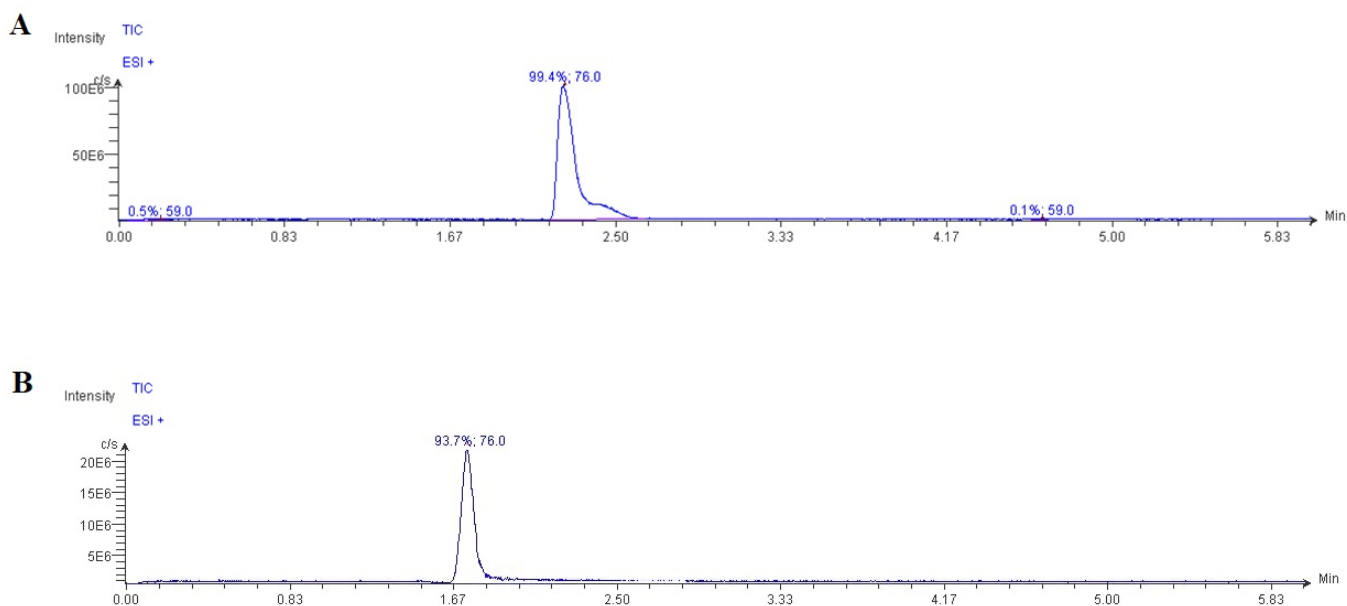


Figure 1.2.2.2^{III}. Typical extracted ion chromatograms from LC/MS analysis of (A) TMAO and (B) glycine standard dilution (ion extracted at $m/z = 76.0$ in positive mode). As glycine is present in plasma and having both the same TMAO molecular weight and ability to be ionized in positive mode, the two different retention times allow to discriminate TMAO in biological fluid from other compounds with similar chemical features [source: (Annunziata et al., 2019b)]

With this study we proposed a useful, rapid, versatile and valid method for detection and quantification of TMAO serum that should be considered for clinical and diagnostic applications. The methods used in our study is an optimization of a MS method previously developed (Beale and Airs, 2016) for quantification of TMAO concentration in seawater. Our validation studies were performed not for a comparison with other previously reported results, but with the aim to confirm the validity of our experiments. Overall, our method has good precision, accuracy and sensitivity.

1.3 Other diseases related to oxidative stress and/or atherosclerotic processes

1.3.1 Aged brain-associated cognitive impairment

The prevalence of age-dependent diseases, mainly brain ageing-related diseases, is dramatically increasing in developed and developing countries, resulting in both social and health-care cost problems. This scenario highlights the need to develop novel strategies to improve the life quality of aged people (Gareri et al., 2002; Hedden and Gabrieli, 2004; Sarubbo et al., 2015). For a general comprehension of this phenomenon, it should be taken into account that aged brain-associated cognitive impairments are just the tip of an iceberg built on a plethora of biochemical and molecular alterations occurring during ageing, and that have been demonstrated to be crucial in the development of neurodegenerative diseases (Gareri et al., 2002; Hedden and Gabrieli, 2004; Sarubbo et al., 2015). In particular, there is evidence that ageing-related alterations of the brain physiology, including cognitive alterations and synaptic dysfunction, are generally due to an increased OxS (Harman, 1956; Sarubbo et al., 2018d, 2018a) and inflammation (Salminen et al., 2008; Sarubbo et al., 2018d, 2018a) and reduced endogenous antioxidant defences (Bishop et al., 2010; Sarubbo et al., 2018d; Venkataraman et al., 2013). Notably, studies reported the association between increased OxS-related biomarkers and raised levels of pro-inflammatory cytokines with cognitive performance in institutionalised elderly people (Liguori et al., 2018).

Interestingly, increased OxS has also been indicated as one of the main causes of neurotransmitter system alterations (Haider et al., 2014; Pieta Dias et al., 2007). Indeed, during ageing the increased oxidative stress negatively affects the activity of limiting enzymes involved in the synthesis of the monoamines, including tryptophan hydroxylase (TPH) and tyrosine hydroxylase (TH); particularly, this reduction of the enzymatic activity is mainly related to oxidative damages and/or inefficient phosphorylations due to ROS injury (Cash, 1998; De La Cruz et al., 1996; Hussain and Mitra, 2000). Reduced activities of both TPH and TH result in decreased levels of monoamines, which is responsible for memory disorders development and neurodegenerative diseases onset (Collier et al., 2004; Cools, 2011; Esteban et al., 2010; Haider et al., 2014).

Another mechanism for the involvement of OxS in neurodegenerative diseases is related to the ability of oxidative status to induce stress granules (SGs) formation. Nuclear SGs contain pre-mRNA processing factors and heat-shock transcription factor 1/2; cytosol SGs contain proteins and non-translating mRNA. Under pathological conditions, SGs form super-stable aggregates that exert protective and anti-apoptotic effects. In cognitive impairment, SGs interfere with neuronal function *via* silencing transcripts and sequestering ribonucleoproteins (Liguori et al., 2018).

Equally noteworthy, altered homeostasis of ROS production and bioactive metals may have a role in pathogenesis of neurodegenerative diseases affecting amyloid-protein precursors or directly binding to

amyloid promoting its aggregation. Also, redox metals promote Tau protein phosphorylation. ROS, amyloid and Tau proteins affect the N-methyl-d-aspartate (NMDA) receptor activity, resulting in triggered excessive Ca^{2+} influx in post-synaptic neurons mediated by NMDA. This, in turn, leads to a cascade of events culminating in increased production of ROS, Tau phosphorylation and oxidative damage (mainly lipid peroxidation), ultimately leading to synaptic dysfunction (Liguori et al., 2018).

1.3.2 Age-related macular degeneration

Age-related macular degeneration (AMD) is an ophthalmology disease affecting about 64 million people worldwide, mainly middle-aged (over 65 years), that can culminate with legal blindness and sight loss (Gehrs et al., 2006). It is defined as a progressive degeneration of macula, a central retina specialized region, responsible for fine and color vision (Pawlowska et al., 2019). In advanced stages, AMD can be classified into two types: dry and wet (Lim et al., 2012). Diagnosis of AMD is based on combination of clinical examination and investigations, including photography, angiography, and optical coherence tomography (OCT) (Lim et al., 2012). The pharmacological treatments currently licensed for AMD comprise intraocular injection of anti-VEGF agents (i.e. ranibizumab and bevacizumab), which tolerability is different among patients (Lim et al., 2012). AMD pathogenesis is multifactorial, and several risk factors are implicated, including age (Pawlowska et al., 2019), genetic factors (Warwick and Lotery, 2018) and environmental/lifestyle factors, such as smoking, obesity, unhealthy diet, prolonged exposure to blue light and UV (Sobrin and Seddon, 2014). Both ageing and environmental/lifestyle factors have been recognized as responsible for increased OxS, whose role in AMD pathogenesis is commonly accepted (Bungau et al., 2019; Pawlowska et al., 2019). More specifically, OxS has been demonstrated to be implicated in AMD development *via* different mechanisms (Datta et al., 2017; Pawlowska et al., 2019), as schematically reported in **Figure 1.3.2**!

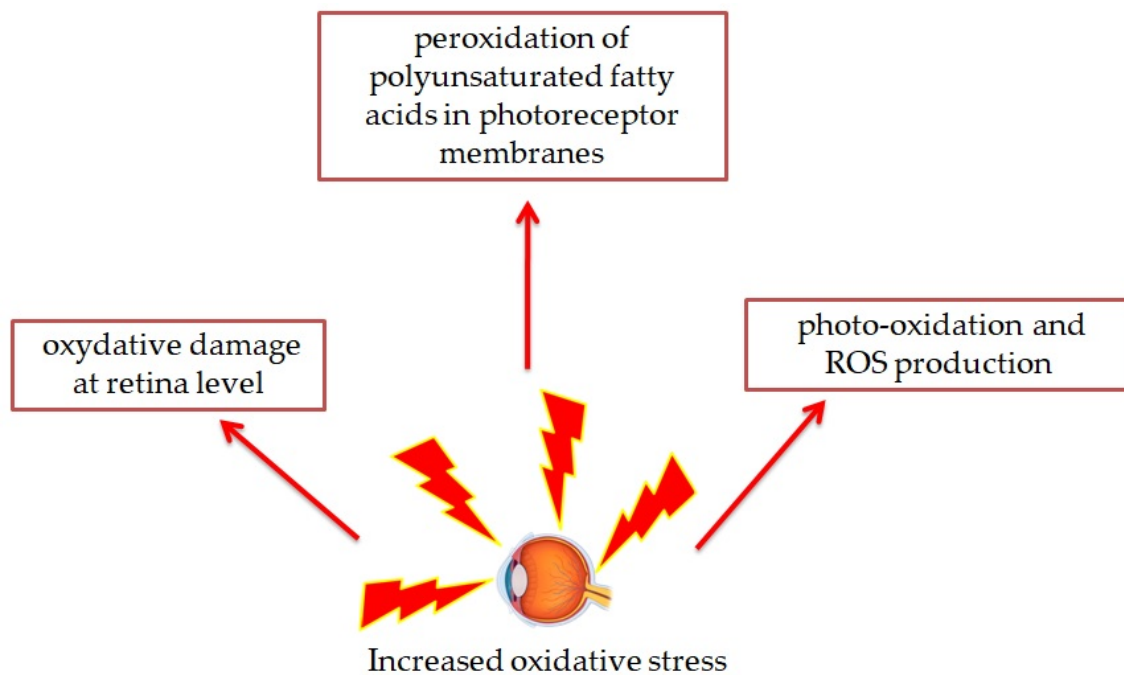


Figure 1.3.2¹. The role of oxidative stress in development of ophthalmology diseases

Additionally, it should be taken into account that ageing, *per se*, features high OxS, due to both reduction in endogenous antioxidant defenses and increase in free radical production (Harman, 1968; Jones et al., 2002; Petersen and Smith, 2016; Sohal and Weindruch, 1996). The involvement of OxS in both AMD development and progression, thus, is rooted in consequences of environmental factors and physiological conditions. From a clinical point of view, increased OxS at eye level is responsible for a progressive degeneration of several inner parts of retina (i.e. macula), resulting in disease development. This, in turn, leads to a progressive clinical evolution, due to limited self-repair and regeneration ability of retina (Pawlowska et al., 2019). In this scenario, therapeutic approaches aimed to counteract the OxS, are considered as effective strategies for AMD patient management.

In addition to OxS, evidence reported the existence of a close correlation between cardiovascular and inflammatory markers AMD (Al-Janabi et al., 2018; Kauppinen et al., 2016; Molins et al., 2018). In particular, thromboembolic and/or atherosclerotic processes are among the leading causes of acute retinal artery occlusion (RAO) (Dunlap et al., 2007; Hayreh, 2011; Hayreh et al., 2009), which clinical evolution leads to development of macular degeneration. According to several studies, AMD is associated with atherosclerosis (Vingerling et al., 1995) that, in turn, is linked to diabetes, obesity and altered gut microbiota (Armstrong et al., 2013; Karlsson et al., 2012; Tang et al., 2013; Turnbaugh et al., 2009). Interestingly, altered gut microbiota has also been reported in AMD patients (Rowan et al., 2017; Zinkernagel et al., 2017), suggesting the possible role played by such gut microbiota-derived metabolites with negative cardiovascular implication in AMD pathogenesis. Among these, TMAO is emerging; studies, indeed, demonstrated higher TMAO serum levels in patients with RAO than in healthy controls (Zysset-Burri et al., 2019).

In general, according to the available literature, AMD can be considered as an OxS-related disease with relative vascular implications. This justifies the use of polyphenol-based nutraceutical formulation that are commonly included in therapeutic schemes in clinical practice. As confirmation of this, it has been demonstrated that orally administered polyphenols can cross the blood-retina barrier (Pawlowska et al., 2019). Also, a number randomized clinical trials investigated the effects of different food-derived bioactive compounds (i.e. polyphenols) on AMD, including the Carotenoids in Age-Related Eye Disease Study (CAREDS), the Antioxydants, Lipides Essentiels, Nutrition et Maladies Oculaires (ALIENOR) study, the Taurine, Omega-3 Fatty Acids, Zinc, Antioxidant, Lutein (TOZAL) study (Carneiro and Andrade, 2017).

Such promising, these results highlight the interest of both researchers and clinicians in individuating novel nutraceutical approaches for the management of this degenerative and debilitating disease.

1.3.3 Endothelial dysfunction

Endothelial dysfunction is recognised as the leading risk factor for several CVD, including stroke, myocardial infarction, heart failure. In particular, endothelial dysfunction and vascular remodelling are considered as early determinants in the development of hypertension and atherosclerosis (Siti et al., 2015).

It is defined as a progressive reduced nitric oxide (NO) production and availability, with or without an imbalance between endothelium-derived contracting and relaxing factors associated with a pro-inflammatory and prothrombotic status (Scioli et al., 2020). Also, for this pathological condition, OxS plays a central role. In particular, ROS are responsible for a disruption of the vaso-protective NO signalling pathways that results in endothelial dysfunction and vascular abnormalities, and culminates in NO synthase (NOS) uncoupling. NOS are enzymes synthesising NO from L-arginine in presence of dioxygen as cofactor, producing superoxide anions. There are three types of NOS identified in different tissues: neuronal NOS (NOS1 or nNOS, type I), inducible NOS (NO₂ or iNOS, type II) and endothelial NOS (NOS3 or eNOS, type 3). NOS1 and 3 are expressed in heart and endothelial cells, and present Ca²⁺-dependent activity, while NOS2 possesses a Ca²⁺-independent activity, and is not constitutively expressed in healthy heart, but it is expressed in pathological conditions (i.e. inflammation) (Loyer et al., 2008; Umar and Van Der Laarse, 2010). NOS uncoupling results in switch from NO to •O₂⁻ production and ONOO⁻ *via* association of the two preceding, causing reduced NO bioavailability and consequent vasoconstriction (Santillo et al., 2015). ONOO⁻ plays a role in atherosclerosis progression by by inhibition of vasorelaxation, decrease in the beneficial effects of NO on platelet aggregation and vascular smooth muscle cell proliferation, and oxidation of DNA and lipids (Cai and Harrison, 2000).

Interestingly, ageing augments OxS in resistance arteries *via* increasing the production of ONOO⁻ (Ma et al., 2014). In healthy humans, brachial artery flow-mediated dilation (that is licensed as the golden

standard for the study of endothelial function) has been found to be negatively related to nitrotyrosine in vascular endothelial cells (Donato et al., 2007). Also, in old adults the expression of endothelin-1 (the main vascular endothelium-derived vasoconstrictor compound) is higher than in young; moreover, it is negatively related to endothelium-dependent dilation and directly related to nitrotyrosine (Donato et al., 2009).

1.4 Nutraceutical, the health-promoting effect from nature

In 1989 Dr. Stephen DeFelice, founder and chairman of the Foundation for Innovation in Medicine coined the term “nutraceutical” as a crasis of the words “nutrition” and “pharmaceutical” (Santini and Novellino, 2014), to describe a novel science studying the effects of food-derived bioactive compounds on human health (Cicero et al., 2017). Although the term nutraceutical let it be understood a potential pharmacological effect of such bioactive substances, it should be taken into account that nutraceuticals cannot be considered as product with prophylactic or therapeutic properties against human diseases (like conventional drugs), since they properly refer to foods, thus their consumption cannot have as ultimate purpose the treatment of diseases (Bianchi et al., 2017). More specifically, the use of nutraceutical supplements in clinical practice is currently licensed as (i) *add-on therapy*, in addition to the standard pharmacological treatment, for management of multi-treated patients, (ii) for long-term treatment of borderline conditions, where the clinical criteria for pharmacological treatments are not met, or (iii) for prevention and maintenance of wellness.

In general, nutraceuticals are considered as food supplements, although this definition is improper. According to the European Committee, indeed, food supplements are defined as food products intended to integrate the common diet and containing a concentrated source of nutrients (i.e. vitamins, minerals, aminoacids, fats, fibre) in pre-dosed formulations (Bianchi et al., 2017; European Parliament and Council, 2002). It appears clear, thus, that, although not considerable as drugs with pharmaceutical properties, nutraceutical products cannot be properly defined as food supplements, since their purpose is not integrate the common diet but support the physiological functions, eventually altered. This discrepancy is probably due to a not complete knowledge and comprehension of the health-promoting effect of nutraceuticals that is far to a mere supplementation with micro- and macronutrients, although no close to pharmaceutical treatments. In a double meaning, nutraceuticals, indeed, take place in the perfect middle between (i) healthy and disease, and (ii) diet and drugs, or more specifically as Prof. Novellino stated “*Beyond diet before drugs*” (Santini and Novellino, 2014).

Marketing researches suggest that the nutritional supplements (and nutraceuticals) business is rapidly and progressively growing among ordinary consumers worldwide. It was described in details in the Euromonitor International “Top 10 Global Consumer trends for 2017” that highlighted an increased appreciation of consumers for nutraceuticals that are associated with the concepts of wellness and prevention (Stallone et al., 2017). This is reinforced by the growing body of studies investigating the health-promoting properties of nutraceutical.

The growing interest of ordinary consumers in using nutraceuticals for preventive purposes has an important role also in reducing the healthcare costs. As an examples, as reported by the Frost&Sullivan

business consulting company involved in market research and analysis, considering the CVR-reducing effect of omega-3, their use as supplements results in a healthcare cost saving of about 13 billion/year in Europe (1.3 billion/year in Italy) (Stallone et al., 2017). This represents, thus, another relevant aspect for the use of nutraceutical. On the other hand, such promising, these data should encourage Government to promote research in this field.

In addition to various Government agencies and organizations, a relevant role is played by the European Food Safety Authority (EFSA) in summarise and evaluate the scientific evidence on nutraceuticals with the purpose to harmonise the legislation of European Member States regarding both nutrition and health claims reported on commercial product labels, in marketing or advertising. A nutrition claim is a statement or suggestion describing the beneficial nutritional properties of a food (i.e. “low fat”, “high in fibre”, “no added sugar”). A health claim refers to the health benefit(s) resulting from consumption of a food or its components (i.e. “Calcium may help improve bone density”, “Plant sterol have shown to reduce cholesterol levels, a risk factor in the development of coronary heart disease”). In addition to these claims (also called “general function health claims”), applicants can submit relative dossiers to the Member States in order to seed a risk assessment from EFSA on new function claims for a specific product. Such dossiers will be based on newly developed scientific evidence and will be transmitted to EFSA for a case-by-case assessment by the EFSA’s Novel Foods and Food Allergens (NDA) Panel (“European Food Safety Authority, EFSA,” 2021). Also, EFSA provide specific indications regarding the dosage of food components administered in nutraceutical forms. This is another crucial aspect regarding both efficacy and safety of nutraceuticals, since pharmacokinetic and optimal dosing studies are not frequently conducted. For example, the Commission Regulation (EC) No. 258/1997 considers 1000mg as the maximum safe polyphenolic extract daily amount compatible with a good health state in human. However, specific maximal doses have been established for some single polyphenols, such as caffeine (200mg), epigallocatechingallate (300mg), flavonoids (1000mg), quercetin (200mg), quercitrin (300mg), rutin (300mg), spiroside (300mg), esperidin (600mg), esperitin (300mg), isoflavones (80mg), lycopene (15g) (Cicero and Colletti, 2017).

1.4.1 The use of agri-food by-products as sources of bioactive compounds

In last few years, scientific research in nutraceutical field focused on the individuation of alternative sources of bioactive compounds, including agro-food *by-products*. This is mainly promoted by both economic (in terms of reduced production costs) and ecological needs (development of eco-friendly productive process aimed to reduce the waste-caused environmental pollution). It should be taken into account, indeed, that about the 60% of raw material used by the food industry represents waste material, that is intended to be used for animal feed or production of fertiliser, compost or biogas. In this context, thus, the proverbial

assumption to convert the necessity into a virtue gained a well-consolidated meaning, representing the *primum movens* of the scientific rationale also for research in nutraceutical field. More specifically, it is widely reported in literature that *by-products* from agro-food industry represent a valid source of bioactive compounds (Teixeira et al., 2014) that, in some cases, are present in greater amount than in the edible part. The most fitting example is represented by polyphenols, bioactive compounds more concentrated under the skin of fruits and vegetables, where protect against UV radiations, pathogens and physic damages (Manach et al., 2004). It appears clear, thus, that *by-products* represent a precious resource for extraction of this class of bioactive compounds.

On the base of these knowledge, last-decade researches demonstrated the nutraceutical potential of such agro-food *by-products* and their useful employment in nutraceutical as well as cosmetic industry (Barbulova et al., 2015). Previous evidence highlighted the significant nutraceutical potential of winemaking *by-products* (Teixeira et al., 2014), also called grape pomace. Studies reported that grape pomace exert a more marked lipid profile-regulating effect *in vivo* than red wine, due to the higher amount of polyphenols (de Oliveira et al., 2017), such as procyanidins A and B (De Camargo et al., 2014; Melo et al., 2015; Oldoni et al., 2016). This makes grape pomace good candidates for production of nutraceuticals. In this sense, remarkable were the studies on the beneficial effects of the polyphenolic fraction from *Aglianico* cultivar red grapes (Carola et al., 2012; Urquiaga et al., 2015).

1.4.2 The antioxidant and cardio-protective activity of polyphenols

Among the food-derived bioactive compounds, polyphenols are undoubtedly the most investigated and abundant. They represent the largest class of bioactive substances present in plants, where are produced as secondary metabolites with protective functions against UV radiations, pathogen aggression, and oxidative stress protection (Annunziata et al., 2020a). The great research interest in this class of bioactive compounds is due to their well-demonstrated beneficial effects on human health, in particular antioxidant and anti-inflammatory activities, that will be discussed in detail in following sections. Interestingly, a large body of evidence reported further activities of polyphenols, including anti-diabetic (Annunziata et al., 2020a, 2019a; Barrea et al., 2019a; Daliu et al., 2020; Tenore et al., 2020), plasma lipid lowering (Farzaei et al., 2019; Feng et al., 2019; Schiano et al., 2020), and antiviral properties against a large number of pathogens, including EpsteinBarr virus (De Leo et al., 2012; Yiu et al., 2010), enterovirus 71 (Zhang et al., 2015), herpes simplex virus (HSV) (Annunziata et al., 2018b; Faith et al., 2006), influenza virus (Lin et al., 2015), MERS-/SARS-coronavirus (Annunziata et al., 2020c) and other virus causing respiratory tract-related infections (Liu et al., 2014; Mastromarino et al., 2015). This latter potential of polyphenols, that at this time (2021 COVID-19 pandemic) gained a relevant interest, seems be due to a viral replication inhibition exerted by polyphenols *via* different mechanisms (Annunziata et al., 2020c): (i) inhibition of immediate-early virus protein

expression (i.e., ICP-4 and-27), (ii) inhibition of the NF κ B signaling pathway, and (iii) activation of the AMPK/Sirt1 axis in the host cell (14).

Polyphenols are a very complex class of food-derived bioactive compounds presenting a variety of chemical, biochemical and pharmacological features that will be presented in the present section.

1.4.2.1 Chemistry and food sources of polyphenols

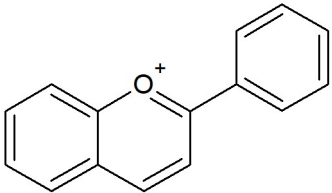
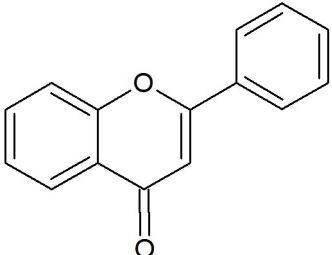
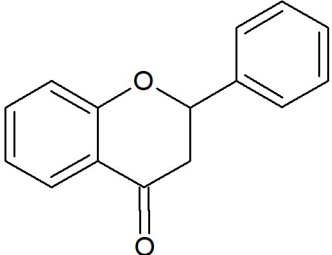
Besides the various thousands of different molecules, polyphenol compounds share the same basic chemical structure based on one or more phenolic rings with hydroxyl groups. The molecular structure of polyphenols derives from phenylalanine (or from its precursor shikimic acid), conjugated with one or more sugars, carboxylic, organic acid, amine, lipid or phenol residues via hydroxyl groups (Kondratyuk and Pezzuto, 2004). Based on their chemical structure, polyphenols are classified into flavonoids, phenolic acids, polyphenolic amides, stilbens and lignans (**Table 1.4.2.1'**).

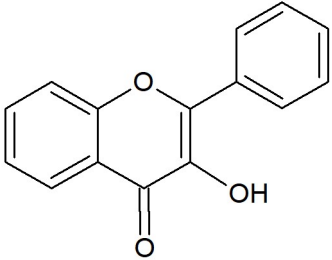
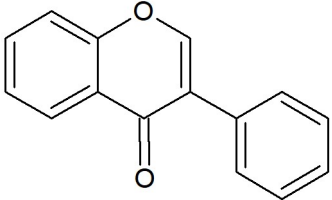
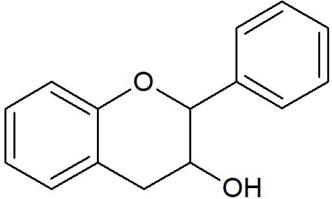
- *Flavonoids* – the general chemical structure is based on two aromatic rings (C₆, A and B rings) bound together by an additional three-carbon atoms ring forming an oxygenated heterocycle (C ring). Based on the type of the heterocycle involved, flavonoids are divided into six different subclasses: flavonols (i.e. quercetin, kaempferol), flavones (i.e. luteolin, apigenin), isoflavones (i.e. Genistein, daidzein, glycitein), flavanones (i.e. naringenin, hesperetin, eriodictyol), anthocyanidins (i.e cyanidin) and flavanols (i.e. catechins, proanthocyanidins). Among the general chemical characteristics, such flavonoids present specific features that result strongly related to their biological activities. The most peculiar example refers to isoflavones that, although they are not steroids, have structural similarities to estrogens, and for this reason they are also named phytoestrogens. More specifically, isoflavones have hydroxyl groups in positions 7 and 4' in a configuration analogous to that of estradiol. This confers their ability to bind to estrogen receptors. The flavonoid distribution in foods varies among the single subclasses. Flavonols are the most ubiquitous in foods, and are generally present in concentrations of about 15-30mg/kg of fresh weight. Their richest sources are onions, curly kale, leeks, broccoli, blueberries, leafy vegetables, cherry tomatoes. Conversely, flavones are less common and mostly identified in parsley and celery. Food source of flavanones are tomatoes, aromatic plants (i.e mint) and fruits (i.e. grapefruits, orange and lemon). Isoflavones are exclusively present in plants belonging to the leguminous botanical family, where soya is the main dietary source; isoflavones content in soybeans ranges 580-3800 mg/kg of fresh weight. Although some fruits (i.e. apricot) and beverages (i.e wine) contain appreciable amounts of catechins (flavanols), tea and chocolate are the richest sources. A green tea infusion, indeed, contains more than 200mg of catechins.

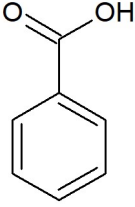
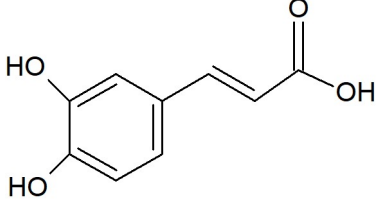
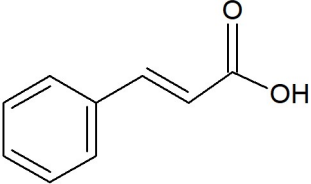
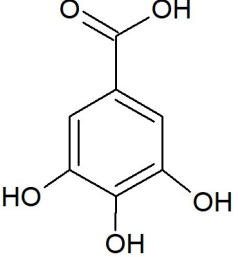
Interestingly, the flavanols content in tea varies on the base of the productive process; in particular, the fermentation of tea leaves used for the production of black teas causes an oxidation of monomer flavanols, resulting in production of condensed polyphenols, such as theaflavin and thearubigin. Finally, the most important dietary sources of anthocyanins are cereals, leafy and root vegetables, fruits (in particular red fruits) and wine, where their content is about 200-300mg/L (Manach et al., 2004).

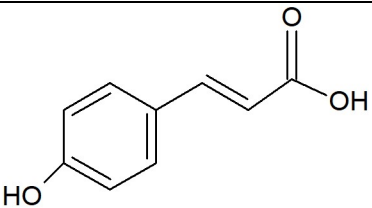
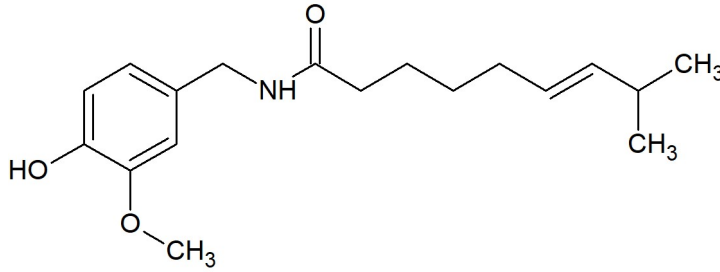
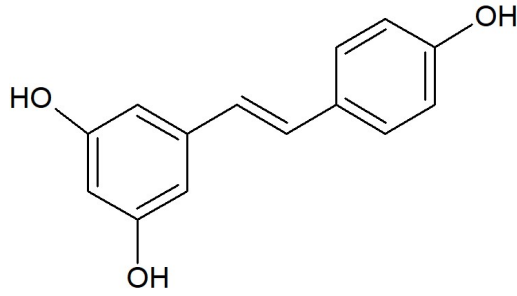
- *Phenolic acids* – compounds belonging to this class are non-flavonoid polyphenols presenting only one phenol ring bound to 1-3 carbon chain. Phenolic acids can be distinguished into two classes: cinnamic acid derivatives (hydroxycinnamic acids) and benzoic acid derivatives (hydroxybenzoic acids). The most representative hydroxycinnamic acids are *p*-cumaric, caffeic, ferulic, and sinapic acids. Generally, there are glycosylated or esterified with quinic, shikimic or tartaric acids. Their main food sources are coffee (70-350mg of chlorogenic acid per cup), fruits (such as blueberries, kiwis, plums, cherries, apples that contain on average 0.5-2.0g of hydroxycinnamic acids per kg of fresh weight) and certain cereals (such as wheat, rice and oat containing on average 0.5-2.0g of ferulic acid/kg of fresh weight). On the other hand, hydroxybenzoic acids are mainly found in red fruits (i.e. strawberries, raspberries, blackberries) and tea leaves (on average 4.5g/kg of fresh weight) (Manach et al., 2004).
- *Phenolic amides* – these are polyphenols with N-containing functional substituents. Among these, capsaicin contained in chilli peppers is the most representative (Annunziata et al., 2020a).
- *Stilbenes and lignans* – stilbenes are phenylpropanoids characterised by a 1,2-diphenylethylene backbone; the most representative and studied is resveratrol. The main sources are medicinal plants, fruits (i.e. grapes) and wine. Lignans are phenylpropanoid dimers containing two phenylpropane units (C6-C3) linked by their carbon 8. Secoisolariciresinol and matairesinol are examples of lignans. The main food source of lignans are cereals, grain, fruit and vegetables; however, the richest one is linseed (Manach et al., 2004).

Table 1.4.2.1'. Classification of the main polyphenols [source: (Annunziata et al., 2020a)]

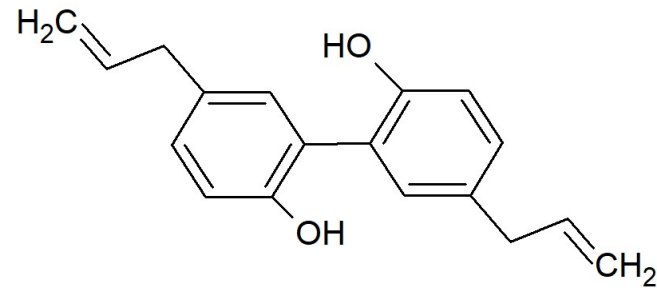
Major class	Basic description	Subclass	Main examples	Dietary source	References
Flavonoids	Two phenolic rings (C6) bounded by an additional carbonyl ring of three carbons (C3)	 <p>Anthocyanins</p>	Aurantidin, Capensinidin, Cyanidin, Delphinidin, Europinidin, Hirsutidin, Malvidin, Pelargonidin, Peonidin, Petunidin, Pulchellidin, Rosinidin	Strawberry, plum, black grape, blueberry, blackcurrant, cherry, rhubarb	(D'Archivio et al., 2010; Pandareesh et al., 2015; Salucci and Falcieri, 2020; Tsao, 2010; Tsopmo et al., 2013; Xiao and Kai, 2012)
		 <p>Flavones</p>	Apigenin, luteolin, tangeritin, chrysin, 6-hydroxyflavone	Parsley, celery, hot pepper, thyme	
		 <p>Flavanones</p>	Blumeatin, butin, eriodictyol, hesperidin, homeoriodictyol, isosakuranetin, naringenin, naringin, pinocembrin, poncirin, sakuranetin, sakuranin, sterubin	Lemon juice, orange juice, grape fruit juice	

		 <p>Flavonols</p>	<p>3-hydroxyflavone, azaleatin, fisetin, gelangin, gossypetin, kaempferide, kaempferol, isorhamnetin, morin, myricetin, natsudaïdain, pachypodol, quercetin, rhamnazin, rhamnetin</p>	<p>Onion, curly kale, leek, cherry, tomato, broccoli, apples, green and black tea, blueberry</p>	
		 <p>Isoflavones</p>	<p>Biochanin A, calycosin, daidzein, formononetin, genistein, glycitein, irilone, orobol, pratensein, prunetin, pseudobaptigenin, puerarin</p>	<p>Legumes, soymilk, tofu, miso</p>	
		 <p>Flavan-3-ols</p>	<p>Catechins and derivatives</p>	<p>Cereals, legumes, fruits, vegetables, wine and tea.</p>	

Phenolic acids	One phenol ring bounded to 1-3 carbon chain		 <p data-bbox="1305 395 1451 419">Benzoic acid</p>	Fruits, vegetables, red fruits, tea, coffee, cider	
			 <p data-bbox="1312 675 1451 699">Caffeic acid</p>		
			 <p data-bbox="1296 951 1469 975">Cinnamic acid</p>		
			 <p data-bbox="1319 1289 1447 1313">Gallic acid</p>		

			 <p>p-Coumaric acid</p>	
Polyphenolic amides	Polyphenol compounds with N-containing functional substituents		 <p>Capsaicin</p>	Chilli pepper
Stilbenes or lignans	<p>Stilbenes: phenylpropanoids characterised by a 1,2-diphenylethylene backbone</p> <p>Lignans:</p>		 <p>Resveratrol (stilbene)</p>	<p>Grains: barley, buckwheat, millet, oat, rye, wheat, brown rice</p> <p>Nuts: cashew,</p>

phenylpropanoid
dimers containing
two phenylpropane
units (C6-C3)
linked by their
carbon 8



Magnolol (lignan)

hazelnut
Seeds:
sesame,
sunflower,
flax,
chickpea,
lentil, pea,
soybean
Fruits: apple,
banana,
cantaloupe,
grape, kiwi,
lemon,
orange,
pineapple,
red
raspberry,
strawberry
Vegetables:
asparagus,
avocado,
cabbage,
carrot,

				cauliflower, cucumber, eggplant, garlic, onion, potato, radish, tomato Coffee and tea Wine	
--	--	--	--	---	--

1.4.2.2 Bioavailability of polyphenols

Bioavailability is defined as “the fraction of both nutrients and non-nutrients that are absorbed and available for the human body, in particular at the site of action, where they can exert their functions” (Annunziata et al., 2020a). In general, this represents a major concern for the nutraceutical industry in order to ensure the optimal absorption of bioactive compounds, including polyphenols. Due to their peculiar chemistry, indeed, polyphenols are rather known for their very low intestinal bioaccessibility and consequent bioavailability. This is mainly due to their hydrophobic nature, that results in low water solubility (Dutta et al., 2018). Moreover, their chemical instability under different physicochemical conditions during the transit in the gastrointestinal tract, the difficult diffusion across the cell membranes and their rapid metabolism also severely impair the polyphenol bioavailability (Dias et al., 2015; Feng et al., 2019). Overall, the main factors affecting the polyphenol bioavailability are represented in **Figure 1.4.2.2**, and summarised as follow:

- degrading factors: natural bioactive compounds (i.e. polyphenols) are particularly susceptible to light, temperature and pH, that cause their degradation and, consequently, bioactivity reduction (Ozkan et al., 2019). Also, once ingested, polyphenol structures are altered by enzyme activity and physico-chemical variations during the transit into the gastrointestinal (GI) tract, resulting in compromising their solubility. Generally, polyphenols present three different features: (i) high solubility and poor permeability across the cell membrane (i.e. epigallocatechin gallate), (ii) low solubility and poor permeability across the cell membrane (i.e. curcumin) and (iii) low solubility and high permeability across the cell membrane (i.e. resveratrol) (Hu et al., 2017)
- release from food matrix: natural bioactive compounds, and in particular polyphenols, exist in glycosidic form, linked to fibre *via* a glycosidic bond with a glucose residue. To promote the permeation across the intestinal barrier, this bond needs to be broken, releasing the aglycon. This occurs not only in foods, but also in nutraceutical formulations, where extracted polyphenols are still linked to residual fibre, resulting in impaired absorption (Annunziata et al., 2018a)
- intestinal permeation: there is no evidence of specific receptors for polyphenols in enterocytes. It is plausible, thus, that polyphenols are absorbed *via* diffusion/efflux mechanisms (Dias et al., 2015). In general, polyphenols with a low molecular weight can be absorbed by passive diffusion (Barrington et al., 2009). On the other hand, some compounds (such as resveratrol) are absorbed *via* mechanisms involving transcellular transports (Kaldas et al., 2003) and other (such as curcumin) *via* passive diffusion, due to their lipophilic nature (Yu and Huang, 2011)

- metabolic transformation: natural bioactive compounds undergo both intestinal and hepatic modification through phase I and II metabolisms (Hu et al., 2017; Rotches-Ribalta et al., 2012; Walle, 2011).

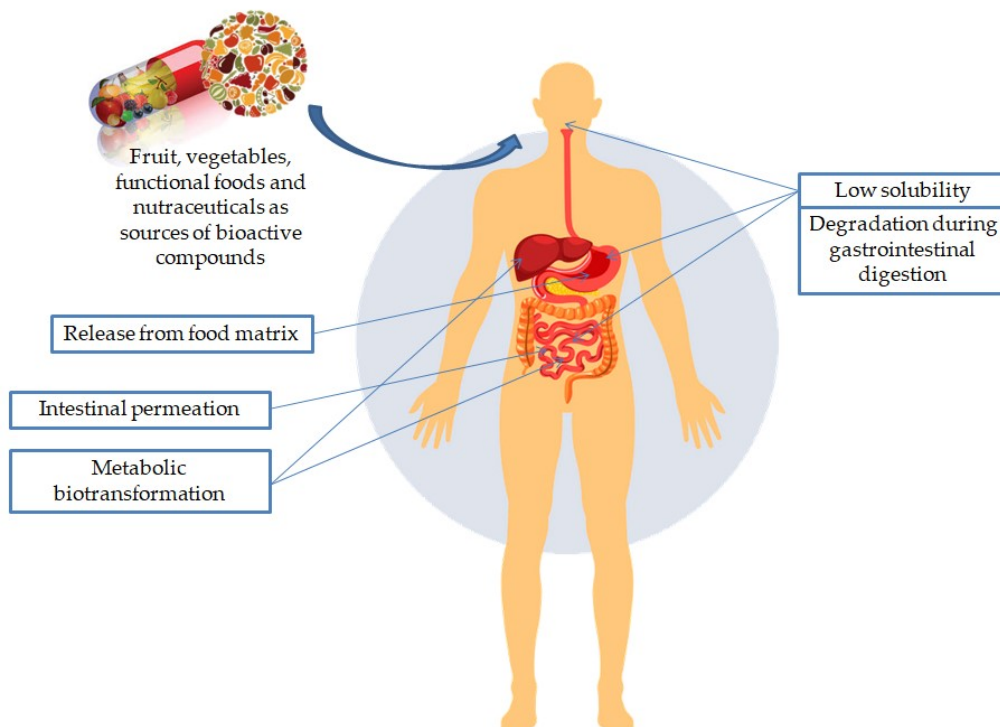


Figure 1.4.2.2¹. Factors affecting polyphenols bioavailability. Fruit, vegetables, functional foods and nutraceuticals are sources of bioactive compounds, mainly polyphenols; their beneficial effects are affected by several factors compromising their bioavailability, in particular, low water solubility. Additionally, after the oral consumption, the polyphenols undergo drastic degradation processes due to the transit in the diverse organs of the gastrointestinal tract, where the unaffected compounds need to be released from the food matrix in order to be absorbable. A further critical point is the scarce permeation through the intestinal barrier; it means that the release into the bloodstream occurred in a very low amount of bioactive compounds which, however, undergo complex metabolism both in gut and liver [source: (Annunziata et al., 2020a)].

The low bioavailability of polyphenols, thus, is a very crucial concern for the biological effects of nutraceutical. Several studies investigated in this sense reporting, for example, the very low bioavailability of orally administered catechins from green tea (<3.5%) (Kida et al., 2000). An interesting study conducted by our research group evaluated both bioaccessibility (using an *in vitro* model of gastrointestinal digestion) and bioavailability (*via* a Caco-2 monolayer permeation model) of tea catechins, reporting that only the 2-15% of the intestinal content permeated across the intestinal barrier model (Tenore et al., 2015). The same *in vitro*

model of bioaccessibility study was used to investigate the digestive fate of tea polyphenol-based nutraceutical formulations. In this study we observed that, in contrast to the low upper intestine bioaccessibility (13.00-23.77%), that at lower intestine level was significantly increased (108-112%), suggesting the potential role played by gut microbiota in metabolism of polyphenols that results in their enhanced absorption rate (Annunziata et al., 2018a). Similarly, we also demonstrated that after gastrointestinal digestion the intestinal bioaccessibility of abscisic acid in an okra-based nutraceutical formulation significantly decreased (Daliu et al., 2020).

As previously reported in this section, the peculiar chemistry of polyphenols plays a key role in their bioavailability. For example, polyphenols with a lipophilic structure have a low intestinal bioaccessibility (due to their low water solubility) but a high ability to permeate across the intestinal barrier (Dias et al., 2015). Resveratrol is among the most investigated polyphenols for its historically-known beneficial effects on human health. Evidence reported that, due to its chemistry, resveratrol is poorly soluble in water (about 0.03 g/L) (Mattarei et al., 2013). Notably, its oral absorption rate in human is relatively high (about 75%); however, due to an extensive metabolism at both intestinal and liver level, its bioavailability is very low (about 1%) (Rotches-Ribalta et al., 2012; Walle, 2011). Furthermore, pharmacokinetic studies reported that, when orally administered, this polyphenol reaches two plasma concentration peaks (at 1h and 6h), suggesting an enteric recirculation, also confirmed by its 9.2h half-life (Almeida et al., 2009; Zu et al., 2016).

1.4.2.3 *Metabolic fate of polyphenols – Absorption, Distribution, Metabolism, Excretion (ADME)*

As per other xenobiotics, polyphenols undergo a very complex metabolism. Once ingested through the diet or nutraceutical formulations, indeed, polyphenols follow the physiological gastrointestinal digestion, undergoing several physico-chemical and biochemical conditions naturally occurring during these processes, which may severely affect both their chemical features and absorption rate. Overall, the metabolic fate of these bioactive compounds can be summarised as following described at different levels:

- stomach: some polyphenols (mainly in glycosidic form) are resistant at gastric acid pH, thus reach the intestine in an intact form (Gee et al., 1998). Also, some flavonoids (i.e. quercetin and daidzein) can be absorbed across the gastric mucosa (Crespy et al., 2002; Piskula et al., 1999).
- upper intestine: the majority of polyphenols are absorbed at intestinal level, although most of them are too hydrophilic to be absorbed across the gut mucosa *via* passive diffusion. Membrane carrier and active transporters have been identified (Ader et al., 1996). In general, only aglycones can be absorbed at intestinal level, while glycosides need to be previously hydrolysed by gut microbiota (Hollman and Katan, 1997; Manach et al., 1995), glucosidases of the brush border of enterocytes (i.e. lactase phloridzine hydrolase) (Day et al., 2000) or cytosolic β -glucosidases (Day et al., 1998) after

being transported into the enterocytes by sodium-dependent transporter (SGLT)-1 (Hollman et al., 1995)

- lower intestine: the enzymatic activities of gut microbiota contribute to further metabolise unabsorbed polyphenols, favouring their absorption in the colon (Manach et al., 2004). In particular, microbiota is particularly able to hydrolyse glycosides into aglycones and aglycones into several aromatic acids (Kuhnau, 1976) that, in turn, are absorbed and further metabolised (mainly conjugated with glycine, glucuronic acid, or sulfate) (Manach et al., 2004).

Additionally, the main pharmacokinetic features may be summarised with the so-called ADME scheme (abbreviation for absorption, distribution, metabolism and excretion):

- A – absorption: as aforementioned, intestinal absorption of polyphenols mainly occurs *via* transcellular transports (Kaldas et al., 2003) or *via* passive diffusion, due to their lipophilic nature (Yu and Huang, 2011), with different efficiency depending on the polyphenol molecule. For example, in human the maximum absorption of quercetin-4'-glucoside occurs 0.5-0.7h after ingestion and 6-9h after ingestion of the same amount of quercetin-3 β -rutinoside (Graefe et al., 2001; Hollman et al., 1999). These differences may be explained by a matrix effect. It has been reported, indeed, that the bioavailability of some polyphenols administered in pure form is greater than that of the same amount in foods (Setchell et al., 2001).
- D – distribution: polyphenol metabolites travel into the bloodstream to free but bound to plasma proteins, mainly albumin, with different affinity depending on the various polyphenolic molecules. For example, quercetin, kaempferol and isorhamnetin have an affinity of about 99% for concentration up to 15 μ mol/L (Boulton et al., 1998; Dangles et al., 2001). Substitution of 3-OH causes reduction of the affinity to albumin (Dangles et al., 1999). The degree of binding to albumin results in clearance of metabolites and affects their cellular and tissue distribution. Conventionally, cellular uptake is proportional to the concentration of unbound metabolites. pH variations cause changes in albumin conformation, resulting in dissociation of the ligand-albumin complex (Horie et al., 1988). It has been reported a high distribution of polyphenols in several tissues (including brain, endothelial cells, heart, kidney, spleen, pancreas, prostate, uterus, ovary, mammary, gland, testes, bladder, bone and skin) with different concentrations ranging from 30 to 3000ng aglycone equivalent/7g tissue depending on the dose administered and the tissue considered (Manach et al., 2004). Endothelium is the main site of flavonoid action, where polyphenols reach with rapid, energy-dependent transport systems (Schramm et al., 1999).

- M – metabolism: after the intestinal absorption, polyphenols undergo several complex metabolic processes at both hepatic and intestinal level. In particular, three main types of conjugations occur: methylation, sulfatation, and glucuronidation. Methylation is performed by catechol-*O*-methyl transferase that catalyses the transfer of a methyl group from *S*-adenosyl-*L*-methionine to polyphenols having an *o*-diphenolic moiety (i.e. quercetin, catechin, caffeic acid, luteolin). This is a reaction generally occurring in the 3' position, but a minor proportion of 4'-*O*-methylated products are also formed. Sulfatation is performed by sulfotransferases that catalyses the transfer of a sulfate moiety from 3'-phosphoadenosine-5'-phosphosulfate to a hydroxyl group. Finally, glucuronidation is performed by UDP-glucuronosyltransferases that catalyses the transfer of a glucuronic acid from UDP-glucuronic acid to polyphenols. Also, once metabolised at intestinal levels, polyphenols undergo further methylation and deglucuronidation reactions in hepatic cells (Manach et al., 2004).
- E – excretion: polyphenol metabolites follow two main excretion pathways: biliary (for large, extensively conjugated metabolites) or urinary (for small conjugates such as monosulfates) route. Biliary excretion is typical of compounds such as genistein, epigallocatechingallate and eriodictyol; some of them may be further metabolised by microbiota β -glucuronidases releasing the relative aglycone that is reabsorbed through the enterohepatic circulation. On the other hand, urinary excretion is typical of flavanones and isoflavones. Some polyphenols (i.e anthocyanins) have a low urinary excretion percentage probably due to pronounced biliary excretion or extensive metabolism. The exact half-life of polyphenols has been calculated not exactly for all molecules. However, evidence a half-life of 2h for compounds such as anthocyanins, 2-3h for flavanols (except for epigallocatechingallate), 4-8h for isoflavones and 11-28 for quercetin. These data suggest that regular and frequent consumption of source of polyphenols is necessary for maintenance of their high plasma concentration (Manach et al., 2004).

1.4.2.4 Nutraceutical properties of polyphenols – focus on the antioxidant and anti-inflammatory activities

It is historically known that polyphenols exert their antioxidant activity through two major levels named (i) ROS-removing level (direct ROS-scavenging and modulation of the endogenous antioxidant defences) and (ii) ROS formation levels (inhibition of both the metal-dependent production of free radicals and ROS-producing enzymes) (Sandoval-Acuña et al., 2014) (**Figure 1.4.2.4'**). With respect to the first point, the scavenging activity of polyphenols is mainly due to their peculiar chemistry. Polyphenols, indeed, are able to react with free radicals directly, including hydroxyl, superoxide, nitric oxide, alkoxyl and peroxy radicals, through their benzene ring-bound hydroxyl groups, by which they transfer an electron to the ROS molecule, stabilising the reactive species (Amic et al., 2007; Bors et al., 1990) and generating a phenoxyl radicals that, in turn, react with a second radical forming a stable quinone structure (Amic et al., 2007).

However, it should be taken into account that depending on their concentration, polyphenols may also act as pro-oxidant (Sandoval-Acuña et al., 2014). Moreover, polyphenols are also able to up-regulate the expression of enzymes involved in the antioxidant cells' defences, including SOD, CAT, GPx. This up-regulation is mainly modulated *via* activation of the Keap1/Nrf2/ARE signalling pathway (Sandoval-Acuña et al., 2014; Tsuji et al., 2013). In addition to these mechanisms, it should be noted that polyphenols can directly counteract the production of ROS chelating iron and copper ions thus preventing their participation in free radical formation reactions or inhibiting the activities of ROS-producing enzymes, such as NOX and monoamine oxidase (MAO) (Sandoval-Acuña et al., 2014).

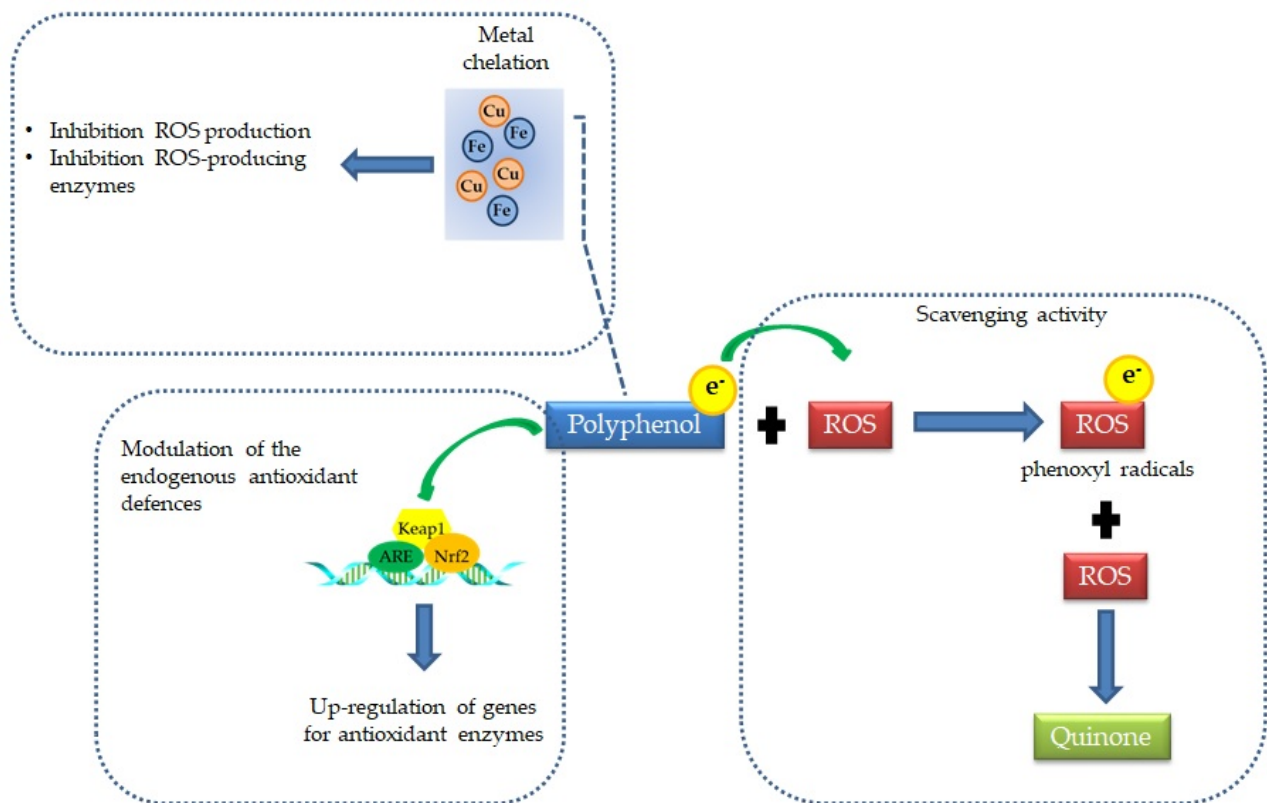


Figure 1.4.2.4¹. Main mechanisms antioxidant mechanisms of polyphenols

In addition to the antioxidant activity, several *in vitro* and *in vivo* studies have investigated the anti-inflammatory activity of polyphenols, suggesting their ability to act on different targets, including inhibition of COXs, phospholipase A2 and lipoxygenases, which result in decreased synthesis of prostanoids and leukotrienes. Moreover, further targets of the anti-inflammatory activity of polyphenols include phosphodiesterase, kinases and transcriptases (Farzaei et al., 2019).

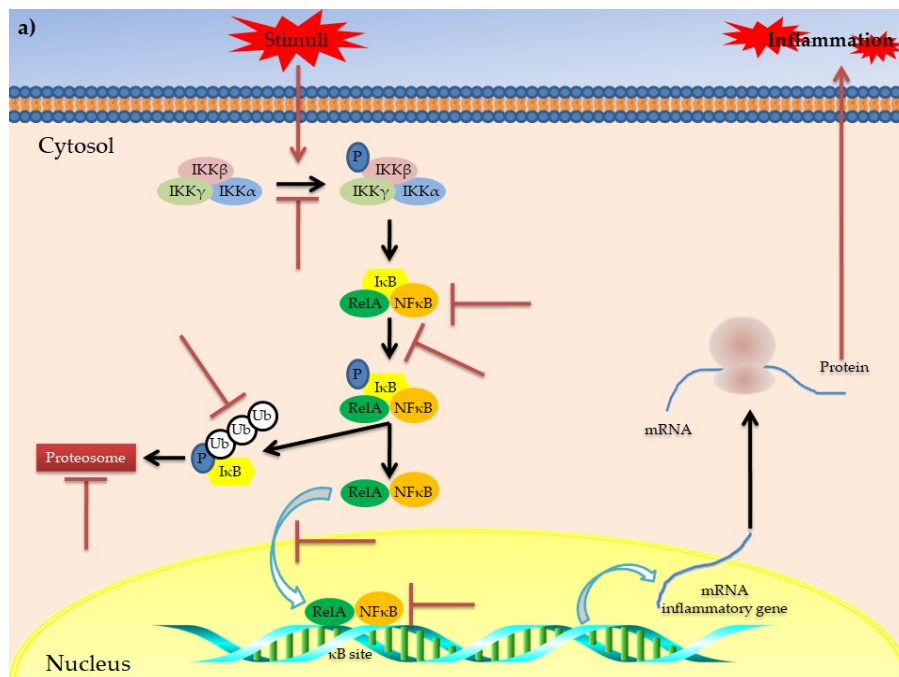
However, besides polyphenols' generic anti-inflammatory potential, evidence has highlighted their role in modulating the obesity-related inflammatory status. Among the various metabolic disorders, obesity is undoubtedly the main disorder strongly related to a chronic low-grade inflammation (Gregor and

Hotamisligil, 2011; Klop et al., 2013). This is evidenced by increased circulating levels of inflammatory biomarkers in obese patients compared to non-obese subjects, mainly released by monocytes, macrophages and dysfunctional adipocytes (Bray et al., 2016; Calder et al., 2011). At molecular level, this is the result of an NF- κ B-induced expression of pro-inflammatory genes. More specifically, NF- κ B is a family of transcription factors (including NF- κ B1 and NF- κ B2) (Chen et al., 1999) normally present in cytoplasm and associated with I κ B, a regulatory protein family that includes I κ B γ , I κ B β , I κ B α , I κ B ϵ , and Bcl-3 (Shirane et al., 1999). When bound to I κ B, NF- κ B is maintained in an inactive state. In response to various stimuli (i.e. increasing oxidative stress and/or inflammation), specific genes such as NF- κ B-inducing kinase (NIK), mitogen activated protein kinase kinase (MEKK), interleukin-1 receptor-associated kinase (IRAK), TNF receptor-associated factor (TRAF), PKC, and VCAM promote the activation of IKK which, in turn, phosphorylates I κ B, resulting in release of NF- κ B (Chen et al., 1995). Once released, NF- κ B translocates into the nucleus, inducing the expression of pro-inflammatory genes (Chen et al., 1999; Israël, 2010). In this context, evidence has demonstrated the ability of polyphenols to modulate the NF- κ B pathway, acting at different levels (Farzaei et al., 2019; Santangelo et al., 2007) (**Figure 1.4.2.4^{II-A}**). In particular, mechanistic studies have reported that polyphenols are able to: (i) counteract the activation of IKK (i.e. EGCG, epicatechin, flavonoids) (Aneja et al., 2004; Mackenzie et al., 2004; Wheeler et al., 2004); (ii) inhibit the phosphorylation of I κ B (i.e. EGCG, quercetin, apigenin, silymarin, kaempferol, and isoliquiritigenin, curcumin) (Bradford, 2013; Comalada et al., 2005; Farzaei et al., 2019; Gonzales and Orlando, 2008; Yang et al., 2001); (iii) inhibit the degradation of I κ B (EGCG, epicatechin, quercetin, apigenin, isoliquiritigenin) (Aneja et al., 2004; Farzaei et al., 2019; Mackenzie et al., 2004; Min et al., 2007; Wheeler et al., 2004); (iv) inhibit the nuclear translocation of NF κ B (quercetin, isoliquiritigenin) (Farzaei et al., 2019; Min et al., 2007); (v) block the DNA binding of NF κ B (EGCG, epicatechin, quercetin, apigenin) (Chen et al., 2005; Farzaei et al., 2019; Ichikawa et al., 2004; Mackenzie et al., 2004).

Another interesting pathway involved in inflammatory response is the so-called “mitogen-activated protein kinases (MAPKs) cascade” (Karin, 2005, 1995; Khan et al., 2006) (**Figure 1.4.2.4^{II-B}**). MAPKs are proteins belonging to Ser/Thr kinases, which regulate various cellular processes *via* modulation of gene expression in response to specific stimuli (Santangelo et al., 2007). In mammals, four groups of MAPKs have been identified: extracellular signal-related kinases (ERK)-1/2, c-Jun amino-terminal kinases (JNK)-1/2/3, p38-MAPK(α - δ) and ERK5. Each one is activated *via* phosphorylation by specific MAP kinase kinases (MAPKKs) (MEK1/2, MKK4/7, MKK3/6 and MEK5, respectively). Each MAPKK is, in turn, phosphorylated and activated by MAP kinase kinase kinases (MAPKKKs) (Chang and Karin, 2001). It has been reported that polyphenols play a role in modulation of the MAPK pathway, acting at different levels (Chen et al., 2004). In particular, polyphenols such as kaempferol, chrysin, apigenin, luteolin, quercetin, catechin, cyanidin-3-O-

glucoside, EGCG have shown to exert inhibitory activities on different MAPKs of the MAPK cascade, resulting in reduced transcription of inflammatory cytokines (Farzaei et al., 2019; Santangelo et al., 2007).

This evidence is corroborated by *in vivo* studies (both animal-based studies and clinical trials) which demonstrate that chronic administration of various polyphenol compounds (such as quercetin, curcumin, resveratrol, gingerols, isoflavones, procyanidins, oleuropein) significantly reduced the levels of pro-inflammatory biomarkers, including TNF α , IL-1, IL-4, INF γ . Interestingly, the expression of these pro-inflammatory genes is mainly mediated by both I κ B/NF κ B and MAPK signalling pathways (Farzaei et al., 2019; Jayarathne et al., 2017; Lozano-Castellón et al., 2020; Rosa et al., 2012; Zhao et al., 2017). This suggests that the ability of polyphenols to modulate these two key pathways represents one of the main mechanisms of action for their anti-inflammatory activity.



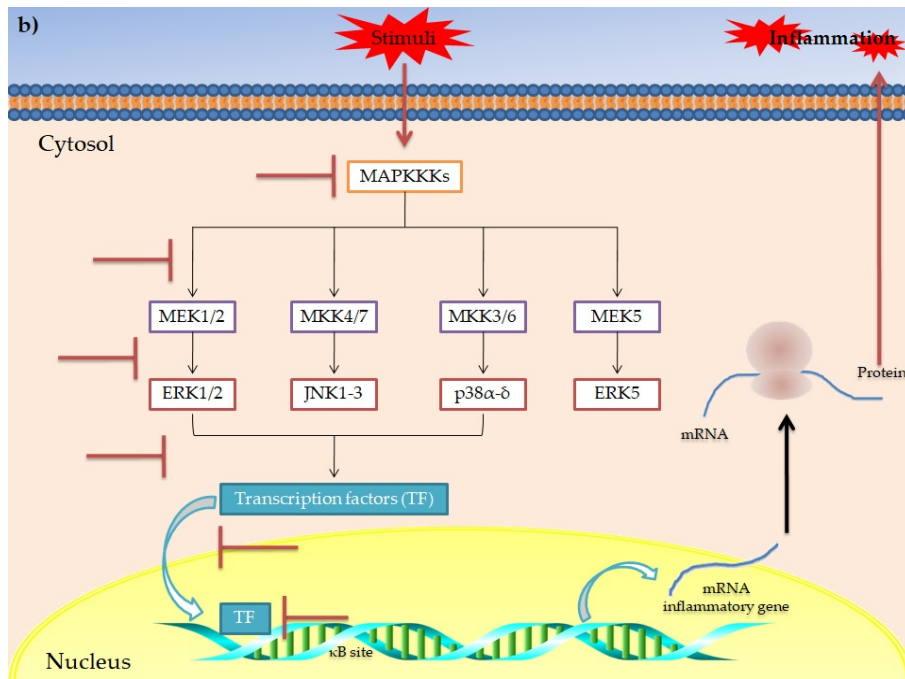


Figure 1.4.2.4ⁱⁱ. Main mechanisms of action for the anti-inflammatory activity of polyphenols in obesity. Schematic representation of the main putative targets of polyphenols in I κ B/NF κ B (a) and MAPK signalling pathways (b) involved in the inflammatory response. The symbol  indicates the targets inhibited/blocked by polyphenols [source: (Deledda et al., 2021)]

2. Taurisolo® nutraceutical formulation

Taurisolo® is a supplement consisting of a polyphenol extract obtained from *Aglianico* cultivar grape, collected during the autumn 2016-2020 harvest. Preliminary studies have been conducted in the NutraPharmaLabs laboratories of the Department of Pharmacy, University of Naples Federico II (Naples, Italy) in order to provide a pilot nutraceutical formulation. Once consolidated the entire productive method, the large-scale production was accomplished by MBMed Company (Turin, Italy).

2.1 *Productive process. The use of microencapsulation as a strategy to enhance the polyphenol bioaccessibility and bioavailability*

To obtain the polyphenol extract, grapes were extracted with water (50 °C), and the solution was filtrated and concentrated and underwent a spray-drying process with maltodextrins as support (5-15%), obtaining a fine microencapsulated powder.

Microencapsulation is a historically-known technological process (Luzzi, 1970; Sliwka, 1975), largely used in the pharmaceutical industry in order to incorporate various compounds into different wall materials, improving their delivery (Annunziata et al., 2020a). Technically, microencapsulation is defined as a “*packaging process by which liquids, solids or gaseous substances are incorporated in microscopic capsules that can measure from millimetre to micrometre, consisting on continuous films of coating materials*” (Annunziata et al., 2020a).

The scientific research in the pharmaceutical technology field developed a large number of techniques to produce stable microencapsulated formulations, including coaservation, ionic gelation, solvent evaporation, lyophilisation and spray-drying (Annunziata et al., 2020a), using different coating materials (Figure 2.1¹).

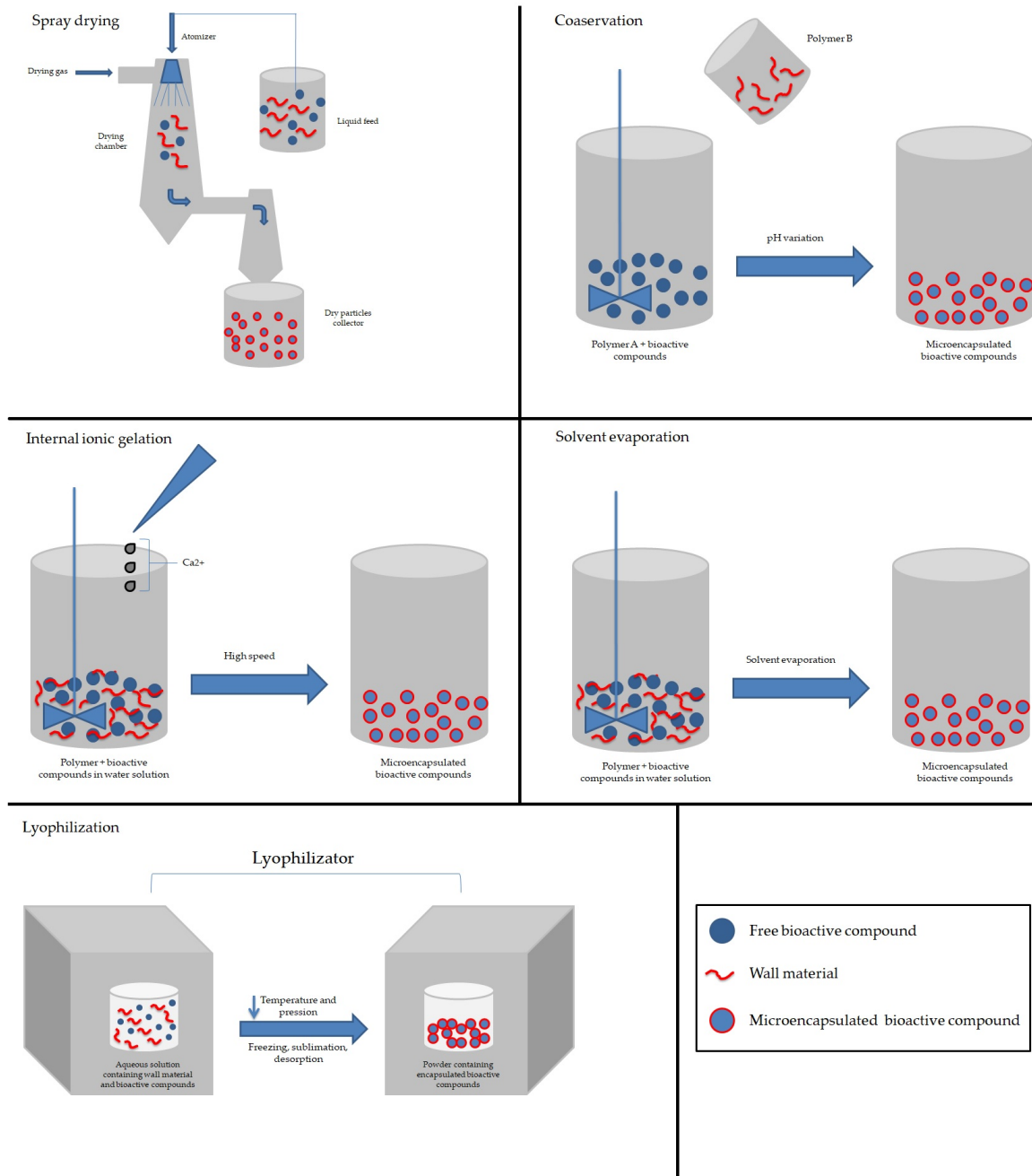


Figure 2.1¹. Some of the main microencapsulation methods schematically represented that are generally used in the nutraceutical and functional food industry [source: (Annunziata et al., 2020a)].

Spray-drying has been used for the production of Taurisolo®. It is undoubtedly, however, that since the final product is intended for human uses, for the microencapsulation processes food-grade and no-toxic solvents and wall materials shall be used (Nazzaro et al., 2012; Ozkan et al., 2019).

Spray-drying is a microencapsulation technique based on the atomization of a liquid solution (containing both the core and the wall material) by a hot drying gas stream included into an injector; the final product obtained is a dry powder (Gharsallaoui et al., 2007; Ozkan et al., 2019). More specifically, the liquid solution is injected into a drying vessel through a nozzle or an atomizer, producing small droplets followed by solvent evaporation (Fatnassi et al., 2013). For this technique various kinds of coating materials can be used, including polysaccharides (i.e. maltodextrins, cyclodextrins and gum arabic), proteins (i.e. soybean proteins, whey proteins and sodium caseinate), chitosan, gelatin and modified starch (Ozkan et al., 2019). The most suitable coating material is established on the base of both its physico-chemical properties and interaction created with the compounds constituting the core material (Annunziata et al., 2020a). In general, cyclodextrins or maltodextrins are used for microencapsulation of polyphenols. Despite the different chemical structures of cyclodextrins and maltodextrins, it can be hypothesised that spray-drying process may induce a modification of the maltodextrin conformation, passing from a linear to a circular structure that mimics that of cyclodextrins, allowing the incorporation of polyphenols (Annunziata et al., 2020a).

In the last decades, microencapsulation has been used also in the nutraceutical industry for the production of supplements and functional foods, as useful strategy to counteract various limits of natural bioactive compounds, such as scarce storage and stability, unpleasant flavour, low water solubility (**Figure 2.1ⁱⁱ**).

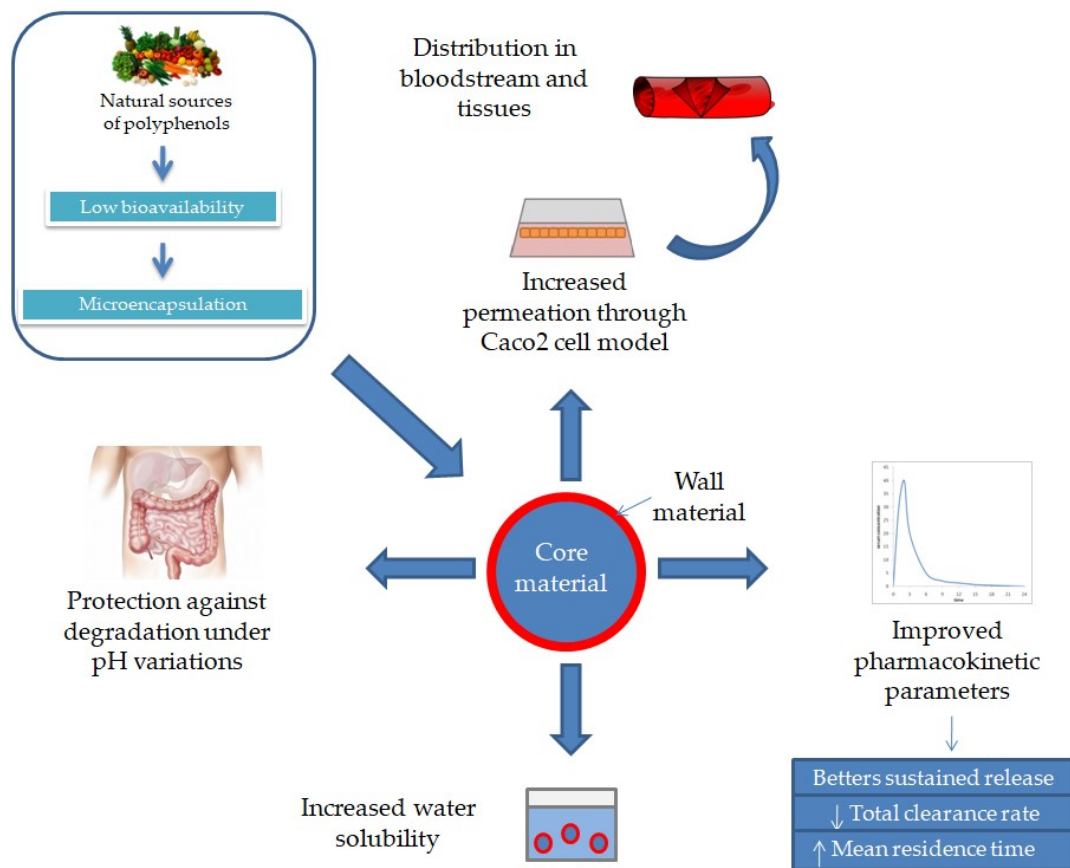


Figure 2.1^{II}. Advantages of microencapsulation. Since polyphenols are characterised by a very low bioaccessibility, due to several factors, the microencapsulation is designed as a strategy to ameliorate this pivotal feature of bioactive compounds. It increases the water solubility of polyphenols and offers protection against biochemical and physicochemical variation occurring during the transit into the gastrointestinal tract. This also allows to increase the intestinal absorption and the consequent distribution in bloodstream and tissues. Overall, the microencapsulation may be considered as a tool to improve the pharmacokinetics of polyphenols [source: (Annunziata et al., 2020a)].

Among these, low stability and water solubility are crucial issues since they are main factors at the basis of the typical low bioavailability (as described in section 1.5.2).

It appears clear, thus, that microencapsulation is a useful tool to enhance the water solubility of polyphenols (resulting in increasing bioaccessibility) and protect them during the digestive processes (resulting in increasing bioavailability) (Cohen et al., 2011; S. Wang et al., 2015). Interestingly, it has been reported that microencapsulation prolongs the intestinal permanence of bioactive substance *via* mucoadhesion and promotes their endocytosis (des Rieux et al., 2006), resulting in increasing absorption across the gut barrier (Hu et al., 2017).

As aforementioned, Taurisolo® is a supplement consisting of grape polyphenol extract microencapsulated in maltodextrins *via* spray-drying process. Scanning Electron Microscopy (SEM) analyses have been performed in to verify the formation of microencapsulation after the spray-drying process, as shown in **Figure 2.1^{III}** (Annunziata et al., 2019c).

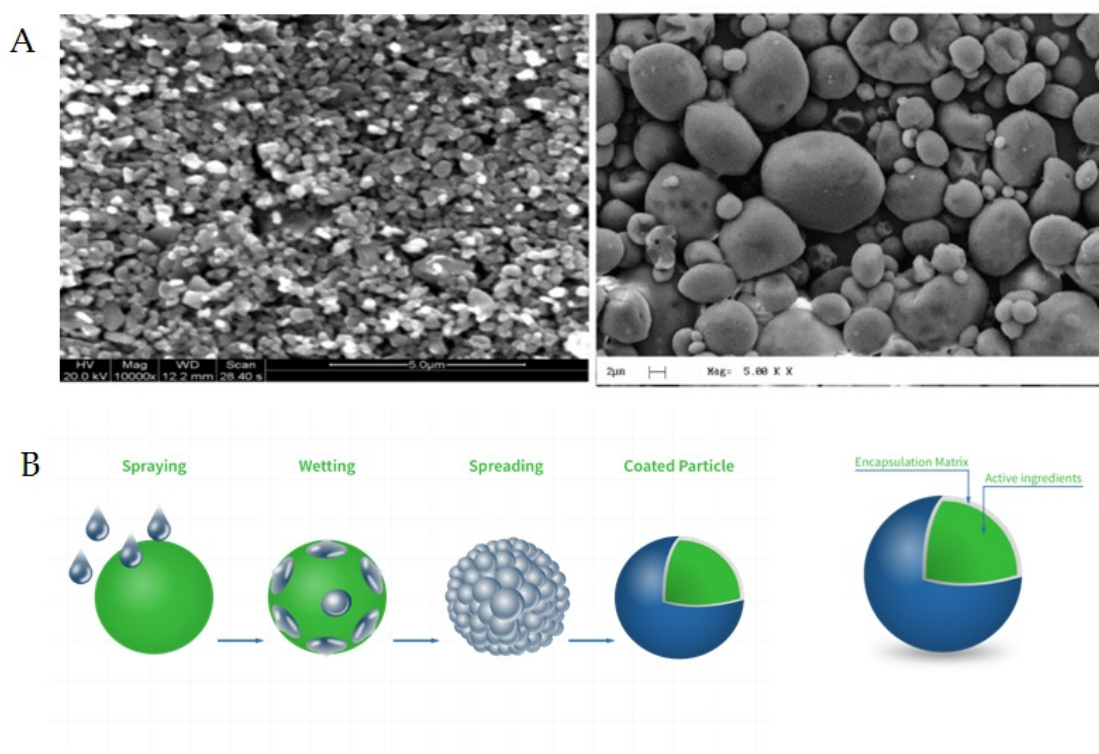


Figure 2.1^{III}. Microencapsulation of grape polyphenolic extract with maltodextrins. (A) Representative microphotographs of the Taurisolo® ultrastructure obtained by SEM analysis. (B) Graphical representation of the microencapsulation after spray-drying process. SEM, Scanning Electron Microscopy [source: (Annunziata et al., 2019c)].

Also, in order to evaluate the intestinal bioaccessibility, both acid-resistant and non-acid-resistant capsules containing Taurisolo® have undergone an *in vitro* simulated GI digestion, according to the method of Annunziata and co-workers (Annunziata et al., 2018a) (methods are detailed in **Appendix A**), followed by High-Performance Liquid Chromatography-diodearray detector (HPLC-DAD, Jasco Inc., Easton, MD, USA). As shown in **Figure 2.1^{IV}**, after *in vitro* GI digestion, the loss of polyphenols was less with acid-resistant (3.7%) than with non-acid resistant formulation (17%) (Annunziata et al., 2019c), suggesting that the use of acid-resistant forms, in combination with the microencapsulation, is a valid strategy to deliver bioactive compounds to the gut, protecting them from the GI digestion.

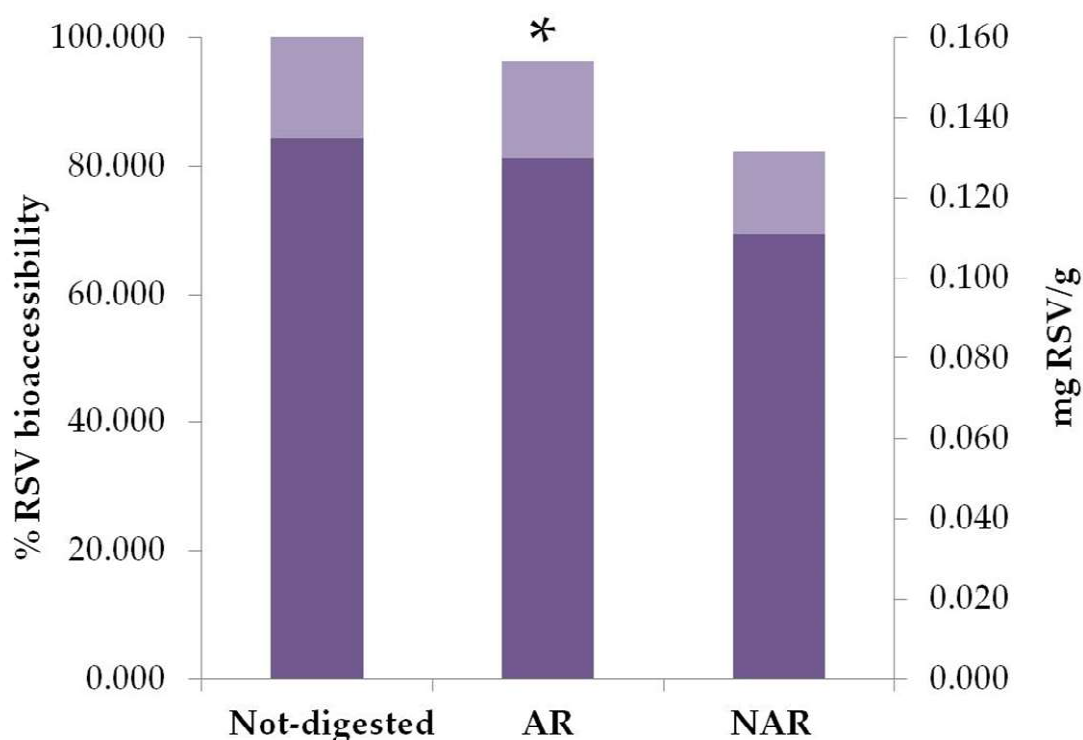


Figure 2.1^{IV}. Intestinal bioaccessibility of RSV contained in Taurisolo® after *in vitro* gastrointestinal digestion on AR and NAR capsules. Data are expressed as mean values in mg RSV per g of extract, and percentage of RSV intestinal bioaccessibility. Statistic significance are calculated by Student’s t-test: * $P = 0.0002$, AR bioaccessibility vs. NAR bioaccessibility. **Abbreviations:** RSV, Resveratrol; AR, Acid-resistant capsule; NAR, Non acid-resistant capsule [source: (Annunziata et al., 2019c)].

2.2 Chemical profile

The polyphenol profile of Taurisolo® before and after *in vitro* simulated GI digestion was evaluated by HPLC-DAD analysis using the method described by Giusti and coworkers (Giusti et al., 2017) (methods are detailed in **Appendix A**). The main polyphenols are reported in **Table 2.2^I**.

Table 2.2^l. High Performance Liquid Chromatography-diode-array detector (HPLC-DAD) analysis of the main polyphenols contained in Taurisolo[®], before and after *in vitro* simulated gastrointestinal digestion. Values are expressed in $\mu\text{g/g}$ Taurisolo[®] \pm standard deviation of three repetitions.

Compound	Mean value ($\mu\text{g/g}$) \pm SD	
	Taurisolo [®]	Digested Taurisolo [®]
Ferulic acid	14.59 \pm 0.98	1.92 \pm 0.11
Resveratrol	12.55 \pm 0.02	0.245 \pm 0.004
Caffeic acid	35.00 \pm 3.00	n.d.
<i>p</i> -cumaric acid	122.75 \pm 2.77	n.d.
Rutin	98.81 \pm 7.31	20.82 \pm 0.20
Quercetin	135.41 \pm 4.69	n.d.
Procyanidin B1 dimer	946.33 \pm 55.20	116.72 \pm 0.52
Procyanidin B2 dimer	645.89 \pm 59.17	169.16 \pm 0.77
Syringic acid	310.95 \pm 0.01	122.57 \pm 0.55
Epicatechin	1696.55 \pm 109.60	1.38 \pm 0.02
Gallic acid	199.46 \pm 4.59	n.d.
Catechin	2499.04 \pm 307.41	77.95 \pm 0.29

2.3 Pharmacokinetic

As previously discussed, polyphenols are characterised by a typical low bioavailability, due to their chemical features. This is a major concern for the nutraceutical industry since, to be effective, after oral administration bioactive compounds should easily reach the bloodstream in optimal concentrations in order to exert their pharmacological activities. The pharmacokinetic profile of nutraceuticals, thus, plays a central role in evaluation of its biological activity. In this sense, the use of specific pharmaceutical technologies (including microencapsulation of bioactive compounds and/or the acid-resistant pharmaceutical forms) is a successful strategy. Pharmacokinetic studies confirmed that microencapsulated polyphenols have a higher absorption rate (mainly evaluated *in vitro* using a Caco-2 monolayer) than free polyphenols (Almeida et al., 2009; Kulandaivelu and Mandal, 2017; Li et al., 2015; Narayanan et al., 2009; Sanna et al., 2013; Singh and Pai, 2014; Yi et al., 2013; Zu et al., 2016).

The pharmacokinetic profile of Taurisolo[®] was evaluated both in human both in acute and chronic (4-week treatment period). Particularly, for the acute study, study participants were administered with 600mg Taurisolo[®] in acid-resistant capsules and blood samples were collected before (time collection: 0 min) and after the administration, at different timepoints (30, 60, 120 and 240 min). Both serum and whole blood concentration of resveratrol were quantified *via* HPLC-DAD analysis. As reported in **Table 2.3^l**, and graphically in **Figure 2.3^l**, 1h after the oral administration, the maximum levels of resveratrol were detected both in serum and whole blood (49.0 \pm 0.55 and 14.2 \pm 0.40 ng/mL, respectively). For the chronic study, serum resveratrol levels were quantified after 4-week treatment with 300mg Taurisolo[®] twice daily. As shown in **Table 2.3^l**, after chronic treatment serum levels of resveratrol were 7.50 \pm 0.04 ng/mL, whereas at time '0 min',

serum polyphenol levels were not-detected (Annunziata et al., 2019c). It can be speculated that the 60-min serum peak of Taurisolo® polyphenols might be due to use of microencapsulation that improves their bioavailability, resulting in a rapid absorption across the intestinal mucosa, reaching the bloodstream.

Table 2.3¹. Pharmacokinetic profile of Taurisolo® [source: (Annunziata et al., 2019c)]

Sample	Time collection	RSV content
		Mean value \pm SD
Serum	0 min	n.d.
	30 min	5.55 \pm 0.02 ^a
	60 min	49.0 \pm 0.55 ^b
	120 min	3.99 \pm 0.04 ^c
	240 min	2.90 \pm 0.06 ^d
Blood	0 min	n.d.
	30 min	10.6 \pm 0.33 ^e
	60 min	14.2 \pm 0.39 ^f
	120 min	8.13 \pm 0.05 ^g
	240 min	7.98 \pm 0.04 ^h
Serum	4 weeks	7.50 \pm 0.04 ⁱ

RSV content quantified in serum and whole blood samples of participants in acute and chronic Taurisolo® administration. Values are expressed in ng per ml of serum or whole blood \pm standard deviation of three repetitions.

^{a,b,c,d,e,f,g,h,i} Mean values with different superscript letters are significantly different by Tukey-Kramer multiple comparison test. n.d.: not detected

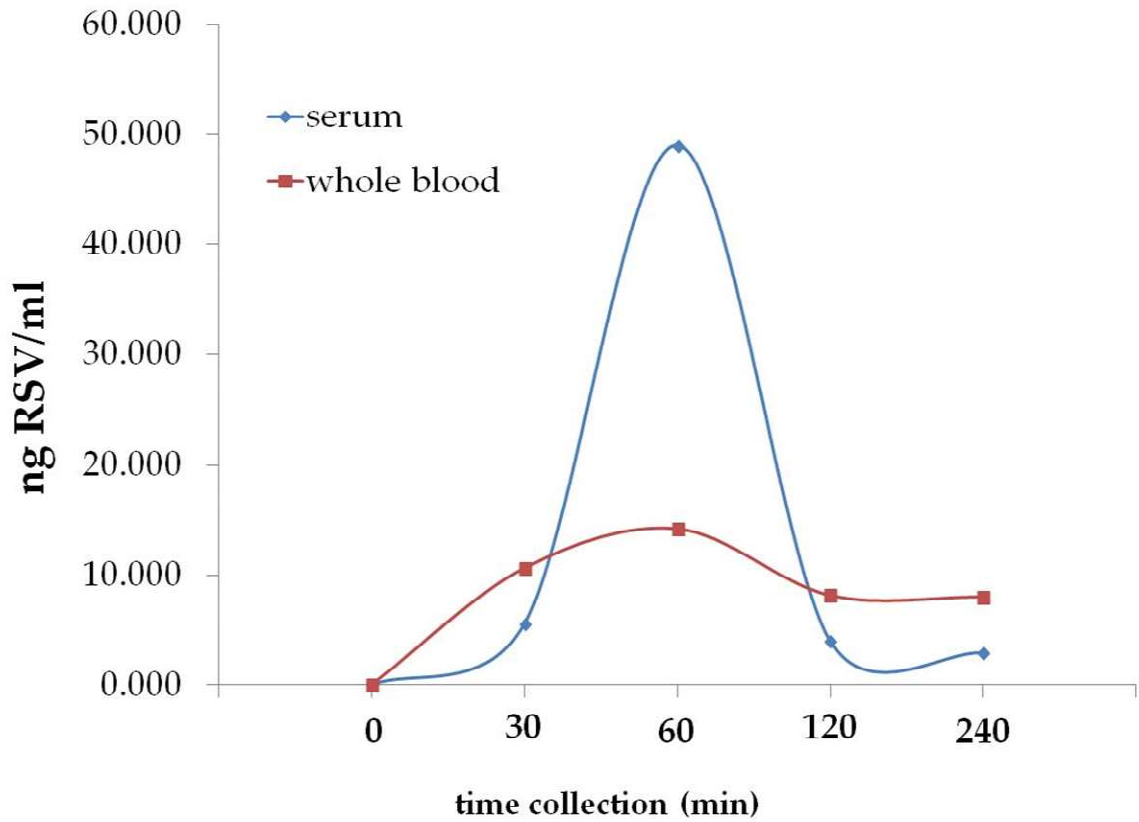


Figure 2.3^l. Bioavailability of RSV in acute. RSV levels evaluated in serum and whole blood samples before (time 0) and after (30, 60, 120 and 240 min) the administration of 2 AR capsules containing 300 mg Taurisolo®. In both serum and whole blood the maximum levels of RSV (49.0 ± 0.55 and 14.2 ± 0.40 ng/ml, respectively) were detected 60 min after the nutraceutical administration [source: (Annunziata et al., 2019c)].

3. Antioxidant activity of Taurisolo®

As described in the previous section, Taurisolo® is a polyphenol rich nutraceutical formulation. Since the literature widely described the ability of polyphenols to contrast OxS (as aforementioned in previous sections), evaluation of the antioxidant activity of Taurisolo® was among our first scopes. This was accomplished performing several studies, as summarized in **Table 3¹**.

Table 3¹. Studies investigating the antioxidant activity of Taurisolo®

Type of study	Experimental model	Main results	References
<i>In vitro</i>	Spectrophotometric assay (DPPH and ABTS assays)	acid-resistant formulation has higher antioxidant activity than non-acid-resistant	(Annunziata et al., 2021)
<i>Ex vivo</i>	Human peripheral blood cells	<ul style="list-style-type: none"> ➤ reduced ROS production ➤ reduced activity of endogenous antioxidant enzymes (in cell medium) ➤ increased intracellular activity of endogenous antioxidant enzymes ➤ reduced oxidative damage 	(Annunziata et al., 2021)
<i>Animal-based</i>	Aged rats	<ul style="list-style-type: none"> ➤ increased antioxidant capacity in muscle sample ➤ increased activity of antioxidant enzymes in muscle sample ➤ reduced lipid and protein oxidative damage in muscle sample ➤ increased expression of antioxidant genes 	(Annunziata et al., 2020b)*
<i>Clinical trial</i>	Human	<ul style="list-style-type: none"> ➤ reduction of oxLDL serum levels 	(Annunziata et al., 2019b)
<i>Clinical trial</i>	Human	<ul style="list-style-type: none"> ➤ reduction of oxLDL and DROMs serum levels 	Article in press

* This study is described in detail in section 5.3.2

The *in vitro* antioxidant activity of Taurisolo® was evaluated before and after simulated gastrointestinal digestion with DPPH and ABTS spectrophotometric assays. Methods are detailed in **Appendix A**. The *in vitro* gastrointestinal digestion was performed on both acid-resistant (AR) and non-acid-

resistant (NAR) capsules containing Taurisolo[®]. Results, expressed in mmol Trolox Equivalent/g and reported in **Table 3ⁱⁱ**, indicate that AR formulation represent a valid and effective strategy to preserve the biological activity of polyphenols against degrading agents during the gastrointestinal digestion (i.e. pH variations, digestive enzymes).

Table 3ⁱⁱ. Antioxidant activity of Taurisolo[®] evaluated by DPPH and ABTS assays. Values are expressed in mmol TE/g \pm SD of three repetition (**unpublished data**)

Sample	DPPH	ABTS
Not digested	3.67 \pm 0.55	3.47 \pm 0.11
AR duodenal phase	2.55 \pm 0.76	2.33 \pm 0.66
NAR duodenal phase	0.67 \pm 0.07	0.55 \pm 0.12

Further *in vitro* studies have been conducted to elucidate the main putative mechanism of action for the antioxidant activity of Taurisolo[®] in biological systems. In particular, in a study conducted during the internship at the Research Group in Community Nutrition and Oxidative Stress and Health Research Institute of the Balearic Islands (IdISBa), University of Balearic Islands, Palma de Mallorca (Spain) as required by this PhD program, we tested the antioxidant activity of Taurisolo[®] on human peripheral blood cells. More specifically, we tested the efficacy of Taurisolo[®] (before and after *in vitro* simulated gastrointestinal digestion) on neutrophils from subjects with metabolic syndrome (MetS) demonstrating its ability to reduce the production of ROS and the activities of antioxidant enzymes in the cell medium, suggesting that the extract was able to contrast the OxS in the external environment resulting in decreased cellular response needs. Interestingly, the intracellular enzymatic activities increased, suggesting a possible role of Taurisolo[®] polyphenols to activate specific nuclear factors, resulting in up-regulation of antioxidant gene expression. Moreover, we demonstrated the ability of Taurisolo[®] to reduce the levels of malondialdehyde (MDA), suggesting its role in prevention of cellular membrane-related OxS damage (Annunziata et al., 2021). Methods are detailed in **Appendix A**.

Study participants were middle-aged and on average overweight/obese. Anthropometric characteristics and metabolic and haematological parameters are reported in **Table 3ⁱⁱⁱ**.

Table 3^{III}. Characteristics of study participants [source: (Annunziata et al., 2021)]

Parameter	Mean ± SEM (n=17)
Age (years)	63.4± 10.9
<i>Anthropometric characteristics</i>	
Weight (kg) (n=16)	91.4±17.4
Height (cm) (n=16)	169.5±12.1
BMI (kg/m ²) (n=16)	31.6±3.14
<i>Metabolic parameters</i>	
Glucose (mg/dL)	103.2±27.5
Hb1A (%)	5.92± 1.23
Triglycerides (mg/dL)	200.6±31.7
HDL-cholesterol (mg/dL)	40.4±8.57
LDL-cholesterol (mg/dL) (n=15)	126.5±28.9
Cholesterol total (mg/dL)	197.1±40.3
Bilirubin (mg/dL) (n=6)	0.683±0.223
AST (U/L) (n=15)	21.2±4.02
ALT (U/L)	24.9±9.96
GGT (U/L)	39.1±31.4
PKC (mg/dL) (n=6)	0.770 ±0.310
<i>Haematological parameters</i>	
Hematocrit (%)	46.0±2.69
Erythrocytes (10 ⁶ /mm ³)	4.99±0.374
Leukocytes (10 ³ /mm ³)	7.83±1.63
Neutrophils (10 ³ /mm ³)	4.30±1.39
Lymphocytes (10 ³ /mm ³)	2.58±0.763
Basophils (10 ³ /mm ³)	0.063±0.038
Monocytes (10 ³ /mm ³)	0.648±0.189
Eosinophils (10 ³ /mm ³)	0.238±0.084
Platelets (10 ³ /mm ³)	218.7±62.5

Firstly, we evaluated *in vitro* the antioxidant activity of Taurisolo® through the FRAP assay, demonstrating a relatively high antioxidant capacity of 0.705±0.04 mM TE. Then, to evaluate the cytotoxicity we performed a MTT-test. The cell viability test revealed that Taurisolo® did not exert any cytotoxic effect at

concentrations ranging from 0.2 mg/mL to 2.0 mg/mL (**Figure 3^l**). The apparently dose-dependent increased cell viability might be explained by the 570 nm absorbance of polyphenols contained in our extract.

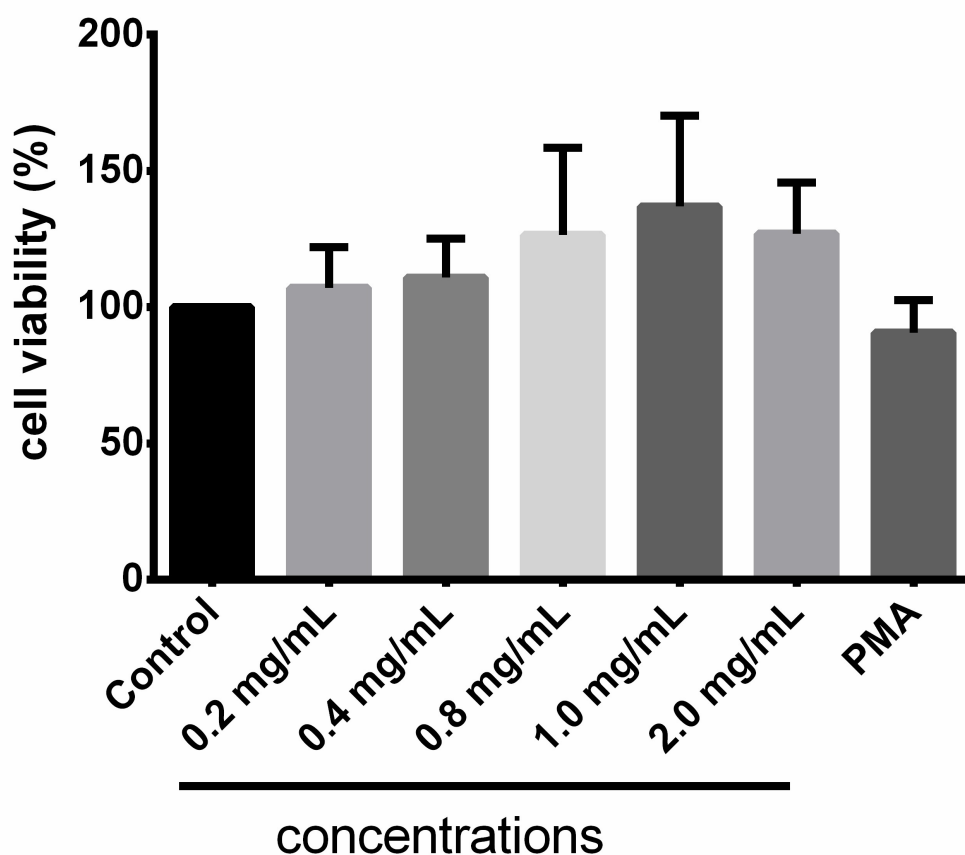


Figure 3^l. Cell viability test. Results are expressed as mean \pm SD of three repetitions [source: (Annunziata et al., 2021)]

Based on the MTT-test we decided to the concentration of 1.0mg/mL for the following experiments. We firstly investigated the ROS production. The levels of ROS were indirectly monitored via evaluation of hydrogen peroxide production in neutrophils incubated with/without Taurisol[®] in the presence or absence of PMA (**Figure 3^{ll}**). As expected, PMA significantly increased the ROS production compared to control (+1214.50%). On the contrary, the incubation with Taurisol[®] and digested-Taurisol[®] significantly reduced the ROS production in absence as well as in presence of PMA (Taurisol[®]: -81.60% compared to Ctr; PMA+Taurisol[®]: -80.23% compared to PMA; digested-Taurisol[®]: -48.86% compared to Ctr; PMA+digested-Taurisol[®]: -20.55% compared to PMA).

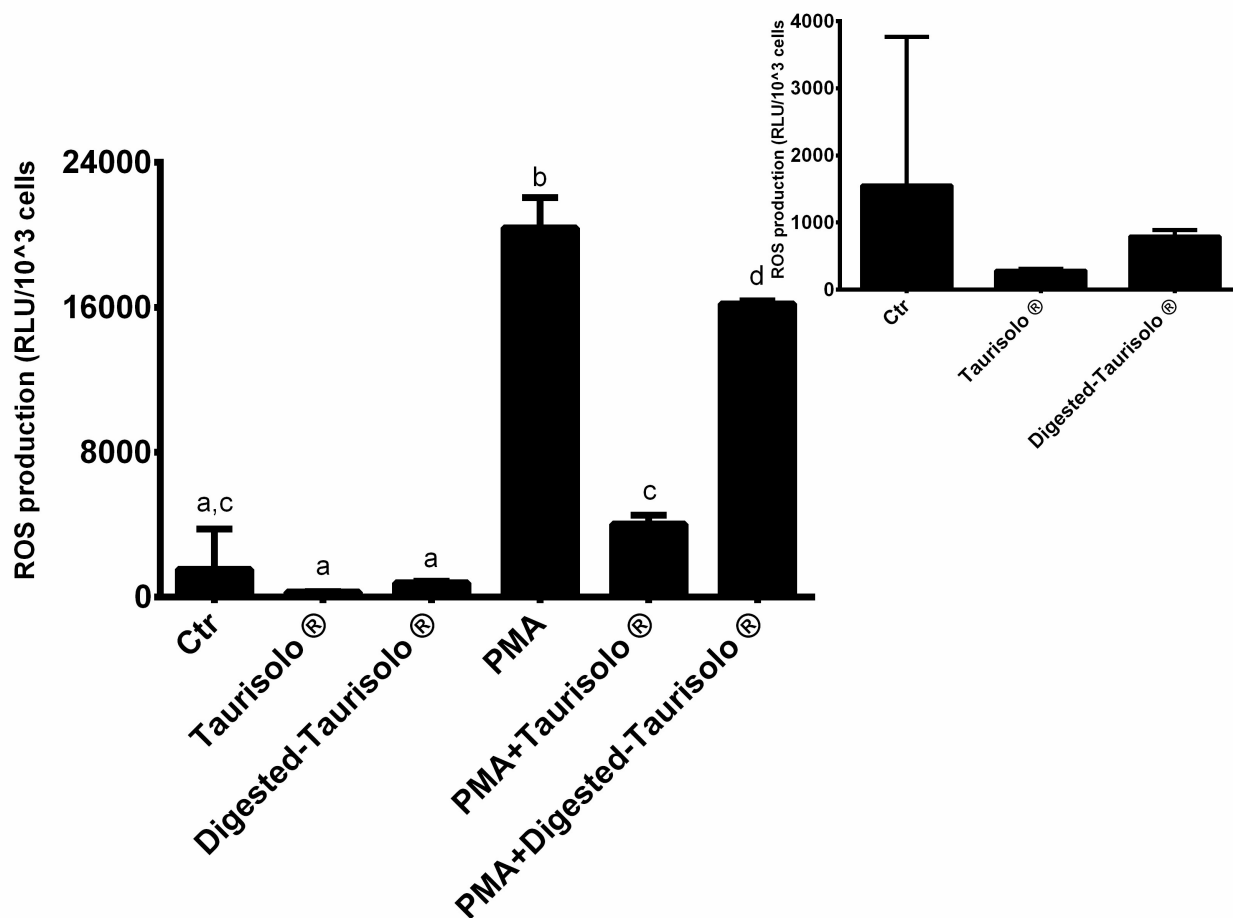


Figure 3^{II}. ROS levels monitored evaluating the production of hydrogen peroxide. Results are expressed as mean±SEM, and $p < 0.05$ was considered statistically significant. ANOVA one-way analysis. Different letters reveal significant differences [source (Annunziata et al., 2021)]

To evaluate the ability of Taurisolo® to modulate the endogenous antioxidant defences, we determined both the extracellular and intracellular enzymatic activities of catalase (CAT) and myeloperoxidase (MPO) (**Figure 3^{III}**). As expected, in extracellular media, PMA significantly increased the activity of both the enzymes when compared to control (+153.28% and +293.94%, CAT and MPO, respectively, $p < 0.001$ for all). On the contrary, the incubation with Taurisolo® and digested-Taurisolo® significantly reduced the enzymatic activities in presence of PMA (CAT = PMA+Taurisolo®: -45.28% compared to PMA, PMA+digested-Taurisolo®: -41.03% compared to PMA; MPO = PMA+Taurisolo®: -90.60% compared to PMA, PMA+digested-Taurisolo®: -62.80% compared to PMA). On the other hand, in intracellular media the trend was diametrically opposed. As shown, indeed, PMA significantly reduced the enzymatic activities of CAT and MPO (-47.43% and -85.46%, respectively), while the incubation with Taurisolo® and digested-Taurisolo® caused their increase (CAT = PMA+Taurisolo®: +86.17% compared to PMA, PMA+digested-Taurisolo®: +99.19% compared to PMA; MPO = PMA+Taurisolo®: +298.46% compared to PMA, PMA+digested-Taurisolo®: 181.54% compared to PMA).

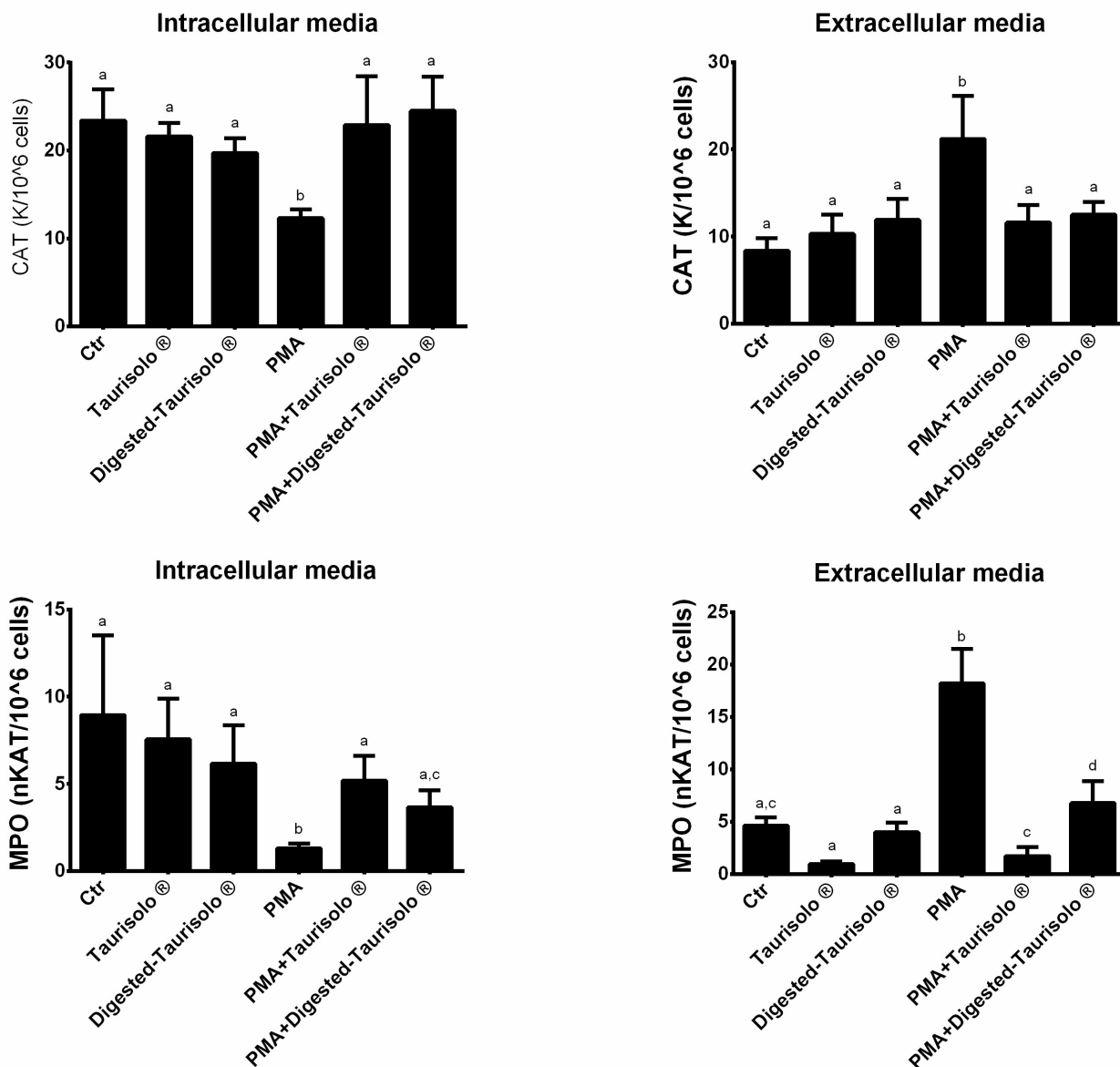


Figure 3^{III}. Enzymatic activities of CAT (a) and MPO (b). Results are expressed mean±SEM and $p < 0.05$ was considered statistically significant. ANOVA one-way analysis. Different letters reveal significant differences [source: (Annunziata et al., 2021)]

Finally, we evaluated the ability of Taurisolo® to prevent oxidative damage, we monitored the levels of malondialdehyde (MDA) as lipid peroxidation marker. As shown in **Figure 3^{IV}** PMA significantly increased MDA levels (+119.86% compared to control), while incubation with Taurisolo® and digested-Taurisolo® significantly reduced (PMA+ Taurisolo®: -52.65% compared to PMA; PMA+digested- Taurisolo®: -56.23% compared to PMA).

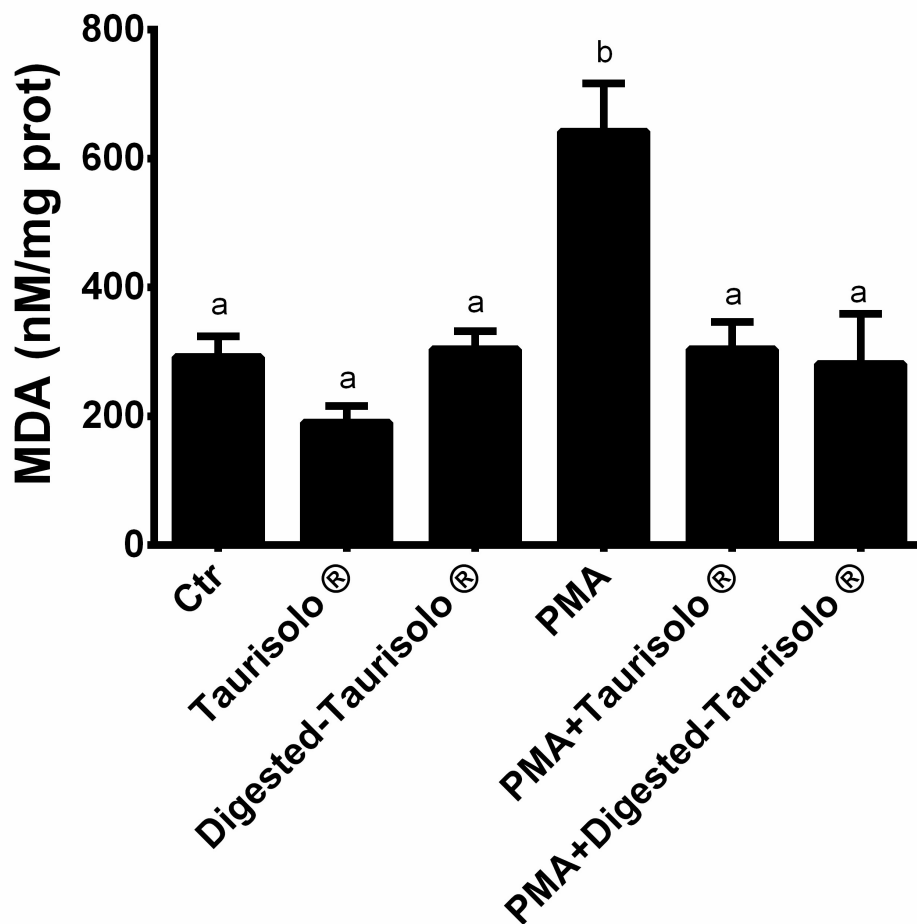


Figure 3^{IV}. Levels of MDA. Results are expressed as mean \pm SEM, and $p < 0.05$ was considered statistically significant. ANOVA one-way analysis. Different letters reveal significant differences [source: (Annunziata et al., 2021)]

The observed reduction of ROS levels is in line with a study conducted by our research group demonstrating ROS-reducing effect of intravenous and oral administration of Taurisolo® in a rat model of brain microvascular alteration induced by diminished cerebral blood flow and subsequent blood flow restoration. These promising results led us to investigate the potential mechanisms of action of Taurisolo® for its antioxidant effects and its role at blood level. For this reason, we decided to test the efficacy of our extract (both in digested and native forms) on human blood cells from subjects with MetS, in which both redox unbalance and inflammation affecting the cellular response and immune cells have been clearly demonstrated (Carrier, 2017; Devaraj et al., 2008; Holvoet, 2008; Khaybullina, 2017). Particularly, a typical feature in this class of subjects is the so-defined chronic low-grade inflammation, also characterized by increased circulating levels of ROS (Ellulu et al., 2017; Marseglia et al., 2015; McMurray et al., 2016). In this sense, as neutrophils are implicated in various anti-pathogen functions, including OxS and inflammation, we decided to use this cellular model to assess the efficacy of Taurisolo®.

As aforementioned, Taurisol[®] is a miscellanea of polyphenols with demonstrated antioxidant activity both *in vitro* and *in vivo*. This articulated polyphenol profile is responsible for the OxS-contrasting effect of Taurisol[®], as shown by its ferric reducing ability (FRAP assay) and free radical scavenging activity (reduction of ROS levels). As widely described in section 1.4.2.4, polyphenols act with both direct and indirect mechanisms in contrasting OxS that explain the ability of Taurisol[®] polyphenols to reduce the levels of ROS herein reported. In our experiments, Taurisol[®] treatment was shown to reduce the ROS levels in control cells, suggesting its ability to contrast the free radical accumulation also in basal conditions. However, to recreate a pathological condition, we stimulated neutrophils with PMA that activates them inducing an oxidative burst with consequent large production of ROS (Niwa et al., 1996). Also in presence of PMA, Taurisol[®] treatment drastically reduced the levels of ROS in the extracellular medium, suggesting its free radical scavenging potential both in normal and pathological conditions.

The increased levels of free radicals in the cellular medium may be considered as the main actor for activation of cell responses, resulting in release of antioxidant enzymes aimed to contrast the ROS accumulation, including CAT and MPO, which decompose H₂O₂ in H₂O before H₂O₂ reacts with metal ions generating hydroxyl radicals (Truong et al., 2018). This mechanism is supported by the observed marked increase in the enzymatic activities of CAT and MPO in the extracellular medium after stimulation with PMA. The PMA-induced neutrophils activation, indeed, causes the degranulation of these cells, with increased activity of MPO and CAT (Niwa et al., 1996). However, after treatment with Taurisol[®] we registered a marked decrease of the activities of these two enzymes. It can be speculated, thus, that the ROS-reducing effect of Taurisol[®]-polyphenols might be responsible for the reduced MPO and CAT enzymatic activities with or without the PMA stimulation, suggesting the ability of antioxidants to contrast the global oxidative stress in the culture medium that results in reducing the need to activate the intracellular defences for neutralization of the dangerous external environment.

Interestingly, when we analysed the enzymatic activities of CAT and MPO in the intracellular medium, we observed an inverse trend. In particular, in cells treated with PMA the activities of CAT and MPO were reduced, while they were increased when cells were treated with Taurisol[®]. This effect may be explained by the ability of polyphenols to modulate the endogenous antioxidant defence (Sandoval-Acuña et al., 2014). More specifically, there is evidence that polyphenols can increase the activities of antioxidant enzymes up-regulating the expression of related genes *via* activation of specific nuclear signalling pathways (Sandoval-Acuña et al., 2014; Tsuji et al., 2013). It has been reported, indeed, that grape-derived polyphenols activate nuclear factors, including nuclear factor-erythroid 2-related factor 2 (Nrf2) and forkhead box O (FOXO) and proliferator-activated receptor gamma coactivator 1 α (PGC-1 α), causing their nuclear translocation. This, in turn, results in enhancement of the expression of responding genes encoding for antioxidant enzymes. In contrast, there is evidence recognizing free radicals as stimuli for activation of the nuclear factor kappa-light-

chain-enhancer of activated B cells (NF- κ B), which nuclear translocation promotes the expression of OxS- and inflammation-related genes. Interestingly, grape polyphenols are capable to suppress the NF- κ B pathways, suggesting a further antioxidant and anti-inflammatory mechanism (Truong et al., 2018). These previously reported mechanisms may be used to explain the observed Taurisol[®]-induced increase of the antioxidant enzyme activities in intracellular medium both in basal condition or under PMA stimulation.

The different trend between the antioxidant enzymatic activities observed in extracellular and intracellular media led us to speculate a dual efficacy of Taurisol[®] in contrasting OxS: on one hand the ROS-reducing effect that results in improving the redox status of the external environment, reducing the needs of the cells to respond with their endogenous antioxidant systems; on the other hand, the intrinsic activation of the antioxidant defenses, probably *via* modulation of the related gene expression.

In summary, with this *ex vivo* study we demonstrated the elevated antioxidant potential of Taurisol[®] on human neutrophils from subjects with MetS. As shown in **Figure 3^v**, due to its antioxidant capacity, Taurisol[®] firstly acts as a ROS scavenger agent, reducing their levels in the extracellular medium. This, in turn, may be responsible for reduced activities of antioxidant enzymes in the same medium, as a result of improved redox status of the external environment with consequent reduction of the cell response need and oxidative damage. In addition, the observed increase of antioxidant enzyme activities in the intracellular medium might reflect the ability of Taurisol[®] polyphenols to up-regulate their gene expression.

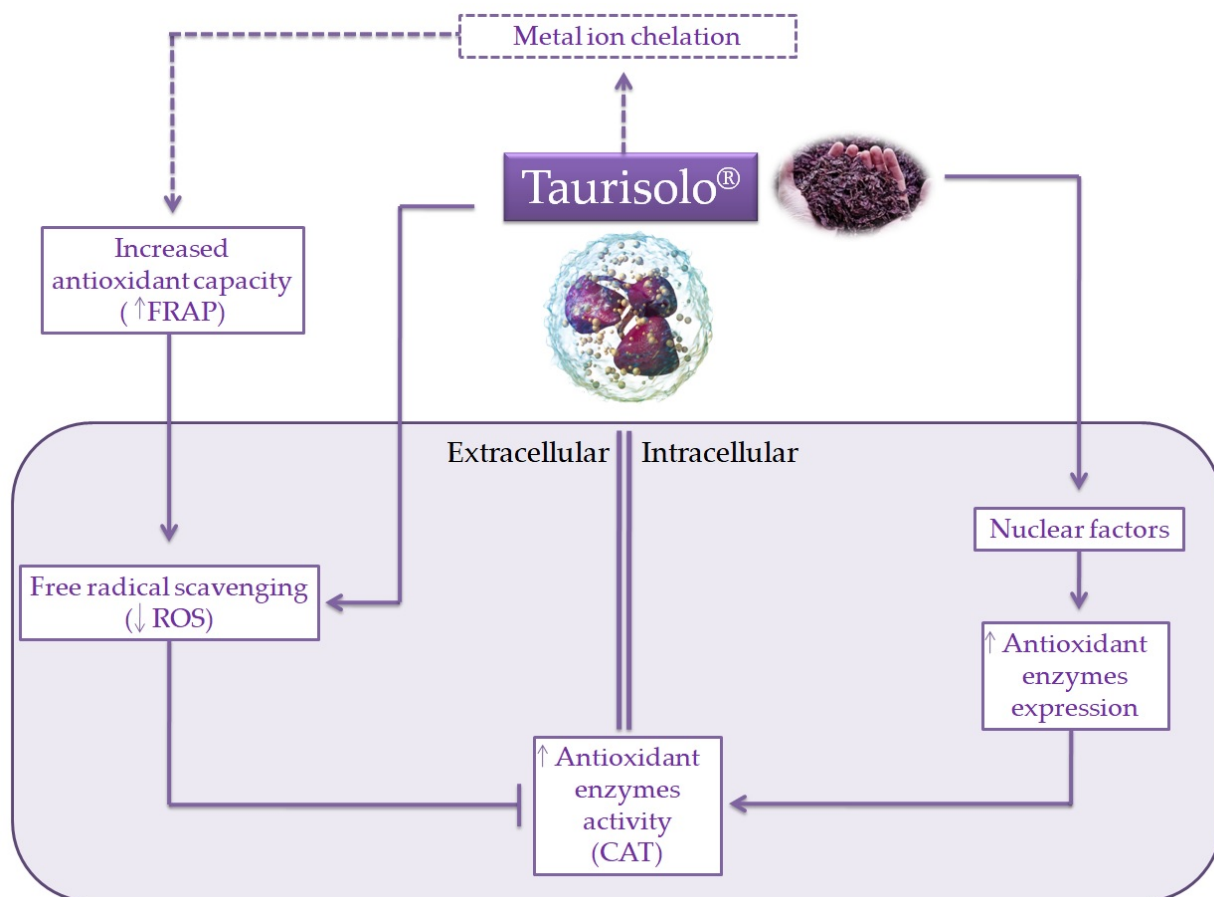


Figure 3^v. Schematic representation of the potential mechanisms of action of Taurisolo®. As a polyphenol-rich extract, Taurisolo® has a marked antioxidant capacity that, in addition to the metal ion chelation activity, acts as free radical scavenging agent, reducing the levels of ROS in the extracellular medium. This improvement of the redox status of the external environment results in reduced needs of the cell to activate their endogenous defences releasing antioxidant enzymes. At nuclear level, indeed, Taurisolo® polyphenols are able to interact with nuclear factors, resulting in enhancing the expression of antioxidant genes.
 — indicates the mechanisms directly observed; ---- indicates the mechanisms/pathways not directly observed, but reported in literature [source: (Annunziata et al., 2021)]

To confirm the antioxidant potential observed *in vitro* and *ex-vivo*, we conducted two randomized clinical trials (RCTs) monitoring the circulating levels of oxLDL and reactive oxygen metabolites (DROMs) after chronic treatment with Taurisolo® (Table 3^{IV}). Study population and designs are detailed in Appendix A and Appendix C.

Table 3^{IV}. RCTs investigating the antioxidant activity of Taurisolo®. Abbreviations: R, randomized; DB, double-blind; PC, placebo-controlled; PA, parallel-arm; CVD, cardiovascular diseases.

Study design	Population	Intervention	Main results	Reference
R, DB, PC, PA	65 overweight/obese subjects	Group A: 300mg Taurisolo® twice daily for 8 weeks Group B: 300mg Taurisolo®+300mg pectin twice daily for 8 weeks	Significant reduction of circulating oxLDL (group A: -76.06%, p=0.03 compared to baseline; group B: -74.02%, p=0.02 compared to baseline)	(Annunziata et al., 2019b)
R, DB, PC	108 subjects with CVD factors	400mg Taurisolo® twice daily for 8 weeks	Significant reduction of oxLDL and DROMs (-65.05% and -49.68%, respectively, p>0.0001 for all compared to baseline)	Article in press

The first RCT was conducted on a cohort of overweight/obese subjects chronically administered (8 weeks) with acid-resistant capsules containing Taurisolo® (300 mg per capsule) or Taurisolo®+pectin (300 mg+300 mg per capsule) twice daily. The study was designed as a 16-week monocentric, double-blind, randomized, placebo-controlled, 2-arm parallel-group trial: 4-week run-in period, 8-week intervention period and a 4-week follow-up period. During the run-in period, subjects were given placebo (maltodextrins). This study was listed on the ISRCTN registry (www.isrctn.com) with ID ISRCTN10794277 (doi: 10.1186/ISRCTN10794277). Serum levels of oxLDL were monitored after 12h of fasting at weeks 0, 4, 8, 12 and 16.

A total of 121 subjects were screened for eligibility; 90 were randomized, while 31 (25.6%) did not pass the screening stage. Selected patients were randomized into groups A and B. The study flow chart according to the CONSORT PRO reporting guideline (Calvert et al., 2013) is represented in Figure 3^{VI}.

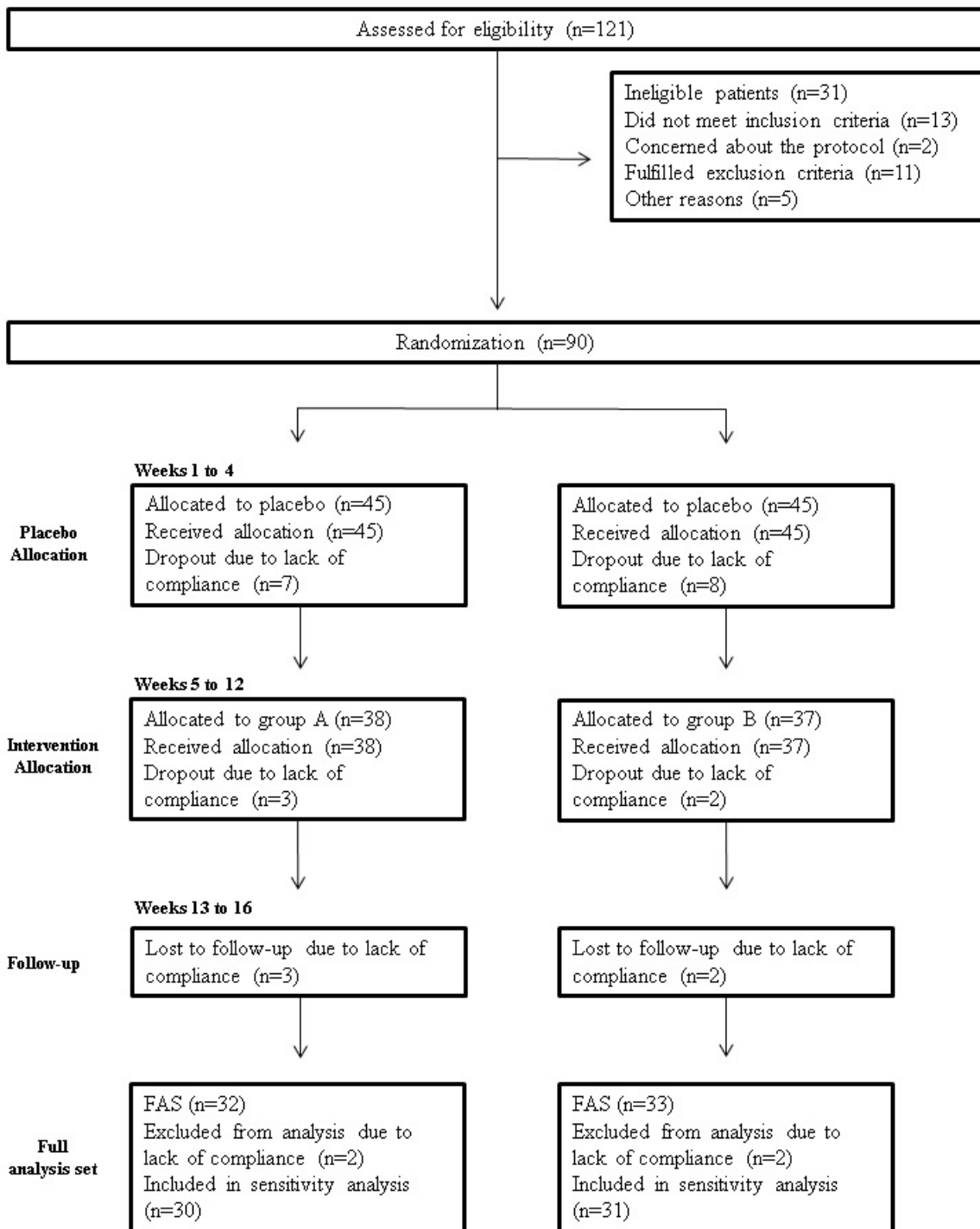


Figure 3^{vi}. Study flowchart according to the consolidated standards of reporting trials (CONSORT) [source: (Annunziata et al., 2019b)].

Baseline characteristics of study participant are reported in **Table 3^v**. As shown, no significant differences were evident between the two intervention groups. After the run-in period, during which participants were given placebo, no differences have been observed in the ox-LDL serum levels. In **Table 3^{vi}** are reported the effect of Taurisolo® or Taurisolo®+pectin on ox-LDL serum levels. In both intervention groups oxLDL serum levels significantly decreased (-76.06% $p = 0.03$ and -74.02% $p = 0.02$, group A and

group B, respectively). No significant differences have been reported between the two interventions after the 8-week treatment period ($p = 0.915$, group A *vs.* group B). After the 4-week follow-up period, the ox-LDL serum levels not significantly increased in both groups (23.85% and 25.83%).

Table 3^v. Baseline characteristics of study participants. No significant differences were evident between the two groups.* Values are expressed as mean \pm SD; statistical significance is calculated by Student's t-test. Abbreviations: BMI, body mass index; WC, waist circumference; HC, hip circumference; WHR, waist-to-hip ratio; SD, standard deviation; TMAO, trimethylamine N-oxide [source: (Annunziata et al., 2019b)].

Parameters	Group A	Group B	<i>p</i>-value
Gender (male (%))	57.14	55.00	$\chi^2 = 0.019, p = 0.890$
Age (years)*	65.14 \pm 10.46	64.50 \pm 11.84	0.855
Physical activity (yes, (%))	14.29	5.00	$\chi^2 = 1.003, p = 0.316$
Weight (kg)*	83.25 \pm 12.54	83.48 \pm 13.53	0.956
Height (m)*	1.64 \pm 0.10	1.63 \pm 0.11	0.732
BMI (kg/m ²)*	31.16 \pm 4.74	31.54 \pm 3.55	0.776
WC (cm)*	107.08 \pm 12.37	106.25 \pm 9.11	0.812
HC (cm)*	113.05 \pm 13.78	110.55 \pm 7.75	0.484
WHR*	0.95 \pm 0.11	0.96 \pm 0.07	0.604
Diabetes mellitus (yes (%))	47.62	45.00	$\chi^2 = 0.028, p = 0.866$
Hypertension (yes (%))	42.86	30.00	$\chi^2 = 0.729, p = 0.393$
Hypercholesterolemia (yes (%))	66.47	60.00	$\chi^2 = 0.196, p = 0.658$
Hypertriglyceridemia (yes (%))	4.76	10.00	$\chi^2 = 0.414, p = 0.520$
TMAO (μ M)*	3.52 \pm 2.95	3.44 \pm 2.04	0.926
Ox-LDL (μ Eq/L)	1041.21 \pm 406.76	941.54 \pm 316.01	0.754

Table 3^{vi}. ox-LDL serum levels of study participants before and after 2-month treatment. Value are expressed as mean \pm SD of three replicates. Decrement percentage between ox-LDL serum levels before and after 8-week treatment was shown. Statistical significance is calculated by Student's t-test. * $P = 0.915$, group A *vs.* group B (after treatment); # $P = 0.897$, group A *vs.* group B (after treatment) [source: (Annunziata et al., 2019b)].

	Ox-LDL serum levels				Δ (%)	<i>p</i> -value
	(μEq/L)					
	Run-in (placebo)	Before treatment	After treatment	Follow- up		
Group A	1102.33 \pm 398.43	1041.21 \pm 406.76	249.2 \pm 47.01	308.64 \pm 52.57	- 76.06	0.03
Group B	822.99 \pm 370.94	941.54 \pm 316.01	244.6 \pm 52.4*	307.76 \pm 100.77	- 74.02	0.02

Similarly, we conducted another RCT aimed to confirm the antioxidant potential of Taurisolo® in a larger cohort of subjects with various risk factors for CVD (n=108), including overweight/obesity, smoking, diabetes or hypertension. This study, conducted in collaboration with the Cardarelli Hospital of Naples (Italy) was designed as a randomised, placebo-controlled, double-blind clinical trial with duration of 14 weeks: 2-week run-in period (with administration of capsules containing only excipients as placebo), followed by 8 weeks of Taurisolo® treatment (400mg twice daily), and 4 weeks of follow-up (without any treatment). Serum levels of oxLDL and DROMs were monitored after 12h of fasting at weeks 0, 2, 6, 10 and 14.

A total of 188 subjects were screened for eligibility; 40 subjects did not pass the screening stage. Overall, 148 subjects were assigned to the group of intervention study. **Figure 3^{vii}** shows the flow of participants through the trials together with the completeness of diary information over the entire treatment period. A total of 37 subjects prematurely terminated study participation (10 during the run-in period and 27 during the intervention period). **Figure 3^{vii}** follows the CONSORT PRO reporting guideline.

Table 3^{viii} reports the demographic and clinical characteristics assessed at the baseline visit of all study participants. Overall, 61% of subjects were male and, on average, middle-aged and overweight. Type 2 diabetes mellitus (T2DM) and hypertension were the most diagnosed diseases among the study participants (26% and 36%, respectively), and for this reason they were considered in further analysis.

Serum levels of oxLDL and D-ROMs were monitored in all study participants at run-in, before starting Taurisolo® treatment (baseline), after 4-week Taurisolo® treatment, after 8-week Taurisolo® treatment and after 4-week follow-up (**Figure 3^{viii}**). oxLDL levels significantly reduced after 4-week Taurisolo® treatment, from 795.95 ± 186.74 $\mu\text{Eq/L}$ to 452.78 ± 100.72 $\mu\text{Eq/L}$ (-43.12%, $p < 0.0001$), and after 8-week Taurisolo® treatment (278.15 ± 24.48 μM , -65.05%, $p < 0.0001$). Similar trend was also observed for D-ROMs levels that significantly reduced after 4-week Taurisolo® treatment, from 477.08 ± 135.38 UCARR to 313.09 ± 96.70 UCARR (-34.37%, $p < 0.0001$), and after 8-week Taurisolo® treatment (240.07 ± 49.44 UCARR, -49.68%, $p < 0.0001$).

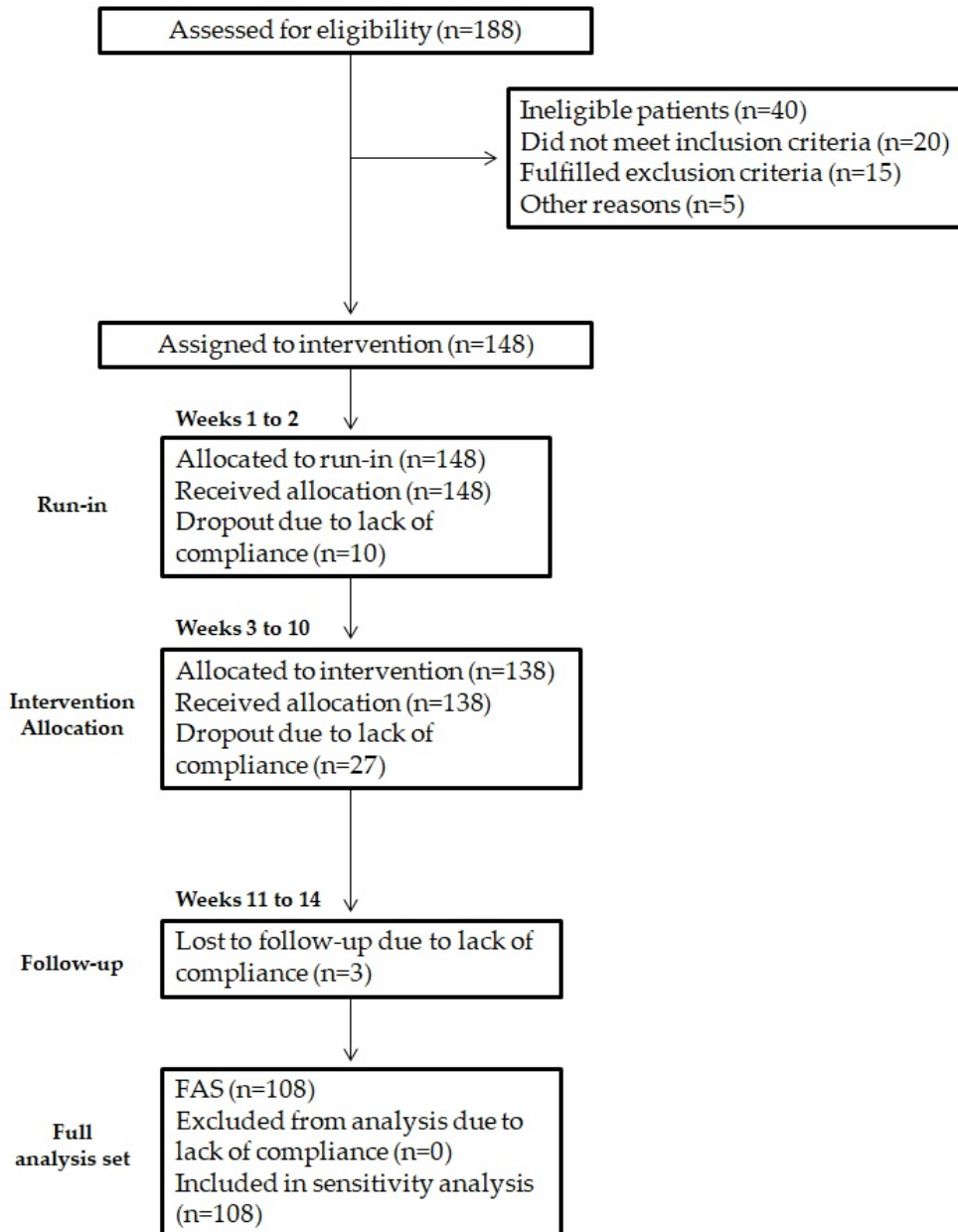


Figure 3^{vii}. Study flowchart. Study flowchart, according to the consolidated standards of reporting trials (CONSORT).

Table 3^{vii}. Baseline characteristics of study participants

Age (year)	60.94±13.55
Gender (M/F)	66/42
BMI (kg/m ²)	28.79±4.17
Smokers (yes (%))	51.54
Physical activity (yes (%))	32.47
T2DM (yes (n.))	28
Hypertension (yes (n.))	39
TMAO (μM)	2.19±2.30
oxLDL (μEq/L)	795.96±189.18
D-ROMs (UCARR)	477.08±135.38

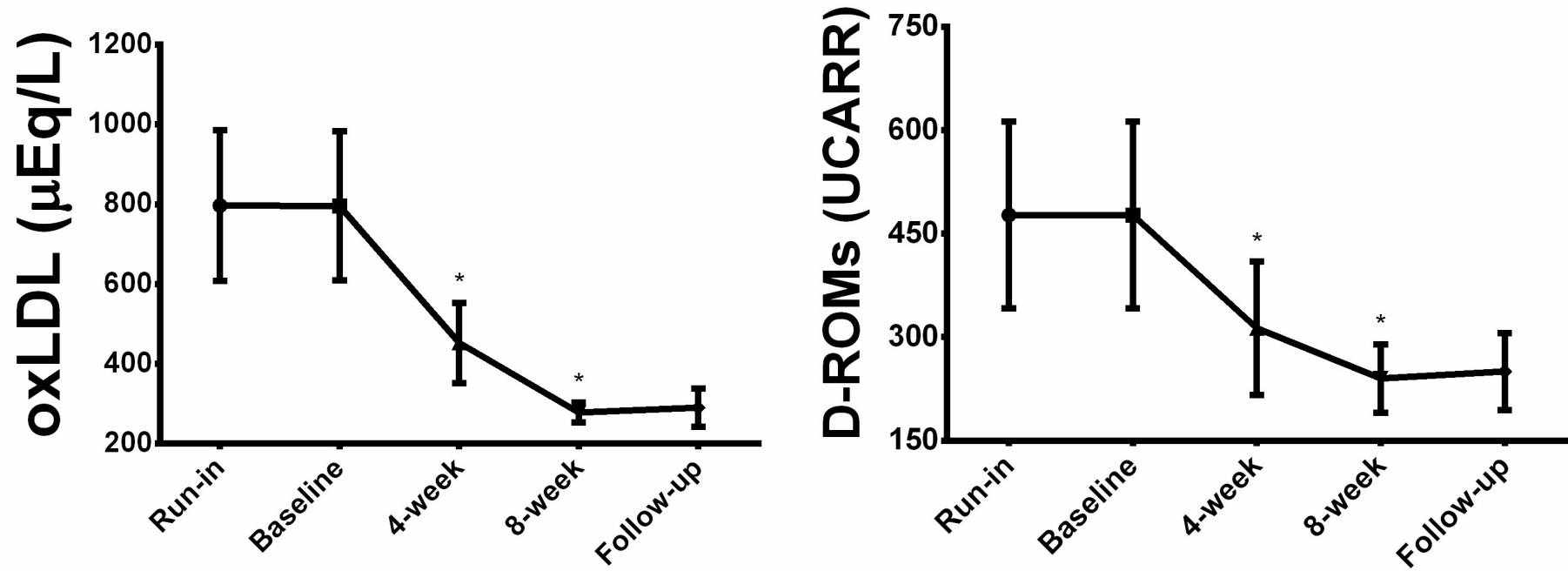


Figure 3^{VIII}. Graphical representation of the oxidative stress-related biomarkers serum levels at the different time points. Values are expressed as mean \pm standard deviation. Statistical significance was calculated with Student's t-test; p-value <0.05 was considered as significant. * $P < 0.0001$, compared to baseline.

In these two RCTs we observed an interesting activity of chronic treatment with Taurisolo® in reducing significantly the serum levels of OxS-related biomarkers (oxLDL and D-ROMs). Besides the well-established antioxidant potential of polyphenols, several studies reported the ability of polyphenols to contrast the LDL oxidizability (Chen et al., 2017; Suzuki-Sugihara et al., 2016). In particular, polyphenols act as hydrogen donors to α -tocopherol radicals, resulting in prevention of LDL oxidation (Zhu et al., 1999). Also, mechanistic studies reported that red wine polyphenols inhibited copper-catalyzed LDL oxidation (Frankel et al., 1993). In these studies, circulating oxLDL were monitored using the LP-CHOLOX test (Diacron, Grosseto, Italy), aimed to measure the levels of lipid peroxidation-derived hydroperoxides, mainly represented by oxidized cholesterol. According to the manufacturer's instructions, oxLDL levels are defined: normal (with values ≤ 599 $\mu\text{Eq/L}$), slightly high (with values ranging from 600 to 799 $\mu\text{Eq/L}$), moderately high (with values ranging from 800 to 999 $\mu\text{Eq/L}$) and very high (with values ≥ 1000 $\mu\text{Eq/L}$) (Macri et al., 2015; Mancini et al., 2017). In agreement with this classification, our results showed that a 8-week treatment with Taurisolo® significantly reduced serum levels of oxLDL in all study participants from a slightly high to normal level.

DROMs are stable and quantifiable oxygen metabolites produced from free radical attacks operated at the expense of biomolecules. The test used in the present study is based on the concept that, according to the Fenton's reaction, DROMs contained in a serum generate, in presence of iron, alkoxy (R-O^*) and peroxy (R-OO^*) radicals which, in turn, oxidize an alkyl-substituted aromatic amine, producing a pink-colored derivative ($[\text{A-NH}_2^*]^+$), photometrically quantified (Alberti et al., 2000; Cesarone et al., 1999; Gerardi et al., 2002; Trotti et al., 2001). DROMs, thus, are useful biomarkers of OxS, determined on the basis of the following ranges: (i) normal: 250-300 UCARR, (ii) border-line: 300-320 UCARR, (iii) low level of oxidative stress: 321-340 UCARR, (iv) middle level of oxidative stress: 341-400 UCARR, (v) high level of oxidative stress: 401-500 UCARR and (vi) very high level of oxidative stress: >500 UCARR, where 1 UCARR=0.08 mg $\text{H}_2\text{O}_2/\text{dL}$ (Alberti et al., 2000; Cesarone et al., 1999; Gerardi et al., 2002; Trotti et al., 2001). According to this classification, our results showed that chronic treatment with Taurisolo® significantly reduced OxS in all study participants, from a very high to normal level. Mechanisms reported in section 1.4.2.4 regarding the antioxidant activity of polyphenols, and more specifically the ROS production inhibition, may serve to explain the *in vivo* results herein reported. It is plausible that these as possible mechanisms since Taurisolo® polyphenols have a very high bioavailability, as previously described in section 2. The presence of Taurisolo® polyphenols (or their metabolites) into the bloodstreams allows speculating their possible involvement in chemical reactions with free radicals, ions, metals or other compounds involved in pro-oxidant processes.

4. Anti-atherosclerotic activity of Taurisolo®

As extensively described in section 1.2.3, TMAO plays a central role in development and progression of atherosclerotic disease. This intriguing knowledge drove our research group to investigate the TMAO-reducing activity of Taurisolo® as a potential mechanism for its anti-atherosclerotic effect. In particular, we conducted three RCTs, summarised in **Table 4¹**. Study design and protocol are detailed in **Appendix A** and **Appendix C**.

Table 4¹. RCTs investigating the TMAO-reducing activity of Taurisolo®. Abbreviations: R, randomized; DB, double-blind; PC, placebo-controlled; PA, parallel-arm; CO, cross-over; CVD, cardiovascular diseases.

Study design	Population	Intervention	Circulating TMAO reduction	Reference
R, DB, PC, CO	20 healthy subjects	300mg Taurisolo® twice daily for 4 weeks	-63.5%	(Annunziata et al., 2019c)
R, DB, PC, PA	65 overweight/obese subjects	Group A: 300mg Taurisolo® twice daily for 8 weeks Group B: 300mg Taurisolo®+300mg pectin twice daily for 8 weeks	Group A: -78.58% Group B: -76.76%	(Annunziata et al., 2019b)
R, DB, PC	108 subjects with CVD factors	400mg Taurisolo® twice daily for 8 weeks	Men: -80.59% Women: -71.22%	Article in press

The first study was conducted on healthy subjects aged 25-35 years randomly divided into two groups (active and placebo). The study followed a cross-over design consisting of 1-week run-in period, 4-week intervention period and 1-week washout period. During the intervention period, each subject was given 300 mg Taurisolo® in acid-resistant capsules or placebo (identically appearing capsules containing only maltodextrin) twice daily. Blood samples were collected after 12h of fasting at days 8, 35, 42 and 70.

A total of 27 subjects were screened for eligibility; 20 were randomised, while 7 (25.9%) did not pass the screening stage. The most common reasons were: 4 subjects did not meet the inclusion criteria at

baseline, 2 subjects did not fulfill exclusion criteria and 1 subject refused to participate for no specific reasons. Selected patients were equally divided into two subgroups. Each subject underwent a 7-day washout period before the 28-day intervention period, according to a crossover plan. All participants complete the study. In **Figure 4** is represented the flow chart of the study according to the CONSORT PRO reporting guideline.

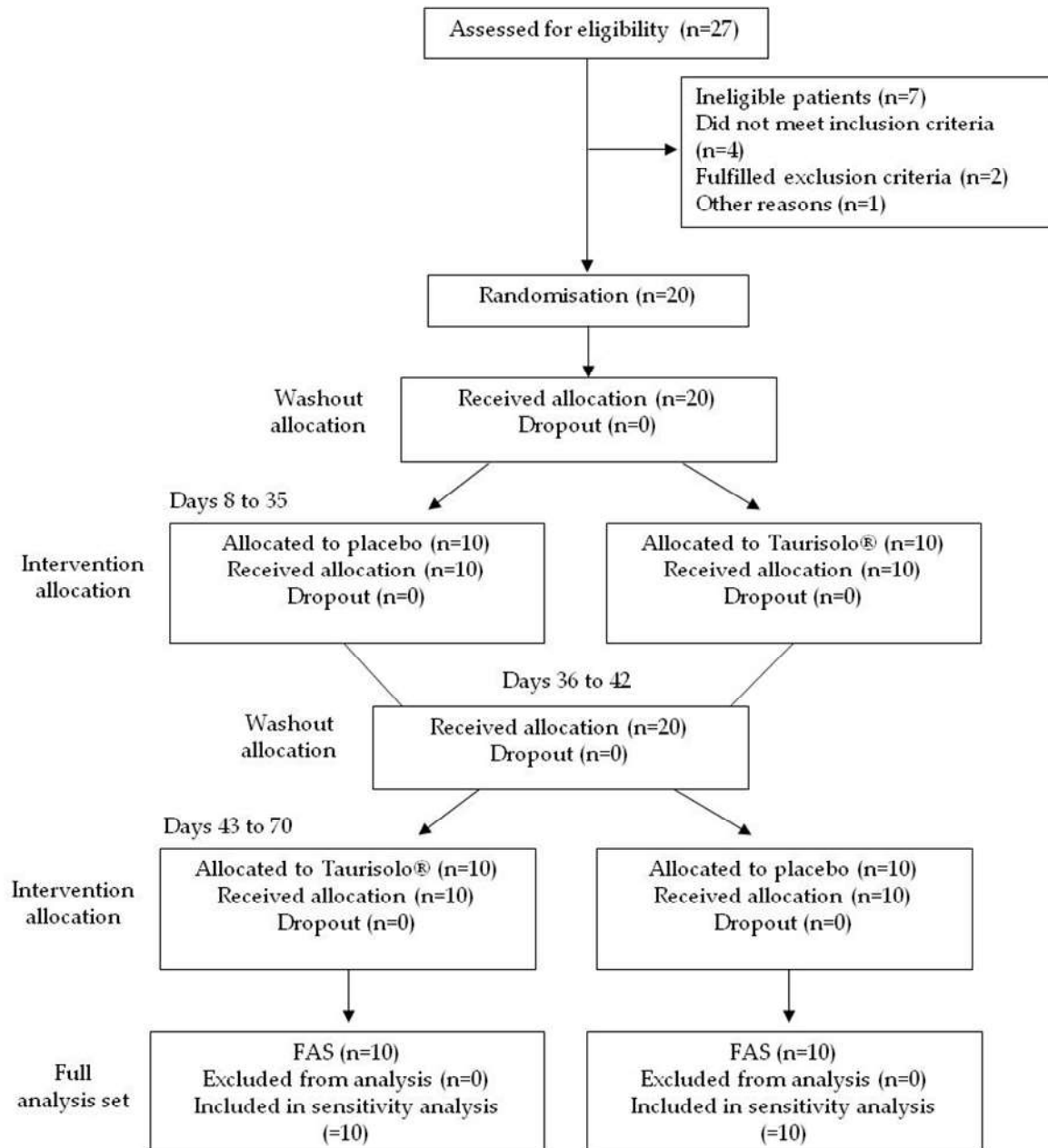


Figure 4. Study flowchart. Study flowchart, according to the consolidated standards of reporting trials (CONSORT) [source: (Annunziata et al., 2019c)].

Table 4ⁱⁱ shows that TMAO serum levels were significantly decreased ($\Delta\% = -63.6\%$) in the Taurisol[®] period compared with placebo period ($P < 0.0001$).

Table 4ⁱⁱ. Effects of Taurisol[®] on TMAO serum levels in healthy subjects (n = 20) [source: (Annunziata et al., 2019c)]

Parameters	Placebo			Taurisol [®]		
	Initial ^a	Final ^a	$\Delta\%$	Initial	Final	$\Delta\%$
Age (years)	30.0 ± 5.0	-	-	-	-	-
Male sex (No (%))	10 (50.0%)	-	-	-	-	-
White ethnicity (No (%))	20 (100.0 %)	-	-	-	-	-
BMI (kg/m ²)	20.8 ± 3.6					
TMAO levels (µM) ± SD	1.86 ± 0.35	1.84 ± 0.34*	- 0.54	1.87 ± 0.33 [#]	0.66 ± 0.44 ^{###}	- 63.5

Value are expressed in µM ± SD of three replicates. Decrement percentage was shown. Statistic significance are calculated by Student's t-test.

^aInitial refers to samples collected at days 8 and 42. Final refers to samples collected at days 35 and 70.

* $P = 0.9297$, initial vs. final (placebo); ** $P < 0.0001$, initial vs. final (Taurisol[®]); # $P = 0.9555$ placebo vs. Taurisol[®] (initial); ## $P < 0.0001$, placebo vs. Taurisol[®] (final)

Encouraged by these results, we decided to investigate the TMAO-reducing ability of Taurisol[®] in subjects with conditions strongly associated with higher levels of this metabolite, such as overweight and obesity. In this study (described in previous section), we administered subjects with two formulations (Taurisol[®] and Taurisol[®]+pectin) in order to evaluate whether the supplementation with prebiotics resulted in greater reduction of TMAO serum levels, maybe through its beneficial effect on gut microbiota. Surprisingly, we observed no significant difference between the two groups at the end of the intervention period, suggesting the observed TMAO-reducing effect was due exclusively to Taurisol[®], and fibre did not represent any added value. In particular, in both intervention groups TMAO serum levels significantly decreased (-78.58% $p=0.006$ and -76.76% $p=0.001$, group A and group B, respectively). No significant differences have been reported between the two interventions after the 8-week treatment period (TMAO: $p=0.897$, group A vs. group B). After the 4-week follow-up period, the TMAO serum levels not significantly increased in both groups (TMAO:33.77% and 37.60%, group A and group B, respectively) (**Table 4ⁱⁱⁱ**, **Figure 4ⁱⁱ**).

Table 4ⁱⁱⁱ. TMAO serum levels of study participants before and after 2-month treatment. Values are expressed as mean \pm SD of three replicates. Statistical significance was calculated by Student's t-test. #P = 0.897, group A vs. group B (after treatment) [source: (Annunziata et al., 2019b)]

	TMAO serum levels (μM)				Δ (%)	<i>p</i> -value
	Run-in(placebo)	Before treatment	After treatment	Follow-up		
Group A	3.47 \pm 2.87	3.52 \pm 2.95	0.75 \pm 1.06	1.00 \pm 0.99	- 78.58	0.006
Group B	3.42 \pm 1.97	3.44 \pm 2.04	0.80 \pm 0.37 [#]	1.10 \pm 0.44	- 76.76	0.001

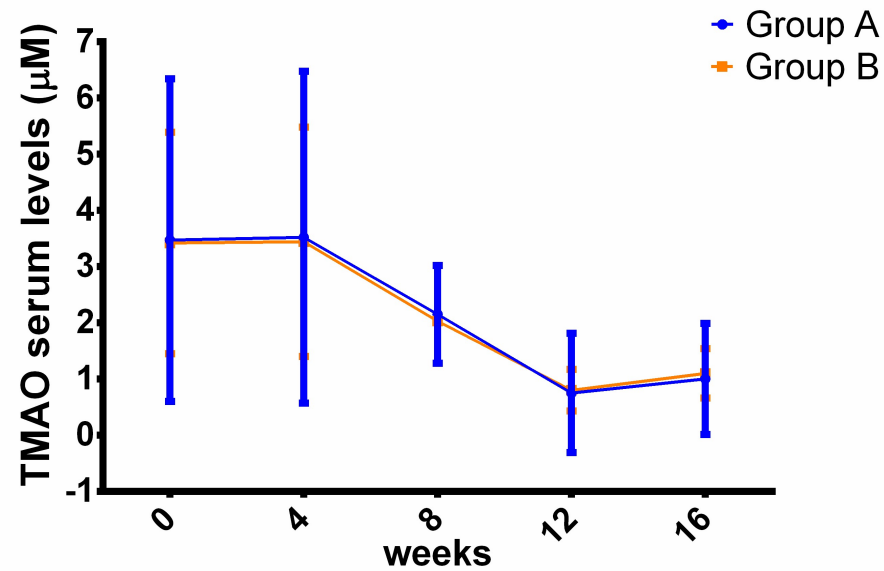


Figure 4ⁱⁱ. Graphical representation of the TMAO serum levels at the different time points [source: (Annunziata et al., 2019b)]

Finally, we conducted a third RCT on subjects with various risk factors for CVD, including overweight/obesity, cigarette smoking, diabetes or hypertension. In this study (described in details in previous section) we performed a number of stratifications and correlation analyses to elucidate both the relationship between TMAO and other risk factors and the role of Taurisolo® in different population subclasses. Firstly, TMAO serum levels were monitored in all study participants at run-in, before starting Taurisolo® treatment (baseline), after 4-week Taurisolo® treatment, after 8-week Taurisolo® treatment and after 4-week follow-up (**Figure 4^{III}**). TMAO serum levels significantly reduced after 4-week Taurisolo® treatment, from $2.91 \pm 2.30 \mu\text{M}$ to $1.10 \pm 1.17 \mu\text{M}$ (-49.78%, $p < 0.0001$), and after 8-week Taurisolo® treatment ($0.53 \pm 0.53 \mu\text{M}$, -75.85%, $p < 0.0001$).

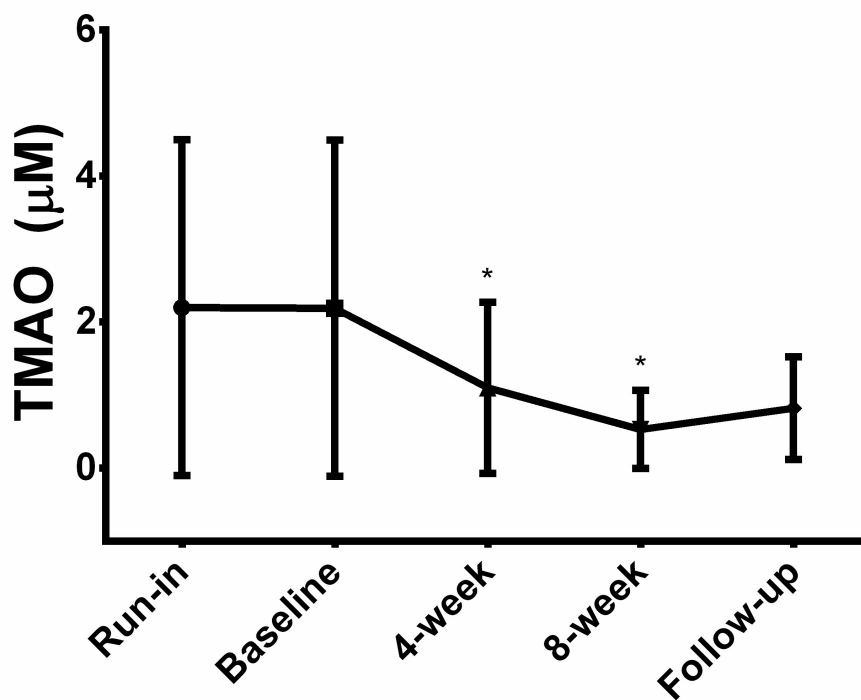


Figure 4^{III}. Graphical representation of the TMAO serum levels at the different time points. Values are expressed as mean \pm standard deviation. Statistical significance was calculated with Student's t-test; p-value < 0.05 was considered as significant. * P < 0.0001 , compared to baseline.

Study participants were then stratified for (i) gender, (ii) diagnosis of diabetes or hypertension, (iii) body mass index (BMI) and (iv) age. The effects of Taurisolo® on TMAO serum levels are reported in **Tables 4^{IV-VII}**.

Finally, a Pearson's correlation analysis was performed between (i) serum levels of TMAO, oxLDL and D-ROMs (at baseline, after 4-week and 8-week Taurisolo® treatment) (**Table 4^{VIII}**) and (ii) variations of

these three parameters during both the 4-week and 8-week treatment periods (indicated as $\Delta\%$ (baseline-t-4wk) and $\Delta\%$ (baseline-t-8wk, respectively) (**Table 4^{ix}**).

Table 4^{iv}. Serum levels of TMAO before and after 4-week and 8-week treatment with Taurisolo® in study participants stratified for gender. Statistical significance was calculated with Student's t-test; p-value <0.05 was considered as significant

	Baseline	t-4wk			t-8wk		
	Mean±SD	Mean±SD	$\Delta\%$	p (vs t0)	Mean±SD	$\Delta\%$	p (vs t0)
		(vs. t0)	(vs. t0)		(vs. t0)	(vs. t0)	
Men (n=66)	2.57±2.71	1.43±1.41	-44.23	<0.0001	0.50±0.38	-80.59	<0.0001
Women (n=42)	2.11±1.53	1.21±0.94	-42.89	<0.0001	0.61±0.67	-71.22	<0.0001

Table 4^v. Serum levels of TMAO before and after 4-week and 8-week treatment with Taurisolo® in study participants stratified for diagnosis of diabetes or hypertension. Statistical significance was calculated with Student's t-test; p-value <0.05 was considered as significant

	Baseline	t-4wk			t-8wk		
	Mean±SD	Mean±SD	$\Delta\%$	p (vs t0)	Mean±SD	$\Delta\%$	p (vs t0)
		(vs. t0)	(vs. t0)		(vs. t0)	(vs. t0)	
Diabetes (n=28)	3.71±2.81	2.11±1.15	-43.15	<0.001	0.73±0.67	-80.31	<0.0001
Hypertension (n=39)	3.02±2.87	1.79±1.42	-40.84	0.0001	0.64±0.64	-78.88	<0.0001
No-diabetes/No-hypertension (n=41)	1.32±1.10	0.66±0.63	-49.82	<0.0001	0.40±0.32	-69.92	<0.0001

Table 4^{vi}. Serum levels of TMAO before and after 4-week and 8-week treatment with Taurisolo® in study participants stratified for BMI. Statistical significance was calculated with Student's t-test; p-value <0.05 was considered as significant

	Baseline	t-4wk			t-8wk		
	Mean±SD	Mean±SD	$\Delta\%$	p (vs t0)	Mean±SD	$\Delta\%$	p (vs t0)
		(vs. t0)	(vs. t0)		(vs. t0)	(vs. t0)	
Normal weight (n=57)	0.96±0.61	0.48±0.29	-50.27	<0.0001	0.33±0.23	-65.53	<0.0001
Overweight (n=21)	1.84±0.59	1.30±0.47	-29.27	<0.001	0.54±0.29	-70.75	<0.0001
Grade I obesity (n=16)	3.62±0.88	2.04±0.76	-43.68	<0.0001	0.72±0.40	-80.12	<0.0001
Grade II obesity (n=14)	7.06±2.45	3.75±0.73	-46.84	0.001	1.14±1.00	-83.86	<0.0001

Table 4^{vii}. Serum levels of TMAO before and after 4-week and 8-week treatment with Taurisolo® in study participants stratified for age. Statistical significance was calculated with Student's t-test; p-value <0.05 was considered as significant

	Baseline	t-4wk			t-8wk		
	Mean±SD	Mean±SD	$\Delta\%$	p (vs t0)	Mean±SD	$\Delta\%$	p (vs t0)
		(vs. t0)	(vs. t0)		(vs. t0)	(vs. t0)	
18-40 years (n=14)	1.89±0.32	0.78±0.56	-58.92	<0.0001	0.75±0.33	-60.08	<0.0001
41-60 years (n=31)	2.53±3.16	1.29±1.32	-49.13	<0.001	0.65±0.80	-74.24	<0.001
>61 years (n=63)	2.55±1.95	1.41±1.29	-44.73	<0.0001	0.46±0.34	-81.87	<0.0001

Table 4^{viii}. Correlation analysis between TMAO, oxLDL and D-ROMs serum levels in all study participants

	TMAO baseline		TMAO t-4wk		TMAO t-8wk	
	Coefficient	<i>p</i> -value	Coefficient	<i>p</i> -value	Coefficient	<i>p</i> -value
<i>OxLDL</i>						
Baseline	0.975	<0.0001	-	-	-	-
t-4wk	-	-	0.969	<0.0001	-	-
t-8wk	-	-	-	-	0.972	<0.0001
<i>D-ROMs</i>						
Baseline	0.975	<0.0001	-	-	-	-
t-4wk	-	-	0.946	<0.0001	-	-
t-8wk	-	-	-	-	0.907	<0.0001

Table 4^{ix}. Correlation analysis between variations of TMAO, oxLDL and D-ROMs serum levels in all study participants

	TMAO Δ% (Baseline-t-4wk)		TMAO Δ% (Baseline-t-8wk)	
	Coefficient	<i>p</i> -value	Coefficient	<i>p</i> -value
<i>OxLDL</i>				
Δ% (Baseline-t-4wk)	0.757	<0.0001	-	-
Δ% (Baseline-t-8wk)	-	-	0.221	<0.05
<i>D-ROMs</i>				
Δ% (Baseline-t-4wk)	0.654	<0.0001	-	-
Δ% (Baseline-t-8wk)	-	-	0.178	0.066

With these studies we demonstrated the ability of Taurisolo® to reduce TMAO serum levels in a large number of subjects, including healthy (Annunziata et al., 2019c), overweight/obese subjects (Annunziata et al., 2019b) and high CVR subjects (**article in press**). Interestingly, our correlation analysis demonstrated that TMAO serum levels correlated positively with circulating oxLDL and DROMs at baseline and after 4- and 8-week treatment with Taurisolo® (**Table 4^{viii}**); similarly, variations of TMAO serum levels during the nutraceutical treatment also correlated positively with variation of oxLDL and DROMs levels (**Table 4^{ix}**). This suggests, on one hand, the link between this microbiota metabolite and OxS-related biomarkers, and on the other hand that chronic treatment with Taurisolo® may represent a valid nutraceutical approach for cardioprotection.

Besides the very large number of paper published on TMAO in last decades, no mechanisms have been proposed for the potential TMAO-reducing effect of drugs or natural compounds. However, studies reported in literature allow speculating possible mechanisms of action. In particular, we hypothesized two different ways by which polyphenols may contribute to reduce TMAO serum levels: antioxidant and/or microbiota remodeling activities.

Polyphenols exert their antioxidant activity through direct and indirect mechanisms (Sandoval-Acuña et al., 2014), including free radical scavenging. In particular, through their benzene ring-bound hydroxyl groups, polyphenols transfer an electron to free radicals, acting, thus, as “electron donors” (Amic et al., 2007; Bors et al., 1990). In contrast, TMAO has been reported to act as an “electron acceptor” in bacteria (Barrett, 1985), leading to a so-called “redox hypothesis”, where both polyphenols and TMAO are two actors of the same redox reaction occurring at blood levels, and resulting in a chemical reduction of TMAO to TMA.

The antioxidant potential of Taurisolo® has been previously reported both in human (Annunziata et al., 2019b) and rats (Annunziata et al., 2020b) (as described in previous section). Similarly, our previous evidence demonstrated a high bioavailability of Taurisolo® polyphenols (Annunziata et al., 2019c), due to the use of microencapsulation in maltodextrins, a useful strategy to enhance the absorption of polyphenols across the intestinal barriers (Annunziata et al., 2020a). It appears clear, thus, that, whether confirmed, the “redox hypothesis” might be a possible mechanism of action for the TMAO-reducing effect of Taurisolo®.

In addition to this hypothesis, we also proposed the so-called “microbiota hypothesis” based on the ability of polyphenols to modulate the growth of different bacterial strains. In particular, it is reported in literature that grape polyphenols are capable to reduce the growth of TMA-producing bacteria (i.e. *Clostridia* and *Bacteroides*) (Lee et al., 2006; Selma et al., 2009) and to increase that of non-TMA-producing ones (i.e. *Lactobacillus* and *Bifidobacterium*) (Chen et al., 2016), resulting in a remodelling of the gut microbiota. According to our “microbiota hypothesis”, after chronic oral administration, Taurisolo® polyphenols might contribute in reduction of TMAO serum levels *via* blocking the colonic production of its precursor, TMA.

This, in turn, might be operated by the antimicrobial activity against TMA-producing strains or a potential inhibition of their metabolism, for example down-regulation/inhibition of target genes/enzymes, such as TMA lyase, carnitine oxygenase and betaine reductase, responsible for the TMA release from food components. This hypothesis is again corroborated by the nature of our nutraceutical formulation, administered in an acid-resistant form. According to our previous investigations, the use of acid-resistant formulation protects polyphenols against degradation during the transit in the gastrointestinal tract, and allows polyphenols reaching the intestine in an active form (Annunziata et al., 2018a). Interestingly, a very recent preprint paper investigated the inhibitory effect of phytochemicals on TMA production (Iglesias-Carres et al., 2021). In particular, it was developed an anaerobic fermentation methodology to study inhibition of choline microbial metabolism into TMA by phenolic compounds (gallic acid and chlorogenic acid) using healthy human faeces as starter. It was reported that both the phenolic compounds exerted a higher TMA inhibitory potential (maximum of 80-90% in TMA production inhibition with IC_{50} around 5mM) than 3,3-dimethyl-1-butanol (DMB) used as positive TMA production inhibitor (acting as TMA-lyase inhibitor). Notably, through cytotoxicity experiments, authors observed that both gallic and chlorogenic acids did not act inhibiting TMA-lyase activity. On the contrary, they speculated that the two phenolic acids reduced TMA production by providing better energy substrates than choline. More specifically, bacteria could use gallic and chlorogenic acids as a more preferred source of energy than choline, resulting in a reduced utilisation of choline as substrate for TMA production. Undoubtedly, both redox and microbiological hypothesis (**Figure 4^V**), need to be further investigated.

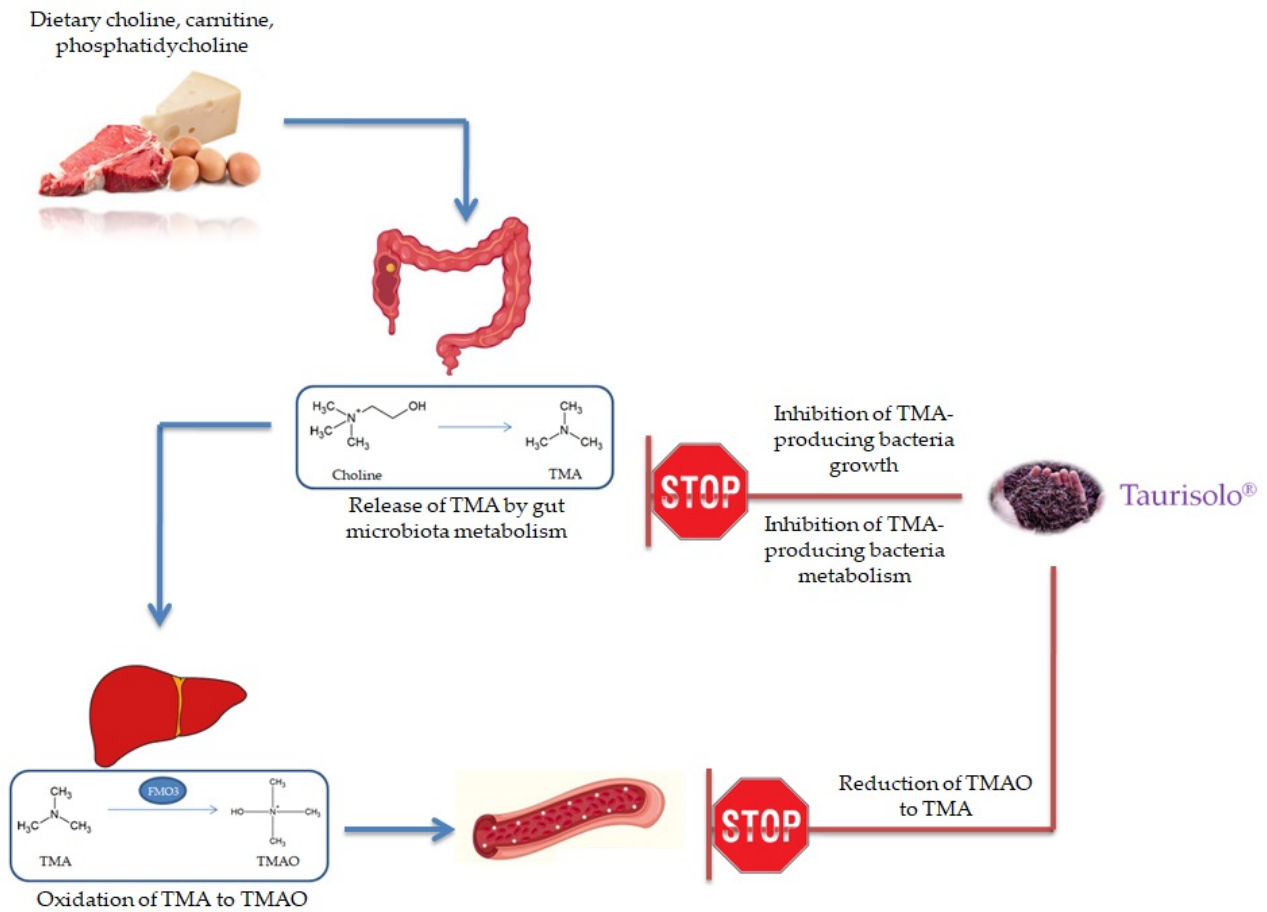


Figure 4^{IV}. Proposed mechanisms of action of Taurisolo® in reducing circulating TMAO levels and, consequently, the risk of atherosclerosis

5. The effects of Taurisolo® on oxidative stress- and atherosclerosis-related diseases

A number of further studies have been conducted, or are still ongoing, to confirm the efficacy of Taurisolo® in pathological conditions related to the CVR. All these studies will be discussed in following sections.

5.1 CVD

To test the cardioprotective effect of Taurisolo® we performed an *in vitro* study on cardiomyoblast H9c2 cells in collaboration with the Departments of Precision Medicine, Experimental Medicine and Advanced Medical and Surgical Sciences of the University of Campania “Luigi Vanvitelli”, Naples (Italy) (Lama et al., 2020). In particular, we investigated the ability of Taurisolo® to contrast both TMAO- and high glucose (HG)-induced cytotoxicity in this cell model. Cell damage was induced with HG (HG-H9c2) and HG+TMAO (THG-H9c2); both experimental cell models were, thus, incubated for 72 h in the presence or absence of Taurisolo®. Methods are detailed in **Appendix A**.

To gain an insight about the mechanism through which Taurisolo® sustained the cardiomyocyte viability, we have damaged the H9c2 cardiomyoblastic cell line with HG concentration (44 mM) and TMAO, a molecule linked to obesity and energy metabolism (**Figure 5.1**¹). H9c2 vitality was detected via MTT assay, while LDH and AST release assays were performed for cellular injury. HG treatment of H9c2 (44 mM) significantly reduced cell viability (~25%; $P = 0.011$) and increased both AST and LDH release ($P = 0.037$ and $P = 0.0074$, respectively) compared with the non-HG (NG)-H9c2 growth in standard condition (5.5 mM glucose). In contrast, treatment with Taurisolo® was able to counteract significantly the decrease of vitality and the AST and LDH release in both HG-H9c2 and THG-H9c2 cells, while at the same concentration, Taurisolo®-treated NG-H9c2 did not produce the same effect. In **Figure 5.1**^{1-D}, we reported the LDH1:LDH2 isoenzyme ratio, observing that increased of about 1,8 and 2,5 fold in HG-H9c2 and THG-H9c2, respectively, compared to NG-H9c2 (LDH1:LDH2 ratio=1). Interestingly, Taurisolo® treatment of THG-H9c2 counteracted the increase of LDH1/LDH2 ratio.

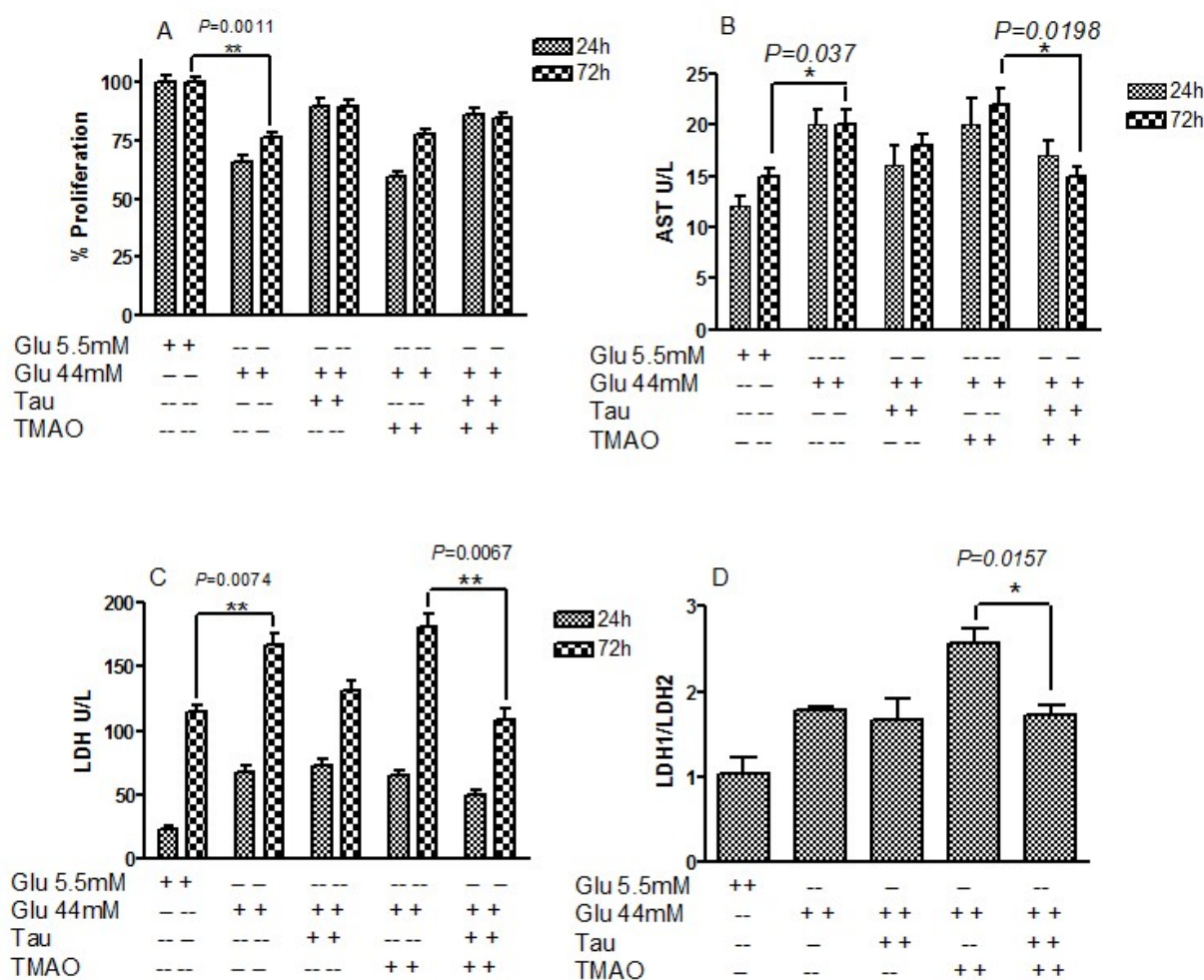


Figure 5.1I. Taurisoló® (Tau) counteracts the H9c2 cell injury induced from TMAO in hyperglycemic condition. H9c2 cells were grown in standard (5.5 mM Glu NG-H9c2) and high glucose (44 mM Glu, HG-H9c2) condition. The HG-H9c2 cells were treated, for 72 h with Tau (0,5 µg/µL), TMAO(50 µM), and TMAO-Tau combination. (a) The cell survival was performed with MTT assay. (b, c) AST and LDH as makers of cell injury were performed by the colorimetric assay. (d) LDH1/LDH2 isoenzymes ratio was evaluated at 72 h by the colorimetric assay. Each experiment was repeated at least three times. Results are expressed as mean ± SD [source: (Lama et al., 2020)]

To demonstrate that the effect of Taurisoló® on proliferation was related to the reduction of ROS production, we evaluated both lipid peroxidation by aldehyde reactive to thiobarbituric acids (TBARS) assay and endogenous free nitric oxide (as NO₂⁻) by the Griess assay (**Figure 5.1II**). We observed a significant increase of TBARS production in THG-H9c2 cells compared to Taurisoló®-treated THG-H9c2 cells (P = 0:0159) and an increase of NO production in the medium of Taurisoló®- treated THG-H9C2 (P=0:038) compared with untreated THG-H9c2 cells.

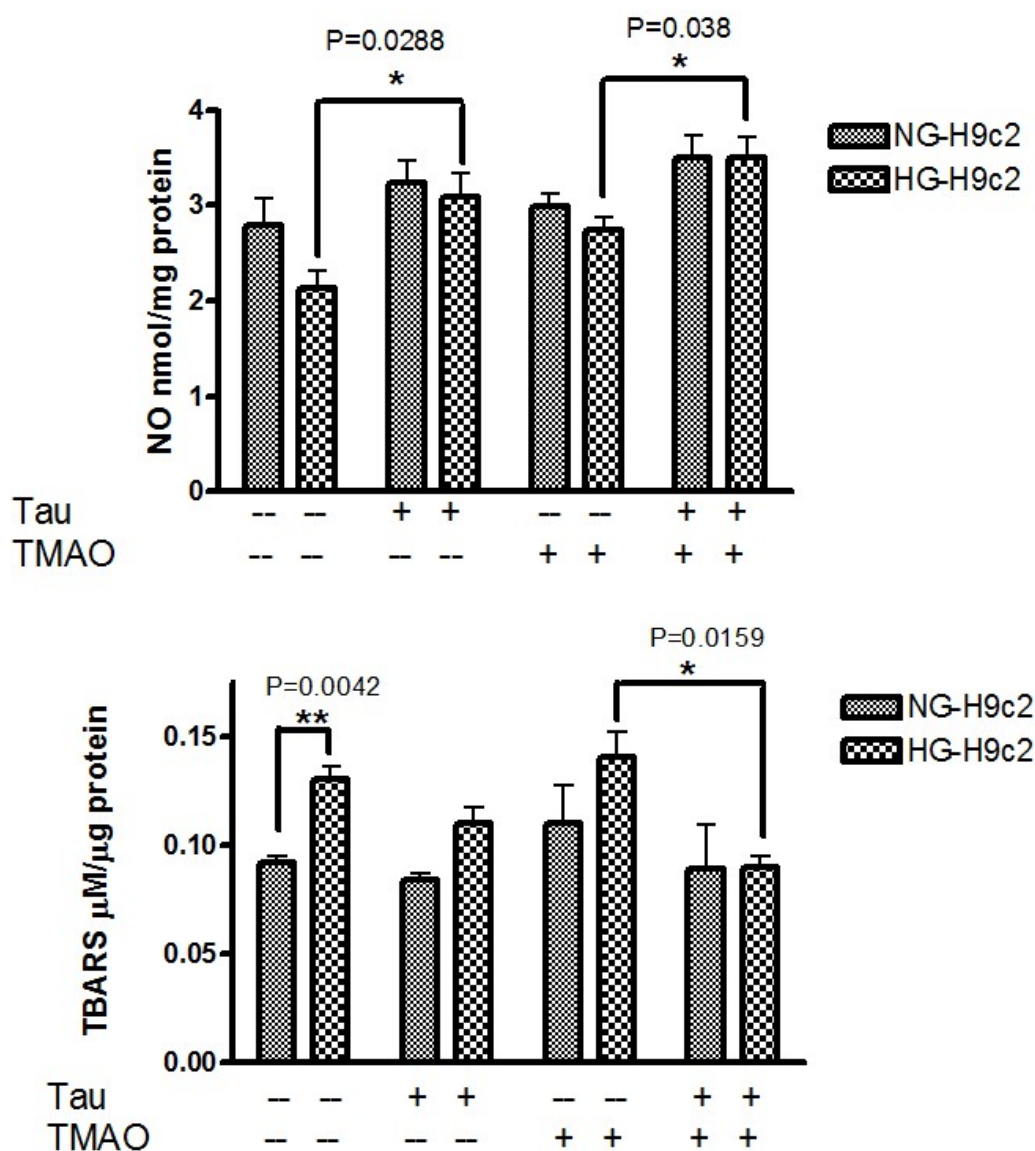


Figure 5.1ⁱⁱ. Taurisolo[®] increased the nitric oxide values in the medium of THG-treated H9c2 cells. The values of NO were evaluated by the Griess assay. H9c2 cells were grown in standard (5.5 mM NG-H9c2) and high glucose (44 mM Glu, HG-H9c2) condition. The NG and HG-H9c2 cells were treated, for 72 h with Tau (0.5 μg/μL), TMAO (50 μM), and TMAO-Tau combination. Absorbance was assayed at 550 nm and compared with a standard curve obtained using sodium nitrite. TBARS were quantified by spectrophotometry at 532 nm. Results were expressed as TBARS M/g of serum proteins. Each data point is the average of triplicate measurements, with each experiment performed in triplicate. Results are expressed as mean ± SD [source: (Lama et al., 2020)]

Furthermore, Taurisolo[®] treatment counteracted the higher expression of Mn-SOD in THG-H9c2 cells (Figure 5.1ⁱⁱⁱ).

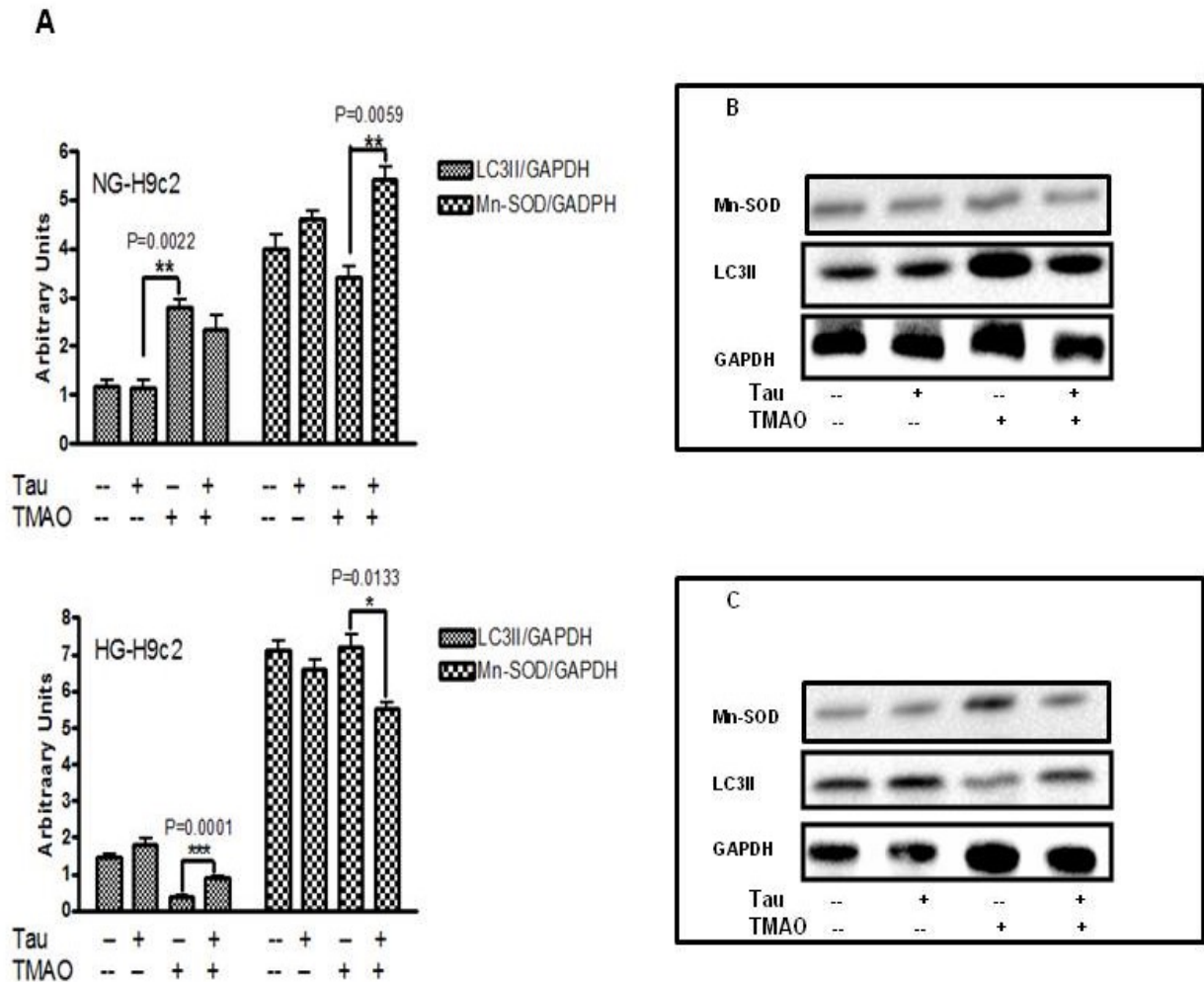


Figure 5.1^{III}. Taurisolol[®] (Tau) increase LC3II expression and counteract high levels of MnSOD. H9c2 cells were grown in standard (5.5 mM Glu NG-H9c2) and high glucose (44 mM Glu, HG9c2) condition. The NG and HG-H9c2 cells were treated, for 72 h with Tau (0.5 $\mu\text{g}/\mu\text{L}$), TMAO (50 μM), and TMAO-Tau combination. (a) Bar graphs show densitometrically quantified LC3II, MnSOD with respect to house-keeping GAPDH in NG (5.5 mM glucose) and HG-H9c2 cells. Representative immunoblots of Tau treated TNG-H9c2 (b) and THG-H9c2 cells (c). Each data point is the average of triplicate measurements, with each experiment performed in triplicate. Results are expressed as mean \pm SD [source: (Lama et al., 2020)]

Extracellular signal-regulated protein kinase (ERK) and its phosphorylated form (pERK) are important mediators of various cellular responses, such as proliferation, differentiation, and cell death. It is noting that chronic HG induced ERK phosphorylation and cell death. We detected ERK activation by evaluating the pERK/ERK ratio by Western blot analysis using phospho-specific antibodies. ERK activation (**Figure 5.1^{IV-A}**) was elevated in HG-H9c2 cells compared to NG-H9c2 cells (**Figure 5.1^{IV}**), while it was significantly reduced after TMAO treatment in both NG and HG-H9c2 cells. Of note, treatment with Taurisolol[®] modulated ERK activation in prosurvival manner both HG and THG-H9c2 cells.

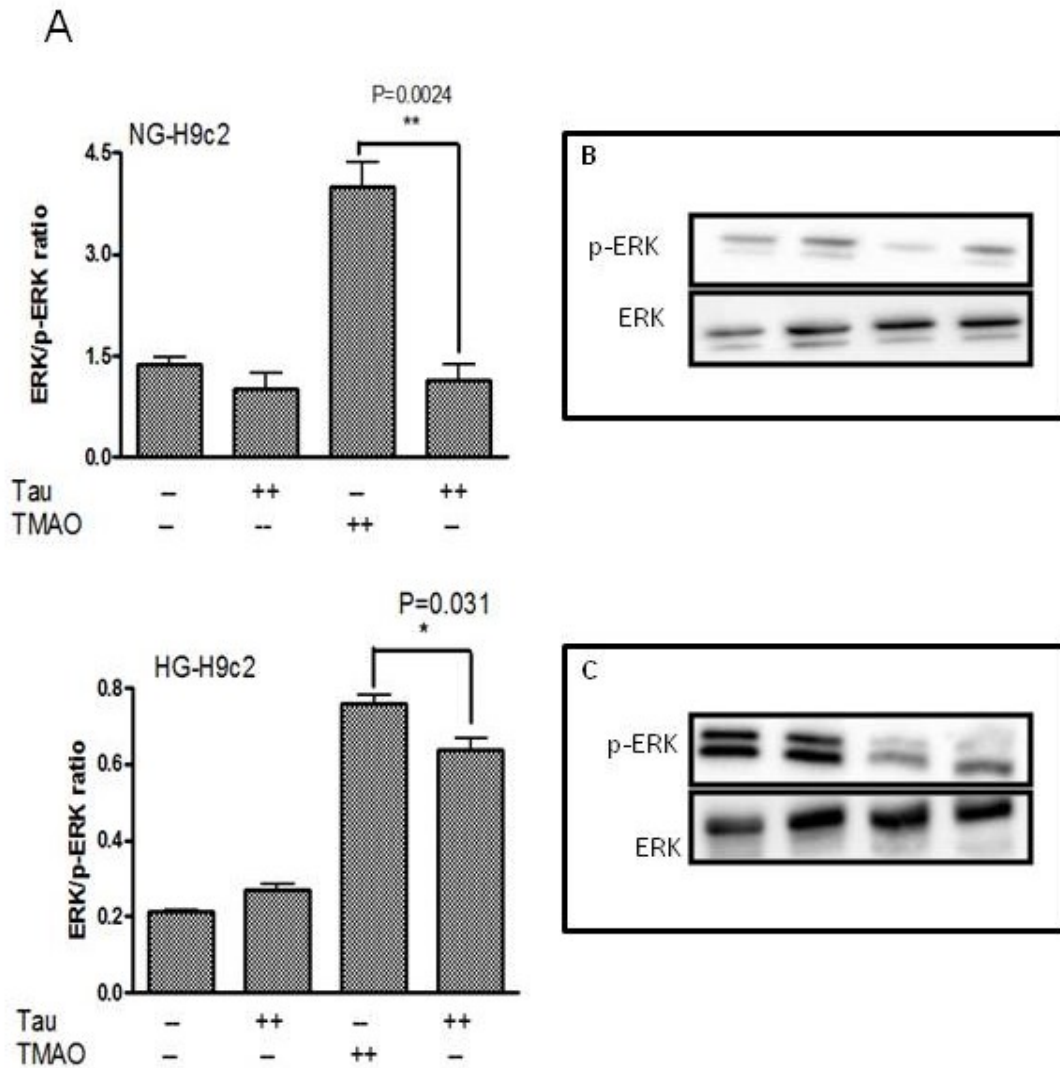


Figure 5.1^{IV}. Taurisolo® modulated ERK activation. H9c2 cells were grown in standard (5.5 mM Glu NG-H9c2) and high glucose (44 mM Glu, HG9c2) condition. The NG and HG-H9c2 cells were treated, for 72 h with Tau (0.5 µg/µL), TMAO (50 µM), and TMAO-Tau combination. (a) Bar graphs show densitometrically quantified ratio of p-ERK/ERK in H9c2 cells. (b) Representative immunoblots of NG-H9c2 cells treated with Tau, TMAO, and Tau-TMAO combination. (c) Representative immunoblots of HG-H9c2 cells treated with Tau, TMAO, and Tau-TMAO combination. Each data point is the average of triplicate measurements, with each experiment performed in triplicate. Results are expressed as mean ± SD [source: (Lama et al., 2020)]

Collectively, these data suggested that the association of 72 h-hyperglycemia and 72 h-TMAO treatment of H9c2 cells led to both cardiac cell cytotoxicity and increase in OS, as mainly indicated by the increases of both lipid peroxidation and antioxidant enzyme levels. Taurisolo® treatment mitigated the increases in AST and LDH levels and increased H9c2 cell viability, suggesting its protective effect on cardiomyocytes during both hyperglycemia- and TMAO-caused damage. Furthermore, these results showed that Taurisolo® reduced THG-induced H9c2 injury by reducing OS. Decreased levels of TBARS are combined

with increase of free NO production, suggesting a potential involvement of Taurisolo® in regulating the balance between NO and peroxynitrite. A protective effect of NO has also been observed in endothelial cells, cardiomyocytes (Santucci et al., 2006), and inflammatory cells (Ronchetti et al., 2009). When MnSOD is overexpressed, more superoxide radicals are converted to H₂O₂, which acts as a cytotoxic agent, and therefore are removed from the physiological equilibrium, causing an increased production of membrane lipid peroxidation. To demonstrate that the cellular damage effect of HG and TMAO was related to increased OxS, we assessed cell vitality after treatment for 24 h with 10 µM N-acetyl cysteine (NAC) widely used as a pharmacological antioxidant and cytoprotective compound. In this experimental condition, we did not observe growth inhibition in both HG and THG-H9c2 cells (data not shown). In conclusion, the protective effect of Taurisolo® on cell viability and cell injury is closely linked to the antioxidant activity of its polyphenol composition. The antioxidant potential of Taurisolo® results in decreased both expression of MnSOD and lipid peroxidation levels. Conversely, the increased release of NO leads to an ERK activation and a consequently pro-survival effect against TMAO damage induced in the H9c2 cells.

As autophagy is important for the maintenance of mitochondrial homeostasis, it was hypothesized that Taurisolo® may preserve the H9c2 from injury induced by TMAO and hyperglycemia via autophagy activation. To prove this hypothesis, we evaluated the autophagy marker protein microtubule-associated protein LC3II expression by Western blot analysis. TMAO treatment of HG-H9c2 induced a down-regulation of autophagy, as evidenced by a decrease in LC3II, compared with the HG-H9c2 cells. 72 h-treatment with TMAO/ Taurisolo® combination of HG-H9c2 cells was able to reverse the decrease of LC3II expression in THG-H9c2 cells (**Figure 5.1^{III-A-C}**).

Morphological changes induced by both HG and TMAO in H9c2 cells were detected by α -actin immunofluorescence by confocal microscopy; the representative results were shown in **Figure 5.1^V**. The α -actin protein (green signal) in Taurisolo®-treated HG-H9c2 cells was uniformly distributed in the cytoplasm, and cells presented a typical elongated form with respect to untreated HG-H9c2 cells where the shape appeared enlarged and rounded; in THG-H9c2 cells, α -actin accumulated, forming evident punctuated signals. Meanwhile, Taurisolo® treatment reduced actin aggregation in THG-H9c2 cells. These results demonstrate that exposure to Taurisolo® in both HG and THG-H9c2 cells induced α -actin spatial organization and a functional cell morphological conformation. The purpose of autophagy is to ensure quality control of organelles and proteins, as well as protection of intracellular homeostasis in stress and nutrient efficiency (Cetrullo et al., 2015; Dunlop and Tee, 2014; Kume and Koya, 2015; Mizushima and Komatsu, 2011; Salminen et al., 2016; Sridharan et al., 2011). Autophagy is involved in the maintenance of organelle integrity, protein quality (Zientara-Rytter and Subramani, 2016), and modulated and to participate in the pathogenesis of human diseases, such as DM, neurodegenerative diseases, aging, and vascular disease (He et al., 2016; Lippai and Szatmari, 2017; Wang et al., 2014). It has been reported that antioxidant molecules

such as resveratrol by increasing autophagic flux ameliorates diabetic cardiomyopathy (Lv et al., 2017). In THG-H9c2 damage cell model cells, we demonstrated that Taurisol[®], restoring the autophagic process, induces a reduction of the actin aggregation, restoring a normal cell morphology.

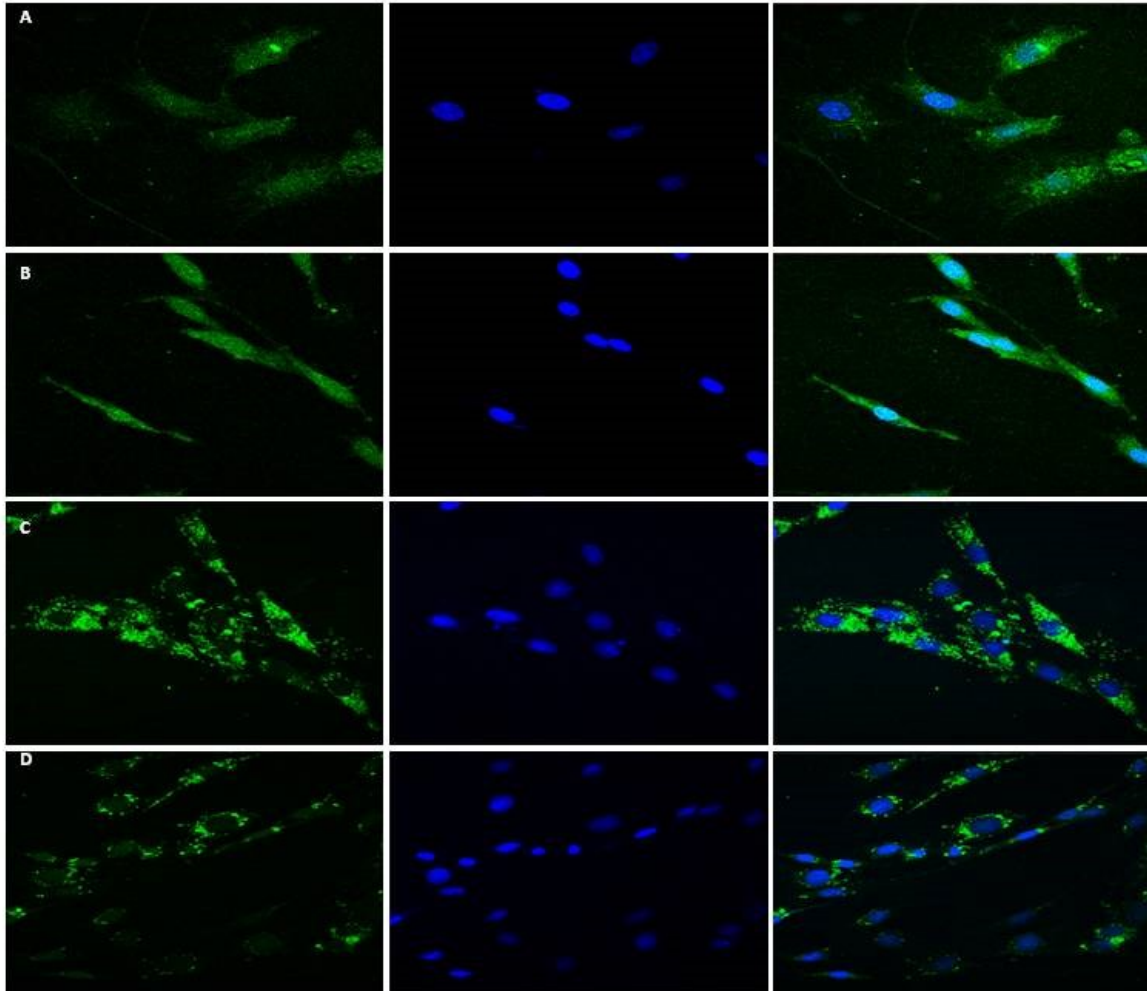


Figure 5.1V. Representative microphotographs of HG-H9c2 cells. Cardiomyocyte was identified with α -actin antibody (green signal), and the nucleus was identified by DAPI (blue signal). (a) H9c2 cell growth with 44 mM glucose (HG-H9c2). (b) HG-H9c2 was treated for 72 h with Tau (0.5 $\mu\text{g}/\mu\text{L}$). (c) HG-H9c2 cell was treated for 72 h with TMAO (50 μM). (d) HG-H9c2 cell was treated for 72 h with TMAO/Tau combination [source: (Lama et al., 2020)].

Sphingolipids (SLs) are molecules implicated in cell survival and autophagy. Bioactive lysolipids, including ceramides (Cer) and sphingosine-1-phosphate, may act as both extracellular and intracellular mediators. We used tandem mass spectrometry to investigate which sphingolipids were secreted in the cell medium in Taurisol[®]-treated HG- and THG-H9c2 cells. In **Figure 5.1VI**, the positive ion mass spectrometry profile of lipid extract in the medium of the HG-H9c2, THG-H9c2, and both Taurisol[®]-treated HG- and THG-H9c2 cells was reported. In both HG- and THG-H9c2 spectra, we identified the following peaks: d18: 1

sphingoid base and phosphocholine headgroup (449 m/z) (Sullards et al., 2011) (Monounsaturated 18-carbon dihydroxylated sphingoid base linked to one chain of palmitic acid denominated 1-O-tricosanoyl-Cer (d18: 1/16: 0) (875 m/z) and N-(hexacosanoyl)- eicosasphinganine-1-O-[D-mannopyranosyl- α 1-2-myo-inositol-1-phosphate] MIPC (d20 : 0/26 : 0) (1111 m/z). We observed in the lipid fingerprint profile of Taurisol[®]-treated HG- and THG-H9c2 cells that the metabolite peaks were centered between 200 and 1500 m/z as sphingosine, C16- C18 sphinganine-1-phosphate, PE-Cer (d16 : 2/20 : 1), SM (d18 : 0/16 : 0), PI-Cer (d18 : 0/16 : 0), 1-O-stearoyl-Cer (d18 : 1/18 : 0)/Or 1-O-eicosanoyl-Cer (d18 : 1/16 : 0), MIPC (18 : /20), PIM2 (16 : 0/18 : 1), and Glu/Gal-ceramide. Cer plays a central role in sphingolipid metabolism. Cer consists of sphingoid long-chain base linked to an acyl chain via an amide bond and synthesized de novo in the endoplasmatic reticulum (ER); it can be modified into Golgi in sphingomyelin (SM), sphingosine, and glycosphingolipids (e.g., galactosylceramide) and are transported to the plasma membrane (PM). Cer can then be metabolized into ceramide-1-phosphate (C1P) and sphingosine-1-phosphate (S1P) or be resynthesized back into SM. Sphingosine was associated with growth arrest (Ballou et al., 1992) (whereas SP1 promoted cell proliferation and prevents programmed cell death (Spiegel and Milstien, 2000)). In H9c2 cells, higher glucose concentration may block the Cer production and then promote transformation in SM and Sph1P, whereas Taurisol[®] treatment of HG and THG-H9c2 cells induced a reprogramming lipid metabolism and increased Cer, SM, and Sph1P productions that may protect the cardiomyocyte from glucose cytotoxicity. Further in vivo researches may serve to license Taurisol[®] as a useful nutraceutical approach in the prevention of heart damage in obese subjects.

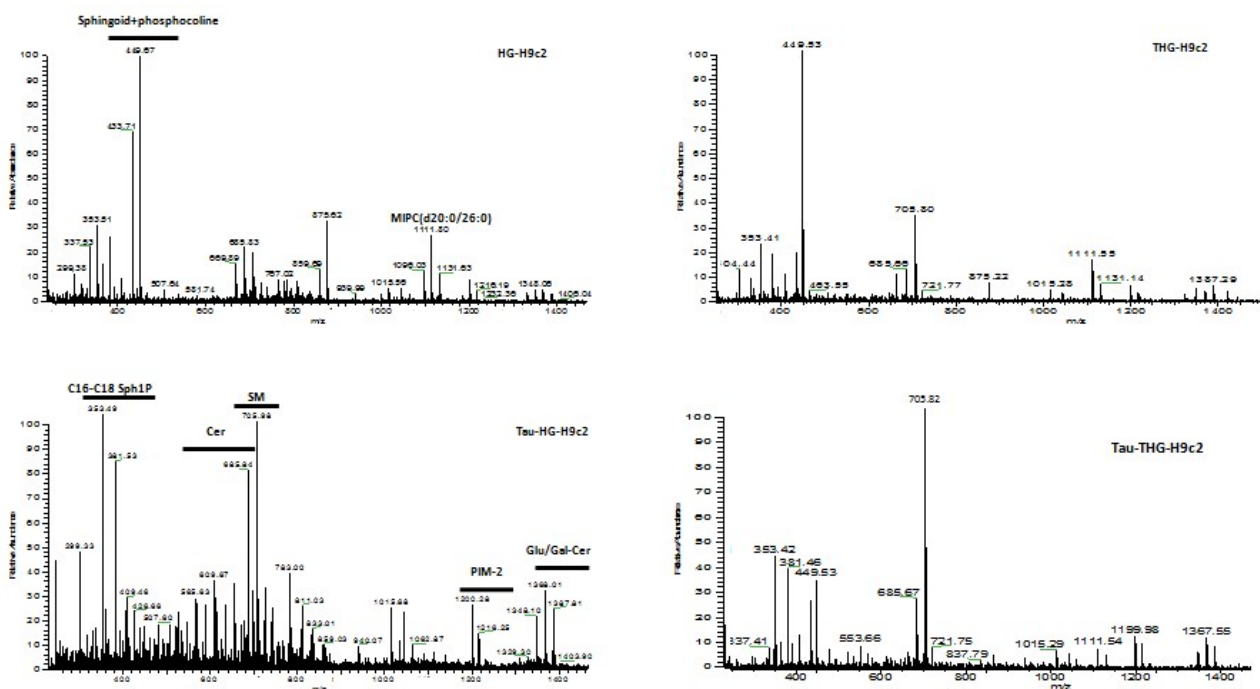


Figure 5.1^{VI}. Positive mass spectra of lipid extracted from media of H9c2 cells. Positive ion electrospray mass spectra of lipid molecular species in lipid extracts from medium of the HG-H9c2 (44 mM glucose) and THG-

H9c2 (44 mM glucose + 50 μ M TMAO) before and after Tau treatment (Tau-HG-H9c2; Tau-THG-H9c2) [source: (Lama et al., 2020)]

5.1.1 Endothelial dysfunction

An interesting multicentric study has been conducted by our research group in cooperation with the Department of Pharmacy of the University of Pisa (Italy), the Department of Translational Medical Sciences and the Department of Clinical Medicine and Surgery of the University of Naples Federico II (Italy) with the scope to elucidate all the possible mechanisms of action of Taurisolo[®] in protection of the endothelial function, using a complete and detailed pharmacological approach (Martelli et al., 2021). This is a very large study consisting of *in vitro* and animal-based studies and a RCT. Overall, materials and methods are detailed in **Appendix A, B** and **C**. To streamline the reading, the entire description of this study has been divided into three subsections: *in vitro*, animal and clinical data.

➤ *In vitro* data

Taurisolo[®] was tested to evaluate its ability to protect both HUVECs and HASMCs against an oxidative stimulus obtained by the administration of H₂O₂. HUVECs were challenged with H₂O₂ 100 μ M and HASMCs with H₂O₂200 μ M, according to preliminary experiments carried out to establish their different sensitivity to the oxidative stimulus (data not shown). The administration of H₂O₂ on HUVECs induced a decrease of cell viability by about 21% (%cell viability *vs* control:78.9 \pm 1.5). This reduction was prevented, in a concentration-dependent manner, by the pre-incubation of three different concentrations of Taurisolo[®] (% cell viability *vs* control for 10 μ g/mL:83.3 \pm 5.6, for 30 μ g/mL: 95.6 \pm 3.2 and for 100 μ g/mL:101.6 \pm 3.2) (**Figure 5.1.1^A**). On the other hand, the administration of H₂O₂ on HASMCs induced a decrease of cell viability by about 24% (% cell viability *vs* control: 75.8 \pm 3.7) and also in HASMCs, the pre-incubation of the three different concentrations of Taurisolo[®] induced a concentration-dependent trend of protection (% cell viability *vs* control for 10 μ g/mL:87.5 \pm 4.9, for 30 μ g/mL: 94.9 \pm 4.2 and for 100 μ g/mL:97.2 \pm 3.4) (**Figure 5.1.1^B**).

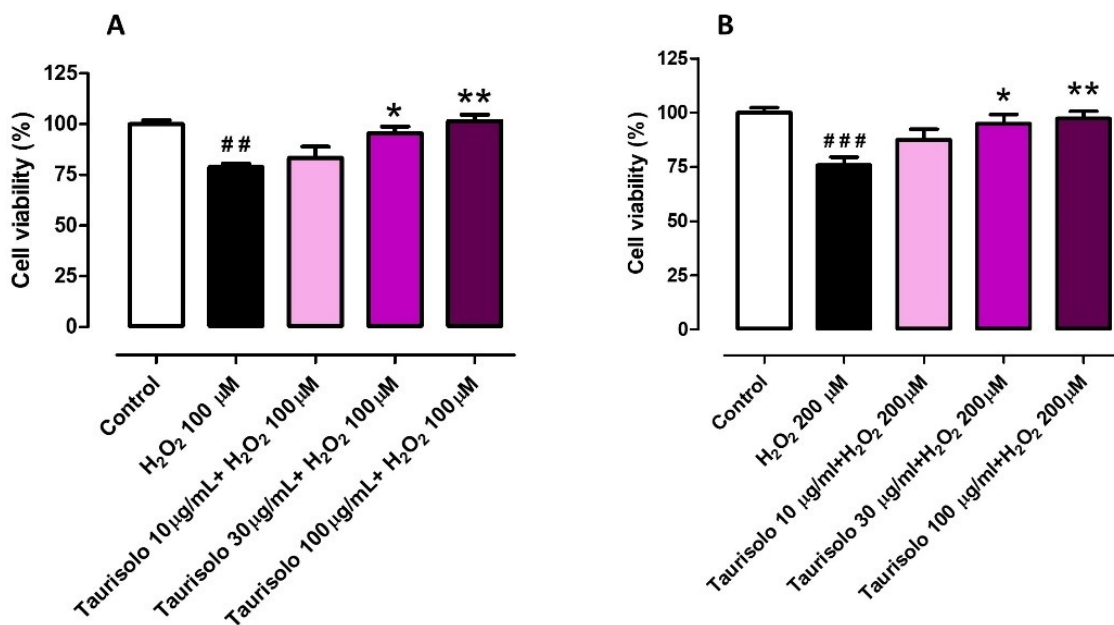


Figure 5.1.1. Evaluation of the protective effect induced by Taurisoló® on HUVECs(A) and HASMCs(B) cell viability, against the H₂O₂-induced oxidative damage. The coloured histograms indicate the % of cell viability of treated cells vs the value of cell viability in cells treated only with vehicle (Control, white histogram). All the experiments were repeated for a minimum of three times and each one was carried out in triplicate (n=9). The symbols indicate the level of statistical significance calculated by ANOVA one-way, followed by Bonferroni post-test: # indicates the significance vs Control, * indicates significance vs cells treated with H₂O₂ (**p<0.01, ***p<0.001; *p<0.05, **p<0.01) [source: (Martelli et al., 2021)].

On the basis of the above results, the concentration of Taurisoló® 100µg/mL, which demonstrated full protection on both HUVECs and HASMCs, was selected for further investigation on the potential mechanisms of action. On the other hand, on the basis of the composition of the extract rich in resveratrol, a possible involvement of the Sirtuins pathway was evaluated. Resveratrol is reported as an activator of Sirtuin-1 but also of the AMP-dependent protein kinase (AMPK), and these targets show a mutual co-activation. Therefore, the involvement of the AMPK pathway was also evaluated. In order to evaluate the involvement of Sirtuins and AMPK in the protective activity of Taurisoló®, the selective blockers of the Sirtuins pathway Sirtinol, and the blocker of the AMPK pathway, Compound C (or Dorsomorphin), were administered, both at 10µM. In this set of experiments, the administration of H₂O₂ 100µM to HUVECs reduced cell viability by about 27% (%cell viability vs control: 73.1 ± 1.9), and the pre-incubation of Taurisoló® 100µg/mL induced an almost full preservation of cell viability (%cell viability vs control: 95.0 ± 1.9). When the administration of Taurisoló® 100µg/mL was preceded by the pre-incubation of Sirtinol 10µM,

Taurisol[®] was unable to protect the endothelial cells against the oxidative damage (%cell viability vs control: 69.3 ± 2.8). The same inability was observed when Taurisol[®] administration was preceded by pre-incubation of Compound C 10µM (%cell viability vs control: 74.0 ± 6.7) and also when the two inhibitors, Sirt and CC, were co-pre-incubated in HUVECs before Taurisol[®] administration (%cell viability vs control: 70.7 ± 3.1) (**Figure 5.1.1^{II-A}**). The same experimental protocol was applied on HASMCs in which the administration of H₂O₂ 200µM reduced the vascular smooth muscle viability by about 28% (%cell viability vs control: 71.8 ± 2.4) and the pre-incubation of Taurisol[®] 100µg/mL prevented this reduction resulting in a %cell viability vs control of 96.4 ± 1.6. As already observed in HUVECs, also in HASMCs both the pre-incubation of Sirtinol and the pre-incubation of Compound C inhibited the protective effect exhibited by Taurisol[®] (%cell viability vs control: 76.7 ± 3.6 and 71.8 ± 4.7 respectively), as well as the co-administration of the two inhibitors (%cell viability vs control: 70.6 ± 1.4) (**Figure 5.1.1^{II-B}**).

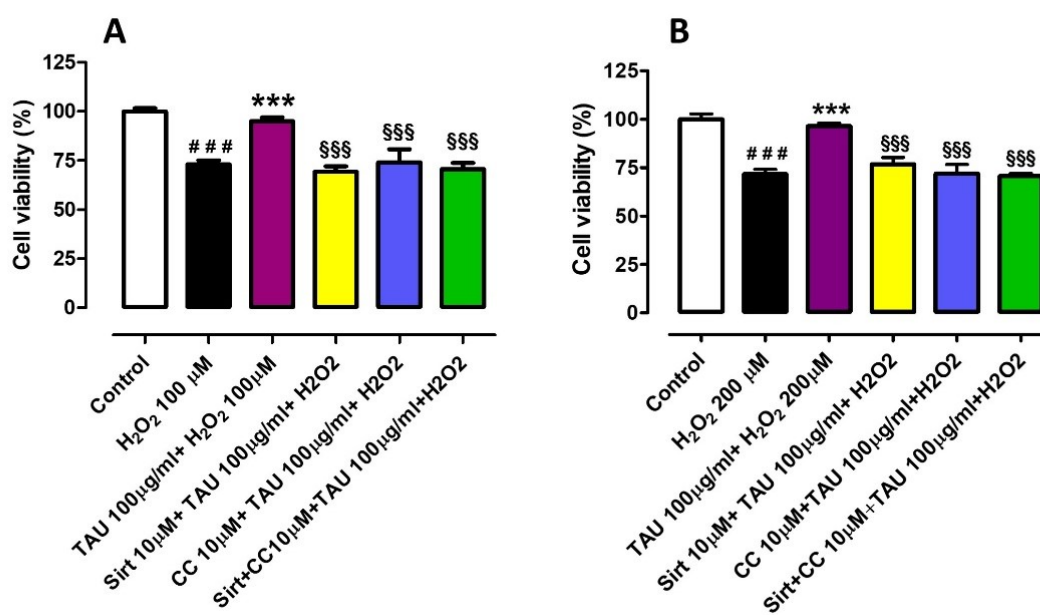


Figure 5.1.1^{II}. Evaluation of the protective effect induced by Taurisol[®] on HUVECs(A) and HASMCs (B) cell viability, against the H₂O₂-induced oxidative damage, in the presence and the absence of selective inhibitors of sirtuin pathway Sirtinol (Sirt) 10µM, of AMPK pathway, Compound C (CC) 10µM, or both. The coloured histograms indicate the % of cell viability of treated cells vs the value of cell viability in cells treated only with vehicle (Control, white histogram). All the experiments were repeated for a minimum of three times and each one was carried out in triplicate (n=9). The symbols indicate the level of statistical significance calculated by ANOVA one-way, followed by Bonferroni post-test: # indicates the significance vs Control, * indicates significance vs cells treated with H₂O₂, §

indicates the significance vs cells treated with Taurisol[®]+H₂O₂ (###p<0.001; ***p<0.001; \$\$\$p<0.001) [source: (Martelli et al., 2021)].

Then, the involvement of sirtuins and AMPK pathways was investigated by the measurement of ROS levels. In particular, in HUVEC cells, the administration of H₂O₂ induced an increase in ROS level by about 40% (%ROS vs control: 141.4 ± 6.7) while the pre-incubation of Taurisol[®] reduced the ROS level at a level even lower than control (%ROS vs control: 83.5 ± 9.0). When Sirtinol, Compound C or both were pre-incubated before Taurisol[®] and H₂O₂, they abolished the preventive effects of Taurisol[®] against ROS production (%ROS+Sirtinol vs control: 129.6 ± 6.7; %ROS+Compound C vs control: 134.9 ± 11.1; %ROS+Sirtinol+Compound C vs control: 141.9 ± 10.2) (Figure 5.1.1^{III-A}). On HASMCs, H₂O₂ evoked an increase of ROS by about 28% (%ROS vs control: 128.0 ± 4.6); pre-incubation of Taurisol[®] prevented this increase maintaining ROS levels lower than those exhibited in control conditions (%ROS vs control: 80.3 ± 5.7). Also in HASMCs, when the administration of Taurisol[®] and H₂O₂ was preceded by pre-incubation of Sirtinol or Compound C or both, the protective effect exhibited by Taurisol[®] against ROS increase was abolished (%ROS+Sirtinol vs control: 138.8 ± 6.8; %ROS+Compound C vs control: 122.1 ± 7.1; %ROS+Sirtinol+Compound C vs control: 147 ± 10.9) (Figure 5.1.1^{III-B}).

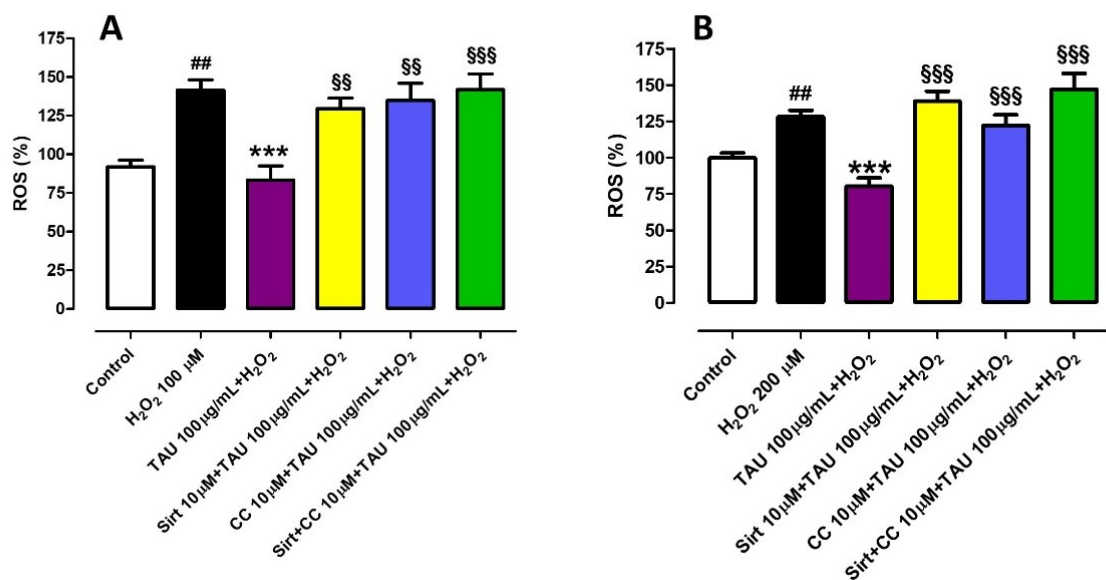


Figure 5.1.1^{III}. Evaluation of the protective effect induced by Taurisol[®] on HUVECs (A) and HASMCs (B) against the H₂O₂-induced ROS-increase, in the presence and in the absence of selective inhibitors of sirtuin pathway Sirtinol (Sirt) 10 µM, of AMPK pathway, Compound C (CC) 10 µM, or both. The coloured histograms indicate the % of ROS levels of treated cells vs the value of ROS levels in cells

treated only with vehicle (Control, white histogram). All the experiments were repeated for a minimum of three times and each one was carried out in triplicate (n=9). The symbols indicate the level of statistical significance calculated by ANOVA one-way, followed by Bonferroni post-test: # indicates the significance vs Control, * indicates significance vs cells treated with H₂O₂, § indicates the significance vs cells treated with Taurisol[®]+H₂O₂ (##p<0.01; ***p<0.001; §§p<0.01,§§§p<0.001) [source: (Martelli et al., 2021)].

The administration of increasing concentrations of Taurisol[®] to endothelium-intact aortic rings pre-contracted with KCl evoked a clear vasorelaxing effect (E_{max}= 80.6 ± 1.9 and pEC₅₀= 1.19 ± 0.03 corresponding about at 0.1mg/ml) which was completely endothelium-dependent and, in particular, nitric oxide (NO)-dependent. Indeed, when the administration of Taurisol[®] was repeated on endothelium-denuded aortic rings or on endothelium-intact aortic rings pre-treated with the inhibitor of NO- biosynthesis L-NAME, the vasorelaxing effect was completely abolished (Figure 5.1.1^{IV}).

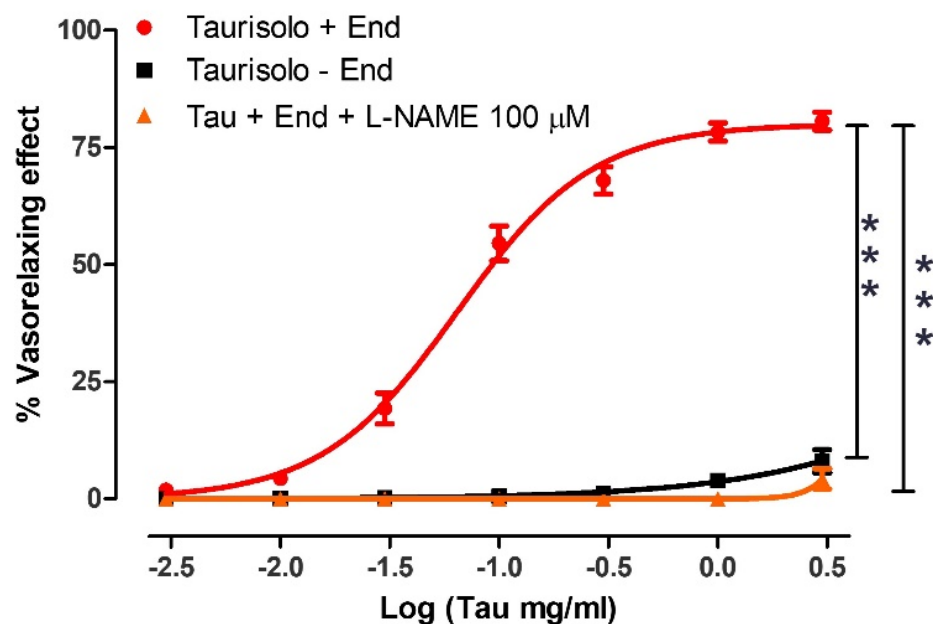


Figure 5.1.1^{IV}. Vasorelaxant effect induced by Taurisol[®] on endothelium-intact or endothelium-denuded rat aortic rings. In the red line the concentration-response curve induced by Taurisol[®] on endothelium-intact rat aortic rings pre-contracted with KCl 25mM. In the black line the concentration-response curve evoked by Taurisol[®] on endothelium-denuded aortic rings. Finally, in the orange line, the concentration-response curve induced by Taurisol[®] on endothelium-intact rat aortic rings in the presence of the inhibitor of the NO biosynthesis, L-NAME 100µM. The vertical bars indicate the SEM. Six different experiments were performed, each with six replicates (n=6). The asterisks indicate a

significant difference from the red curve obtained on endothelium-intact aortic rings (** $p < 0.001$) [source: (Martelli et al., 2021)].

The vasorelaxant concentration-response curve induced by Taurisol[®] was repeated on endothelium-intact rat aortic rings, in the presence of the inhibitor of Sirtuin pathway Sirtinol (Sirt 100 μ M), or the inhibitor of AMPK pathway Compound C (CC 100 μ M). In the aortic rings pre-incubated with Sirtinol, similar values of E_{max} but reduced values of pEC_{50} were observed ($E_{max} = 76.4 \pm 3.8$ and $pEC_{50} = 0.63 \pm 0.05$) if compared to the aortic rings in the absence of inhibitors (red line). The same behaviour was observed in aortic rings pre-incubated with Compound C which exhibited similar E_{max} but reduced pEC_{50} ($E_{max} = 73.7 \pm 3.8$ and $pEC_{50} = 0.57 \pm 0.06$). Finally, when the two inhibitors (Sirt and CC) were pre-incubated together on endothelium-intact rat aortic rings, they evoked again a similar value of E_{max} but a further reduction of pEC_{50} value even if compared with the vasorelaxing curve in the presence of a single inhibitor ($E_{max} = 76.5 \pm 1.8$ and $pEC_{50} = 0.27 \pm 0.04$) (Figure 5.1.1^V).

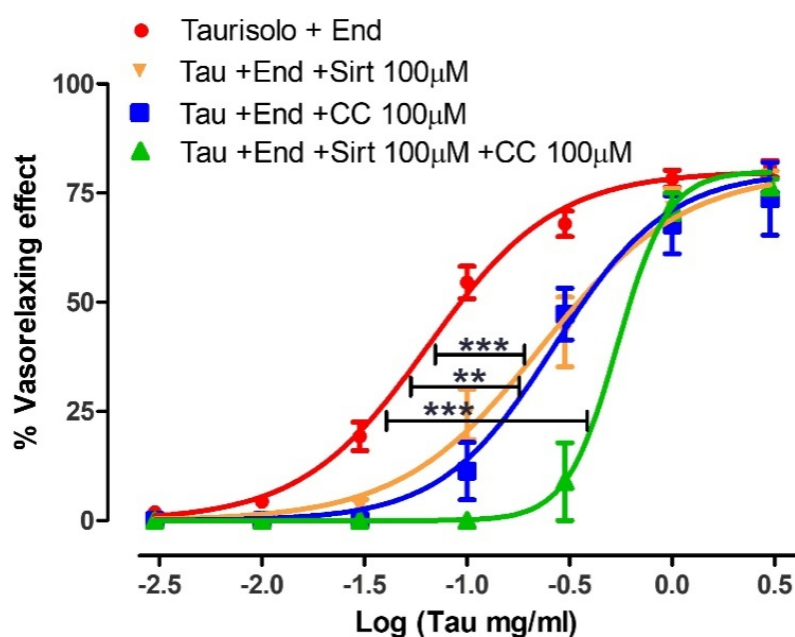


Figure 5.1.1^V. Vasorelaxant effect induced by Taurisol[®] on endothelium-intact in the absence or in the presence of Sirtuins and AMPK pathways inhibitors. In the red line the concentration-response curve induced by Taurisol[®] on endothelium-intact rat aortic rings, pre-contracted with KCl 25mM. In the orange line the concentration-response curve evoked by Taurisol[®] on endothelium-intact aortic rings pre-treated with the inhibitors of Sirtuins pathway, Sirtinol (Sirt 100 μ M). In the blue line, the concentration-response curve induced by Taurisol[®] on endothelium-intact rat aortic rings in the presence of the inhibitor of the AMPK pathway, Compound C (CC 100 μ M). In the green line, the

concentration-response curve induced by Taurisolo® on endothelium-intact rat aortic rings in the presence of both the inhibitors Sirt and CC 100µM. The vertical bars indicate the SEM. Six different experiments were performed, each with six replicates (n=6). The asterisks indicate a significant difference from the red curve obtained on endothelium-intact aortic rings (**p<0.01, ***p<0.001) [source: (Martelli et al., 2021)].

Besides the direct vasodilating effect, Taurisolo® was also able to inhibit the NA-induced vasoconstriction. In particular, in control endothelium-intact aortic rings, the administration of cumulative concentrations of NA induced a vasoconstricting concentration-response curve reaching an Emax of 88.9 ± 2.9 and a pEC50 of 7.21 ± 0.09. The pre-incubation of endothelium-intact aortic rings with Taurisolo® 10 or 30 or 100µg/mL, induced a concentration-dependent reduction both of Emax (Emax with Tau 10µg/mL= 75.4 ± .4; Emax with Tau 30µg/mL= 60.9 ± 5.9; Emax with Tau 100µg/mL= 52.0 ± 5.1) and of pEC50 values (pEC50 with Tau 10µg/mL= 6.81 ± 0.20; pEC50 with Tau 30µg/mL=6.84 ± 0.18; pEC50 with Tau 100µg/mL=6.86 ± 0.11) (Figure 5.1.1^{VI}).

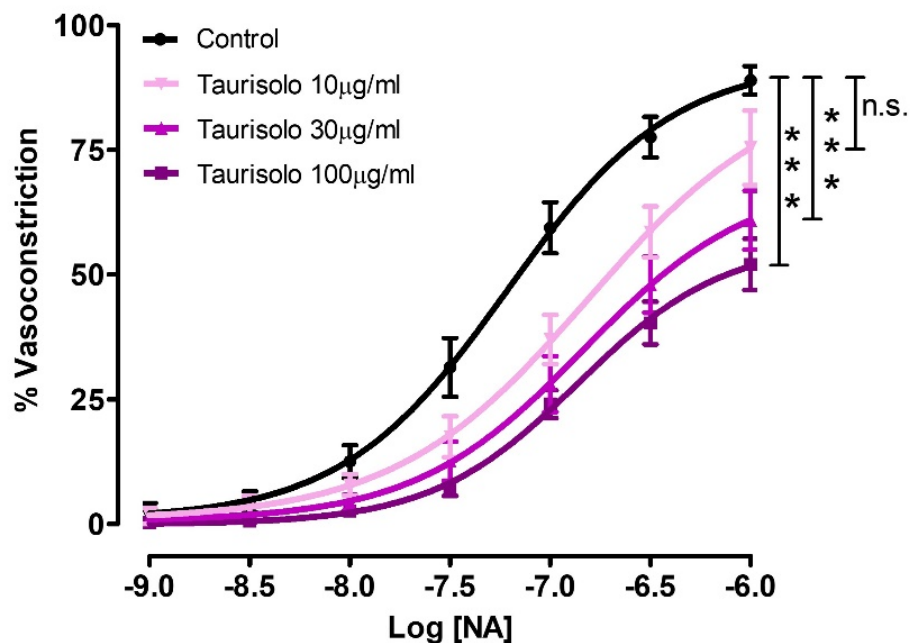


Figure 5.1.1^{VI}. Inhibition of NA-induced vasoconstriction by three different concentrations of Taurisolo®. The curves represent the vasoconstrictant response to cumulative concentrations of NA in endothelium-intact aortic rings pre-incubated with vehicle (Control) or Taurisolo® at the concentrations of 10, 30 and 100 µg/mL. The vasoconstrictant effects are expressed as a% of the contractile responses induced by the administration of KCl 60mM. The vertical bars indicate the SEM. Six different experiments were performed, each with six replicates (n=6).The asterisks indicate a

significant difference from the Control vasoconstriction curve (line in black).(n.s.= not significant; ***p<0.001) [source: (Martelli et al., 2021)].

As reported in scientific literature, resveratrol exerts many of its cardiovascular protective effects, especially against endothelial dysfunction, through the activation of Sirtuin-1 and AMPK (San Cheang et al., 2019). The results obtained on HUVECs and HASMCs confirmed that also Taurisol[®] exhibited a protective effect against endothelium and vascular smooth muscle oxidative processes, through the activation of Sirtuin and AMPK pathways. The involvement of the Sirtuins-AMPK pathways in the cardiovascular effects of Taurisol[®] seems to be confirmed in the experiments on the rat aortic rings, in which the endothelium-dependent/NO-dependent vasodilation induced by Taurisol[®] was impaired when Sirtuins-AMPK pathways were inhibited by the administration of selective blockers. These findings are consistent with the evidence widely described in the literature for resveratrol: activation of Sirtuin-1/AMPK-pathway induces the phosphorylation of eNOS which leads to an increase in NO biosynthesis and to vasodilation (Bonnefont-Rousselot, 2016; Xia et al., 2014).

➤ Animal data

We firstly evaluated the effect of chronic administration with Taurisol[®] on systolic blood pressure values in spontaneously hypertensive rats (SHRs). As expected, between the 6th and the 10th week of age, SHRs showed a progressive increase in blood pressure. In particular, during the 4 weeks of treatment, the systolic blood pressure of SHRs belonging to the “Control group” increased by about 50mmHg reaching values of 234 ± 2 mmHg. In SHRs which received Taurisol[®] 10mg/Kg/die the increase of systolic blood pressure was slightly restrained to 225 ± 1 mmHg, while in the SHRs which received Taurisol[®] 20mg/Kg/die the increase of systolic blood pressure values was significantly inhibited, reaching, at the end of the 4th week, values of 200 ± 2 mmHg similar to those recorded in SHRs treated with the reference drug Captopril 20mg/Kg/die (190 ± 3 mmHg) (**Figure 5.1.1^{VII}**).

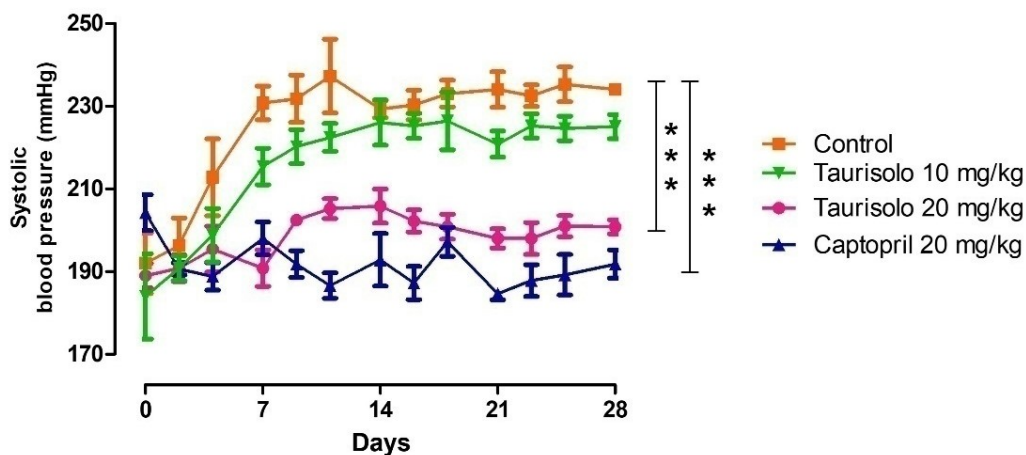


Figure 5.1.1^{vii}. Daily recordings of systolic blood pressure values in SHR_s during the *in vivo*, 4-weeks long chronic, *per os* treatment with: drinking water (Control group, orange line), Taurisol[®] 10mg/Kg/die (green line), Taurisol[®] 20mg/Kg/die (pink line), Captopril 20mg/Kg/die (blue line). The vertical bars indicate the SEM. The asterisks indicate a significant difference from the Control SHR_s group. (***p<0.001) [source: (Martelli et al., 2021)].

The same recordings were then grouped to express the weekly means of systolic blood pressure values before and during the *in vivo*, chronic, *per os* treatment (**Table 5.1.1ⁱ**).

Table 5.1.1ⁱ. Weekly mean of the systolic blood pressure values (mmHg) recorded in SHR_s during the *in vivo*, chronic, oral treatment with: tap water (Control), Taurisol[®] 10mg/Kg/die, Taurisol[®] 20mg/Kg/die, Captopril 20mg/Kg/die [source: (Martelli et al., 2021)].

Week	Control	Taurisol [®] 10mg/Kg/die	Taurisol [®] 20mg/Kg/die	Captopril 20mg/Kg/die
0	184 ± 6	178 ± 7	185 ± 4	194 ± 2
1	212 ± 4	202 ± 3	192 ± 3**	193 ± 2**
2	233 ± 5	223 ± 4	205 ± 2***	191 ± 3***
3	232 ± 3	224 ± 4	200 ± 2***	190 ± 2***
4	234 ± 2	225 ± 1	200 ± 2***	189 ± 3***

*Significance level vs weekly mean values (mmHg) of the Control SHR_s: **p<0.01, ***p<0.001

At the end of the 4-week-long chronic treatment, aorta of SHR_s was excised and aortic rings were mounted in a bath in order to perform the endothelium functionality test. The aortic rings belonging to SHR_s treated only with tap water (Control group) exhibited a reduced vasorelaxing response after Ach administration ($E_{max} = 59.6 \pm 3.6$), giving evidence of an endothelial dysfunction. The aortic rings from SHR_s treated with Taurisol[®]10mg/Kg/die exhibited a partial but significant recovery of the endothelial function ($E_{max} = 74.5 \pm 2.8$) similar to that induced by Captopril 20mg/Kg/die ($E_{max} = 80.2 \pm 3.7$). Finally, the aortic rings deriving from SHR_s treated with Taurisol[®] 20mg/Kg/die exhibited the maximum protection of the endothelial function giving a significant, almost full, vasorelaxing effect ($E_{max} = 88.9 \pm 1.5$) (**Figure 5.1.1^{viii}**).

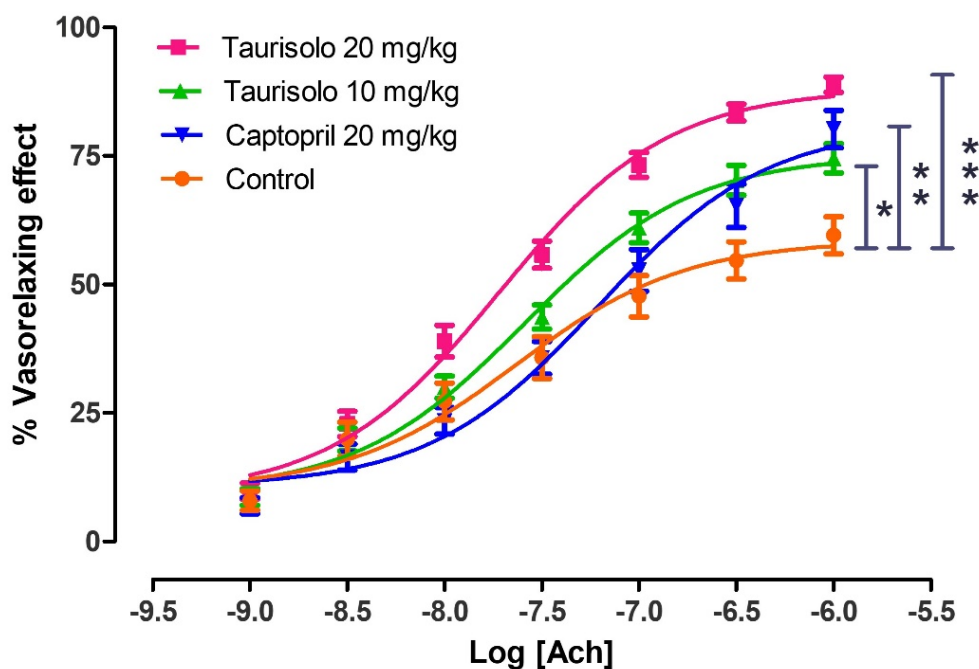


Figure 5.1.1^{viii}. Evaluation of endothelial dysfunction in aortic rings excised by SHR treated for 4 weeks, orally with: tap water (Control, orange line), Taurisolo® 10mg/Kg (green line), Taurisolo® 20mg/Kg (pink line), and the reference drug Captopril 20mg/Kg (blue line). The experiments were carried out in 5 replicates and the five rings derived from 5 different SHRs (n=5). The vertical bars indicate the SEM. The asterisks indicate a significant difference from the Control SHRs group. (*p<0.05, **p<0.01, ***p<0.001) [source: (Martelli et al., 2021)].

In order to demonstrate that the impaired ACh-induced vasorelaxation observed in control SHRs actually derived from the dysfunction of the endothelial tissue (i.e. reduced biosynthesis of endothelial NO), and was not due to a reduced sensitivity of vascular smooth muscle to NO, the vasorelaxing activity of sodium nitroprusside (SNP) was tested. Indeed, SNP is a NO-donor i.e. a vasorelaxant compound which generates exogenous NO independently from the vascular endothelium. In particular, SNP concentration-response curves were performed on aortic rings deriving from SHRs belonging to the different groups of chronic treatments. The administration of cumulative concentrations of SNP to aortic rings from SHRs treated with tap water (Control), Taurisolo® 10mg/Kg/die, Taurisolo® 20mg/Kg/die and Captopril 20mg/Kg/die evoked almost fully comparable vasorelaxing effects (**Figure 5.1.1^{ix}**). This confirmed the exclusive role of endothelial dysfunction in the reduced ACh-induced vasorelaxation.

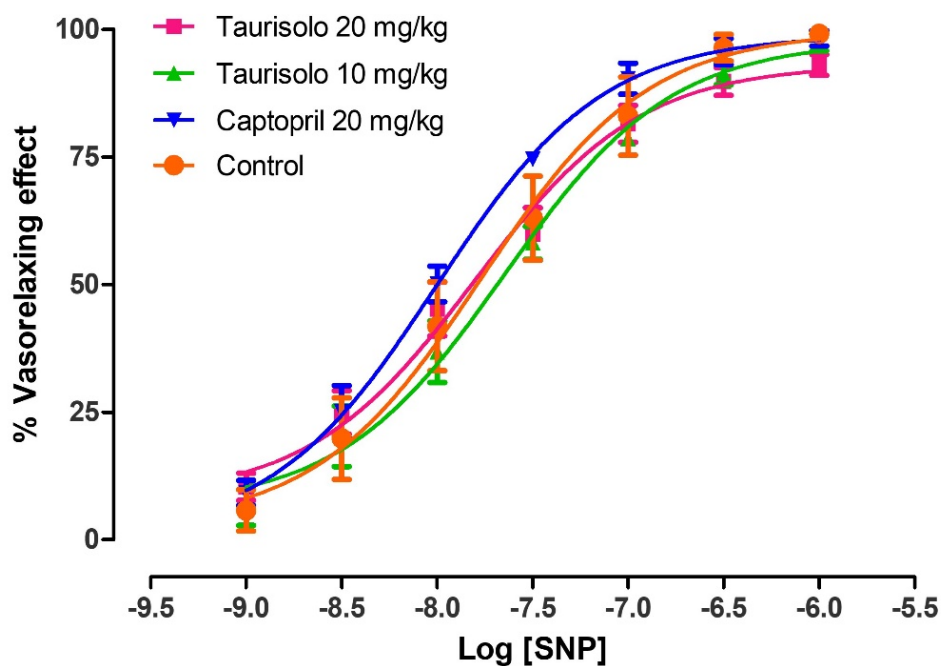


Figure 5.1.1^X. Evaluation of smooth muscle functionality in the aortic rings excised by SHRs treated for 4 weeks, orally with: tap water (Control, orange line), Taurisol® 10mg/Kg (green line), Taurisol® 20mg/Kg (pink line), and the reference drug Captopril 20mg/Kg (blue line). The experiments were carried out in 3 replicates and the five rings derived from 5 different SHRs(n=5). The vertical bars indicate the SEM [source: (Martelli et al., 2021)].

As the increase of blood pressure values in SHRs is coupled with the development of cardiac hypertrophy, at the end of the 4-week-long treatment the heart of SHRs was excised and weighted. In particular, the reference drug Captopril, as other ACE-inhibitors which are gold standards in the prevention/reversion of cardiac hypertrophy, induced a significant anti-hypertrophic effect if compared to the hearts of the Control group (heart weight/rat weight= 3.87 ± 0.10 g/Kg *vs* 4.30 ± 0.03 , respectively). Taurisol® 10mg/Kg/die induced a slight, non-significant reduction of the cardiac hypertrophy (heart weight/rat weight= 4.16 ± 0.09 g/Kg) while the hearts deriving from SHRs treated with Taurisol® 20mg/Kg/die exhibited a value of cardiac hypertrophy significantly different from that exhibited by the hearts excised by SHRs belonging to the control group (heart weight/rat weight= 3.96 ± 0.09 vs 4.30 ± 0.03) (Figure 5.1.1^X).

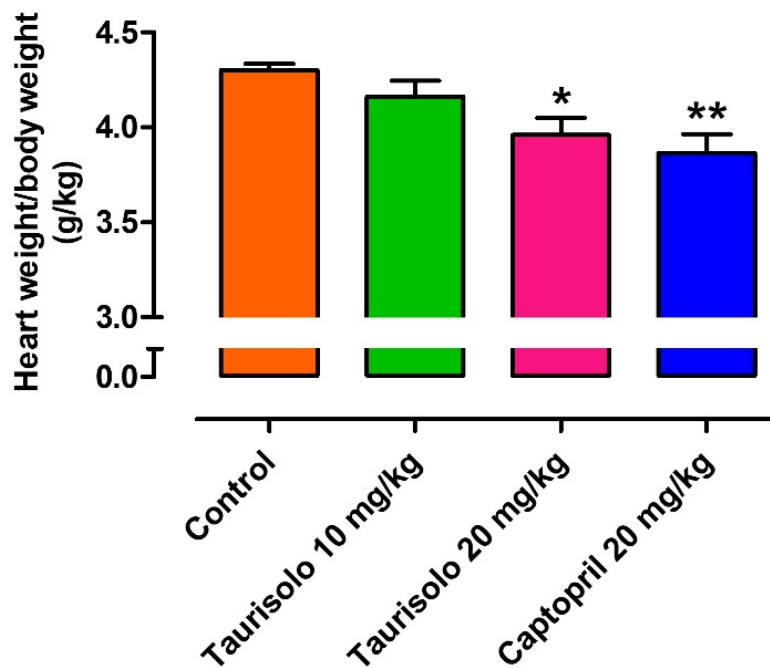


Figure 5.1.1^X. Evaluation of the anti-hypertrophic effect induced by Taurisolo[®] 10mg/Kg (green line), Taurisolo[®] 20mg/Kg (pink line), and the reference drug Captopril 20mg/Kg (blue line) on the SHR hearts after 4 weeks of chronic, oral treatment. The experiments were carried out on the hearts from 5 different SHRs for each treatment (n=5). The vertical bars indicate the SEM. The asterisks indicate a significant difference from the hearts deriving from the Control group. (*p<0.05, **p<0.01) [source: (Martelli et al., 2021)].

Finally, we investigated the indirect effect of Taurisolo[®] on platelet activation performing a murine ex vivo model of clot retraction. Results were assessed by macroscopic clots morphology (**Figure 5.1.1^{XI-A-D}**) and numerically (clot score) by clots weights (**Figure 5.1.1^{XI-E}**) and residual serum volumes (**Figure 5.1.1^{XI-F}**). It was observed that samples from Taurisolo[®]-treated mice (10 and 20 mg/Kg; p.o.) were less retracted compared to Control group ($p \leq 0.05$ vs Ctrl, **Figure 5.1.1^{XI-E}**), suggesting that Taurisolo[®] administrated at the higher doses of 10 and 20 mg/Kg decreased the clot retraction rates of platelets. No significant differences were found in the production of serum (**Figure 5.1.1^{XI-F}**). Successively, we analyzed the effect of Taurisolo[®] on the biochemical indicators of coagulation. As shown in **Figure 5.1.1^{XI-I}** the administration of Taurisolo[®] at the dose of 10 and 20 mg/kg induced a significant decrease of fibrinogen (expressed as mg/dl) compared to Control group ($p \leq 0.05$; $p \leq 0.01$ respectively for Taurisolo[®]10 and 20 mg/Kg). No significant differences were found for serum concentrations of prothrombin time and partial thromboplastin time (expressed as seconds) in all experimental groups (**Figure 5.1.1^{XI-G,H}**).

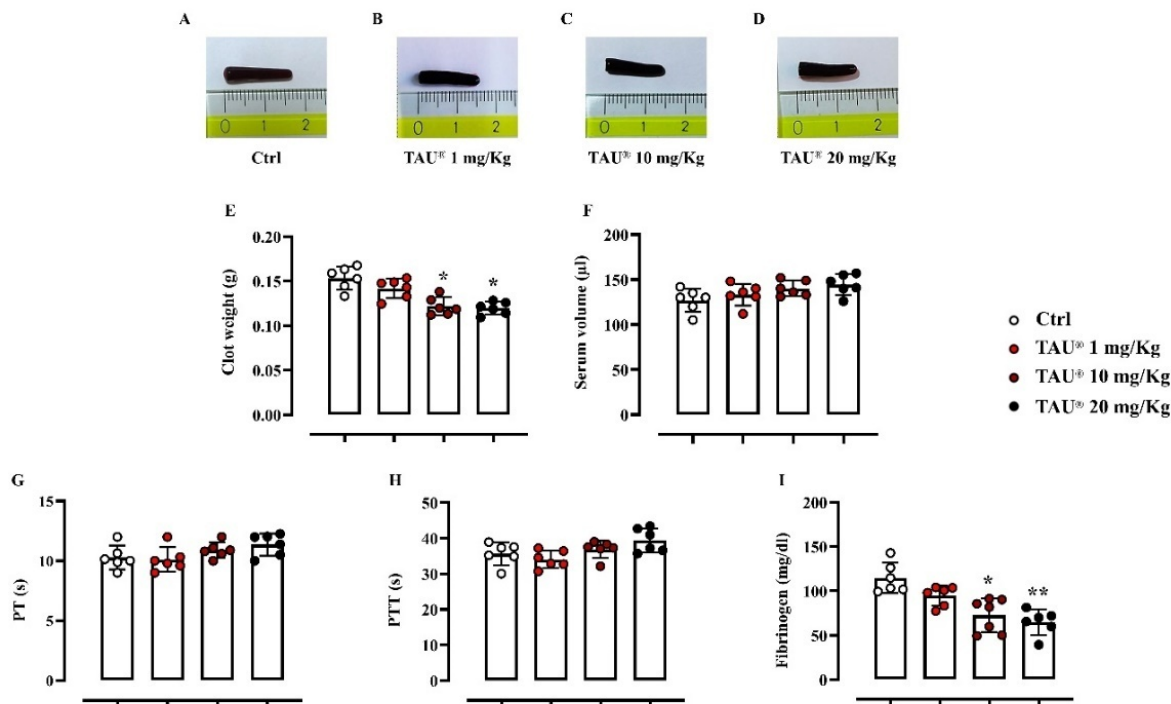


Figure 5.1.1^{XI}. Effect of Taurisol® (TAU®) on ex vivo clot retraction and coagulation's indexes (PT, PTT, fibrinogen). The impact of TAU® (1-20 mg/Kg) on platelet activation was evaluated by clots morphology (A-D), quantification of clot weights (E) and residual serum volumes (F). The effect on coagulation process and fibrinolytic activity were also determined by measuring PT, PTT and fibrinogen levels (G-I). Data are presented as means \pm SD of n=6 mice per group. Statistical analysis was conducted by one-way ANOVA followed by Bonferroni's for multiple comparisons. *p \leq 0.05, **p \leq 0.01 vs Ctrl-treated group [source: (Martelli et al., 2021)].

The results obtained in *in vitro* experiments were translated in the *in vivo* pre-clinical model represented by SHRs, which is a recognized animal model of hypertension, endothelial dysfunction, and cardiac hypertrophy. The sphygmomanometric "tail-cuff" method allows to better reproduce the situation more similar to the clinic one because SHRs are conscious. On the other hand, to avoid the possible alteration of blood pressure due to the animal manipulation, SHRs were trained, for two weeks before the beginning of compound administration, to be handled and to allow blood pressure procedures. As the aim of our work was to evaluate potential prevention of hypertension, endothelial dysfunction, and cardiac hypertrophy by Taurisol®, the SHRs were selected and treated from the 6th to the 10th week of age, since in that interval their blood pressure values, and the consequent degeneration of endothelial and myocardial tissues, are not yet well-established but are in progress. The choice of Captopril as a reference drug was due to its recognized properties to control blood pressure levels and to protect cardiovascular tissues from degenerative processes, especially myocardial remodeling which leads to cardiac hypertrophy. The Taurisol® doses were selected on the basis of previous studies that demonstrated a protective effect by Taurisol® against rat brain ischemia-reperfusion injury (Lapi et al., 2020) and to the observation that the

doses 10mg/Kg and 20mg/Kg in SHRs correspond to about 115mg and 230mg/die in humans of about 70Kg (Reagan-Shaw et al., 2008). These doses are well compatible with a daily assumption of this supplement. During the chronic, 4-week long *in vivo* treatment, oral Taurisolo®20mg/Kg/die, demonstrated a significant inhibition of blood pressure increase, from the first week of treatment to the end of the study. As expected, the metabolic parameter represented by fasting blood glucose level and lipidic panel were not altered in SHRs belonging to the Control group and the administration of Taurisolo® did not change significantly the normal metabolic profile of this pre-clinical animal model. Instead, the evaluation of Taurisolo®'s impact on endothelial dysfunction highlighted a marked protection of endothelial function by Taurisolo® which reaches the statistical significance at the lowest dosage of 10mg/Kg/die and which was even better than that exhibited by Captopril at the dosage of 20mg/Kg/die. Finally, Taurisolo® 20mg/Kg/die induced also significant prevention of the cardiac hypertrophy developed by SHRs, for which the gold standard is represented by ACE-inhibitors like Captopril.

These evidences were also supported by data from *ex vivo* clot retraction and coagulation's indexes. In particular, chronic treatment with Taurisolo® at dose of 10 and 20 mg/kg was able to modify platelet activation and clot formation in mice. Accordingly, fibrinogen levels were down-regulated in Taurisolo®-treated mice compared to Ctrl (without any effect on PT and PTT time) suggesting an extrinsic modulation of coagulation's cascade.

➤ Clinical data

In order to translate both the *in vitro* and the animal-based results into the clinical practice, we also investigated the effects of Taurisolo® on endothelial function in humans. The RCT was conducted on young adults, healthy volunteers. Overall study duration was 12 weeks: 2-week run-in period (without any treatment); 8-week intervention period and 2-week follow-up period. The examinations were performed in an outpatient setting. Clinical examinations and blood sampling were performed after 12h of fasting at weeks 2 and 10. Study participants were randomized into two treatment arms: active group and placebo group. This study was conducted both in acute and chronic. For the acute study, 800mg of Taurisolo® or maltodextrins were administered to each study participant randomized into the relative intervention group. For the chronic study, subjects in the active group were administered with 400mg Taurisolo® twice daily, while subjects in the placebo group were administered with equivalent dose of maltodextrins.

A total of 30 human subjects were screened for eligibility; 4 subjects did not pass the screening phase. Overall, 26 subjects were randomized into active group (n=13) and placebo group (n=13). According to CONSORT PRO guidelines. **Figure 5.1.1^{XII}** shows the flow of study participants through the trial together with the completeness of diary information over the entire treatment period.

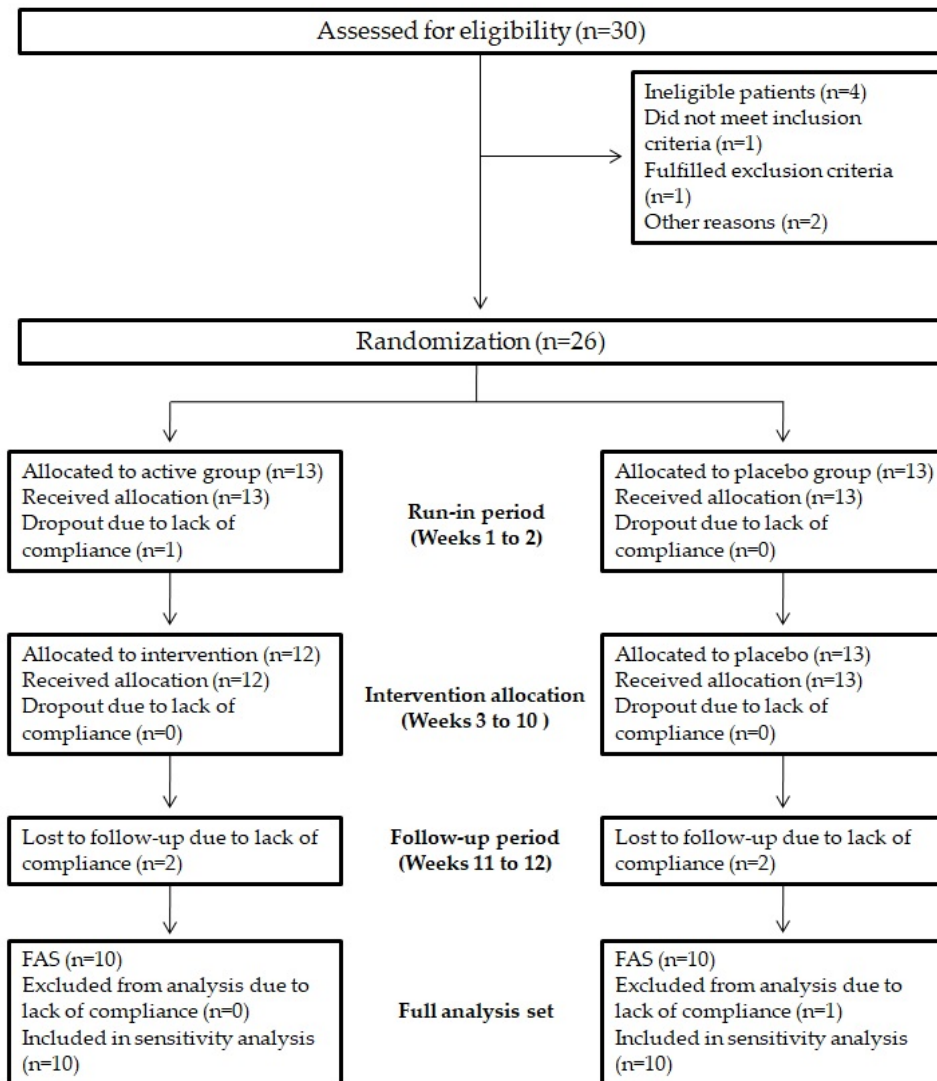


Figure 5.1.1^{xii}. Study flowchart. Study flowchart, according to the consolidated standards of reporting trials (CONSORT) [source: (Martelli et al., 2021)].

Table 5.1.1ⁱⁱ reports baseline demographic and clinical characteristics of the 20 subjects completing the study. Overall, the mean age was 24±3years and BMI 22.3±5kg/m². The majority of study participants (65%) were non-current smokers and regular physical activity practitioners (55%). Serum levels of metabolic parameters were within the normal range for age and sex; serum levels of ox-LDL reflected a strong alteration, while D-ROMs levels fell within the normal range value.

Clinical characteristic variation before and after 8-week treatment with Taurisolo® or placebo are reported in **Table 5.1.1ⁱⁱⁱ**.

Table 5.1.1^{II}. Baseline characteristics of study participants [source: (Martelli et al., 2021)].

Variable	Value \pm SD
<i>Demographic characteristics</i>	
Subjects (No)	20
Age (years)	24.46 \pm 2.99
Male sex (No (%))	11 (55%)
White ethnicity (No (%))	20 (100%)
Smokers (No (%))	7 (35%)
Regular physical activity (No (%))	11 (55%)
<i>Anthropometric characteristics</i>	
Weight (Kg)	66.03 \pm 11.79
Height (cm)	1.69 \pm 0.10
BMI (Kg/m ²)	22.30 \pm 4.87
WC (cm)	76.82 \pm 11.52
HC (cm)	98.09 \pm 5.37
WHR	0.72 \pm 0.25
<i>Serum parameters</i>	
Glycaemia (mg/dl)	66.78 \pm 12.71
TC (mg/dl)	145.85 \pm 32.82
TG (mg/dl)	51.92 \pm 16.86
HDL-c (mg/dl)	49.22 \pm 12.14
LDL-c (mg/dl)	84.05 \pm 34.00

OxLDL ($\mu\text{Eq/L}$)	1031.15 \pm 676.50
D-ROMs (UCARR)	259.33 \pm 104.94
<hr/>	
<i>Endothelial function</i>	
<hr/>	
FMD (%)	6.48 \pm 3.28
RHI	3.26 \pm 1.24
<hr/>	

Table 5.1.1^{III}. Differences between the two intervention groups before and after the 8-week treatment. No significant differences were evident between the two groups before treatment. *Values are expressed as mean \pm SD (three repetitions); statistical significance is calculated by Student's t-test [source: (Martelli et al., 2021)].

Parameters	Taurisolo® (n = 10)		Placebo (n = 10)		p-value		
	Initial	Final	Initial	Final	Initial (Taurisolo® vs. Placebo)	Taurisolo® (initial vs. final)	Placebo (initial vs. final)
Age (years)	24.17 \pm 0.98	-	24.71 \pm 4.11	-	0.757	-	-
Male sex (No (%))	6 (60%)	-	5 (50%)	-	$\chi^2 = 0.202$; $p = 0.653$	-	-
Smokers (No (%))	4 (40%)	-	3 (30%)	-	$\chi^2 = 0.219$; $p = 0.639$	-	-
Regular physical activity (No (%))	5 (50%)	-	6 (60%)	-	$\chi^2 = 0.202$; $p = 0.653$	-	-
Weight (Kg)	67.53 \pm 11.82	67.33 \pm 11.23	64.52 \pm 12.67	64.35 \pm 13.13	0.679	0.672	0.602
Height (cm)	1.67 \pm 0.10	-	1.71 \pm 0.11	-	0.499	-	-
BMI (Kg/m ²)	24.24 \pm 2.59	24.19 \pm 2.42	21.97 \pm 2.26	21.89 \pm 2.39	0.136	0.738	0.524
WC (cm)	78.75 \pm 15.15	78.38 \pm 15.19	74.50 \pm 5.72	74.64 \pm 5.06	0.570	0.188	0.744
HC (cm)	101.92 \pm 2.15	101.60 \pm 2.54	93.50 \pm 4.24	93.28 \pm 4.25	0.002	0.242	0.189
WHR	0.77 \pm 0.14	0.77 \pm 0.13	0.80 \pm 0.05	0.80 \pm 0.05	0.716	0.475	0.403
Glycaemia (mg/dl)	63.32 \pm 11.55	74.68 \pm 5.82	69.76 \pm 13.77	72.66 \pm 6.50	0.386	0.234	0.420
TC (mg/dl)	143.67 \pm 39.88	154.25 \pm 14.48	147.71 \pm 28.63	142.57 \pm 18.87	0.835	0.055	0.318
TG (mg/dl)	56.83 \pm 17.88	52.25 \pm 27.28	47.71 \pm 16.04	51.57 \pm 18.83	0.353	0.474	0.125
HDL-c (mg/dl)	43.63 \pm 5.77	53.75 \pm 6.55	54.01 \pm 14.46	51.56 \pm 12.95	0.129	0.062	0.122

LDL-c (mg/dl)	88.67 ± 37.61	90.05 ± 20.73	80.10 ± 33.06	80.70 ± 23.09	0.670	0.744	0.910
oxLDL (μEq/L)	1005.00 ± 389.81	639.50 ± 188.74	1053.57 ± 887.36	1051.43 ± 889.95	0.904	0.043	0.945
D-ROMs (UCARR)	297.08 ± 84.06	227.75 ± 20.01	226.97 ± 116.16	227.11 ± 88.26	0.246	0.008	0.995
FMD (%)	6.67 ± 4.56	12.61 ± 2.92	6.31 ± 2.03	6.24 ± 1.62	0.852	0.019	0.763
RHI	2.95 ± 1.10	4.15 ± 1.03	3.63 ± 1.43	3.69 ± 1.60	0.394	0.079	0.920

Endothelial function was evaluated at baseline, in the acute phase (1h after administration of Taurisolo® 800 mg or placebo) and in long-term phase (after 8-week treatment with Taurisolo®400 mg twice daily or placebo). As shown in **Figure 5.1.1^{xiii}**, we observed significant increases in FMD both in acute (p versus baseline =0.021) and during long-term supplementation (p versus baseline =0.019) in active group. Also, in active group RHI did not show any change in the acute phase (p versus baseline =0.613), whereas a trend toward increase was found after 8-week supplementation of Taurisolo® (p versus baseline =0.079). No significant changes were observed for FMD and RHI in placebo group during the study observation time.

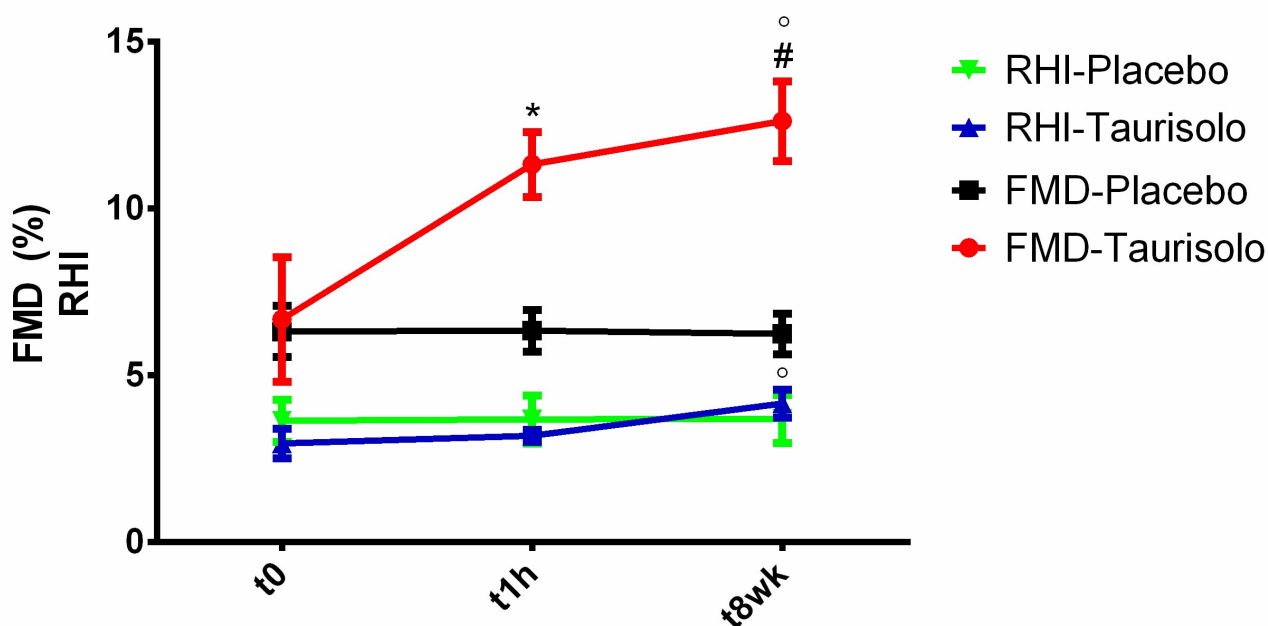


Figure 5.1.1^{xiii}. Acute and chronic effect of Taurisolo® on FMD and RHI. The effect of Taurisolo® on endothelial function was evaluated by monitoring FMD and RHI both in acute and after 8-week treatment period. Values are expressed as mean ± SD (three repetitions); statistical significance is calculated by Student’s t-test. *p < 0.05 t0 vs. t1h; # p < 0.05 t0 vs. t8wk; °p < 0.05 t1h vs. t8wk [source: (Martelli et al., 2021)].

The acute effect may be explained by the high bioavailability of Taurisolo® polyphenols. The acute effects herein observed are in line with previous studies reporting the ability of grape polyphenols to increase FMD within one hour after oral administration (Boban et al., 2006; Hampton et al., 2010; Karatzi et al., 2008, 2007; Lekakis et al., 2005; Li et al., 2013; Papamichael et al., 2004; Wong et al., 2013). Similarly, a number of studies reported the effects of chronic administration of grape polyphenols on endothelial function in terms of increased FMD (Akbari et al., 2019; Barona et al., 2012; Clifton, 2004). Also in this case, our results in humans reflect what previously published. According to the available literature, the most relevant mechanism of action for the FMD-increasing effect of chronic polyphenol administration is related to their action on NO production and release that, in turn, is strongly related to FMD. In this sense, our results demonstrating the endothelium-dependent/NO-dependent vasodilation induced by Taurisolo® may

serve to provide a solid explanation for our clinic observation, representing a potential mechanism of action for both acute and chronic FMD-increasing effects of Taurisolo®.

Since the endothelial function is susceptible to oxidative stress, we also investigated the effects of chronic Taurisolo® administration on oxLDL and D-ROMs, as oxidative stress-related serum biomarkers. Serum levels of oxLDL and D-ROMs were monitored in all study participants before and after 8-week treatment with Taurisolo® (Figure 5.1.1^{XIV}). oxLDL and D-ROMs serum levels significantly reduced by 36.36% ($p=0.043$) and 23.33% ($p=0.008$), respectively, in active group, while no significant variations were observed in placebo group.

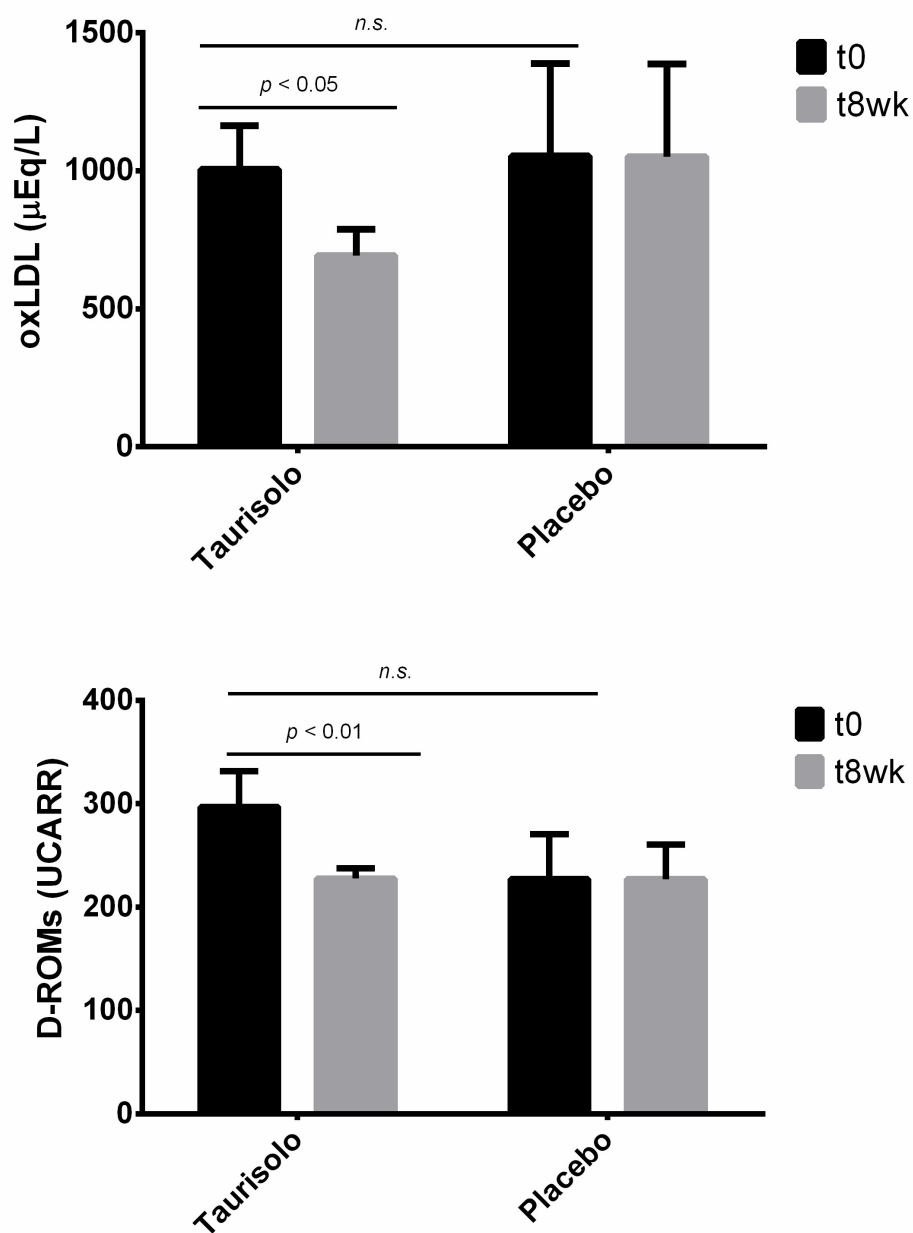


Figure 5.1.1^{xiv}. Chronic effect of Taurisolo[®] on oxidative stress-related biomarkers. Serum levels of oxLDL and D-ROMs, as oxidative stress-related biomarkers, were monitored before and after 8-week treatment with Taurisolo[®] or placebo. Values are expressed as mean \pm SD (three repetitions); statistical significance is calculated by Student's t-test [source: (Martelli et al., 2021)].

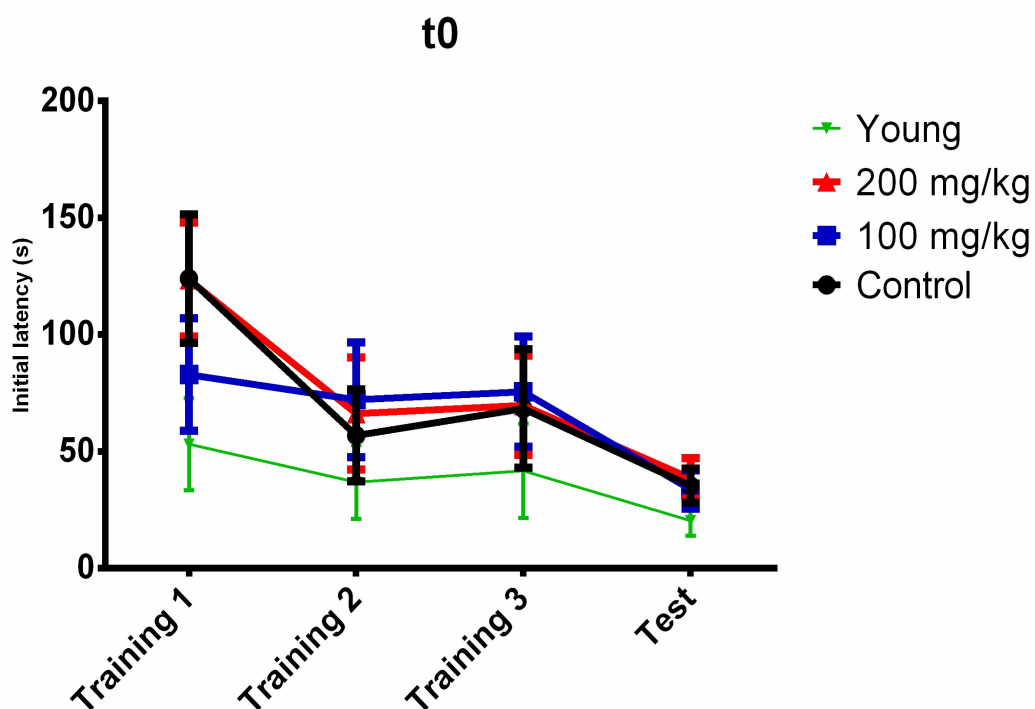
The main putative mechanisms for the oxLDL- and DROMs-reducing effects of Taurisolo[®] have been discussed in section 3.

In conclusion, the pharmacological characterization carried out on the cardiovascular properties exhibited by Taurisolo[®], demonstrated that it represents a nutraceutical product able to induce a protective effect on both endothelium and smooth muscle of the vascular wall, against oxidative stimuli. Taurisolo[®], thus, emerged as a nutraceutical particularly useful for the prevention of the CVD starting with the alteration of the integrity and the functionality of the vascular wall. These phenomena are mainly based on oxidative processes that characterize the gradual ageing of tissues and which are caused by a fat-rich diet or metabolic disorders like metabolic syndrome, obesity, diabetes, and hypercholesterolemia. Both the gradual chronic degeneration due to ageing and the acute attack by cytokines due to infections lead to a dysfunctional endothelium unable to perform its vasodilating and antiplatelet effects mediated by NO, leading to thromboembolic complications. The results obtained in this study confirmed the ability of Taurisolo[®] to arrest the deterioration of the vessels and to protect the endothelial function, inducing the prevention of cardiovascular diseases like hypertension, myocardial infarct, stroke, erectile dysfunction, and cognitive impairment.

5.2 Neurodegenerative disorders

The protective effect of Taurisolo® on brain health, and in particular on aged brain-associated cognitive decline, was evaluated with an animal-based study conducted during the internship at the Research Group in Community Nutrition and Oxidative Stress and Health Research Institute of the Balearic Islands (IdISBa), University of Balearic Islands, Palma de Mallorca (Spain) as required by this PhD program, and in collaboration with the Laboratory of Neurophysiology, Biology Department of the same University (**article in press**). The study (which methods are detailed in **Appendix B**) was conducted on aged rats (20 months aged, n=24) randomly allocated into three groups: control (Ctr; administered with 50 mg/kg maltodextrins daily; n=8), active group 1 (100; administered with 100 mg/kg Taurisolo® daily; n=8) and active group 2 (200; administered with 200 mg/kg Taurisolo® daily; n=8). An additional group of young rats (3 months aged, n=8) were treated with 50 mg/kg maltodextrins, and used as positive control (young). Both treatments (maltodextrins and Taurisolo®) were orally administered for 30 days. Behavioural tests licensed for the study of cognitive and motor functions (Barnes Maze test and Rotarod test) were conducted before and after treatment period.

The effects of chronic treatment with Taurisolo® on learning and memory were evaluated with the Barnes Maze Test. At the start of the treatment (t0), both the initial and the final latency were no significantly different in animals from the three aged treatment groups, among the three training sessions and the test (**Figure 5.2'**). As expected, the initial latency of young rats was lower than aged; however, in young rats, the final latency was surprisingly higher, in particular during the third training.



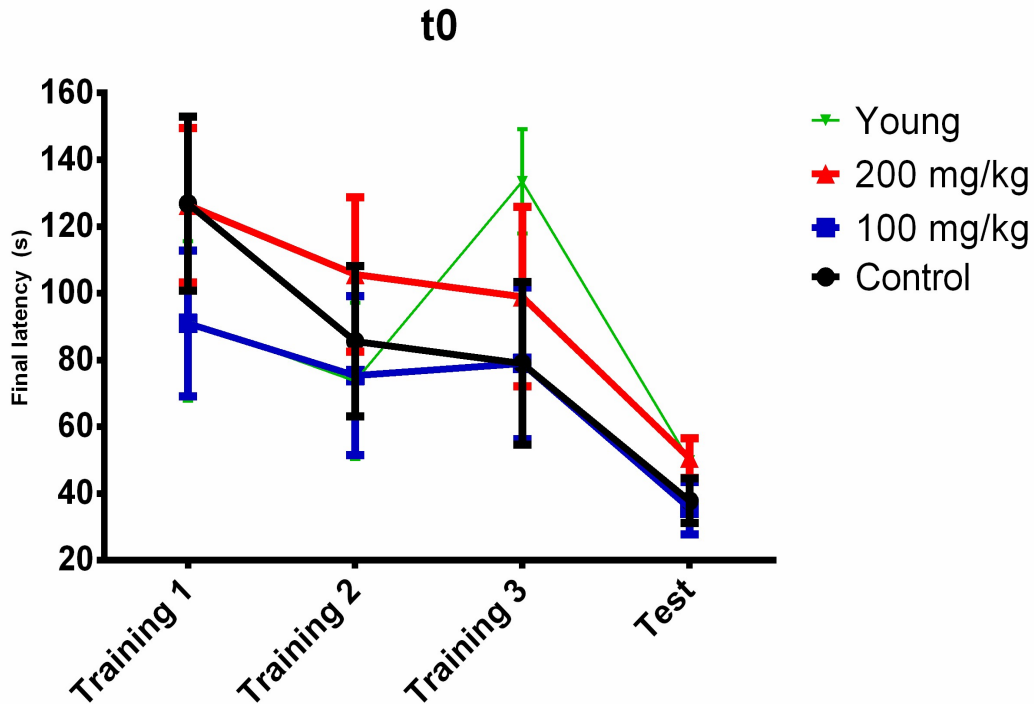


Figure 5.2^I. Barnes Maze Test. Initial and final latency at the start of the treatment.

On the contrary, at the end of the treatment (t30) significant differences were observed, as shown in **Figure 5.2^{II}**. At t30 the initial latency of both the animal groups treated with Taurisol® was lower than the aged rats control group, although only the differences between the control group and the 100-group registered during the training 3 were significant (90.38 ± 75.47 sec *vs.* 35.62 ± 37.60 sec, Ctr *vs.* 100, $p < 0.05$). On the other hand, the final latency of the 200-group was almost similar to Ctr, while that of the 100-group was lower; however, also in this case, the differences between the 100-group and the Ctr were significant at the training 3 (104.13 ± 66.28 sec *vs.* 37.87 ± 37.52 sec, Ctr *vs.* 100, $p < 0.05$). The observed reduction of the latency during both the training sessions and the test suggests an improvement of the visuospatial memory. The animals, indeed, spent a minor time to reach the target, demonstrating their ability to preserve the memory of the black box position in the maze, during the test duration. Interestingly, although both the initial and final latency of young rats was lower than aged rats, the differences between 100-group and young-group were not significant during the training 2 and 3 and the test.

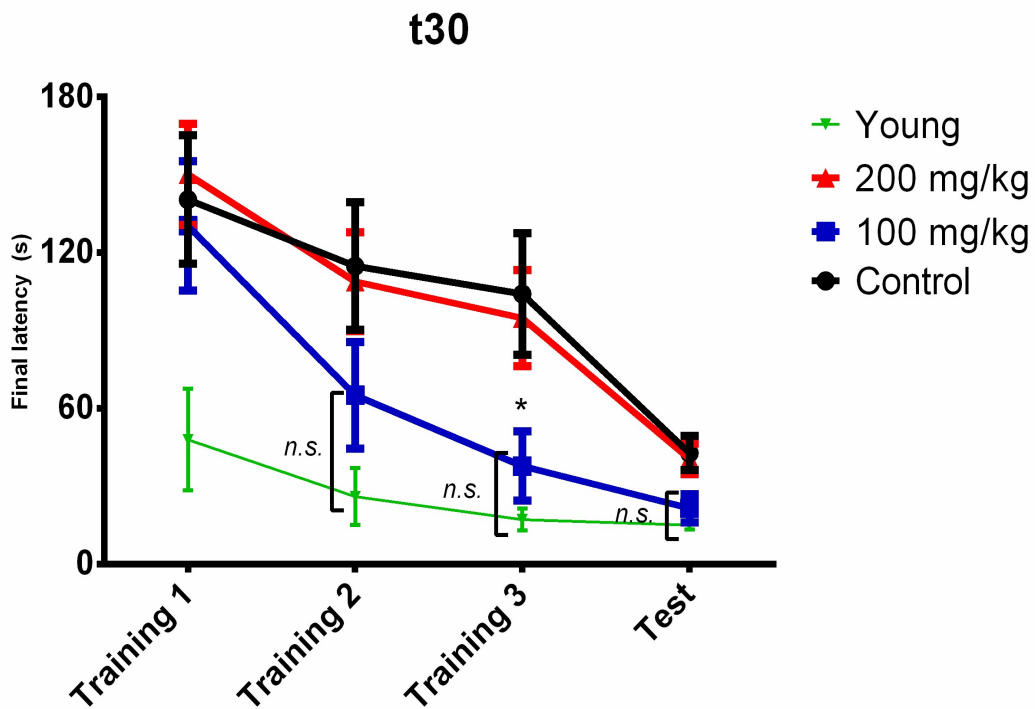
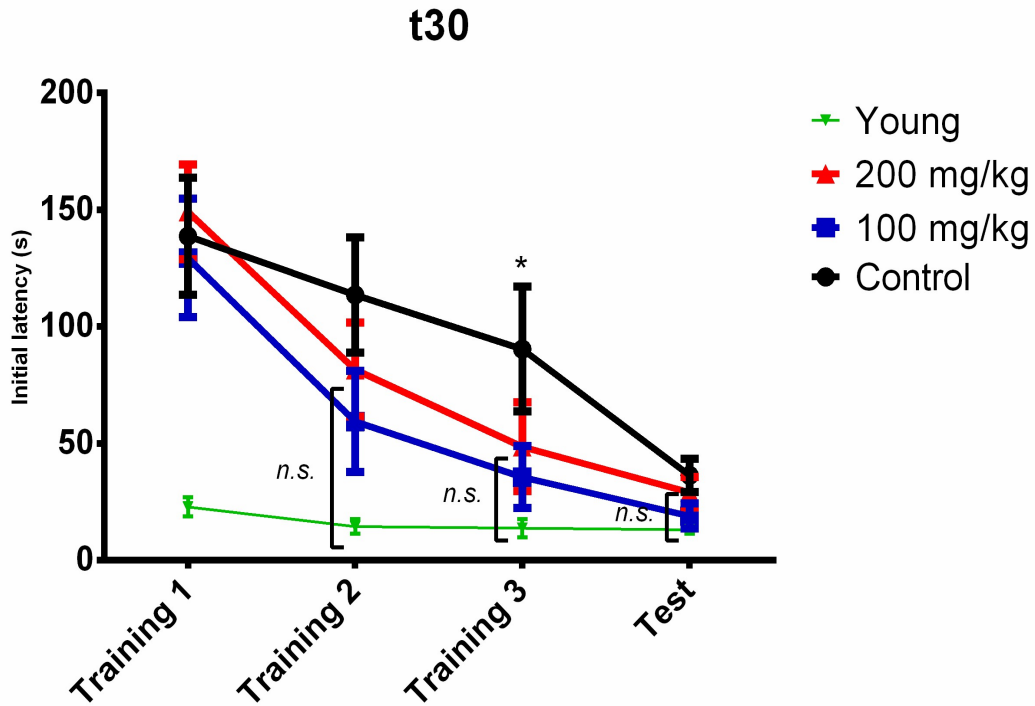
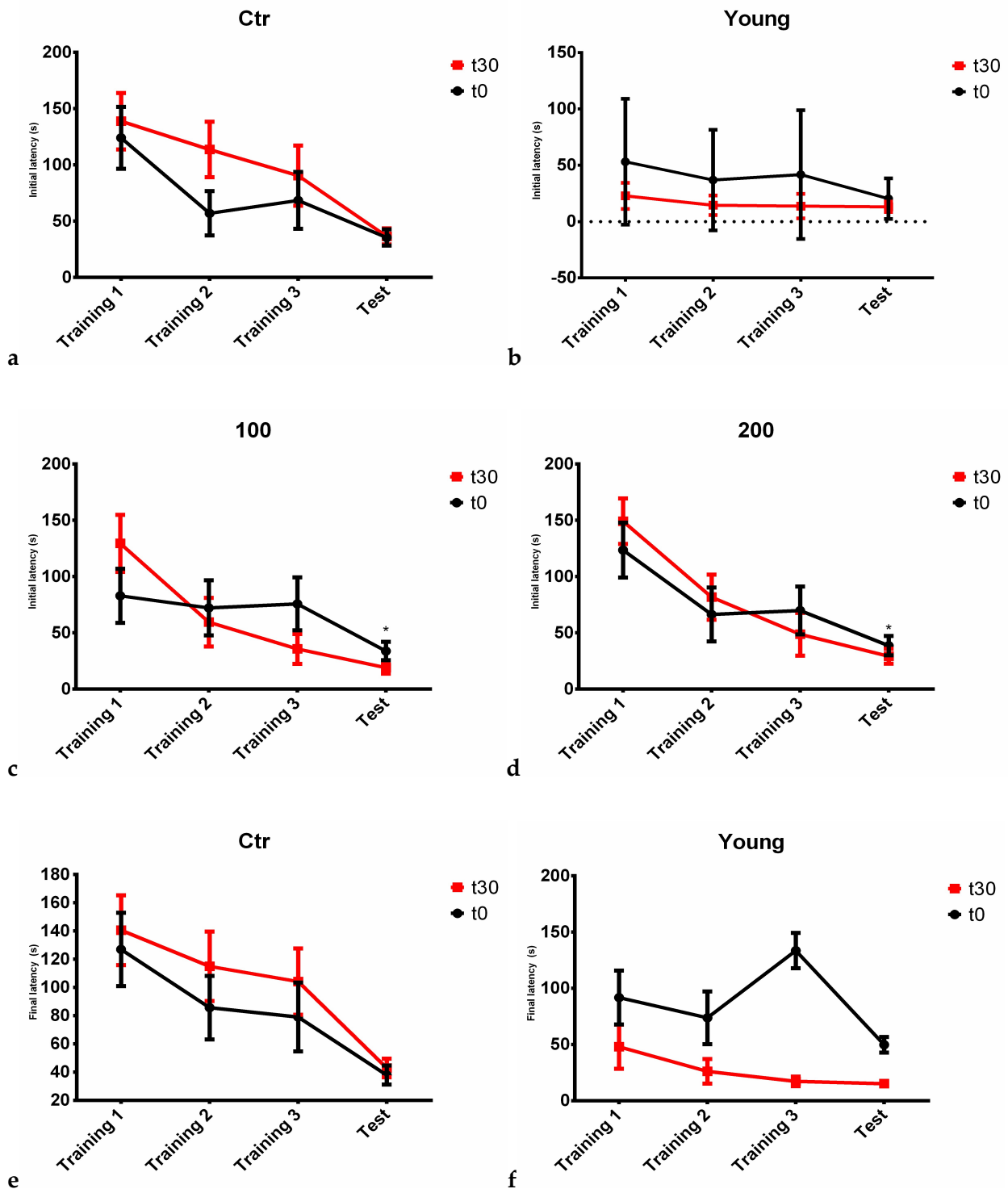


Figure 5.2^{II}. Barnes Maze Test. Initial and final latency at the end of the treatment. * $p < 0.05$ (Control vs. 100 mg/kg Taurisol[®])

Moreover, analysing the results within each group, we observed that at t30 in the two animal groups treated with Taurisol[®], both the initial and final latency rapidly decreased during the training session (Figure 5.2^{III}), reaching the statistic significance between the training 1 and the test (Initial latency – 100

mg/kg: 129.37 ± 71.72 sec vs. 19.00 ± 15.17 sec; 200 mg/kg: 149.13 ± 57.20 sec vs. 29.13 ± 18.64 sec; Final latency – 100 mg/kg: 130.37 ± 70.31 sec vs. 21.26 ± 22.19 sec; 200 mg/kg: 150.25 ± 55.11 sec vs. 40.63 ± 16.80 sec; training 1 vs. test; $p < 0.05$ for all). These data appear particularly interesting since they suggest the improved learning of the Taurisol[®]-treated animals. The latencies of the animals in the two active groups, indeed, in addition to being lower at t30 compared with t0, highlight a continue and gradual downward trend during the Barnes Maze test period, revealing the ability of the treated rats to learn the faster route to reach the target in the minor time.



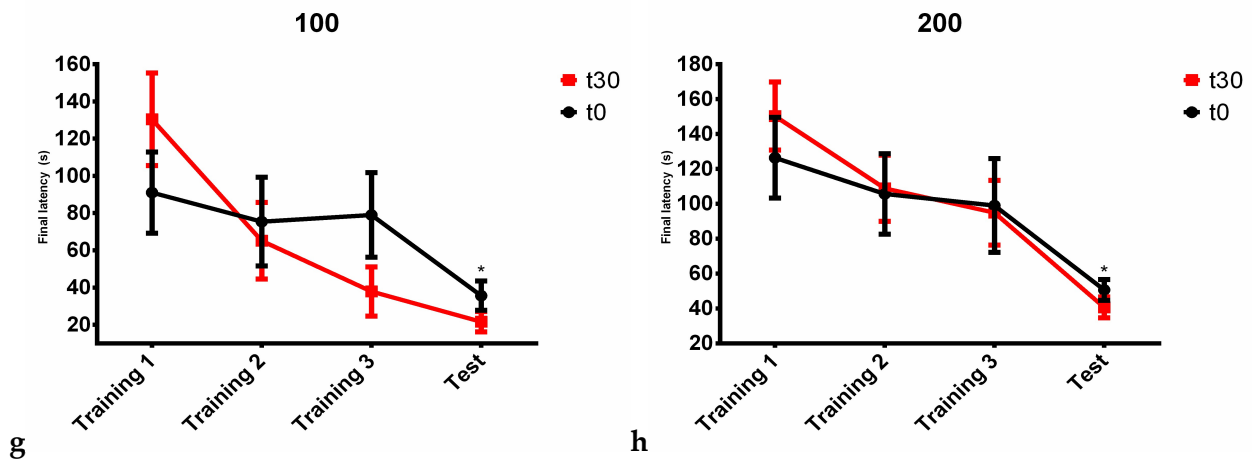


Figure 5.2^{III}. Barnes Maze Test, comparison between t0 and t30 latencies within each group. Letters a-d refer to initial latency; e-h refer to final latency. * $p < 0.05$, training 1 vs. test.

The motor coordination was evaluated with the Rotarod test, taking into account the permanence time on the Rotarod during the five repeated sessions (Figure 5.2^{IV}). At t0, the permanence time between the three groups of aged rats were not significantly different (15.94 ± 6.27 sec, 19.20 ± 7.23 sec and 19.98 ± 9.74 sec, Ctr, 100 and 200, respectively); on the contrary, as expected, the permanence time of young rats was significantly higher (30.85 ± 10.74 sec, $p < 0.01$). At t30, the permanence time (i) not significantly decreased in the control group (13.86 ± 5.33 sec), (ii) remained almost unchanged in both the 200 and young groups (20.77 ± 5.93 sec and 29.75 ± 7.06 sec, respectively) and (iii) significantly increased in the 100 group (24.75 ± 2.44 sec, $p < 0.05$); in this last group, the observed results are still significant when compared to control ($p < 0.01$). Interestingly, although the permanence time at t0 was significantly different between the 100 and young groups ($p < 0.01$), at the end of the treatment no significant differences were observed.

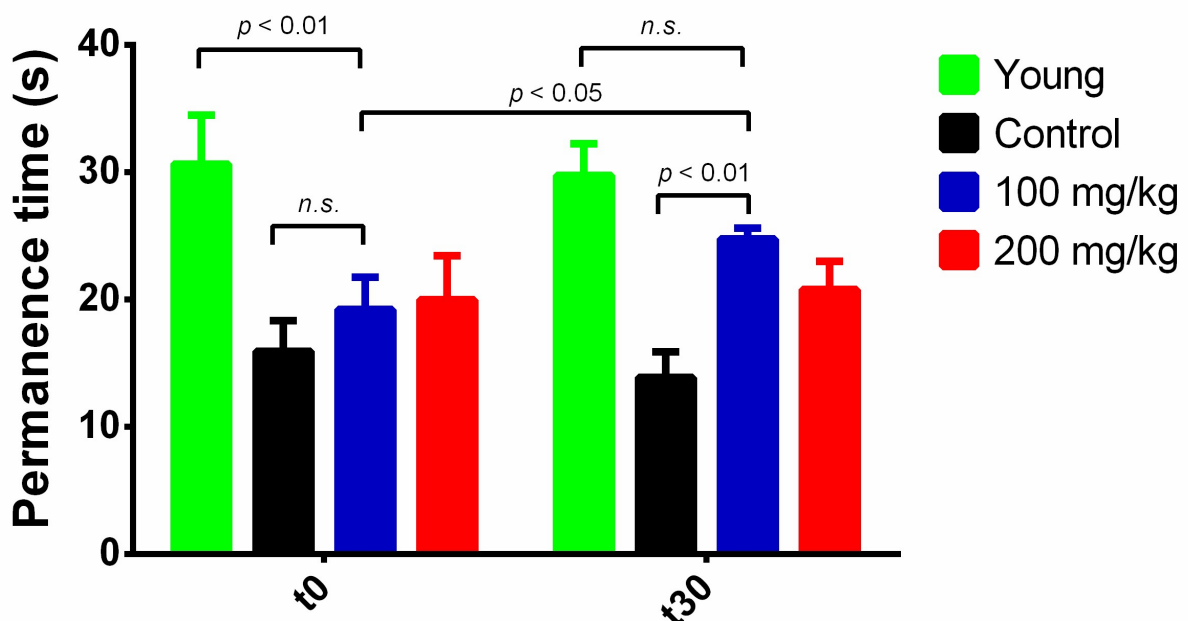


Figure 5.2^{IV}. Motor coordination. Permanence time evaluated with the Rotarod test before (t0) and after treatment (t30).

These observed results clearly indicate that chronic treatment with Taurisol[®] significantly improved both cognitive (visuospatial memory and learning) and motor functions in aged rats compared to controls. These results are in line with the evidence from previous studies reporting these peculiar effects of polyphenols (Flowers et al., 2015; Sarubbo et al., 2018b, 2015). All these studies are concord in indicating the antioxidant activity of polyphenols as the main mechanism of action for their neuroprotective effect. Due to its specific metabolic pathways, indeed, the brain is a body tissue with the largest oxygen consumption, resulting in a relevant sensitivity to oxidative damages. In addition, the endogenous antioxidant defences suffer a gradual decline during the ageing (Keller et al., 2005), resulting in increased OxS which, in turn, has been correlated to cognitive impairment and neurodegenerative changes in both aged human and rodents. Interestingly, increased OxS has also been indicated as one of the main causes of neurotransmitter system alterations (Haider et al., 2014; Pieta Dias et al., 2007). Indeed, during ageing the increased OxS negatively affects the activity of limiting enzymes involved in the synthesis of the monoamines, including TPH and TH; particularly, this reduction of the enzymatic activity is mainly related to oxidative damages and/or inefficient phosphorylations due to ROS injury (Cash, 1998; De La Cruz et al., 1996; Hussain and Mitra, 2000). Reduced activities of both TPH and TH result in decreased levels of monoamines, which is responsible for memory disorders development and neurodegenerative diseases onset (Collier et al., 2004; Cools, 2011; Esteban et al., 2010; Haider et al., 2014).

In vivo evidence demonstrated the anti-ageing activity of dietary antioxidants, including melatonin (Esteban et al., 2010; Moranta et al., 2014), tocopherol (Ramis et al., 2016) and resveratrol (Sarubbo et al., 2015). In general, it has been reported that polyphenols are able to exert various beneficial effects on brain ageing, including improvements in cognition, learning and memory (Ansari et al., 2009; Liu et al., 2006; Sarubbo et al., 2018a, 2015), reduced dementia risk (Sarubbo et al., 2018a; Truelsen et al., 2002) and prevention of neurodegenerative diseases onset (Gomez-Pinilla and Nguyen, 2012; Sarubbo et al., 2018a; A. Scalbert et al., 2005; Augustin Scalbert et al., 2005). In this sense, studies reported that polyphenol treatment significantly increases the brain levels of monoamines, such as serotonin (5-HT), noradrenaline (NA) and dopamine (DA), *via* increasing the activity of limiting enzymes (Sarubbo et al., 2018d, 2015). In particular, polyphenols efficiently protect these enzymes against the activity of oxidising agents (Rose et al., 2014; Y. Wang et al., 2011) and increase their expression *via* activation of SIRT1 (Chen et al., 2007; Kumar et al., 2007; Li et al., 2014; Ranney and Petro, 2009; Sarubbo et al., 2018a). Animal-based studies demonstrated that chronic treatment with polyphenols, including resveratrol and quercetin, increased the levels of monoamines in specific brain regions directly involved in both motor and cognitive processes, including hippocampus and striatum (Sarubbo et al., 2018d, 2015), providing a biochemical explanation for the

improvements observed during the behaviour tests, such as the Barnes Maze Test and the Rotarod Test. Moreover, studies reported the ability of such polyphenols to inhibit both the catabolism and the reuptake of monoamines (Chen et al., 2015; Yanez et al., 2006), resulting in a further mechanism for the increased monoamines levels. Among the various mechanisms proposed for the neuroprotective effects of polyphenols, their antioxidant and anti-inflammatory properties remain the most relevant. In particular, it has been well established the ability of polyphenols to protect DNA, proteins, lipids and carbohydrates from oxidative damage (Cirillo et al., 2016; Karimi et al., 2011; Khurana et al., 2013; Sarubbo et al., 2018a), as well as their efficacy in increasing the endogenous antioxidant defence systems, including GPx and SOD (de Groot and Rauen, 1998; Nencini et al., 2007; Sarubbo et al., 2018a). Interestingly, polyphenols have been demonstrated to control the neuroinflammatory status efficiently (Sarubbo et al., 2018a; Venigalla et al., 2015), *via* specific mechanisms involving the reduction of the activation of intracellular signalling pathways, such as MAPK and NF- κ B (Rice-Evans et al., 1996; Santangelo et al., 2007; Sarubbo et al., 2018a; Spencer, 2010, 2009a, 2009b).

According to this evidence, thus, and taking into account the high antioxidant potential of Taurisolo[®], it is plausible to speculate that it might promote the enhancement of limiting enzyme activities, with consequent increase in brain levels of monoamines, resulting in the observed improvements in both cognitive and motor functions, although this mechanism needs to be proved. However, assessment of the monoamines levels in the single brain regions of our study animals are still ongoing in order to confirm the results.

5.3 Ageing-related chronic diseases

Ageing is a biological process characterized by a progressive functional decline involving the whole body (Laurent et al., 2012). A large body of evidence demonstrated the main putative mechanisms at the basis of ageing and, among them, the increased OxS seems to play a central role. In this sense, in the 1968 Harman postulated the so-called “*Free radical theory*” where OxS has been indicated as the major causal factor of senescence (Harman, 1968; Sohal and Weindruch, 1996). More specifically, a progressive decline of endogenous antioxidant defences occurs during ageing, resulting in alteration of the pro-/antioxidant balance and consequent increased OxS. This, in turn, is responsible for cell damages that cannot be counteracted by endogenous defences, causing a drastic organ mass and functionality loss and culminating in system dysfunction (Jones et al., 2002; Petersen and Smith, 2016). Also, ageing-related diseases are characterised by a chronic inflammatory state that travel in parallel to OxS, sharing some of the main mechanisms/pathways. This comprehension leads to propose the so-called *theory of ageing or oxi-inflamm-aging*, where ageing is defined as a “*loss of homeostasis due to a chronic OxS that affects especially the regulatory systems, such as nervous, endocrine, and immune systems. The consequent activation of the immune system induces an inflammatory state that creates a vicious circle in which chronic oxidative stress and inflammation feed each other, and consequently, increases the age-related morbidity and mortality*” (Liguori et al., 2018). Among the ageing-related disorders, we investigated the effects of Taurisolo® polyphenols on macular degeneration and muscle decline, as extensively described in following sections.

5.3.1 Age-related macular degeneration

The effects of Taurisolo® polyphenols on AMD (for more detailed see section 1.3.2) were evaluated in a randomised clinical trial conducted on both diabetic and non-diabetic patients in collaboration with the Ocular Immunopathology Unit, Department of Ophthalmology of the Antonio Cardarelli Hospital, Naples (Italy) (**article in press**). Primary outcomes of this study were improvements in central foveal thickness (CFT) measured by Optical Coherence Tomography (OCT) and visual acuity measured by a distance Snellen chart design. Study design, population and methods are detailed in **Appendix A** and **Appendix C**. In a first part of the study, participants were chronically administered (6 months) with 400mg Taurisolo® polyphenols twice daily and divided into two groups according to the diabetes diagnosis. After this 6-month period, participants were randomised (independently from the diabetes diagnosis) into two groups: active group (400mg Taurisolo® polyphenols twice daily) and placebo group (400mg maltodextrins twice daily); both the treatments were followed for 3 months.

In this study a total of 37 patients with AMD (23 men and 14 women) with a mean age of 67.59±6.00 years and an average BMI of 31.18±6.83 kg/m² were assigned to the study. AMD patients with cataract were also included in the study; however, none needed cataract surgery during the entire study duration. AMD

patients were stratified in diabetics and non-diabetics (n=19 and n=18, respectively). Demographic, anthropometric and clinical characteristics are reported in **Table 5.3.1**¹. As shown, no significant differences were evident for demographic, oxidative stress-related biomarkers and diagnosed diseases, except for diabetes mellitus. No subjects prematurely terminated study participation.

Table 5.3.1¹. Baseline characteristics of study participants. No significant differences were evident between the two groups, except for anthropometric characteristics, metabolism blood parameters and diagnosis of diabetes mellitus. *Values are expressed as mean \pm SD; statistical significance is calculated by Student's t-test. BMI, body mass index; WC, waist circumference; HC, hip circumference; WHR, waist-to-hip ratio; HDL-c, high-density lipoprotein cholesterol; LDL-c, low-density lipoprotein cholesterol; TMAO, trimethylamine N-oxide; D-ROMs, reactive oxygen metabolites; ox-LDL, oxidized LDL cholesterol.

Parameters	Diabetics (n=19)	Non-diabetics (n=18)	p-value
<i>Demographic characteristics</i>			
Gender [male (%)]	73.33	50.00	$\chi^2 = 2.204, p = 0.138$
Age (years)*	65.93 \pm 5.60	69.67 \pm 6.07	0.110
Smokers [yes (%)]	40.00	33.33	$\chi^2 = 0.302, p = 0.582$
Physical activity [yes (%)]	13.33	16.67	$\chi^2 = 0.005, p = 0.942$
<i>Anthropometric characteristics</i>			
Weight (kg)*	84.70 \pm 15.58	67.92 \pm 1.31	0.007
Height (m)*	1.68 \pm 0.12	1.59 \pm 0.09	0.032
BMI (kg/m ²)*	34.36 \pm 6.35	27.21 \pm 5.33	0.004
WC (cm)*	106.00 \pm 9.48	94.33 \pm 12.23	0.010
HC (cm)*	108.40 \pm 10.73	101.00 \pm 11.18	0.093
WHR*	0.98 \pm 0.08	0.93 \pm 0.08	0.124
<i>Blood parameters</i>			
Metabolism			
Glucose (mg/dl)*	139.60 \pm 28.78	93.39 \pm 9.87	<0.0001
Insulin (μ IU/ml)*	9.44 \pm 2.35	7.81 \pm 0.91	0.032
Cholesterol (mg/dl)*	199.61 \pm 47.93	165.33 \pm 29.87	0.041
HDL-c (mg/dl)*	43.74 \pm 13.77	56.12 \pm 16.83	0.045
LDL-c (mg/dl)*	122.38 \pm 45.07	87.53 \pm 27.66	0.027
Triglycerides (mg/dl)*	167.47 \pm 21.62	108.42 \pm 56.26	<0.001

Oxidative stress			
TMAO (μM)*	3.94 \pm 3.10	4.10 \pm 2.40	0.879
D-ROMs (UCARR)*	520.27 \pm 74.12	503.07 \pm 2.71	0.815
Ox-LDL ($\mu\text{Eq/L}$)*	778.20 \pm 321.34	747.36 \pm 365.92	0.811
<i>Diagnosed diseases</i>			
Diabetes mellitus [yes (%)]	100.00	0.00	1.00
Hypertension [yes (%)]	66.67	41.67	$\chi^2 = 2.165, p = 0.141$
Hypercholesterolemia [yes (%)]	53.33	41.67	$\chi^2 = 0.248, p = 0.618$
Hypertriglyceridemia [yes (%)]	6.67	8.33	$\chi^2 = 0.424, p = 0.515$

After 6-month treatment with Taurisolo[®] polyphenols we observed changes in CFT and visual acuity on right and left eye. In particular, significant reductions in CFT and improvements in visual acuity were experienced in 63.1% and 52.6%, respectively, of diabetics AMD patients, while in non-diabetics were observed in 55.5% and 54.4%, respectively. As shown in **Figure 5.3.1I**, at the end of the treatment period, globally CFT significantly reduced in both diabetics (right eye: from 442.889 \pm 54.091 μm to 334.364 \pm 39.721 μm , $p=0.01$; left eye: from 474.818 \pm 66.473 μm to 307.111 \pm 18.165 μm , $p=0.006$) and non-diabetics (right eye: from 370.889 \pm 49.087 μm to 287.222 \pm 39.496 μm , $p=0.002$; left eye: from 321.667 \pm 47.238 μm to 301.333 \pm 50.416 μm , $p=0.06$). Similarly, visual acuity significantly improved in both diabetics (right eye: from 0.325 \pm 0.082 to 0.463 \pm 0.094, $p=0.004$; left eye: from 0.192 \pm 0.052 to 0.317 \pm 0.085, $p=0.02$) and non-diabetics (right eye: from 0.120 \pm 0.020 to 0.186 \pm 0.014; left eye: from 0.165 \pm 0.067 to 0.375 \pm 0.077, $p=0.001$).

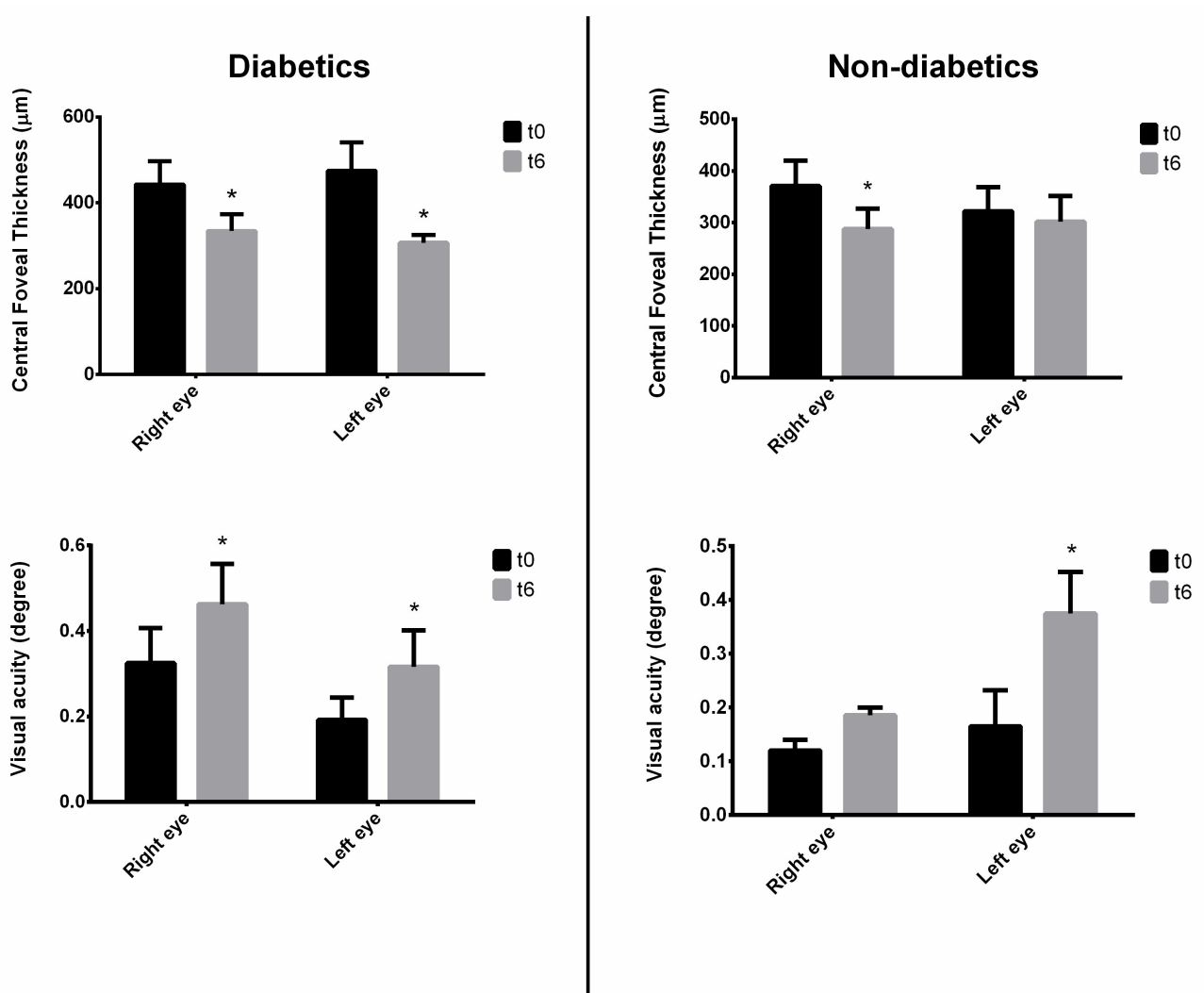


Figure 5.3.1¹. Effects of 6-month Taurisolo® treatment on central foveal thickness and visual acuity in both diabetic and non-diabetic patients with age-related macular degeneration. t0 and t6 refer to baseline and after 6-month treatment, respectively. Data are expressed as mean±SEM. Statistic significance was calculated by Student's *t*-test. * indicates a significant difference between t0 and t6 ($p < 0.05$).

In **Figure 5.3.1^{II}** OCT images from the same study participants before and after treatment with Taurisolo[®] are reported.

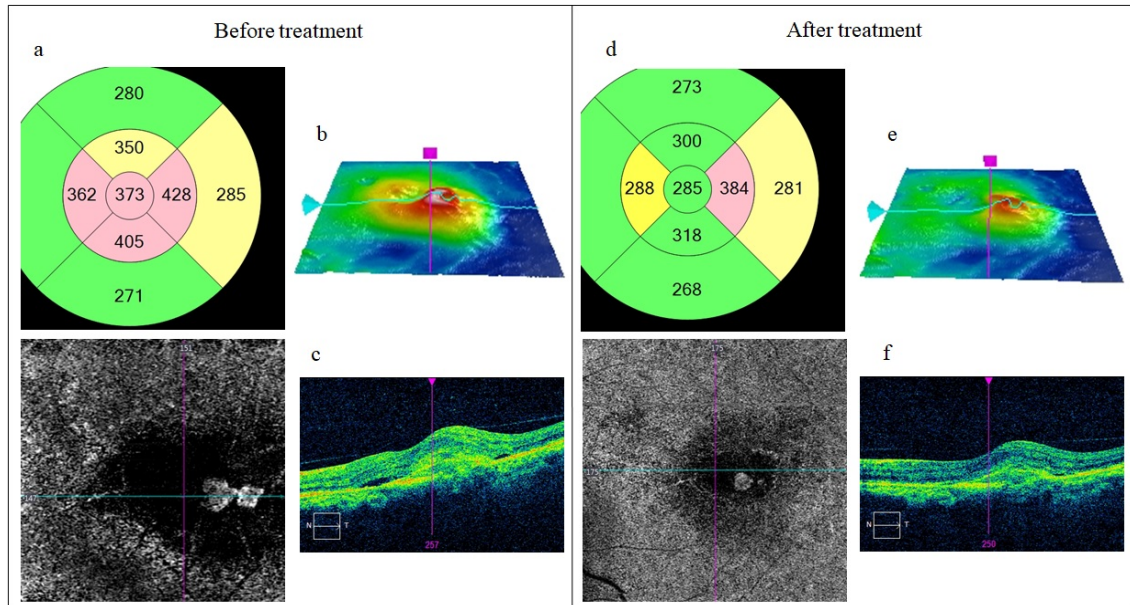


Figure 5.3.1^{II}. Optical Coherence Tomography (OCT) before and after 6-month treatment with Taurisolo[®] (a) OCT-Angiography performed above the plane of the retinal pigment epithelium – the neovascular network is perfectly visualized. There are peripheral anastomoses corresponding to the outer edge of the lesion. (b) The OCT mapping confirms the presence of an abnormal retinal thickening. (c) Horizontal OCT B-scan (passing through the lesion) shows subretinal edema associated with a hyper-reflective subretinal lesion. (d) OCT-Angiography highlights the neovascular network is smaller and the disappearance of peripheral anastomoses. (e) The OCT mapping shows the reduction of central retinal thickness. (f) Horizontal OCT B-scan (passing through the lesion) shows total absence of perilesional subretinal edema.

As AMD is a disease strongly associated with both OxS and atherosclerotic processes, we also monitored the circulating related biomarkers, such as TMAO, D-ROMs and oxLDL. All monitored markers significantly reduced at the end of the treatment period in both diabetics (TMAO: from $3.937 \pm 0.800 \mu\text{M}$ to $2.019 \pm 0.568 \mu\text{M}$, $p=0.014$; D-ROMs: from $520.30 \pm 19.14 \text{ UCARR}$ to $251.90 \pm 16.93 \text{ UCARR}$, $p<0.001$; oxLDL: from $778.20 \pm 82.97 \mu\text{Eq/L}$ to $415.50 \pm 66.18 \mu\text{Eq/L}$, $p<0.001$) and non-diabetics (TMAO: from $4.097 \pm 0.642 \mu\text{M}$ to $1.716 \pm 0.532 \mu\text{M}$, $p<0.001$; D-ROMs: from $503.10 \pm 72.65 \text{ UCARR}$ to $258.10 \pm 27.61 \text{ UCARR}$, $p=0.016$; oxLDL: from $747.40 \pm 97.80 \mu\text{Eq/L}$ to $344.70 \pm 59.37 \mu\text{Eq/L}$, $p=0.002$) (**Figure 5.3.1^{III}**).

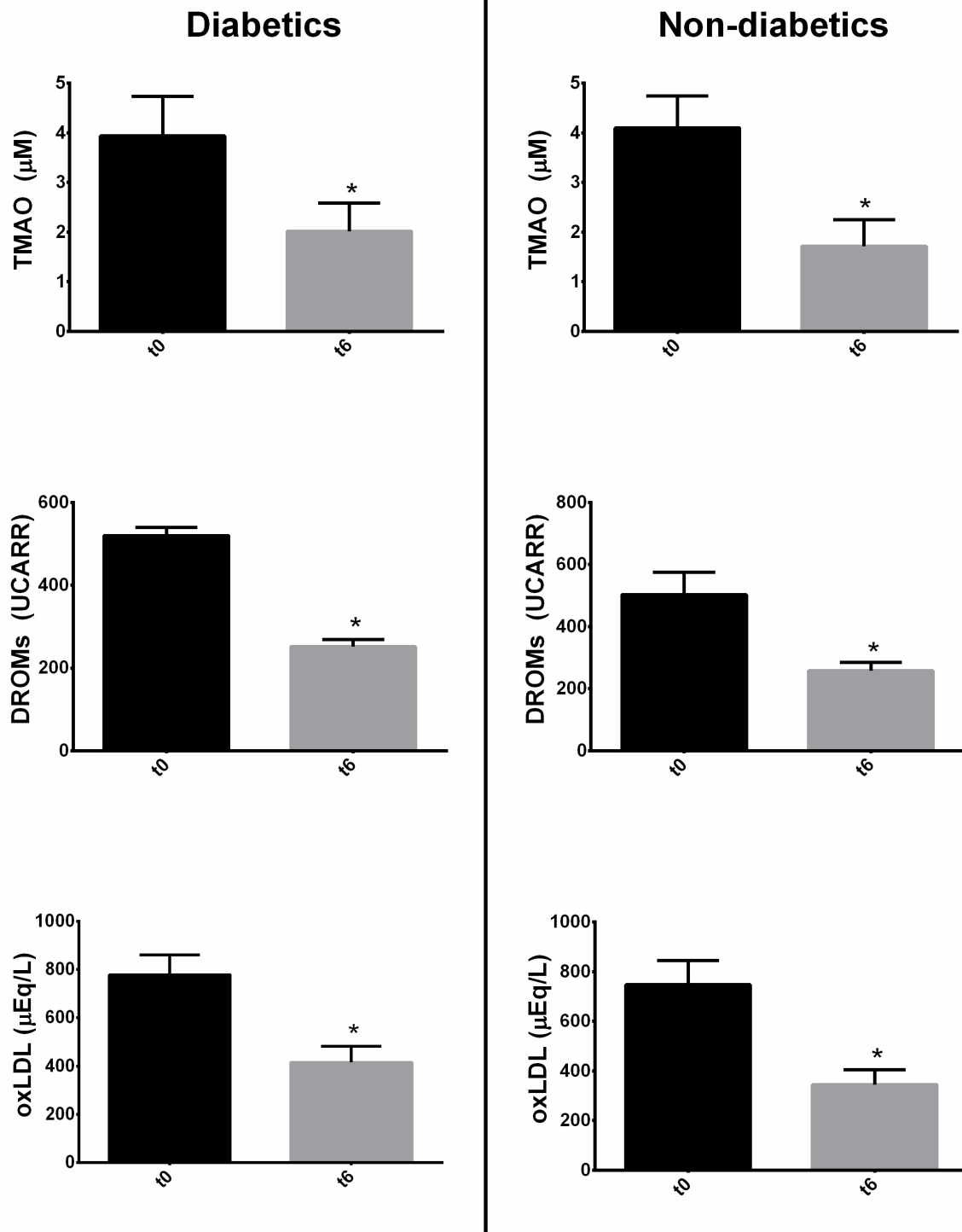


Figure 5.3.1^{III}. Effects of 6-month Taurisolo® treatment on serum oxidative stress-related biomarkers in both diabetic and non-diabetic patients with age-related macular degeneration. t0 and t6 refer to baseline and after 6-month treatment, respectively. Data are expressed as mean±SEM. Statistic significance was calculated by Student's t-test. * indicates a significant difference between t0 and t6 (p<0.05). *Abbreviations:* TMAO, trimethylamine N-oxide; D-ROMs, reactive oxygen metabolites; ox-LDL, oxidized LDL cholesterol.

To test the efficacy of Taurisolo® to reduce serum levels of OxS-related biomarkers compared to placebo, all AMD patients were randomised into active and placebo. TMAO, DROMs and oxLDL were monitored before and after treatment. As shown in **Table 5.3.1ⁱⁱ**, Taurisolo® significantly reduced serum levels of TMAO, DROMs and oxLDL (-16.57%, -17.92% and -27.71%, respectively) compared to placebo (+30.95%, +46.68% and +19.90%, respectively).

Table 5.3.1ⁱⁱ. Effects of Taurisolo® on TMAO, DROMs and oxLDL serum levels on AMD patients after 3-month treatment. Values are expressed as mean±SD of three repetitions. “Initial” and “final” refer to samples collected at months 6 and 9, respectively. Statistic significance was calculated by Student’s t-test. *p<0.05, initial vs. final (active); ** p<0.0001, initial vs. final (placebo); ° p<0.05, active vs. placebo (final); † p<0.0001, active vs. placebo (final). TMAO, trimethylamine N-oxide; D-ROMs, reactive oxygen metabolites; ox-LDL, oxidized LDL cholesterol.

	TMAO (µM)		DROMs (UCARR)		oxLDL (µEq/L)	
	Initial	Final	Initial	Final	Initial	Final
Active group	2.10±1.05	1.75±0.93 [°]	235.47±96.73	193.27±49.43 [†]	421.47±211.81	304.67±139.96 [†]
Placebo group	2.98±2.11	3.91±2.25 ^{**}	298.93±82.58	417.93±107.32 ^{**}	541.71±263.36	649.50±252.31 ^{**}

Also, a Pearson correlation analysis has been performed between TMAO, DROMs and oxLDL serum levels and measured values of CFT and visual acuity. Results reported in **Table 5.3.1ⁱⁱⁱ** indicate that OxS-related biomarkers positively correlate with CFT and negatively with visual acuity, suggesting that increased oxidative status and atherosclerotic process have a role in macular degeneration and, consequently, in visual acuity. The absence of statistic significance (except for correlation between DROMs levels and right eye CFT) may be due to the small sample size.

Table 5.3.1ⁱⁱⁱ. Correlation analysis between ophthalmic outcomes and oxidative stress-related biomarkers at baseline in AMD patients. Pearson correlation coefficients between indicated parameters are represented; values in bold type are statistically significant (p< 0.05). TMAO, trimethylamine N-oxide; D-ROMs, reactive oxygen metabolites; ox-LDL, oxidized LDL cholesterol.

	TMAO levels		DROMs levels		oxLDL levels	
	Coefficient	p-value	Coefficient	p-value	Coefficient	p-value
<i>Central Foveal Thickness</i>						
Left eye	0.133	0.638	0.242	0.304	0.195	0.454
Right eye	0.391	0.297	0.607	0.036	0.161	0.636

<i>Visual acuity</i>						
Left eye	-0.195	0.487	-0.193	0.495	-0.374	0.140
Right eye	-0.012	0.975	-0.350	0.365	-0.039	0.942

In order to elucidate any eventual involvement of the antioxidant activity of Taurisolo® (in terms of TMAO-, D-ROMs- and oxLDL-reducing effects) in improvement of ophthalmic outcomes, a correlation analysis has been performed. In particular, a Pearson correlation analysis has been performed between (i) variations (defined as the variation between values measured at the end of the treatment period (t6) and at baseline (t0), and indicated as “Δ% (t0-t6)”) of TMAO, D-ROMs and oxLDL and (ii) ophthalmic outcomes (CFT and visual acuity). For these last two parameters, values referring to right eye and left eye were correlated. As shown in **Table 5.3.1^{IV}**, in AMD patients (i) significant positive correlation has been found between variations of CFT and TMAO, D-ROMs and oxLDL, and (ii) significant negative correlation has been found between variations of visual acuity and D-ROMs, while non-significant negative correlation was observed for TMAO and oxLDL.

Table 5.3.1^{IV}. Correlation analysis between ophthalmic outcomes and oxidative stress-related biomarkers at the end of the treatment period in AMD patients. Pearson correlation coefficients between indicated parameters are represented; values in bold type are statistically significant ($p < 0.05$). “Δ% (t0-t6)” refers to variations observed between values measured at the end of the treatment period (t6) and at baseline (t0). TMAO, trimethylamine N-oxide; D-ROMs, reactive oxygen metabolites; ox-LDL, oxidized LDL cholesterol.

	TMAO Δ% (t0-t6)		DROMs Δ% (t0-t6)		oxLDL Δ% (t0-t6)	
	Coefficient	p-value	Coefficient	p-value	Coefficient	p-value
<i>Central Foveal Thickness Δ% (t0-t6)</i>						
Left eye	0.764	<0.0001	0.927	<0.0001	0.953	<0.0001
Right eye	0.595	0.041	0.858	<0.0001	0.867	<0.0001
<i>Visual acuity Δ% (t0-t6)</i>						
Left eye	-0.533	0.091	-0.532	0.034	-0.413	0.126
Right eye	-0.687	0.132	-0.968	0.032	-0.760	0.136

With this study we demonstrated that chronic treatment (6 months) with Taurisolo® polyphenols significantly reduces CFT and increases visual acuity in both diabetic and non-diabetic patients with AMD. This beneficial activity is related to a marked effect in reducing serum levels of TMAO (as a pro-atherogenic agent) and OxS-related biomarkers (DROMs and oxLDL), as evidenced by our correlation analyses. Such promising, these results allow indicating these effects as potential mechanisms of action for the beneficial

role played by Taurisolo® polyphenols on eye diseases, providing novel insights on the use of nutraceutical for management of OxS- and vascular alteration-related diseases, including ophthalmological disease (Figure 5.3.1^{IV}).

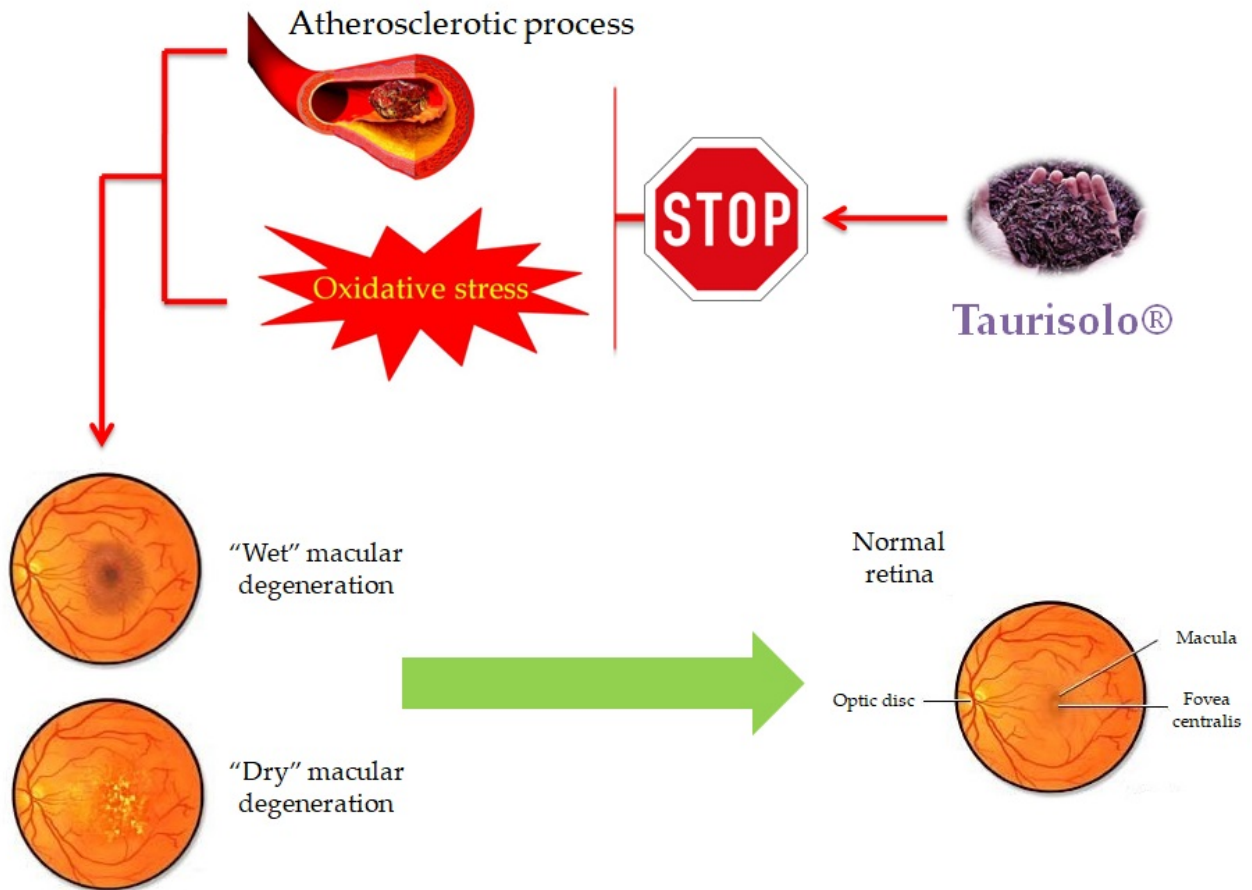


Figure 5.3.1^{IV}. Effect of Taurisolo® in improving macular degeneration. Thromboembolic and/or atherosclerotic processes, in addition to OxS, are closely implicated in pathogenesis of AMD. Taurisolo®, reducing serum levels of TMAO, as pro-atherogenic agent, and DROMs and oxLDL, as OxS-related biomarkers, significantly ameliorates ophthalmic outcomes in patients with AMD, improving the global eye health.

5.3.2 Age-related muscle decline

As aforementioned, OxS is strongly related in structural and functional alterations of several organs, including skeletal muscle (Lee et al., 2017; Lourenço dos Santos et al., 2015; Marzetti et al., 2013; Romanello and Sandri, 2016; Roseno et al., 2015), mainly *via* producing free radicals, with the consequent increased oxidative damage such as lipid peroxidation, resulting in affected muscle quality and strength. Also, the aged-dependent reduction of the muscle ability to counteract the increased production of ROS results in an oxidative damage accumulation, causing a loss of the tissue homeostasis (Jackson and Mcardle, 2011). In this sense, animal-based studies reported higher levels of ROS in aged rats than in young ones (Charles et al., 2013). Furthermore, in human serum levels of OxS-related biomarkers were found to be elevated in elderly subjects with a diagnosis of sarcopenia (Bellanti et al., 2018; Howard et al., 2007), suggesting that OxS may contribute to the age-related muscular decline.

A considerable body of evidence reported the role played by polyphenols in prevention of ageing-related muscle impairment, in particular contrasting the OxS (Charles et al., 2013). More specifically, resveratrol, one of the main polyphenols in grape, was demonstrated to prevent the muscle atrophy in a large number of catabolic conditions (Furtado et al., 2020; Shadfar et al., 2011; Sun et al., 2017), counterbalancing the ageing-induced muscular oxidative damage (Wang et al., 2018). In aged rats resveratrol prevents the muscle atrophy ameliorating the mitochondrial function and reducing the OxS through the PKA/LKB1/AMPK pathway. Also, studies reported the ability of resveratrol to activate Sirtuin 1 (Sirt1) (Huang et al., 2019; Sharples et al., 2015), which beneficial role in various ageing-related conditions, including muscle mass and functional decline is well established (Huang et al., 2019).

According to the available literature, we evaluated the efficacy of Taurisol[®] polyphenols in ameliorating the status of OxS markers as parameters of muscle quality in aged rats. This study was conducted during the internship at the Research Group in Community Nutrition and Oxidative Stress and Health Research Institute of the Balearic Islands (IdISBa), University of Balearic Islands, Palma de Mallorca (Spain) as required by this PhD program. The study consisted of chronic treatment with Taurisol[®] (100mg/kg) or placebo (maltodextrin, 50mg/kg) to aged rats, with a young rats as positive control group. Functional (motor coordination test) and biochemical (on gastrocnemius) analyses were performed in order to evaluate the efficacy on muscle quality. Methods are detailed in **Appendix A** and **Appendix B** (Annunziata et al., 2020b).

The motor coordination was evaluated with the Rotarod test, taking into account the permanence time on the Rotarod during the five repeated sessions (**Figure 5.3.2¹**). At t₀, the permanence time between the two groups of aged rats was not significantly different (15.94 ± 6.27 s and 19.20 ± 7.23 s, for control old rats and treated old rats, respectively). On the contrary, the permanence time of young rats was significantly

higher (30.85 ± 10.74 sec, $p < 0.01$). At t30, the permanence time (i) did not significantly decrease in the aged control group (13.86 ± 5.33 sec) and (ii) significantly increased in the treated old rats (24.75 ± 2.44 sec, $p < 0.05$); in this last group, the observed results are still significant when compared to aged control ($p < 0.01$). Interestingly, although the permanence time at t0 was significantly different between the old treated and young groups ($p < 0.01$), at the end of the treatment no significant differences were observed.

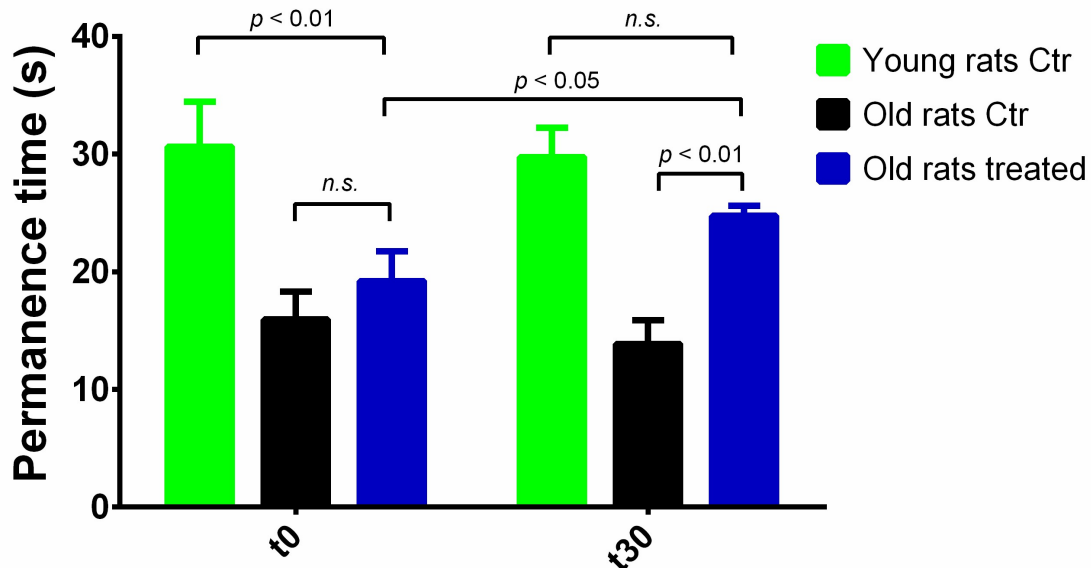


Figure 5.3.2¹. Motor coordination. Permanence time evaluated with the Rotarod test before (t0) and after treatment (t30). Results are expressed as mean \pm SEM of the number of determinations. Statistic significance was calculated by Student's t-test. Old rats Ctr refers to old animals treated with placebo; Old rats treated refers to old animals treated with Taurisolo[®]; Young rats Ctr refers to young animals treated with placebo. T0 refers to the beginning of the treatment and t30 refers to the end of the treatment [source: (Annunziata et al., 2020b)].

Rotarod test is generally used to evaluate the motor coordination mainly in aged brain-associated cognitive decline; however, we used these data to assess the effects of Taurisolo[®] polyphenol treatment on muscle skills, eventually impaired by ageing. Our results suggest that Taurisolo[®] polyphenols ameliorated the altered motor coordination in aged rats, maybe *via* increasing the levels of monoamine in specific brain regions involved in motor processes, including hippocampus and striatum (Sarubbo et al., 2018c, 2018d). On the other hand, it is plausible to speculate a direct improvement of muscular skills, as a result of the ameliorated muscle functionality. As previously reported, polyphenols improve exercise capacity and endurance in rats probably *via* reducing OxS in muscle and improving vascular and endothelial function (Lambert et al., 2018; Matsumura et al., 2018; Yoshida et al., 2018), resulting in a global amelioration of the skeletal muscle health.

To elucidate and confirm the antioxidant potential of Taurisolo® we performed various biochemical assays on rat muscle samples (gastrocnemius). Firstly, the antioxidant capacity was evaluated using the FRAP assay. As shown in **Figure 5.3.2ⁱⁱ**, in old rats treated with placebo the antioxidant capacity was significantly lower than in young rats (0.21 ± 0.08 mM Trolox Equivalents (TE) and 0.24 ± 0.06 mM TE, respectively; $p < 0.05$). On the other hand, in old rats treated with Taurisolo® the antioxidant capacity was significantly higher than in old rats control (0.26 ± 0.11 mM TE, $p < 0.05$). Interestingly, no significant differences were observed between old rats treated with Taurisolo® and young rats.

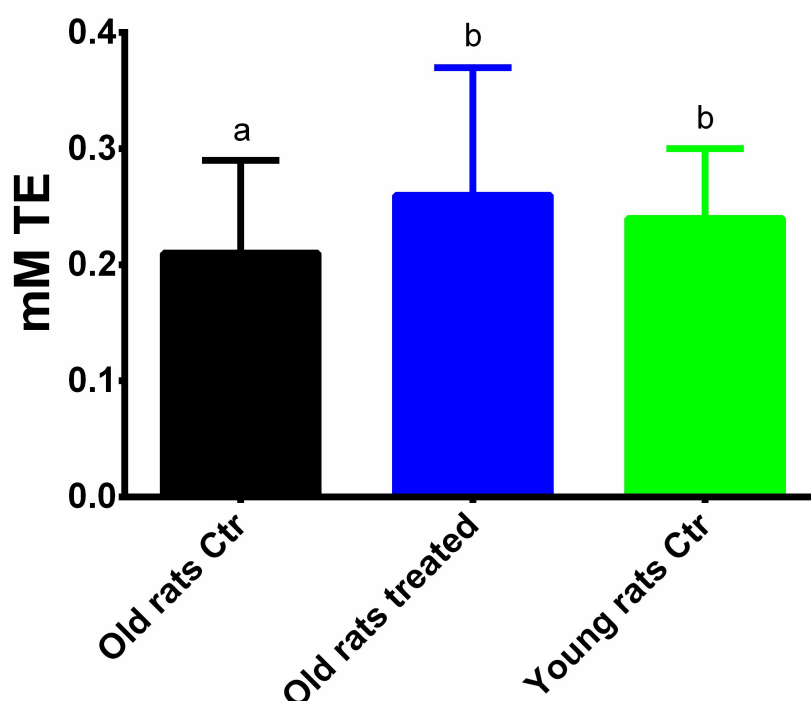


Figure 5.3.2ⁱⁱ. Antioxidant capacity determined with the FRAP assay in muscles of rats. Results are expressed as mean \pm SEM, and $p < 0.05$ was considered statistically significant. ANOVA one-way analysis. Different letters reveal significant differences. Old rats Ctr refers to old animals treated with placebo; Old rats treated refers to old animals treated with Taurisolo®; Young rats Ctr refers to young animals treated with placebo [source: (Annunziata et al., 2020b)].

FRAP test measures the ferric reducing ability of a sample and it is licensed as a useful method for assessing the antioxidant power (Benzie and Strain, 1996). Since the FRAP assay provides a putative index of reducing and antioxidant potential of biological samples, the results observed provide intriguing insights about the OxS-reducing effect of chronic Taurisolo® administration at the muscular level. Notably, it could be speculated that through the bloodstream, polyphenols or their metabolites, are able to reach the muscle (Fernández-Quintela et al., 2017; Koenig et al., 2011) and exert *in situ* their antioxidant activity counteracting the ROS production by chelating iron ions, or inhibiting their reduction. This, in turn, provides a first important mechanism for the reduction of the OxS in muscle, resulting in ameliorating the muscle quality.

In order to evaluate the effects of Taurisolo® polyphenols on endogenous antioxidant defences, we monitored the enzymatic activities of catalase (CAT), superoxide dismutase (SOD), glutathione peroxidase (GPx) and glutathione reductase (GRd) (**Figure 5.3.2^m**). In old rats control the activities of antioxidant enzymes were lower than in young rats (GRd = Old rats control: 8.59 ± 0.57 pKat/mg prot, Young rats control: 12.50 ± 0.41 pKat/mg prot; GPx = Old rats control: 4.75 ± 0.25 nKat/mg prot, Young rats control: 5.99 ± 0.52 nKat/mg prot; CAT = Old rats control: 4.94 ± 0.36 mKat/mg prot, Young rats control: 10.90 ± 0.54 mKat/mg prot). No differences in SOD activity were observed between the different groups. Interestingly, in animals treated with Taurisolo® the activities of GRd, GPx and CAT were significantly higher than in old rats treated with placebo (GRd = 11.30 ± 0.59 pKat/mg prot; GPx = 4.86 ± 0.37 nKat/mg prot; CAT = 6.70 ± 0.22 mKat/mg prot, $p < 0.05$ for all).

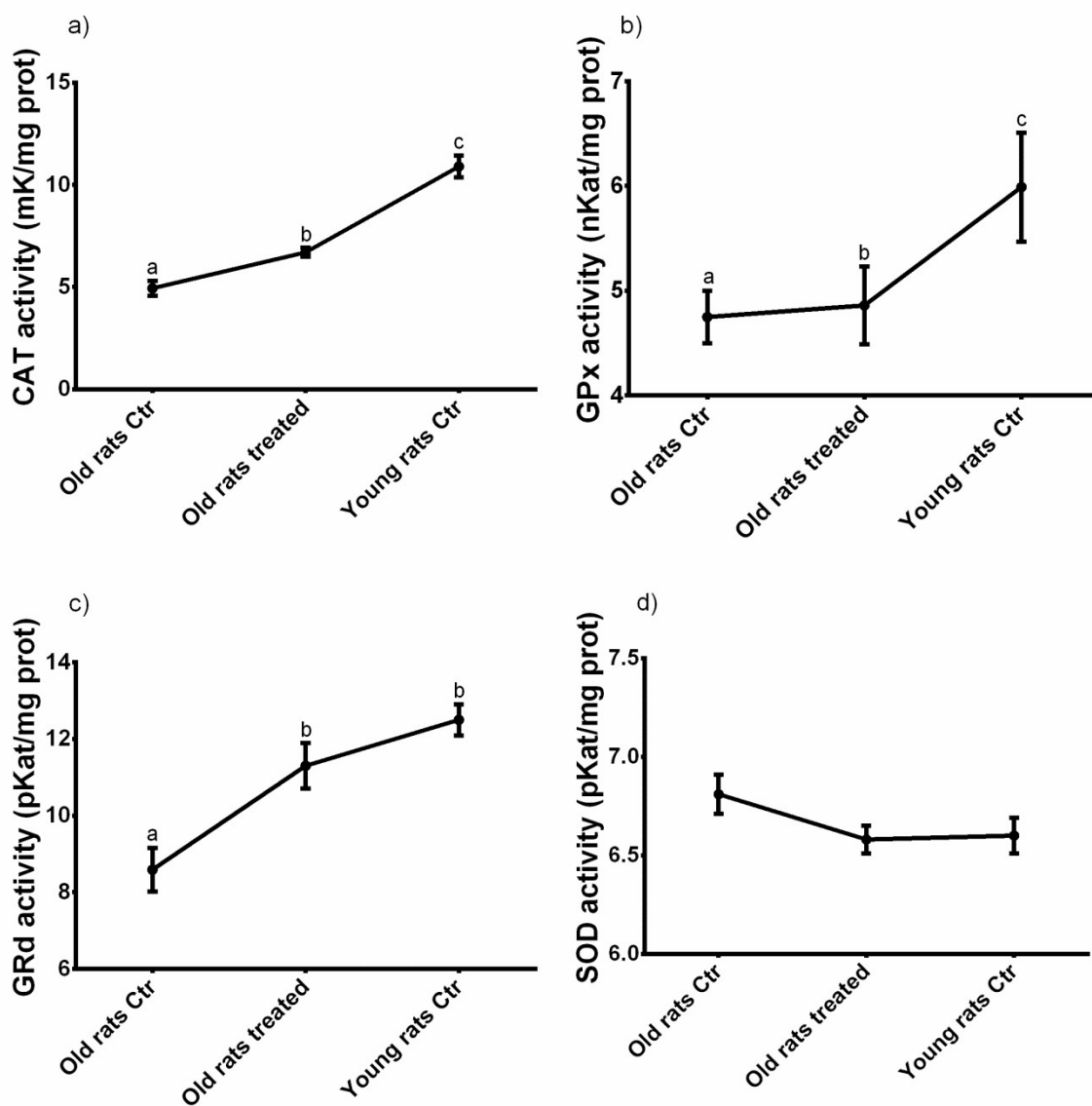


Figure 5.3.2^{III}. Enzymatic activity of (a) CAT, (b) GPx, (c) GRd and (d) SOD. Results are expressed as mean \pm SEM, and $p < 0.05$ was considered statistically significant. ANOVA one-way analysis. Different letters reveal significant differences. Old rats Ctr refers to old animals treated with placebo; Old rats treated refers to old animals treated with Taurisol[®]; Young rats Ctr refers to young animals treated with placebo. Abbreviations: GRd, glutathione reductase; GPx, glutathione peroxidase; CAT, catalase; SOD, superoxide dismutase [source: (Annunziata et al., 2020b)].

Also, we monitored the expression of targeted OxS- and inflammation-related genes. As shown in **Table 5.3.2^I**, in old rats treated with placebo it was registered a reduced expression of antioxidant genes, including CAT, GPx, Sirt1 and Mn-SOD, and increased pro-inflammatory genes expression, including IL-6 and -10, in comparison to young animals. In contrast, we observed that the chronic treatment with Taurisol[®] was able to counteract the negative influence of ageing on both OxS- and inflammation-related genes.

Table 5.3.2^I. Effect of Taurisol[®] chronic treatment on oxidative stress- and inflammation-related genes [source: (Annunziata et al., 2020b)]

	Young rats Ctr	Old rats Ctr	Old rats treated
CAT	1.00 \pm 0.36 ^a	0.18 \pm 0.04 ^b	0.68 \pm 0.32 ^a
GPx	1.00 \pm 0.19 ^{ab}	0.68 \pm 0.09 ^a	1.47 \pm 0.38 ^b
IL6	1.00 \pm 0.24 ^a	4.84 \pm 1.46 ^b	1.20 \pm 0.25 ^a
Sirt1	1.00 \pm 0.21 ^{ab}	0.73 \pm 0.13 ^a	1.72 \pm 0.17 ^{ab}
Mn-SOD	1.00 \pm 0.21	0.79 \pm 0.06	1.58 \pm 0.58
IL10	1.00 \pm 0.16	1.44 \pm 0.09	1.39 \pm 0.19

Results are expressed as mean \pm SEM, and $p < 0.05$ was considered statistically significant. ANOVA one-way analysis. Different letters reveal significant differences

In addition to a direct activity of polyphenols in reducing OxS in muscle, we observed a significant increase of key antioxidant enzymes activity (GRd, GPx and CAT). These enzymes are part of the so-called endogenous antioxidant defence system acting *via* neutralizing free radicals (Truong et al., 2018). In particular, CAT decomposes H₂O₂ in H₂O before H₂O₂ reacts with metal ions generating hydroxyl radicals, while GRd and GPx regulate the maintenance of the balance between reduced and oxidized forms of glutathione (GSH) that acts as a free radical scavenging agent (Truong et al., 2018). The ability of polyphenols to enhance the activities of such antioxidant enzymes, including CAT, SOD and GPx has been previously reported (Truong et al., 2018). In general, it can be speculated that the observed increase in the activity of endogenous antioxidant enzymes might be due to both a direct effect of polyphenols in enhancing their enzymatic activities or an up-regulation of their expression. This up-regulation is mainly modulated *via*

activation of the Keap1/Nrf2/ARE signalling pathway (Sandoval-Acuña et al., 2014; Tsuji et al., 2013). Another interesting signalling pathway involves Sirtuin 1 (Sirt1), an NAD⁺-dependent deacetylase playing a pivotal role in several biological processes, including ageing. Sirt1 modulates various nuclear factors, including forkhead box 0 (FOX0) and proliferator-activated receptor gamma coactivator 1α (PGC-1α), regulating the expression of antioxidant and antiageing-related genes (Truong et al., 2018). Additionally, in muscles, PGC-1α stimulates the mitochondrial biogenesis activating the nuclear respiratory factor (NRF1) (Baur et al., 2006; Lin et al., 2005; Truong et al., 2018), and representing a further protective mechanism contributing to the muscle improvement. Polyphenols such as resveratrol have been demonstrated to indirectly activate Sirt1 through activation of the AMP-activated protein kinase (AMPK) (Park et al., 2012). The Sirt1-mediated regulation of FOX0 and PGC-1α results in enhanced expression of antioxidant genes, including SOD, GPx and CAT (Brunet et al., 2004; St-Pierre et al., 2006). Interestingly, it has been reported that, in gastrocnemius muscle of aged rats, the supplementation with red grape polyphenolic extract increased both the expression of PGC-1α and the activation of AMPK (Laurent et al., 2012), providing further evidence for the involvement of polyphenols in these specific signalling pathways. In this sense, the observed enhanced Sirt1 expression in muscle of aged rats treated with Taurisol[®] might be responsible for an up-regulation of the antioxidant enzymes that, in turn, may explain the observed increased enzymatic activities of CAT, GPx and GRd. Moreover, it is possible an enhanced mitochondriogenesis *via* PGC-1α activation explaining the contrasted muscle decline, as shown by the increased permanence time of old rats treated on the rotarod, as an indicator of motor resistance. In contrast, evidence reported that polyphenols are able to suppress the nuclear factor kappa-light-chain-enhancer of activated B cells (NF-κB) pathway that has been recognized as responsible for the increased expression of pro-oxidant and pro-inflammatory genes. More specifically, NF-κB is physiologically inactive in the cytosol by interaction with IκB. ROS and reactive nitrogen species (RNS) are stimuli causing the activation of NF-κB that translocates into the nucleus promoting the expression of pro-inflammatory mediators/cytokines- and OxS-related genes (Truong et al., 2018). In line with this evidence, our results demonstrated the ability of the chronic Taurisol[®] administration to down-regulate the expression of pro-inflammatory genes, including IL6.

To evaluate the effects of Taurisol[®] in contrasting oxidative damages, we monitored the levels of MDA as a marker of lipid peroxidation indicative of oxidative damage to lipids, and N-tyrosine (N-Tyr) as a marker of protein damage. As shown in **Figure 5.3.2^{IV}**, chronic treatment with Taurisol[®] counteracted significantly the increase in MDA levels induced by ageing (650±82.7 mM/mg prot vs. 526±16.7 mM/mg prot, Old rats control vs. Old rats treated, p< 0.05; Young rats control: 470±13.1 mM/mg prot).

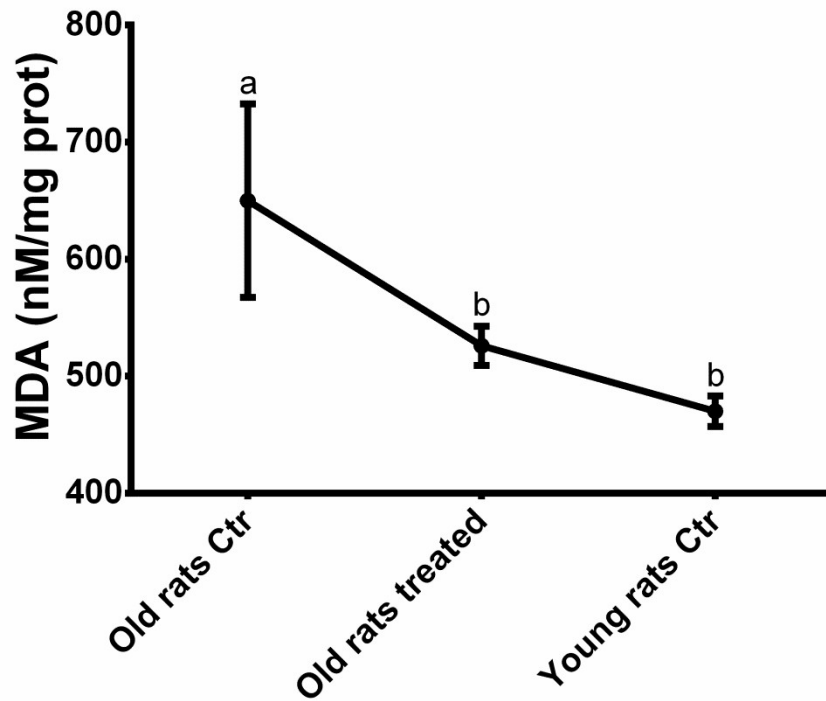


Figure 5.3.2^{iv}. Levels of MDA. Results are expressed as mean \pm SEM, and $p < 0.05$ was considered statistically significant. ANOVA one-way analysis. Different letters reveal significant differences. Old rats Ctr refers to old animals treated with placebo; Old rats treated refers to old animals treated with Taurisolo[®]; Young rats Ctr refers to young animals treated with placebo. Abbreviations: MDA, malondialdehyde [source: (Annunziata et al., 2020b)].

Similarly, the chronic treatment with Taurisolo[®] counteracted the increase in N-Tyr levels induced by ageing ($208 \pm 15.2\%$ vs. $171 \pm 14.3\%$, Old rats control vs. Old rats treated, $p = 0.06$; Young rats control: $100 \pm 11.9\%$) (**Figure 5.3.2^v**).

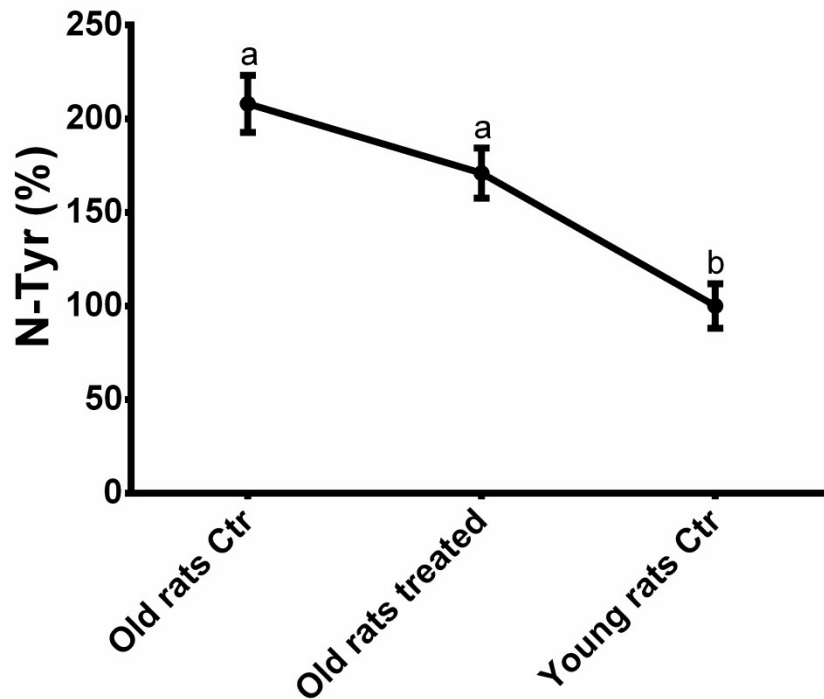


Figure 5.3.2^v. Levels of N-Tyr. Results are expressed as mean \pm SEM, and $p < 0.05$ was considered statistically significant. ANOVA one-way analysis. Different letters reveal significant differences. Old rats Ctr refers to old animals treated with placebo; Old rats treated refers to old animals treated with Taurisolo®; Young rats Ctr refers to young animals treated with placebo. Abbreviations: N-Tyr, nitrotyrosine [source: (Annunziata et al., 2020b)].

Lipid peroxidation is a direct consequence of OxS and it leads to both alteration of membrane biological function and cell damage (Bellanti et al., 2018). In particular, ROS and RNS play a central role in promoting lipid peroxidation (Truong et al., 2018). This is a chain-reaction process producing a large variety of reactive aldehydes, including MDA (Esterbauer et al., 1991, 1982; Negre-Salvayre et al., 2008), which in turn, are stable and diffuse across the membranes attacking biomolecules in various sites, and causing biological and biochemical alterations leading to disease development (Caruso et al., 2004; Kurutas, 2016; Valko et al., 2007). In this sense, MDA can be considered as a marker of injury and its levels have been found increased in sarcopenic subjects (Bellanti et al., 2018). There is evidence about the activity of free radical scavenging agents to inhibit the lipid peroxidation, in particular polyphenols including resveratrol (Stojanović et al., 2001), due to its ability to donate hydrogen, generating phenoxyl radicals (Brito et al., 2002; Castaldo et al., 2019; Olas et al., 2006). ROS and RNS are also involved in protein oxidation processes leading to the formation of both protein carbonyls and advanced oxidation protein products (Truong et al., 2018) which have been found age-dependently increased in human (Pandey et al., 2010). Particularly, among the various free radicals, RNS are implicated in reactions with amino acid side chains such as tyrosine, forming nitrogenated proteins (i.e. N-Tyr) (Lü et al., 2010). Polyphenols have been demonstrated to efficiently

counteract the ROS/RSN-mediated protein oxidation (Truong et al., 2018), contributing to the maintenance of cellular proteostasis (Matos et al., 2017).

Overall, with this study we demonstrates that chronic treatment with Taurisolo[®] significantly improved the muscle quality in aged rats *via* reducing OxS at a muscular level. More specifically, we observed that Taurisolo[®] polyphenols (i) increase the total antioxidant capacity of muscles, (ii) increase the activities of antioxidant enzymes, (iii) reduce both the lipid and protein oxidation and (iv) modulate the expression of OxS- and inflammation-related genes (**Figure 5.3.2^{VI}**).

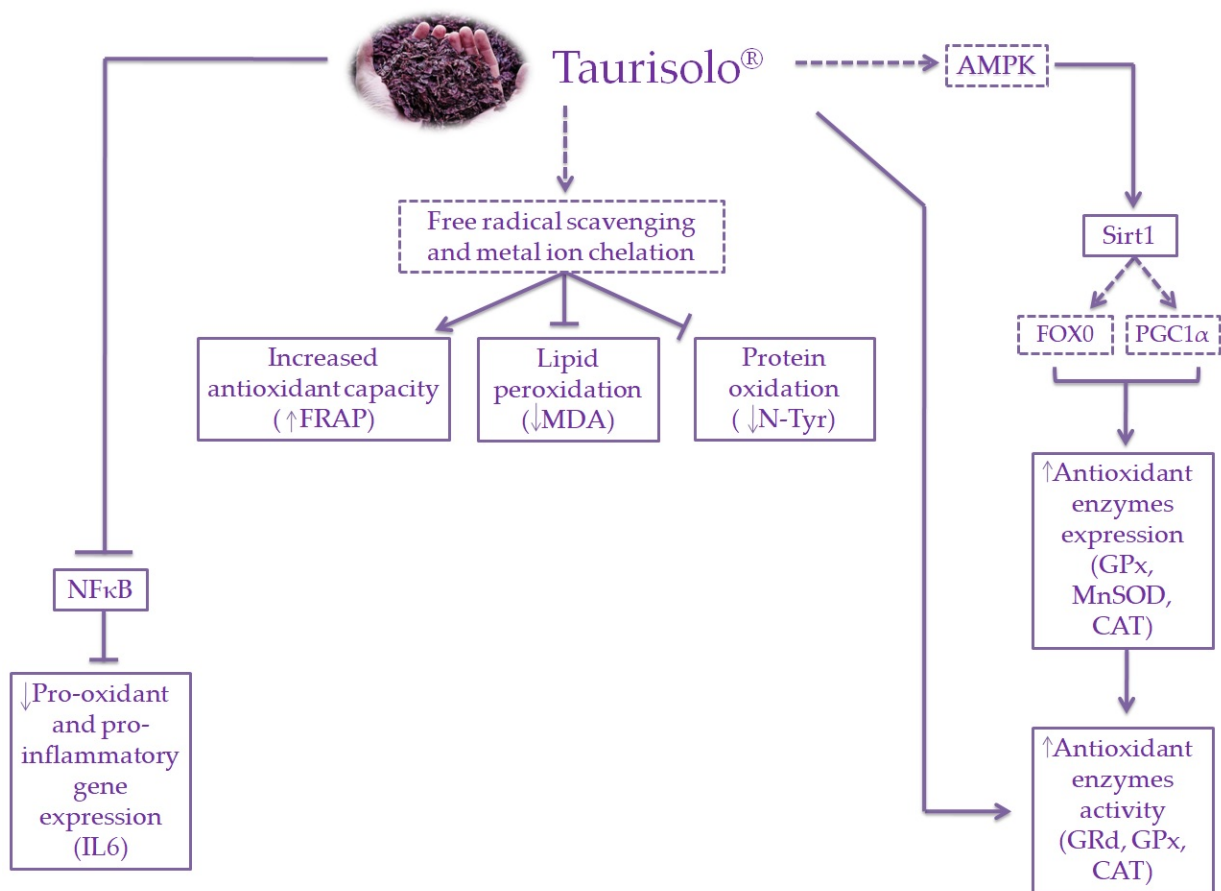


Figure 5.3.2^{VI}. Schematic representation of the potential mechanisms of action of Taurisolo[®].

— indicates the mechanisms directly observed; ---- indicates the mechanisms/pathways not directly observed, but reported in the literature [source: (Annunziata et al., 2020b)].

6. Conclusion and future perspectives

The present document reports all the results obtained from studies performed during this three-year PhD project, aimed to evaluate the nutraceutical potential of Taurisolo[®], a novel grape polyphenol-based nutraceutical formulation.

Working in collaboration with the MBMed Company of Turin, Italy (industrial partner of this PhD project), Taurisolo[®] was firstly formulated and characterised, and the productive process was optimised in accordance to both its polyphenol profile and the bioaccessibility of its components. Once obtained the final formulation, the large-scale production was accomplished by the MBMed Company, and the product used for pre-clinical and clinical studies.

In particular, starting from the large body of evidence reporting the well-known and -established cardioprotective role of grape polyphenols, we decided to investigate the effects of Taurisolo[®] in management of CVR, acting in reducing the risk factors related to CVD, by *in vitro*, *ex-vivo*, animal based-studies and clinical trials. Overall, our results suggest that Taurisolo[®] exerts its cardioprotective effect *via* two main mechanism: antioxidant and anti-atherosclerotic activities. Among these, the anti-atherosclerotic activity, mainly exerted *via* reducing the serum levels of TMAO (which pro-atherogenic role has been widely described) appears such promising as a novel interpretation of the cardioprotective effect of polyphenols, and is driving our further studies. In particular, we are currently investigating the ability of Taurisolo[®] to reduce circulating TMAO *via* inhibiting the intestinal production of its precursor (TMA), thus, acting on gut microbiota. In this sense, we are performing two studies:

- animal-based study aimed to investigate the microbiota-remodelling ability of chronic treatment with Taurisolo[®] in mice fed with normal and high-fat diet. In particular, we are monitoring the relative abundances (and eventual changes) of selected bacterial strains (belonging to *Bacteroidetes* and *Firmicutes*) by assessing the levels of bacterial DNA *via* real time-PCR on stool samples.
- Acute clinical trial on healthy subjects aimed to evaluate the ability of Taurisolo[®] to reduce serum levels of TMAO after consumption of 2g L-carnitine. In basal conditions (without treatment with Taurisolo[®]) we observed a serum peak of TMAO 12h after ingestion of L-carnitine that disappears after administration of 800mg Taurisolo[®]. In particular, we observed on average a marked reduction of the AUC from 107.02 to 38.56 μ M (basal and Taurisolo[®], respectively). The study will proceed in order to enlarge the sample size, reaching a number of study participants necessary to evidence any statistical difference.

Furthermore, taking into account the strong relationship between OxS and inflammation, we are also investigating the anti-inflammatory potential of Taurisolo® in human, with particular interest in pulmonary inflammation. In this sense, we developed a novel Taurisolo® formulation for aerosol administration that we are testing in both healthy subjects and patients with diagnosed pulmonary diseases. In particular, we observed significant acute reduction of DROMs (as OxS-related biomarker) and IL6 (as inflammation-related biomarker) in healthy current smokers and patients with diagnosis of tuberculosis. These results encouraged us to follow our research in this field. More specifically, during the first months of 2020, in concomitance with the global Sars-CoV2 pandemic, we started a multicentric clinical trial on patients with COVID-19 in hospital setting. Preliminary data from this study, conducted in cooperation with the Ospedale dei Colli (Naples, Italy), are really promising and evidence marked reduction of both IL6 and PCR as serum biomarkers related to pulmonary inflammation after chronic aerosol administration of Taurisolo®.

Overall, results from our study on the nutraceutical efficacy of the tested product allow concluding that Taurisolo® may represent a very effective and valid support for management of both OxS- and atherosclerosis-related diseases. Also, the pharmacological approach used (in terms of preclinical studies) provide solid evidence for comprehension of the main mechanisms of action at the basis of the clinical effects observed, and open the way to a novel research method for the study of nutraceutical. This is remarkable considering that, although of natural origin, food-derived bioactive compounds are chemical molecules able to exert biological effects on human health, being involved in specific pathways. Based on this evidence, thus, research should move in this direction, in order to provide increasingly strong proves about the efficacy of nutraceutical products in prevention of several diseases or in management of borderline conditions, by placing Nutraceutical in its proper position, *“beyond diet, before drugs”*.

7. References

- Abete, P., Napoli, C., Santoro, G., Al., E., 1999. Age-related decrease in cardiac tolerance to oxidative stress. *J Mol Cell Cardiol* 31, 227–236.
- Acharya, A., Das, I., Chandhok, D., Saha, T., 2010. Redox regulation in cancer: A double-edged sword with therapeutic potential. *Oxid. Med. Cell. Longev.* 3, 23–34. <https://doi.org/10.4161/oxim.3.1.10095>
- Ader, P., Grenacher, B., Langguth, P., Scharrer, E., Wolfram, S., 1996. Cinnamate uptake by rat small intestine: Transport kinetics and transepithelial transfer. *Exp. Physiol.* 81, 943–955. <https://doi.org/10.1113/expphysiol.1996.sp003995>
- Aebi, H., 1984. Catalase in Vitro. *Methods Enzymol.* 105, 121–6. [https://doi.org/10.1016/S0076-6879\(84\)05016-3](https://doi.org/10.1016/S0076-6879(84)05016-3)
- Akbari, M., Tamtaji, O.R., Lankarani, K.B., Tabrizi, R., Dadgostar, E., Kolahdooz, F., Jamilian, M., Mirzaei, H., Asemi, Z., 2019. The effects of resveratrol supplementation on endothelial function and blood pressures among patients with metabolic syndrome and related disorders: a systematic review and meta-analysis of randomized controlled trials. *High Blood Press. Cardiovasc. Prev.* 26, 305–319.
- Al-Janabi, A., Lightman, S., Tomkins-Netzer, O., 2018. Statins in retinal disease. *Eye* 32, 981–991. <https://doi.org/10.1038/s41433-018-0066-7>
- Al-Obaide, M., Singh, R., Datta, P., Rewers-Felkins, K., Salguero, M., Al-Obaidi, I., Kottapalli, K., Vasylyeva, T., 2017. Gut Microbiota-Dependent Trimethylamine-N-oxide and Serum Biomarkers in Patients with T2DM and Advanced CKD. *J. Clin. Med.* 6, 86. <https://doi.org/10.3390/jcm6090086>
- Albert, C.L., Tang, W.H.W., 2018. Metabolic Biomarkers in Heart Failure. *Heart Fail. Clin.* <https://doi.org/10.1016/j.hfc.2017.08.011>
- Alberti, A., Bolognini, L., Macciantelli, D., Caratelli, M., 2000. The radical cation of N,N-diethyl-para-phenylendiamine: A possible indicator of oxidative stress in biological samples. *Res. Chem. Intermed.* 26, 253–267. <https://doi.org/10.1163/156856700X00769>
- Alexander, S.P.H., Roberts, R.E., Broughton, B.R.S., Sobey, C.G., George, C.H., Stanford, S.C., Cirino, G., Docherty, J.R., Giembycz, M.A., Hoyer, D., Insel, P.A., Izzo, A.A., Ji, Y., MacEwan, D.J., Mangum, J., Wonnacott, S., Ahluwalia, A., 2018. Goals and practicalities of immunoblotting and immunohistochemistry: A guide for submission to the British Journal of Pharmacology. *Br. J. Pharmacol.* <https://doi.org/10.1111/bph.14112>

- Almeida, L., Vaz-da-Silva, M., Falcão, A., Soares, E., Costa, R., Loureiro, A.I., Fernandes-Lopes, C., Rocha, J.F., Nunes, T., Wright, L., Soares-da-Silva, P., 2009. Pharmacokinetic and safety profile of trans-resveratrol in a rising multiple-dose study in healthy volunteers. *Mol. Nutr. Food Res.*
<https://doi.org/10.1002/mnfr.200800177>
- Amic, D., Davidovic-Amic, D., Beslo, D., Rastija, V., Lucic, B., Trinajstic, N., 2007. SAR and QSAR of the Antioxidant Activity of Flavonoids. *Curr. Med. Chem.* 14, 827–45.
<https://doi.org/10.2174/092986707780090954>
- Anderson, E.J., Kypson, A.P., Rodriguez, E., Anderson, C.A., Lehr, E.J., Neuffer, P.D., 2009. Substrate-Specific Derangements in Mitochondrial Metabolism and Redox Balance in the Atrium of the Type 2 Diabetic Human Heart. *J. Am. Coll. Cardiol* 54, 1891–1898.
- Aneja, R., Hake, P.W., Burroughs, T.J., Denenberg, A.G., Wong, H.R., Zingarelli, B., 2004. Epigallocatechin, a green tea polyphenol, attenuates myocardial ischemia reperfusion injury in rats. *Mol. Med.* 10, 55–62.
<https://doi.org/10.2119/2004-00032.aneja>
- Annunziata, G., Barrea, L., Ciampaglia, R., Cicala, C., Arnone, A., Savastano, S., Nabavi, S.M., Tenore, G.C., Novellino, E., 2019a. *Arctium lappa* contributes to the management of type 2 diabetes mellitus by regulating glucose homeostasis and improving oxidative stress: A critical review of in vitro and in vivo animal-based studies. *Phyther. Res.* 33, 2213–2220. <https://doi.org/10.1002/ptr.6416>
- Annunziata, G., Capó, X., Quetglas-Llabrés, M.M., Monserrat-Mesquida, M., Tejada, S., Tur, J.A., Ciampaglia, R., Guerra, F., Maisto, M., Tenore, G.C., Novellino, E., Sureda, A., 2021. Ex Vivo Study on the Antioxidant Activity of a Winemaking By-Product Polyphenolic Extract (Taurisolo®) on Human Neutrophils. *Antioxidants (Basel)* 10, 1009. <https://doi.org/10.3390/antiox10071009>
- Annunziata, G., Jiménez-García, M., Capó, X., Moranta, D., Arnone, A., Tenore, G.C., Sureda, A., Tejada, S., 2020a. Microencapsulation as a tool to counteract the typical low bioavailability of polyphenols in the management of diabetes. *Food Chem. Toxicol.* 139, 111248. <https://doi.org/10.1016/j.fct.2020.111248>
- Annunziata, G., Jimenez-García, M., Tejada, S., Moranta, D., Arnone, A., Ciampaglia, R., Tenore, G.C., Sureda, A., Novellino, E., Capó, X., 2020b. Grape polyphenols ameliorate muscle decline reducing oxidative stress and oxidative damage in aged rats. *Nutrients* 12, 1280.
<https://doi.org/10.3390/nu12051280>
- Annunziata, G., Maisto, M., Schisano, C., Ciampaglia, R., Daliu, P., Narciso, V., Tenore, G.C., Novellino, E., 2018a. Colon bioaccessibility and antioxidant activity of white, green and black tea polyphenols extract after in vitro simulated gastrointestinal digestion. *Nutrients* 10, 1711.

<https://doi.org/10.3390/nu10111711>

- Annunziata, G., Maisto, M., Schisano, C., Ciampaglia, R., Narciso, V., Hassan, S.T.S., Tenore, G.C., Novellino, E., 2019b. Effect of grape pomace polyphenols with or without pectin on TMAO serum levels assessed by LC/MS-based assay: A preliminary clinical study on overweight/obese subjects. *Front. Pharmacol.* 10, 575. <https://doi.org/10.3389/fphar.2019.00575>
- Annunziata, G., Maisto, M., Schisano, C., Ciampaglia, R., Narciso, V., Tenore, G.C., Novellino, E., 2019c. Effects of grape pomace polyphenolic extract (Taurisolo®) in reducing tmao serum levels in humans: Preliminary results from a randomized, placebo-controlled, cross-over study. *Nutrients* 11, 139. <https://doi.org/10.3390/nu11010139>
- Annunziata, G., Maisto, M., Schisano, C., Ciampaglia, R., Narciso, V., Tenore, G.C., Novellino, E., 2018b. Resveratrol as a novel anti-herpes simplex virus nutraceutical agent: An overview. *Viruses* 10, 473. <https://doi.org/10.3390/v10090473>
- Annunziata, G., Sanduzzi Zamparelli, M., Santoro, C., Ciampaglia, R., Stornaiuolo, M., Tenore, G.C., Sanduzzi, A., Novellino, E., 2020c. May Polyphenols Have a Role Against Coronavirus Infection? An Overview of in vitro Evidence. *Front. Med.* 7, 240. <https://doi.org/10.3389/fmed.2020.00240>
- Ansari, M.A., Abdul, H.M., Joshi, G., Opii, W.O., Butterfield, D.A., 2009. Protective effect of quercetin in primary neurons against A β (1-42): relevance to Alzheimer's disease. *J. Nutr. Biochem.* <https://doi.org/10.1016/j.jnutbio.2008.03.002>
- Armstrong, E.J., Rutledge, J.C., Rogers, J.H., 2013. Coronary artery revascularization in patients with diabetes mellitus. *Circulation* 128, 1675–85. <https://doi.org/10.1161/CIRCULATIONAHA.113.002114>
- Ascher, S., Reinhardt, C., 2018. The gut microbiota: An emerging risk factor for cardiovascular and cerebrovascular disease. *Eur. J. Immunol.* 48, 564–575. <https://doi.org/10.1002/eji.201646879>
- Ayesh, R., Mitchell, S.C., Zhang, A., Smith, R.L., 1993. The fish odour syndrome: Biochemical, familial, and clinical aspects. *Br. Med. J.* 307, 655–657. <https://doi.org/10.1136/bmj.307.6905.655>
- Ballou, L., Chao, C., Holness, M., Barker, S., Raghov, R., 1992. Interleukin-1-mediated PGE2 production and sphingomyelin metabolism. Evidence for the regulation of cyclooxygenase gene expression by sphingosine and ceramide. *J. Biol. Chem.* 267, 20044–20050.
- Barbulova, A., Colucci, G., Apone, F., 2015. New Trends in Cosmetics: By-Products of Plant Origin and Their Potential Use as Cosmetic Active Ingredients. *Cosmetics* 2, 82–92. <https://doi.org/10.3390/cosmetics2020082>

- Barona, J., Aristizabal, J.C., Blesso, C.N., Volek, J.S., Fernandez, M., 2012. Grape polyphenols reduce blood pressure and increase flow-mediated vasodilation in men with metabolic syndrome. *J. Nutr.* 142, 1626–1632.
- Barrea, L., Annunziata, G., Muscogiuri, G., Arnone, A., Tenore, G.C., Colao, A., Savastano, S., 2019a. Could hop-derived bitter compounds improve glucose homeostasis by stimulating the secretion of GLP-1? *Crit. Rev. Food Sci. Nutr.* 59, 528–535. <https://doi.org/10.1080/10408398.2017.1378168>
- Barrea, L., Annunziata, G., Muscogiuri, G., Di Somma, C., Laudisio, D., Maisto, M., de Alteriis, G., Tenore, G.C., Colao, A., Savastano, S., 2018. Trimethylamine-N-oxide (TMAO) as novel potential biomarker of early predictors of metabolic syndrome. *Nutrients* 10, 1971. <https://doi.org/10.3390/nu10121971>
- Barrea, L., Annunziata, G., Muscogiuri, G., Laudisio, D., Di Somma, C., Maisto, M., Tenore, G.C., Colao, A., Savastano, S., 2019b. Trimethylamine N-oxide, Mediterranean diet, and nutrition in healthy, normal-weight adults: also a matter of sex? *Nutrition* 62, 7–17. <https://doi.org/10.1016/j.nut.2018.11.015>
- Barrea, L., Fabbrocini, G., Annunziata, G., Muscogiuri, G., Donnarumma, M., Marasca, C., Colao, A., Savastano, S., 2019c. Role of nutrition and adherence to the mediterranean diet in the multidisciplinary approach of hidradenitis suppurativa: Evaluation of nutritional status and its association with severity of disease. *Nutrients* 11, 57. <https://doi.org/10.3390/nu11010057>
- Barrea, L., Muscogiuri, G., Annunziata, G., Laudisio, D., Tenore, G.C., Colao, A., Savastano, S., 2019d. A new light on vitamin d in obesity: A novel association with trimethylamine-n-oxide (tmao). *Nutrients* 11, 1310. <https://doi.org/10.3390/nu11061310>
- Barrett, E., 1985. Bacterial Reduction of Trimethylamine Oxide. *Annu. Rev. Microbiol.* 39, 131–49. <https://doi.org/10.1146/annurev.micro.39.1.131>
- Barrett, G.L., Bennie, A., Trieu, J., Ping, S., Tsafoulis, C., 2009. The chronology of age-related spatial learning impairment in two rat strains, as tested by the Barnes maze. *Behav. Neurosci.* 123, 533–538.
- Barrington, R., Williamson, G., Bennett, R.N., Davis, B.D., Brodbelt, J.S., Kroon, P.A., 2009. Absorption, conjugation and efflux of the flavonoids, kaempferol and galangin, using the intestinal CaCo-2/TC7 cell model. *J. Funct. Foods.* <https://doi.org/10.1016/j.jff.2008.09.011>
- Baur, J.A., Pearson, K.J., Price, N.L., Jamieson, H.A., Lerin, C., Kalra, A., Prabhu, V. V., Allard, J.S., Lopez-Lluch, G., Lewis, K., Pistell, P.J., Poosala, S., Becker, K.G., Boss, O., Gwinn, D., Wang, M., Ramaswamy, S., Fishbein, K.W., Spencer, R.G., Lakatta, E.G., Le Couteur, D., Shaw, R.J., Navas, P., Puigserver, P., Ingram, D.K., De Cabo, R., Sinclair, D.A., 2006. Resveratrol improves health and survival of mice on a

high-calorie diet. *Nature* 444, 337–342. <https://doi.org/10.1038/nature05354>

- Beale, R., Airs, R., 2016. Quantification of glycine betaine, choline and trimethylamine N-oxide in seawater particulates: Minimisation of seawater associated ion suppression. *Anal. Chim. Acta* 938, 114–122. <https://doi.org/10.1016/j.aca.2016.07.016>
- Bellanti, F., Romano, A.D., Lo Buglio, A., Castriotta, V., Guglielmi, G., Greco, A., Serviddio, G., Vendemiale, G., 2018. Oxidative stress is increased in sarcopenia and associated with cardiovascular disease risk in sarcopenic obesity. *Maturitas* 109, 6–12. <https://doi.org/10.1016/j.maturitas.2017.12.002>
- Benjamin, E.J., Blaha, M.J., Chiuve, S.E., Cushman, M., Das, S.R., Deo, R., De Ferranti, S.D., Floyd, J., Fornage, M., Gillespie, C., Isasi, C.R., Jimenez, M.C., Jordan, L.C., Judd, S.E., Lackland, D., Lichtman, J.H., Lisabeth, L., Liu, S., Longenecker, C.T., MacKey, R.H., Matsushita, K., Mozaffarian, D., Mussolino, M.E., Nasir, K., Neumar, R.W., Palaniappan, L., Pandey, D.K., Thiagarajan, R.R., Reeves, M.J., Ritchey, M., Rodriguez, C.J., Roth, G.A., Rosamond, W.D., Sasson, C., Towfighi, A., Tsao, C.W., Turner, M.B., Virani, S.S., Voeks, J.H., Willey, J.Z., Wilkins, J.T., Wu, J.H.Y., Alger, H.M., Wong, S.S., Muntner, P., 2017. Heart Disease and Stroke Statistics'2017 Update: A Report from the American Heart Association. *Circulation* 135, e146–e603. <https://doi.org/10.1161/CIR.0000000000000485>
- Benzie, I.F.F., Strain, J.J., 1996. The ferric reducing ability of plasma (FRAP) as a measure of “antioxidant power”: The FRAP assay. *Anal. Biochem.* 239, 70–76. <https://doi.org/10.1006/abio.1996.0292>
- Berlett, B.S., Stadtman, E.R., 1997. Protein oxidation in aging, disease, and oxidative stress. *J. Biol. Chem.* 272, 20313–6. <https://doi.org/10.1074/jbc.272.33.20313>
- Bertini, S., Calderone, V., Carboni, I., Maffei, R., Martelli, A., Martinelli, A., Minutolo, F., Rajabi, M., Testai, L., Tuccinardi, T., 2010. Synthesis of heterocycle-based analogs of resveratrol and their antitumor and vasorelaxing properties. *Bioorg. Med. Chem.* 18, 6715–6724.
- Bhatti, J.S., Bhatti, G.K., Reddy, P.H., 2017. Mitochondrial dysfunction and oxidative stress in metabolic disorders—A step towards mitochondria based therapeutic strategies. *Biochim. Biophys. Acta-Mol. Basis Dis* 1863, 1066–1077.
- Bianchi, M.A., Crenna, P., Punginelli, M., 2017. Aspetti normativi dei nutraceutici, in: Cicero, A.F.G., Colletti, A., Di Pierro, F. (Eds.), *Trattato Italiano Di Nutraceutica Clinica*. Scripta Manent Edizioni, pp. 29–36.
- Bishop, N.A., Lu, T., Yankner, B.A., 2010. Neural mechanisms of ageing and cognitive decline. *Nature*. <https://doi.org/10.1038/nature08983>
- Boban, M., Modun, D., Music, I., Vukovic, J., Brizic, I., Salamunic, I., Obad, A., Palada, I., Dujic, Z., 2006. Red

- wine induced modulation of vascular function: separating the role of polyphenols, ethanol, and urates. *J. Cardiovasc. Pharmacol.* 47, 695–701.
- Bonnefont-Rousselot, D., 2016. Resveratrol and cardiovascular diseases. *Nutrients* 8, 250.
- Bors, W., Heller, W., Michel, C., Saran, M., 1990. Flavonoids as antioxidants: Determination of radical-scavenging efficiencies. *Methods Enzymol.* 186, 343–55. [https://doi.org/10.1016/0076-6879\(90\)86128-I](https://doi.org/10.1016/0076-6879(90)86128-I)
- Boulton, D.W., Walle, U.K., Walle, T., 1998. Extensive binding of the bioflavonoid quercetin to human plasma proteins. *J. Pharm. Pharmacol.* 50, 243–249. <https://doi.org/10.1111/j.2042-7158.1998.tb06183.x>
- Bøyum, A., 1964. Separation of white blood cells. *Nature* 204, 793–4. <https://doi.org/10.1038/204793a0>
- Bradford, M.M., 1976. A rapid and sensitive method for the quantitation of microgram quantities of protein utilizing the principle of protein-dye binding. *Anal Biochem* 72, 248–254. <https://doi.org/10.1006/abio.1976.9999>
- Bradford, P.G., 2013. Curcumin and obesity. *BioFactors* 39, 78–87. <https://doi.org/10.1002/biof.1074>
- Brand-Williams, W., Cuvelier, M.E., Berset, C., 1995. Use of free radical method to evaluate antioxidant activity. *LWT-Food Sci. Technol* 28, 25–30.
- Bray, G.A., Frühbeck, G., Ryan, D.H., Wilding, J.P.H., 2016. Management of obesity. *Lancet* 387, 1947–56. [https://doi.org/10.1016/S0140-6736\(16\)00271-3](https://doi.org/10.1016/S0140-6736(16)00271-3)
- Breschi, M.C., Calderone, V., Digiacomo, M., Macchia, M., Martelli, A., Martinotti, E., Minutolo, F., Rapposelli, S., Rossello, A., Testai, L., 2006. New NO-releasing pharmacodynamic hybrids of losartan and its active metabolite: design, synthesis, and biopharmacological properties. *J. Med. Chem.* 49, 2628–2639.
- Breschi, M.C., Calderone, V., Digiacomo, M., Martelli, A., Martinotti, E., Minutolo, F., Rapposelli, S., Balsamo, A., 2004. NO-sartans: a new class of pharmacodynamic hybrids as cardiovascular drugs. *J. Med. Chem.* 47, 5597–5600.
- Brito, P., Almeida, L.M., Dinis, T.C.P., 2002. The interaction of resveratrol with ferrylmyoglobin and peroxynitrite; protection against LDL oxidation. *Free Radic. Res.* 36, 621–631. <https://doi.org/10.1080/10715760290029083>
- Brunet, A., Sweeney, L.B., Sturgill, J.F., Chua, K.F., Greer, P.L., Lin, Y., Tran, H., Ross, S.E., Mostoslavsky, R., Cohen, H.Y., Hu, L.S., Cheng, H.L., Jedrychowski, M.P., Gygi, S.P., Sinclair, D.A., Alt, F.W., Greenberg, M.E., 2004. Stress-Dependent Regulation of FOXO Transcription Factors by the SIRT1 Deacetylase.

Science (80-.). 303, 2011–2015. <https://doi.org/10.1126/science.1094637>

Bugger, H., Pfeil, K., 2020. Mitochondrial ROS in myocardial ischemia reperfusion and remodeling. *Biochim. Biophys. Acta-Mol. Basis Dis* 1866, 165768.

Bungau, S., Abdel-Daim, M.M., Tit, D.M., Ghanem, E., Sato, S., Maruyama-Inoue, M., Yamane, S., Kadonosono, K., 2019. Health Benefits of Polyphenols and Carotenoids in Age-Related Eye Diseases. *Oxid. Med. Cell. Longev.* 2019, 9783429. <https://doi.org/10.1155/2019/9783429>

Burgoyne, J.R., Mongue-Din, H., Eaton, P., Shah, A.M., 2012. Redox signaling in cardiac physiology and pathology. *Circ. Res.* 111, 1091–1106.

Burton, G.J., Jauniaux, E., 2011. Oxidative stress. *Best Pract. Res. Clin. Obstet. Gynaecol.* 25, 287–299.

Busquets-Cortés, C., Capó, X., Argelich, E., Ferrer, M.D., Mateos, D., Bouzas, C., Abbate, M., Tur, J.A., Sureda, A., Pons, A., 2018. Effects of micromolar steady-state hydrogen peroxide exposure on inflammatory and redox gene expression in immune cells from humans with metabolic syndrome. *Nutrients* 10, 1920. <https://doi.org/10.3390/nu10121920>

Cai, H., Harrison, D.G., 2000. Endothelial dysfunction in cardiovascular diseases: The role of oxidant stress. *Circ. Res.* <https://doi.org/10.1161/01.RES.87.10.840>

Calder, P.C., Ahluwalia, N., Brouns, F., Buetler, T., Clement, K., Cunningham, K., Esposito, K., Jönsson, L.S., Kolb, H., Lansink, M., Marcos, A., Margioris, A., Matusheski, N., Nordmann, H., O'Brien, J., Pugliese, G., Rizkalla, S., Schalkwijk, C., Tuomilehto, J., Wärnberg, J., Watzl, B., Winklhofer-Roob, B.M., 2011. Dietary factors and low-grade inflammation in relation to overweight and obesity. *Br. J. Nutr.* 106, S5–78. <https://doi.org/10.1017/s0007114511005460>

Calderone, V., Fiamingo, F.L., Giorgi, I., Leonardi, M., Livi, O., Martelli, A., Martinotti, E., 2006. Heterocyclic analogs of benzanilide derivatives as potassium channel activators. *Eur. J. Med. Chem.* 41, 761–767.

Calderone, V., Martelli, A., Testai, L., Martinotti, E., Breschi, M.C., 2007. Functional contribution of the endothelial component to the vasorelaxing effect of resveratrol and NS 1619, activators of the large-conductance calcium-activated potassium channels. *Naunyn. Schmiedebergs. Arch. Pharmacol.* 375, 73–80.

Calvert, M., Blazeby, J., Altman, D., Revicki, D., Moher, D., Brundage, M., and CONSORT PRO Group, 2013. Reporting of patient-reported outcomes in randomized trials: the CONSORT PRO extension. *JAMA* 309, 814–822.

- Capeillère-Blandin, C., 1998. Oxidation of guaiacol by myeloperoxidase: A two-electron-oxidized guaiacol transient species as a mediator of NADPH oxidation. *Biochem. J.* 336, 395–404.
<https://doi.org/10.1042/bj3360395>
- Carneiro, Â., Andrade, J.P., 2017. Nutritional and Lifestyle Interventions for Age-Related Macular Degeneration: A Review. *Oxid. Med. Cell. Longev.* 2017, 6469138. <https://doi.org/10.1155/2017/6469138>
- Carola, A., Tito, A., Bimonte, M., Mustilli, A., Cucchiara, M., Monoli, I., Hill, J., Apone, F., G., C., 2012. Liposoluble extracts of *Vitis vinifera* grape marc and cell cultures with synergistic anti-ageing effects. *Househ. Pers. Care Today* 7, 42–46.
- Carrier, A., 2017. Metabolic Syndrome and Oxidative Stress: A Complex Relationship. *Antioxid. Redox Signal.* 26, 429–431. <https://doi.org/10.1089/ars.2016.6929>
- Caruso, F., Tanski, J., Villegas-Estrada, A., Rossi, M., 2004. Structural basis for antioxidant activity of trans-resveratrol: Ab initio calculations and crystal and molecular structure. *J. Agric. Food Chem.* 52, 7279–7285. <https://doi.org/10.1021/jf048794e>
- Cash, C., 1998. Why tryptophan hydroxylase is difficult to purify: a reactive oxygen-derived species-mediated phenomenon that may be implicated in human pathology. *Gen. Pharmacol.* 30, 569–574.
- Castaldo, L., Narváez, A., Izzo, L., Graziani, G., Gaspari, A., Minno, G. Di, Ritieni, A., 2019. Red wine consumption and cardiovascular health. *Molecules.* <https://doi.org/10.3390/molecules24193626>
- Castro, L., Freeman, B.A., 2001. Reactive oxygen species in human health and disease. *Nutrition* 17, 161–165.
[https://doi.org/10.1016/S0899-9007\(00\)00570-0](https://doi.org/10.1016/S0899-9007(00)00570-0)
- Cesarone, M.R., Belcaro, G., Carratelli, M., Cornelli, U., De Sanctis, M.T., Incandela, L., Barsotti, A., Terranova, R., Nicolaidis, A., 1999. A simple test to monitor oxidative stress. *Int. Angiol.* 18, 127–30.
- Cetrullo, S., D'Adamo, S., Tantini, B., Borzi, R., Flamigni, F., 2015. mTOR, AMPK, and Sirt1: key players in metabolic stress management. *Crit. Rev. Eukaryot. Gene Expr.* 25, 59–75.
- Cháfer-Pericás, C., Herráez-Hernández, R., Campíns-Falcó, P., 2004. Selective determination of trimethylamine in air by liquid chromatography using solid phase extraction cartridges for sampling. *J. Chromatogr. A* 1042, 219–223. <https://doi.org/10.1016/j.chroma.2004.05.042>
- Chang, L., Karin, M., 2001. Mammalian MAP kinase signalling cascades. *Nature* 410, 37–40.
<https://doi.org/10.1038/35065000>
- Charles, A.L., Meyer, A., Dal-Ros, S., Auger, C., Keller, N., Ramamoorthy, T.G., Zoll, J., Metzger, D., Schini-

- Kerth, V., Geny, B., 2013. Polyphenols prevent ageing-related impairment in skeletal muscle mitochondrial function through decreased reactive oxygen species production. *Exp. Physiol.* 98, 536–545. <https://doi.org/10.1113/expphysiol.2012.067496>
- Chen, C.C., Chow, M.P., Huang, W.C., Lin, Y.C., Chang, Y.J., 2004. Flavonoids inhibit tumor necrosis factor- α -induced up-regulation of intercellular adhesion molecule-1 (ICAM-1) in respiratory epithelial cells through activator protein-1 and nuclear factor- κ B: Structure-activity relationships. *Mol. Pharmacol.* 66, 683–93. <https://doi.org/10.1124/mol.66.3>.
- Chen, F., Castranova, V., Shi, X., Demers, L.M., 1999. New insights into the role of nuclear factor- κ B, a ubiquitous transcription factor in the initiation of diseases. *Clin. Chem.* 45, 7–17. <https://doi.org/10.1093/clinchem/45.1.7>
- Chen, H., Li, J., Li, N., Liu, H., Tang, J., 2019. Increased circulating trimethylamine N-oxide plays a contributory role in the development of endothelial dysfunction and hypertension in the RUPP rat model of preeclampsia. *Hypertens. Pregnancy* 38, 96–104. <https://doi.org/10.1080/10641955.2019.1584630>
- Chen, J., Lin, D., Zhang, C., Li, G., Zhang, N., Ruan, L., Yan, Q., Li, J., Yu, X., Xie, X., Al, E., 2015. Antidepressant-like effects of ferulic acid: involvement of serotonergic and norepinephrine systems. *Metab. Brain Dis.* 30, 129–136.
- Chen, J.C., Ho, F.M., Chao, P.D.L., Chen, C.P., Jeng, K.C.G., Hsu, H.B., Lee, S.T., Wen, T.W., Lin, W.W., 2005. Inhibition of iNOS gene expression by quercetin is mediated by the inhibition of I κ B kinase, nuclear factor- κ B and STAT1, and depends on heme oxygenase-1 induction in mouse BV-2 microglia. *Eur. J. Pharmacol.* 521, 9–20. <https://doi.org/10.1016/j.ejphar.2005.08.005>
- Chen, J.H., Lee, M.S., Wang, C.P., Hsu, C.C., Lin, H.H., 2017. Autophagic effects of Hibiscus sabdariffa leaf polyphenols and epicatechin gallate (ECG) against oxidized LDL-induced injury of human endothelial cells. *Eur. J. Nutr.* 56, 1963–1981. <https://doi.org/10.1007/s00394-016-1239-4>
- Chen, L.W., Wang, Y.Q., Wei, L.C., Shi, M., Chan, Y.S., 2007. Chinese herbs and herbal extracts for neuroprotection of dopaminergic neurons and potential therapeutic treatment of Parkinson's disease. *CNS Neurol. Disord. Drug Targets* 6, 273–281.
- Chen, M.L., Yi, L., Zhang, Y., Zhou, X., Ran, L., Yang, J., Zhu, J.D., Zhang, Q.Y., Mi, M.T., 2016. Resveratrol attenuates trimethylamine-N-oxide (TMAO)-induced atherosclerosis by regulating TMAO synthesis and bile acid metabolism via remodeling of the gut microbiota. *MBio* 7, e02210-15. <https://doi.org/10.1128/mBio.02210-15>

- Chen, Z., Hagler, J., Palombella, V.J., Melandri, F., Scherer, D., Ballard, D., Maniatis, T., 1995. Signal-induced site-specific phosphorylation targets I κ B α to the ubiquitin-proteasome pathway. *Genes Dev.* 9, 1586–97. <https://doi.org/10.1101/gad.9.13.1586>
- Cheng, S., Shah, S.H., Corwin, E.J., Fiehn, O., Fitzgerald, R.L., Gerszten, R.E., Illig, T., Rhee, E.P., Srinivas, P.R., Wang, T.J., Jain, M., 2017. Potential Impact and Study Considerations of Metabolomics in Cardiovascular Health and Disease: A Scientific Statement from the American Heart Association. *Circ. Cardiovasc. Genet.* 10. <https://doi.org/10.1161/HCG.0000000000000032>
- Chou, R.H., Chen, C.Y., Chen, I.C., Huang, H.L., Lu, Y.W., Kuo, C.S., Chang, C.C., Huang, P.H., Chen, J.W., Lin, S.J., 2019. Trimethylamine N-Oxide, Circulating Endothelial Progenitor Cells, and Endothelial Function in Patients with Stable Angina. *Sci. Rep.* 12, 4249. <https://doi.org/10.1038/s41598-019-40638-y>
- Cicero, A.F.G., Colletti, A., 2017. Disposizioni ministeriali sulle quantità di principio attivo inseribili in un integratore, in: *Trattato Italiano Di Nutraceutica Clinica*. Scripta Manent Edizioni, pp. 603–606.
- Cicero, A.F.G., Colletti, A., Di Pierro, F. (Eds.), 2017. *Trattato italiano di nutraceutica clinica*. Scripta Manent Edizioni. <https://doi.org/978-88-908455-7-4>
- Cirillo, G., Curcio, M., Vittorio, O., Iemma, F., Restuccia, D., Spizzirri, U.G., Puoci, F., Picci, N., 2016. Polyphenol Conjugates and Human Health: A Perspective Review. *Crit. Rev. Food Sci. Nutr.* 56, 326–337.
- Clifton, P.M., 2004. Effect of grape seed extract and quercetin on cardiovascular and endothelial parameters in high-risk subjects. *J. Biomed. Biotechnol.* 2004, 272–278.
- Cohen, R., Schwartz, B., Peri, I., Shimoni, E., 2011. Improving bioavailability and stability of genistein by complexation with high-amylose corn starch, in: *Journal of Agricultural and Food Chemistry*. <https://doi.org/10.1021/jf2013277>
- Collier, T.J., Greene, J.G., Felten, D.L., Stevens, S.Y., Collier, K.S., 2004. Reduced cortical noradrenergic neurotransmission is associated with increased neophobia and impaired spatial memory in aged rats. *Neurobiol. Aging* 25, 209–211.
- Comalada, M., Camuesco, D., Sierra, S., Ballester, I., Xaus, J., Gálvez, J., Zarzuelo, A., 2005. In vivo quercitrin anti-inflammatory effect involves release of quercetin, which inhibits inflammation through down-regulation of the NF- κ B pathway. *Eur. J. Immunol.* 35, 584–92. <https://doi.org/10.1002/eji.200425778>
- Cools, R., 2011. Dopaminergic control of the striatum for high-level cognition. *Curr. Opin. Neurobiol.* 21, 402–407.

- Corretti, M.C., Anderson, T.J., Benjamin, E.J., Celermajer, D., Charbonneau, F., Creager, M.A., Deanfield, J., Drexler, H., Gerhard-Herman, M., Herrington, D., 2002. Guidelines for the ultrasound assessment of endothelial-dependent flow-mediated vasodilation of the brachial artery: a report of the International Brachial Artery Reactivity Task Force. *J. Am. Coll. Cardiol.* 39, 257–265.
- Crespy, V., Morand, C., Besson, C., Manach, C., Demigne, C., Remesy, C., 2002. Quercetin, but not its glycosides, is absorbed from the rat stomach. *J. Agric. Food Chem.* 50, 618–621.
<https://doi.org/10.1021/jf010919h>
- Curtis, M.J., Alexander, S., Cirino, G., Docherty, J.R., George, C.H., Giembycz, M.A., Hoyer, D., Insel, P.A., Izzo, A.A., Ji, Y., MacEwan, D.J., Sobey, C.G., Stanford, S.C., Teixeira, M.M., Wonnacott, S., Ahluwalia, A., 2018. Experimental design and analysis and their reporting II: updated and simplified guidance for authors and peer reviewers. *Br. J. Pharmacol.* <https://doi.org/10.1111/bph.14153>
- D'Archivio, M., Filesi, C., Vari, R., Sczzocchio, B., Masella, R., 2010. Bioavailability of the polyphenols: Status and controversies. *Int. J. Mol. Sci.* 11, 1321–1342. <https://doi.org/10.3390/ijms11041321>
- Daliu, P., Annunziata, G., Tenore, G.C., Santini, A., 2020. Abscisic acid identification in Okra, *Abelmoschus esculentus* L. (Moench): perspective nutraceutical use for the treatment of diabetes. *Nat. Prod. Res.* 34, 3–9. <https://doi.org/10.1080/14786419.2019.1637874>
- Dangles, O., Dufour, C., Bret, S., 1999. Flavonol-serum albumin complexation. Two-electron oxidation of flavonols and their complexes with serum albumin. *J Chem Soc 2*, 737–744.
- Dangles, O., Dufour, C., Manach, C., Morand, C., Remesy, C., 2001. Binding of flavonoids to plasma proteins. *Methods Enzymol.* 335, 319–333. [https://doi.org/10.1016/S0076-6879\(01\)35254-0](https://doi.org/10.1016/S0076-6879(01)35254-0)
- Datta, S., Cano, M., Ebrahimi, K., Wang, L., Handa, J.T., 2017. The impact of oxidative stress and inflammation on RPE degeneration in non-neovascular AMD. *Prog. Retin. Eye Res.* 60, 201–218.
<https://doi.org/10.1016/j.preteyeres.2017.03.002>
- Day, A.J., Cañada, F.J., Díaz, J.C., Kroon, P.A., McLauchlan, R., Faulds, C.B., Plumb, G.W., Morgan, M.R.A., Williamson, G., 2000. Dietary flavonoid and isoflavone glycosides are hydrolysed by the lactase site of lactase phlorizin hydrolase. *FEBS Lett.* 468, 166–170. [https://doi.org/10.1016/S0014-5793\(00\)01211-4](https://doi.org/10.1016/S0014-5793(00)01211-4)
- Day, A.J., Dupont, M.S., Ridley, S., Rhodes, M., Rhodes, M.J. c., Morgan, M.R. a., Williamson, G., 1998. Deglycosylation of flavonoid and isoflavonoid glycosides by human small intestine and liver β -glucosidase activity. *FEBS Lett.* 436, 71–75. [https://doi.org/10.1016/S0014-5793\(98\)01101-6](https://doi.org/10.1016/S0014-5793(98)01101-6)
- De Camargo, A.C., Regitano-D'Arce, M.A.B., Biasoto, A.C.T., Shahidi, F., 2014. Low molecular weight

- phenolics of grape juice and winemaking byproducts: Antioxidant activities and inhibition of oxidation of human low-density lipoprotein cholesterol and DNA strand breakage. *J. Agric. Food Chem.* 62, 12159–71. <https://doi.org/10.1021/jf504185s>
- de Groot, H., Rauen, U., 1998. Tissue injury by reactive oxygen species and the protective effects of flavonoids. *Fundam. Clin. Pharmacol.* 12, 249–255.
- De La Cruz, C.P., Revilla, E., Venero, J.L., Ayala, A., Cano, J., Machado, A., 1996. Oxidative inactivation of tyrosine hydroxylase in substantia nigra of aged rat. *Free Radic. Biol. Med.* 20, 53–61.
- De Leo, A., Arena, G., Lacanna, E., Oliviero, G., Colavita, F., Mattia, E., 2012. Resveratrol inhibits Epstein Barr Virus lytic cycle in Burkitt's lymphoma cells by affecting multiple molecular targets. *Antiviral Res.* 96, 196–202. <https://doi.org/10.1016/j.antiviral.2012.09.003>
- de Oliveira, W.P., Biasoto, A.C.T., Marques, V.F., dos Santos, I.M., Magalhães, K., Correa, L.C., Negro-Dellacqua, M., Miranda, M.S., de Camargo, A.C., Shahidi, F., 2017. Phenolics from Winemaking By-Products Better Decrease VLDL-Cholesterol and Triacylglycerol Levels than Those of Red Wine in Wistar Rats. *J. Food Sci.* 82, 2432–2437. <https://doi.org/10.1111/1750-3841.13841>
- Deacon, R.M., Rawlins, J.N., 2002. Learning impairments of hippocampal-lesioned mice in a paddling pool. *Behav. Neurosci.* 116, 472–478.
- Deidda, M., Piras, C., Dessalvi, C.C., Locci, E., Barberini, L., Torri, F., Ascedu, F., Atzori, L., Mercurio, G., 2015. Metabolomic approach to profile functional and metabolic changes in heart failure. *J. Transl. Med.* 13. <https://doi.org/10.1186/s12967-015-0661-3>
- Deledda, A., Annunziata, G., Tenore, G., Palmas, V., Manzin, A., Velluzzi, F., 2021. Diet-Derived Antioxidants and Their Role in Inflammation, Obesity and Gut Microbiota Modulation. *Antioxidants* 10, 708. <https://doi.org/10.3390/antiox10050708>
- des Rieux, A., Fievez, V., Garinot, M., Schneider, Y.J., Pr at, V., 2006. Nanoparticles as potential oral delivery systems of proteins and vaccines: A mechanistic approach. *J. Control. Release.* <https://doi.org/10.1016/j.jconrel.2006.08.013>
- Devaraj, S., Goyal, R., Jialal, I., 2008. Inflammation, oxidative stress, and the metabolic syndrome. *US Endocrinol.* 4, 32–37. <https://doi.org/10.17925/use.2008.04.2.32>
- Di Minno, A., Gentile, M., Iannuzzo, G., Calcaterra, I., Tripaldella, M., Porro, B., Cavalca, V., Di Taranto, M.D., Tremoli, E., Fortunato, G., 2020. Endothelial function improvement in patients with familial hypercholesterolemia receiving PCSK-9 inhibitors on top of maximally tolerated lipid lowering

therapy. *Thromb. Res.* 194, 229–236.

- Di Minno, M.N.D., Ambrosino, P., Buonomo, A.R., Pinchera, B., Calcaterra, I., Crispo, M., Scotto, R., Borgia, F., Mattia, C., Gentile, I., 2020. Direct-acting antivirals improve endothelial function in patients with chronic hepatitis: a prospective cohort study. *Intern. Emerg. Med.* 15, 263–271.
- Dias, M.I., Ferreira, I.C.F.R., Barreiro, M.F., 2015. Microencapsulation of bioactives for food applications. *Food Funct.* <https://doi.org/10.1039/c4fo01175a>
- Donato, A.J., Eskurza, I., Silver, A.E., Levy, A.S., Pierce, G.L., Gates, P.E., Seals, D.R., 2007. Direct evidence of endothelial oxidative stress with aging in humans: Relation to impaired endothelium-dependent dilation and upregulation of nuclear factor- κ B. *Circ. Res.* 100, 1659–1666. <https://doi.org/10.1161/01.RES.0000269183.13937.e8>
- Donato, A.J., Gano, L.B., Eskurza, I., Silver, A.E., Gates, P.E., Jablonski, K., Seals, D.R., 2009. Vascular endothelial dysfunction with aging: Endothelin-1 and endothelial nitric oxide synthase. *Am. J. Physiol. - Hear. Circ. Physiol.* 297. <https://doi.org/10.1152/ajpheart.00689.2008>
- Dong, Z., Liang, Z., Guo, M., Hu, S., Shen, Z., Hai, X., 2018. The Association between Plasma Levels of Trimethylamine N-Oxide and the Risk of Coronary Heart Disease in Chinese Patients with or without Type 2 Diabetes Mellitus. *Dis. Markers* 2018, 1578320. <https://doi.org/10.1155/2018/1578320>
- Dowling, D.K., Simmons, L.W., 2009. Reactive oxygen species as universal constraints in life-history evolution. *Proc. R. Soc. B Biol. Sci.* 276, 1737–45. <https://doi.org/10.1098/rspb.2008.1791>
- Dubois-Deruy, E., Peugnet, V., Turkieh, A., Pinet, F., 2020. Oxidative Stress in Cardiovascular Diseases. *Antioxidants* 9, 864.
- Dunlap, A.B., Kosmorsky, G.S., Kashyap, V.S., 2007. The fate of patients with retinal artery occlusion and Hollenhorst plaque. *J. Vasc. Surg.* 46, 1125–9. <https://doi.org/10.1016/j.jvs.2007.07.054>
- Dunlop, E., Tee, A., 2014. mTOR and autophagy: a dynamic relationship governed by nutrients and energy. *Semin. Cell&Developmental Biol.* 36, 121–129.
- Dutta, S., Moses, J.A., Anandharamakrishnan, C., 2018. Encapsulation of Nutraceutical Ingredients in Liposomes and Their Potential for Cancer Treatment. *Nutr. Cancer.* <https://doi.org/10.1080/01635581.2018.1557212>
- Ellulu, M.S., Patimah, I., Khaza'ai, H., Rahmat, A., Abed, Y., 2017. Obesity & inflammation: The linking mechanism & the complications. *Arch. Med. Sci.* 13, 851–863. <https://doi.org/10.5114/aoms.2016.58928>

- Erickson, J.R., Mei-ling, A.J., Guan, X., Kutschke, W., Yang, J., Oddis, C.V., Bartlett, R.K., Lowe, J.S., O'Donnell, S.E., Aykin-Burns, N., Al., E., 2008. A Dynamic Pathway for Calcium-Independent Activation of CaMKII by Methionine Oxidation. *Cell* 133, 462–474.
- Esteban, S., Garau, C., Aparicio, S., Moranta, D., Barcelo, P., Fiol, M.A., Rial, R., 2010. Chronic melatonin treatment and its precursor L-tryptophan improve the monoaminergic neurotransmission and related behavior in the aged rat brain. *J. Pineal Res.* 48, 170–177.
- Esterbauer, H., Cheeseman, K.H., Dianzani, M.U., Poli, G., Slater, T.F., 1982. Separation and characterization of the aldehydic products of lipid peroxidation stimulated by ADP-Fe²⁺ in rat liver microsomes. *Biochem. J.* 208, 129–140. <https://doi.org/10.1042/bj2080129>
- Esterbauer, H., Schaur, R.J., Zollner, H., 1991. Chemistry and biochemistry of 4-hydroxynonenal, malonaldehyde and related aldehydes. *Free Radic. Biol. Med.* 11, 81–128. [https://doi.org/10.1016/0891-5849\(91\)90192-6](https://doi.org/10.1016/0891-5849(91)90192-6)
- European Food Safety Authority, EFSA [WWW Document], 2021. URL <https://www.efsa.europa.eu/en>
- European Parliament and Council, 2002. Directive 2002/46/EC.
- Faith, S.A., Sweet, T.J., Bailey, E., Booth, T., Docherty, J.J., 2006. Resveratrol suppresses nuclear factor- κ B in herpes simplex virus infected cells. *Antiviral Res.* 72, 242–251. <https://doi.org/10.1016/j.antiviral.2006.06.011>
- Farzaei, M.H., Singh, A.K., Kumar, R., Croley, C.R., Pandey, A.K., Coy-Barrera, E., Patra, J.K., Das, G., Kerry, R.G., Annunziata, G., Tenore, G.C., Khan, H., Micucci, M., Budriesi, R., Momtaz, S., Nabavi, S.M., Bishayee, A., 2019. Targeting inflammation by flavonoids: Novel therapeutic strategy for metabolic disorders. *Int. J. Mol. Sci.* 20, 4957. <https://doi.org/10.3390/ijms20194957>
- Fatnassi, M., Tourné-Péteilh, C., Peralta, P., Cacciaguerra, T., Dieudonné, P., Devoisselle, J.M., Alonso, B., 2013. Encapsulation of complementary model drugs in spray-dried nanostructured materials. *J. Sol-Gel Sci. Technol.* <https://doi.org/10.1007/s10971-013-3170-y>
- Feng, L., Yang, X., Shi, Y., Liang, S., Zhao, T., Duan, J., Sun, Z., 2018. Co-exposure subacute toxicity of silica nanoparticles and lead acetate on cardiovascular system. *Int. J. Nanomedicine* 13, 7819–7834.
- Feng, X., Sureda, A., Jafari, S., Memariani, Z., Tewari, D., Annunziata, G., Barrea, L., Hassan, S.T.S., Smejkal, K., Malaník, M., Sychrová, A., Barreca, D., Ziberna, L., Mahomoodally, M.F., Zengin, G., Xu, S., Nabavi, S.M., Shen, A.Z., 2019. Berberine in cardiovascular and metabolic diseases: From mechanisms to therapeutics. *Theranostics* 9, 1923–1951. <https://doi.org/10.7150/thno.30787>

- Fennema, D., Phillips, I.R., Shephard, E.A., 2016. Trimethylamine and trimethylamine N-oxide, a Flavin-Containing Monooxygenase 3 (FMO3)-mediated host-microbiome metabolic axis implicated in health and disease. *Drug Metab. Dispos.* 44, 1839–1850. <https://doi.org/10.1124/dmd.116.070615>
- Fernández-Quintela, A., Milton-Laskibar, I., González, M., Portillo, M.P., 2017. Antiobesity effects of resveratrol: Which tissues are involved? *Ann. N. Y. Acad. Sci.* <https://doi.org/10.1111/nyas.13413>
- Fihn, S.D., Gardin, J.M., Abrams, J., Berra, K., Blankenship, J.C., Dallas, A.P., Douglas, P.S., Foody, J.M., Gerber, T.C., Hinderliter, A.L., King, S.B., Kligfield, P.D., Krumholz, H.M., Kwong, R.Y.K., Lim, M.J., Linderbaum, J.A., MacK, M.J., Munger, M.A., Prager, R.L., Sabik, J.F., Shaw, L.J., Sikkema, J.D., Smith, C.R., Smith, S.C., Spertus, J.A., Williams, S. V., 2012. 2012 ACCF/AHA/ACP/AATS/PCNA/SCAI/STS guideline for the diagnosis and management of patients with stable ischemic heart disease: *Circulation* 126, 3097–3137. <https://doi.org/10.1161/CIR.0b013e3182776f83>
- Flohe, L., Gunzler, W., 1984. Assay of glutathione peroxidase. *Methods Enzymol.* 105, 114–121.
- Flowers, A., Lee, J.Y., Acosta, S., Hudson, C., Small, B., Sanberg, C.D., Bickford, P., 2015. NT-020 treatment reduces inflammation and augments Nrf-2 and Wnt signaling in aged rats. *J. Neuroinflammation* 12, 174.
- Fortuño, A., José, G.S., Moreno, M.U., Beloqui, O., Díez, J., Zalba, G., 2006. Phagocytic NADPH oxidase overactivity underlies oxidative stress in metabolic syndrome. *Diabetes* 55, 209–215.
- Frankel, E.N., German, J.B., Kinsella, J.E., Parks, E., Kanner, J., 1993. Inhibition of oxidation of human low-density lipoprotein by phenolic substances in red wine. *Lancet* 341, 454–7. [https://doi.org/10.1016/0140-6736\(93\)90206-V](https://doi.org/10.1016/0140-6736(93)90206-V)
- Fruchart, J.C., Sacks, F., Hermans, M.P., Assmann, G., Brown, W.V., Ceska, R., Chapman, M.J., Dodson, P.M., Fioretto, P., Ginsberg, H.N., Kadowaki, T., Lablanche, J.M., Marx, N., Plutzky, J., Reiner, Ž., Rosenson, R.S., Staels, B., Stock, J.K., Sy, R., Wanner, C., Zambon, A., Zimmet, P., 2008. The Residual Risk Reduction Initiative: A Call to Action to Reduce Residual Vascular Risk in Patients with Dyslipidemia. *Am. J. Cardiol.* 102, 1K-34K. <https://doi.org/10.1016/j.amjcard.2008.10.002>
- Furtado, G.E., Carvalho, H.M., Loureiro, M., Patrício, M., Uba-Chupel, M., Colado, J.C., Hogervorst, E., Ferreira, J.P., Teixeira, A.M., 2020. Chair-based exercise programs in institutionalized older women: Salivary steroid hormones, disabilities and frailty changes. *Exp. Gerontol.* 130. <https://doi.org/10.1016/j.exger.2019.110790>
- Gareri, P., De Fazio, P., De Sarro, G., 2002. Neuropharmacology of depression in aging and age-related

diseases. *Ageing Res. Rev.* [https://doi.org/10.1016/S0047-6374\(01\)00370-0](https://doi.org/10.1016/S0047-6374(01)00370-0)

Gee, J.M., Dupont, M.S., Rhodes, M.J.C., Johnson, I.T., 1998. Quercetin glucosides interact with the intestinal glucose transport pathway. *Free Radic. Biol. Med.* 25, 19–25. [https://doi.org/10.1016/S0891-5849\(98\)00020-3](https://doi.org/10.1016/S0891-5849(98)00020-3)

Gehrs, K.M., Anderson, D.H., Johnson, L. V., Hageman, G.S., 2006. Age-related macular degeneration - Emerging pathogenetic and therapeutic concepts. *Ann. Med.* 38, 405–71. <https://doi.org/10.1080/07853890600946724>

Geng, J., Yang, C., Wang, B., Zhang, X., Hu, T., Gu, Y., Li, J., 2018. Trimethylamine N-oxide promotes atherosclerosis via CD36-dependent MAPK/JNK pathway. *Biomed. Pharmacother.* 97, 941–947. <https://doi.org/10.1016/j.biopha.2017.11.016>

George, C.H., Stanford, S.C., Alexander, S., Cirino, G., Docherty, J.R., Giembycz, M.A., Hoyer, D., Insel, P.A., Izzo, A.A., Ji, Y., MacEwan, D.J., Sobey, C.G., Wonnacott, S., Ahluwalia, A., 2017. Updating the guidelines for data transparency in the *British Journal of Pharmacology* – data sharing and the use of scatter plots instead of bar charts. *Br. J. Pharmacol.* <https://doi.org/10.1111/bph.13925>

George, T.W., Waroonphan, S., Niwat, C., Gordon, M.H., Lovegrove, J.A., 2012. The Glu298Asp single nucleotide polymorphism in the endothelial nitric oxide synthase gene differentially affects the vascular response to acute consumption of fruit and vegetable puree based drinks. *Mol. Nutr. Food Res.* 56, 1014–24. <https://doi.org/10.1002/mnfr.201100689>

Gerardi, G.M., Usberti, M., Martini, G., Albertini, A., Sugherini, L., Pompella, A., Di Lorenzo, D., 2002. Plasma total antioxidant capacity in hemodialyzed patients and its relationships to other biomarkers of oxidative stress and lipid peroxidation. *Clin. Chem. Lab. Med.* 40, 104–10. <https://doi.org/10.1515/CCLM.2002.019>

Gharsallaoui, A., Roudaut, G., Chambin, O., Voilley, A., Saurel, R., 2007. Applications of spray-drying in microencapsulation of food ingredients: An overview. *Food Res. Int.* <https://doi.org/10.1016/j.foodres.2007.07.004>

Giusti, F., Caprioli, G., Ricciutelli, M., Vittori, S., Sagratini, G., 2017. Determination of fourteen polyphenols in pulses by high performance liquid chromatography-diode array detection (HPLC-DAD) and correlation study with antioxidant activity and colour. *Food Chem.* 221, 689–697. <https://doi.org/10.1016/j.foodchem.2016.11.118>

Goldberg, D.M., Spooner, R., 1984. Glutathione reductase, in: Verlagchemie, B. (Ed.), *Methods of Enzymatic*

Analysis. Enzyme 1: Oxidoreductases, Transferases. pp. 258–265.

- Gomez-Monterrey, I., Campiglia, I., Aquino, C., Al., E., 2011. Design, synthesis, and cytotoxic evaluation of acyl derivatives of 3- aminonaphtho[2,3-b]thiophene-4,9-dione, a quinone-based system. *J. Med. Chem.* 54, 4077–4091.
- Gomez-Pinilla, F., Nguyen, T.T.J., 2012. Natural mood foods: The actions of polyphenols against psychiatric and cognitive disorders. *Nutr. Neurosci.* <https://doi.org/10.1179/1476830511Y.0000000035>
- Gonzales, A.M., Orlando, R.A., 2008. Curcumin and resveratrol inhibit nuclear factor-kappaB-mediated cytokine expression in adipocytes. *Nutr. Metab.* 5, 17. <https://doi.org/10.1186/1743-7075-5-17>
- Graefe, E.U., Wittig, J., Mueller, S., Riethling, A.K., Uehleke, B., Drewelow, B., Pforte, H., Jacobasch, G., Derendorf, H., Veit, M., 2001. Pharmacokinetics and bioavailability of quercetin glycosides in humans. *J. Clin. Pharmacol.* 41, 492–499. <https://doi.org/10.1177/00912700122010366>
- Gregor, M.F., Hotamisligil, G.S., 2011. Inflammatory mechanisms in obesity. *Annu. Rev. Immunol.* 29, 415–445. <https://doi.org/10.1146/annurev-immunol-031210-101322>
- Gregory, J.C., Buffa, J.A., Org, E., Wang, Z., Levison, B.S., Zhu, W., Wagner, M.A., Bennett, B.J., Li, L., DiDonato, J.A., Lusic, A.J., Hazen, S.L., 2015. Transmission of atherosclerosis susceptibility with gut microbial transplantation. *J. Biol. Chem.* 290, 5647–5660. <https://doi.org/10.1074/jbc.M114.618249>
- Haghikia, Arash, Li, X.S., Liman, T.G., Bledau, N., Schmidt, D., Zimmermann, F., Kränkel, N., Widera, C., Sonnenschein, K., Haghikia, Aiden, Weissenborn, K., Fraccarollo, D., Heimesaat, M.M., Bauersachs, J., Wang, Z., Zhu, W., Bavendiek, U., Hazen, S.L., Endres, M., Landmesser, U., 2018. Gut microbiota-dependent trimethylamine N-oxide predicts risk of cardiovascular events in patients with stroke and is related to proinflammatory monocytes. *Arterioscler. Thromb. Vasc. Biol.* 38, 2225–2235. <https://doi.org/10.1161/ATVBAHA.118.311023>
- Haider, S., Saleem, S., Perveen, T., Tabassum, S., Batool, Z., Sadir, S., Liaquat, L., Madiha, S., 2014. Age-related learning and memory deficits in rats: role of altered brain neurotransmitters, acetylcholinesterase activity and changes in antioxidant defense system. *Age (Omaha)*. 36, 9653.
- Hampton, S., Isherwood, C., Kirkpatrick, V., Lynne-Smith, A., Griffin, B., 2010. The influence of alcohol consumed with a meal on endothelial function in healthy individuals. *J. Hum. Nutr. Diet.* 23, 120–125.
- Harman, D., 1968. Free radical theory of aging: effect of free radical reaction inhibitors on the mortality rate of male LAF mice. *J. Gerontol.* 23, 476–82. <https://doi.org/10.1093/geronj/23.4.476>

- Harman, D., 1956. Aging: a theory based on free radical and radiation chemistry. *J. Gerontol.*
<https://doi.org/10.1093/geronj/11.3.298>
- Hayreh, S.S., 2011. Acute retinal arterial occlusive disorders. *Prog. Retin. Eye Res.* 30, 359–94.
<https://doi.org/10.1016/j.preteyeres.2011.05.001>
- Hayreh, S.S., Podhajsky, P.A., Zimmerman, M.B., 2009. Retinal Artery Occlusion. Associated Systemic and Ophthalmic Abnormalities. *Ophthalmology* 116, 1928–36. <https://doi.org/10.1016/j.ophtha.2009.03.006>
- He, Q., Sha, S., Sun, L., Zhang, J., Dong, M., 2016. GLP-1 analogue improves hepatic lipid accumulation by inducing autophagy via AMPK/mTOR pathway. *Biochem. Biophys. Res. Commun.* 476, 196–203.
- Hedden, T., Gabrieli, J.D., 2004. Insights into the ageing mind: a view from cognitive neuroscience. *Nat. Rev. Neurosci.* 5, 87–96.
- Hollman, P.C.H., Bijlsman, M.N.C.P., Van Gameren, Y., Cnossen, E.P.J., De Vries, J.H.M., Katan, M.B., 1999. The sugar moiety is a major determinant of the absorption of dietary flavonoid glycosides in man. *Free Radic. Res.* 31, 569–573. <https://doi.org/10.1080/10715769900301141>
- Hollman, P.C.H., De Vries, J.H.M., Van Leeuwen, S.D., Mengelers, M.J.B., Katan, M.B., 1995. Absorption of dietary quercetin glycosides and quercetin in healthy ileostomy volunteers. *Am. J. Clin. Nutr.* 62, 1276–1282. <https://doi.org/10.1093/ajcn/62.6.1276>
- Hollman, P.C.H., Katan, M.B., 1997. Absorption, metabolism and health effects of dietary flavonoids in man. *Biomed. Pharmacother.* 51, 305–310. [https://doi.org/10.1016/S0753-3322\(97\)88045-6](https://doi.org/10.1016/S0753-3322(97)88045-6)
- Holvoet, P., 2008. Relations between metabolic syndrome, oxidative stress and inflammation and cardiovascular disease. *Verh. K. Acad. Geneesk. Belg.* 70, 193–219.
- Horie, T., Mizuma, T., Kasai, S., Awazu, S., 1988. Conformational change in plasma albumin due to interaction with isolated rat hepatocyte. *Am. J. Physiol. - Gastrointest. Liver Physiol.* 254. <https://doi.org/10.1152/ajpgi.1988.254.4.g465>
- Howard, C., Ferrucci, L., Sun, K., Fried, L.P., Walston, J., Varadhan, R., Guralnik, J.M., Semba, R.D., 2007. Oxidative protein damage is associated with poor grip strength among older women living in the community. *J. Appl. Physiol.* 103, 17–20. <https://doi.org/10.1152/jappphysiol.00133.2007>
- Hsu, W.Y., Lo, W.Y., Lai, C.C., Tsai, F.J., Tsai, C.H., Tsai, Y., Lin, W. De, Chao, M.C., 2007. Rapid screening assay of trimethylaminuria in urine with matrix-assisted laser desorption/ionization time-of-flight mass spectrometry. *Rapid Commun. Mass Spectrom.* 21, 1915–1919. <https://doi.org/10.1002/rcm.3043>

- Hu, B., Liu, X., Zhang, C., Zeng, X., 2017. Food macromolecule based nanodelivery systems for enhancing the bioavailability of polyphenols. *J. Food Drug Anal.* <https://doi.org/10.1016/j.jfda.2016.11.004>
- Huang, Y., Zhu, X., Chen, K., Lang, H., Zhang, Y., Hou, P., Ran, L., Zhou, M., Zheng, J., Yi, L., Mi, M., Zhang, Q., 2019. Resveratrol prevents sarcopenic obesity by reversing mitochondrial dysfunction and oxidative stress via the PKA/LKB1/AMPK pathway. *Aging (Albany, NY)*. 11, 2217–2240. <https://doi.org/10.18632/aging.101910>
- Hussain, A.M., Mitra, A.K., 2000. Effect of aging on tryptophan hydroxylase in rat brain: implications on serotonin level. *Drug Metab. Dispos.* 28, 1038–1042.
- Ichikawa, D., Matsui, A., Imai, M., Sonoda, Y., Kasahara, T., 2004. Effect of various catechins on the IL-12p40 production by murine peritoneal macrophages and a macrophage cell line, J774.1. *Biol. Pharm. Bull.* 27, 1353–8. <https://doi.org/10.1248/bpb.27.1353>
- Iglesias-Carres, L., Essenmacher, L.A., Racine, K.C., Neilson, A.P., 2021. Development of a High Throughput Method to Study the Inhibitory Effect of Phytochemicals on Trimethylamine Formation. *Nutrients* 13, 1466. <https://doi.org/10.3390/nu13051466>
- Israël, A., 2010. The IKK complex, a central regulator of NF-kappaB activation. *Cold Spring Harb. Perspect. Biol.* 2, a000158. <https://doi.org/10.1101/cshperspect.a000158>
- Jackson, M.J., Mcardle, A., 2011. Age-related changes in skeletal muscle reactive oxygen species generation and adaptive responses to reactive oxygen species, in: *Journal of Physiology*. *J Physiol*, pp. 2139–2145. <https://doi.org/10.1113/jphysiol.2011.206623>
- Jaipersad, A.S., Lip, G.Y.H., Silverman, S., Shantsila, E., 2014. The role of monocytes in angiogenesis and atherosclerosis. *J. Am. Coll. Cardiol.* 63, 1–11. <https://doi.org/10.1016/j.jacc.2013.09.019>
- Janeiro, M.H., Ramírez, M.J., Milagro, F.I., Martínez, J.A., Solas, M., 2018. Implication of trimethylamine n-oxide (TMAO) in disease: Potential biomarker or new therapeutic target. *Nutrients*. <https://doi.org/10.3390/nu10101398>
- Jayarathne, S., Koboziev, I., Park, O.H., Oldewage-Theron, W., Shen, C.L., Moustaid-Moussa, N., 2017. Anti-Inflammatory and Anti-Obesity Properties of Food Bioactive Components: Effects on Adipose Tissue. *Prev. Nutr. Food Sci.* 22, 251–262. <https://doi.org/10.3746/pnf.2017.22.4.251>
- Jeong, E.M., Chung, J., Liu, H., Al, E., 2016. Role of Mitochondrial Oxidative Stress in Glucose Tolerance, Insulin Resistance, and Cardiac Diastolic Dysfunction. *J. Am. Hear. Assoc* 5, 003046.

- Jones, D.P., Mody, V.C., Carlson, J.L., Lynn, M.J., Sternberg, P., 2002. Redox analysis of human plasma allows separation of pro-oxidant events of aging from decline in antioxidant defenses. *Free Radic. Biol. Med.* 33, 1290–300. [https://doi.org/10.1016/S0891-5849\(02\)01040-7](https://doi.org/10.1016/S0891-5849(02)01040-7)
- Kaldas, M.I., Walle, U.K., Walle, T., 2003. Resveratrol transport and metabolism by human intestinal Caco-2 cells. *J. Pharm. Pharmacol.* <https://doi.org/10.1211/002235702612>
- Karatzis, K., Papamichael, C., Karatzis, E., Papaioannou, T.G., Voidonikola, P.T., Lekakis, J., Zampelas, A., 2007. Acute smoking induces endothelial dysfunction in healthy smokers. Is this reversible by red wine's antioxidant constituents? *J. Am. Coll. Nutr.* 26, 10–15.
- Karatzis, K., Papamichael, C., Karatzis, E., Papaioannou, T.G., Voidonikola, P.T., Vamvakou, G.D., Lekakis, J., Zampelas, A., 2008. Postprandial improvement of endothelial function by red wine and olive oil antioxidants: a synergistic effect of components of the Mediterranean diet. *J. Am. Coll. Nutr.* 27, 448–453.
- Karimi, G., Vahabzadeh, M., Lari, P., Rashedinia, M., Moshiri, M., 2011. "Silymarin", a promising pharmacological agent for treatment of diseases. *Iran. J. Basic Med. Sci.* 14, 308–317.
- Karin, M., 2005. Inflammation-activated protein kinases as targets for drug development. *Proc. Am. Thorac. Soc.* 2, 386–90. <https://doi.org/10.1513/pats.200504-034SR>
- Karin, M., 1995. The regulation of AP-1 activity by mitogen-activated protein kinases. *J. Biol. Chem.* 270, 16483–6. <https://doi.org/10.1074/jbc.270.28.16483>
- Karlsson, F.H., Fåk, F., Nookaew, I., Tremaroli, V., Fagerberg, B., Petranovic, D., Bäckhed, F., Nielsen, J., 2012. Symptomatic atherosclerosis is associated with an altered gut metagenome. *Nat. Commun.* 3, 1245. <https://doi.org/10.1038/ncomms2266>
- Kauppinen, A., Paterno, J.J., Blasiak, J., Salminen, A., Kaarniranta, K., 2016. Inflammation and its role in age-related macular degeneration. *Cell. Mol. Life Sci.* 73, 1765–86. <https://doi.org/10.1007/s00018-016-2147-8>
- Keller, J.N., Schmitt, F.A., Scheff, S.W., Ding, Q., Chen, Q., Butterfield, D.A., Markesbery, W., 2005. Evidence of increased oxidative damage in subjects with mild cognitive impairment. *Neurology* 64, 1152–1156.
- Khan, N., Afaq, F., Saleem, M., Ahmad, N., Mukhtar, H., 2006. Targeting multiple signaling pathways by green tea polyphenol (-)-epigallocatechin-3-gallate. *Cancer Res.* 66, 2500–5. <https://doi.org/10.1158/0008-5472.CAN-05-3636>
- Khaybullina, Z.R., 2017. Inflammation and Oxidative Stress: Critical Role for Metabolic Syndrome. *J Vasc*

Med Surg 5, 302.

- Khurana, S., Venkataraman, K., Hollingsworth, A., Piche, M., Tai, T.C., 2013. Polyphenols: Benefits to the cardiovascular system in health and in aging. *Nutrients*. <https://doi.org/10.3390/nu5103779>
- Kida, K., Suzuki, M., Matsumoto, N., Nanjo, F., Hara, Y., 2000. Identification of biliary metabolites of (-)-epigallocatechin gallate in rats. *J. Agric. Food Chem.* 48, 4151–4155. <https://doi.org/10.1021/jf000386x>
- Kilkenny, C., Browne, W., Cuthill, I.C., Emerson, M., Altman, D.G., 2010. Animal research: reporting in vivo experiments: the ARRIVE guidelines. *Br. J. Pharmacol.* 160, 1577–1579.
- Kim, S., Foong, D., Cooper, M.S., Seibel, M.J., Zhou, H., 2018. Comparison of blood sampling methods for plasma corticosterone measurements in mice associated with minimal stress-related artefacts. *Steroids* 135, 69–72. <https://doi.org/10.1016/j.steroids.2018.03.004>
- Klop, B., Elte, J.W.F., Cabezas, M.C., 2013. Dyslipidemia in Obesity: Mechanisms and Potential Targets. *Nutrients* 5, 1218–40. <https://doi.org/10.3390/nu5041218>
- Koenig, R.T., Dickman, J.R., Wise, M.L., Ji, L.L., 2011. Avenanthramides Are bioavailable and accumulate in hepatic, cardiac, and skeletal muscle tissue following oral gavage in rats. *J. Agric. Food Chem.* 59, 6438–6443. <https://doi.org/10.1021/jf2002427>
- Koeth, R.A., Wang, Z., Levison, B.S., Buffa, J.A., Org, E., Sheehy, B.T., Britt, E.B., Fu, X., Wu, Y., Li, L., Smith, J.D., Didonato, J.A., Chen, J., Li, H., Wu, G.D., Lewis, J.D., Warriar, M., Brown, J.M., Krauss, R.M., Tang, W.H.W., Bushman, F.D., Lusic, A.J., Hazen, S.L., 2013. Intestinal microbiota metabolism of l-carnitine, a nutrient in red meat, promotes atherosclerosis. *Nat. Med.* 19, 576–585. <https://doi.org/10.1038/nm.3145>
- Kondratyuk, T.P., Pezzuto, J.M., 2004. Natural Product Polyphenols of Relevance to Human Health. *Pharm. Biol.* 42, 46–63. <https://doi.org/10.3109/13880200490893519>
- Kuhnau, J., 1976. The flavonoids. A class of semi-essential food components: their role in human nutrition. *World Rev Nutr Diet* 24, 117–191.
- Kulandaivelu, K., Mandal, A.K.A., 2017. Improved bioavailability and pharmacokinetics of tea polyphenols by encapsulation into gelatin nanoparticles. *IET Nanobiotechnology*. <https://doi.org/10.1049/iet-nbt.2016.0147>
- Kumar, A., Naidu, P.S., Seghal, N., Padi, S.S., 2007. Neuroprotective effects of resveratrol against intracerebroventricular colchicine-induced cognitive impairment and oxidative stress in rats. *Pharmacology* 79, 17–26.

- Kume, S., Koya, D., 2015. Autophagy: a novel therapeutic target for diabetic nephropathy. *Diabetes Metab. J.* 39, 451–460.
- Kurutas, E.B., 2016. The importance of antioxidants which play the role in cellular response against oxidative/nitrosative stress: Current state. *Nutr. J.* 15, 71. <https://doi.org/10.1186/s12937-016-0186-5>
- Kwan, H.S., Barrett, E.L., 1983. Purification and properties of trimethylamine oxide reductase from *Salmonella typhimurium*. *J. Bacteriol.* 155, 1455–1458. <https://doi.org/10.1128/jb.155.3.1455-1458.1983>
- Lam, C.W., Law, C.Y., To, K.K.W., Cheung, S.K.K., Lee, K. chung, Sze, K.H., Leung, K.F., Yuen, K.Y., 2014. NMR-based metabolomic urinalysis: A rapid screening test for urinary tract infection. *Clin. Chim. Acta* 436, 217–223. <https://doi.org/10.1016/j.cca.2014.05.014>
- Lama, S., Monda, V., Rizzo, M.R., Dacrema, M., Maisto, M., Annunziata, G., Tenore, G.C., Novellino, E., Stiuso, P., 2020. Cardioprotective Effects of Taurisolo® in Cardiomyoblast H9c2 Cells under High-Glucose and Trimethylamine N-Oxide Treatment via De Novo Sphingolipid Synthesis. *Oxid. Med. Cell. Longev.* 2020, 2961406.
- Lambert, K., Hokayem, M., Thomas, C., Fabre, O., Cassan, C., Bourret, A., Bernex, F., Feuillet-Coudray, C., Notarnicola, C., Mercier, J., Avignon, A., Bisbal, C., 2018. Combination of nutritional polyphenols supplementation with exercise training counteracts insulin resistance and improves endurance in high-fat diet-induced obese rats. *Sci. Rep.* 8. <https://doi.org/10.1038/s41598-018-21287-z>
- Lancel, S., Qin, F., Lennon, S.L., Zhang, J., Tong, X., Mazzini, M.J., Kang, Y.J., Siwik, D.A., Cohen, R.A., Colucci, W.S., 2010. Oxidative posttranslational modifications mediate decreased SERCA activity and myocyte dysfunction in Galphaq-overexpressing mice. *Circ. Res* 107, 228–232.
- Lapi, D., Stornaiuolo, M., Sabatino, L., Sommella, E., Tenore, G., Daglia, M., Scuri, R., Di Maro, M., Colantuoni, A., Novellino, E., 2020. The Pomace Extract Taurisolo Protects Rat Brain From Ischemia-Reperfusion Injury. *Front. Cell. Neurosci.* 14, 3. <https://doi.org/10.3389/fncel.2020.00003>
- Laurent, C., Chabi, B., Fouret, G., Py, G., Sairafi, B., Elong, C., Gaillet, S., Cristol, J.P., Coudray, C., Feillet-Coudray, C., 2012. Polyphenols decreased liver NADPH oxidase activity, increased muscle mitochondrial biogenesis and decreased gastrocnemius age-dependent autophagy in aged rats. *Free Radic. Res.* 46, 1140–1149. <https://doi.org/10.3109/10715762.2012.694428>
- Law, D.A., DeGuzman, F.R., Heiser, P., Ministri-Madrid, K., Killeen, N., Phillips, D.R., 1999. Integrin cytoplasmic tyrosine motif is required for outside-in α IIb β 3 signalling and platelet function. *Nature* 401, 808–811. <https://doi.org/10.1038/44599>

- Lee, H., Lim, J.Y., Choi, S.J., 2017. Oleate Prevents Palmitate-Induced Atrophy via Modulation of Mitochondrial ROS Production in Skeletal Myotubes. *Oxid. Med. Cell. Longev.* 2017. <https://doi.org/10.1155/2017/2739721>
- Lee, H.C., Jenner, A.M., Low, C.S., Lee, Y.K., 2006. Effect of tea phenolics and their aromatic fecal bacterial metabolites on intestinal microbiota. *Res. Microbiol.* 157, 876–84. <https://doi.org/10.1016/j.resmic.2006.07.004>
- Lekakis, J., Rallidis, L.S., Andreadou, I., Vamvakou, G., Kazantzoglou, G., Magiatis, P., Skaltsounis, A.-L., Kremastinos, D.T., 2005. Polyphenols compounds from red grapes acutely improve endothelial function in patients with coronary heart disease. *Eur. J. Prev. Cardiol.* 12, 596–600.
- Lever, M., George, P.M., Slow, S., Bellamy, D., Young, J.M., Ho, M., McEntyre, C.J., Elmslie, J.L., Atkinson, W., Molyneux, S.L., Troughton, R.W., Frampton, C.M., Richards, A.M., Chambers, S.T., 2014. Betaine and trimethylamine-N-oxide as predictors of cardiovascular outcomes show different patterns in diabetes mellitus: An observational study. *PLoS One* 9, e114969. <https://doi.org/10.1371/journal.pone.0114969>
- Li, J., Feng, L., Xing, Y., Wang, Y., Du, L., Xu, C., Cao, J., Wang, Q., Fan, S., Liu, Q., Al., E., 2014. Radioprotective and antioxidant effect of resveratrol in hippocampus by activating Sirt1. *Int. J. Mol. Sci.* 15, 5928–5939.
- Li, J.M., Gall, N.P., Grieve, D.J., Chen, M., Shah, A.M., 2002. Activation of NADPH oxidase during progression of cardiac hypertrophy to failure. *Hypertension* 40, 477–484.
- Li, M., Cui, J., Ngadi, M.O., Ma, Y., 2015. Absorption mechanism of whey-protein-delivered curcumin using Caco-2 cell monolayers. *Food Chem.* <https://doi.org/10.1016/j.foodchem.2015.01.132>
- Li, S.-H., Tian, H.-B., Zhao, H.-J., Chen, L.-H., Cui, L.-Q., 2013. The acute effects of grape polyphenols supplementation on endothelial function in adults: meta-analyses of controlled trials. *PLoS One* 8, e69818.
- Li, X.S., Obeid, S., Klingenberg, R., Gencer, B., Mach, F., Räber, L., Windecker, S., Rodondi, N., Nanchen, D., Muller, O., Miranda, M.X., Matter, C.M., Wu, Y., Li, L., Wang, Z., Alamri, H.S., Gogonea, V., Chung, Y.M., Tang, W.H.W., Hazen, S.L., Lüscher, T.F., 2017. Gutmicrobiota-dependent trimethylamine N-oxide in acute coronary syndromes: A prognostic marker for incident cardiovascular events beyond traditional risk factors. *Eur. Heart J.* 38, 814–824. <https://doi.org/10.1093/eurheartj/ehw582>
- Liang, Z., Dong, Z., Guo, M., Shen, Z., Yin, D., Hu, S., Hai, X., 2019. Trimethylamine N-oxide as a risk marker

for ischemic stroke in patients with atrial fibrillation. *J. Biochem. Mol. Toxicol.* 33, e22246.
<https://doi.org/10.1002/jbt.22246>

- Liguori, I., Russo, G., Curcio, F., Bulli, G., Aran, L., Della-Morte, D., Gargiulo, G., Testa, G., Cacciatore, F., Bonaduce, D., Abete, P., 2018. Oxidative stress, aging and diseases. *Clin. Interv. Aging* 13, 757–772.
- Lim, L.S., Mitchell, P., Seddon, J.M., Holz, F.G., Wong, T.Y., 2012. Age-related macular degeneration. *Lancet* 379, 1728–38. [https://doi.org/10.1016/S0140-6736\(12\)60282-7](https://doi.org/10.1016/S0140-6736(12)60282-7)
- Lin, C.J., Lin, H.J., Chen, T.H., Hsu, Y.A., Liu, C.S., Hwang, G.Y., Wan, L., 2015. *Polygonum cuspidatum* and its active components inhibit replication of the influenza virus through Toll-like receptor 9-induced interferon beta expression. *PLoS One* 10. <https://doi.org/10.1371/journal.pone.0117602>
- Lin, J., Handschin, C., Spiegelman, B.M., 2005. Metabolic control through the PGC-1 family of transcription coactivators. *Cell Metab.* <https://doi.org/10.1016/j.cmet.2005.05.004>
- Lippai, M., Szatmari, Z., 2017. Autophagy from molecular mechanisms to clinical relevance. *Cell Biol. Toxicol.* 33, 145–168.
- Liu, J., Yu, H., Ning, X., 2006. Effect of quercetin on chronic enhancement of spatial learning and memory of mice. *Sci. China, Ser. C Life Sci.* <https://doi.org/10.1007/s11427-006-2037-7>
- Liu, T., Zang, N., Zhou, N., Li, W., Xie, X., Deng, Y., Ren, L., Long, X., Li, S., Zhou, L., Zhao, X., Tu, W., Wang, L., Tan, B., Liu, E., 2014. Resveratrol Inhibits the TRIF-Dependent Pathway by Upregulating Sterile Alpha and Armadillo Motif Protein, Contributing to Anti-Inflammatory Effects after Respiratory Syncytial Virus Infection. *J. Virol.* 88, 4229–4236. <https://doi.org/10.1128/jvi.03637-13>
- Lourenço dos Santos, S., Baraibar, M.A., Lundberg, S., Eeg-Olofsson, O., Larsson, L., Friguet, B., 2015. Oxidative proteome alterations during skeletal muscle ageing. *Redox Biol.* 5, 267–274. <https://doi.org/10.1016/j.redox.2015.05.006>
- Loyer, X., Heymes, C., Samuel, J.-L., 2008. CONSTITUTIVE NITRIC OXIDE SYNTHASES IN THE HEART FROM HYPERTROPHY TO FAILURE. *Clin. Exp. Pharmacol. Physiol.* 35, 483–488. <https://doi.org/10.1111/j.1440-1681.2008.04901.x>
- Lozano-Castellón, J., López-Yerena, A., Rinaldi de Alvarenga, J.F., Romero del Castillo-Alba, J., Vallverdú-Queralt, A., Escribano-Ferrer, E., Lamuela-Raventós, R.M., 2020. Health-promoting properties of oleocanthal and oleacein: Two secoiridoids from extra-virgin olive oil. *Crit. Rev. Food Sci. Nutr.* 60, 2532–2548. <https://doi.org/10.1080/10408398.2019.1650715>

- Lozano, R., Naghavi, M., Foreman, K., Al., E., 2012. Global and regional mortality from 235 causes of death for 20 age groups in 1990 and 2010: a systematic analysis for the Global Burden of Disease Study. *Lancet* 380, 2095–2128.
- Lü, J.M., Lin, P.H., Yao, Q., Chen, C., 2010. Chemical and molecular mechanisms of antioxidants: Experimental approaches and model systems. *J. Cell. Mol. Med.* 14, 840–860. <https://doi.org/10.1111/j.1582-4934.2009.00897.x>
- Luo, J., Mills, K., le Cessie, S., Noordam, R., van Heemst, D., 2020. Ageing, age-related diseases and oxidative stress: What to do next? *Ageing Res. Rev.* 57, 100982. <https://doi.org/10.1016/j.arr.2019.100982>
- Luzzi, L.A., 1970. Microencapsulation. *J. Pharm. Sci.* <https://doi.org/10.1002/jps.2600591002>
- Lv, X., Liu, S., Hu, Z., 2017. Autophagy-inducing natural compounds: a treasure resource for developing therapeutics against tissue fibrosis. *J. Asian Nat. Prod. Res.* 19, 101–108.
- Ma, L., Wang, K., Shang, J., Cao, C., Zhen, P., Liu, X., Wang, W., Zhang, H., Du, Y., Liu, H., 2014. Anti-Peroxynitrite Treatment Ameliorated Vasorelaxation of Resistance Arteries in Aging Rats: Involvement with NO-sGC-cGKs Pathway. *PLoS One* 9, e104788. <https://doi.org/10.1371/journal.pone.0104788>
- Mackenzie, G.G., Carrasquedo, F., Delfino, J.M., Keen, C.L., Fraga, C.G., Oteiza, P.I., 2004. Epicatechin, catechin, and dimeric procyanidins inhibit PMA-induced NF-kappaB activation at multiple steps in Jurkat T cells. *FASEB J.* 18, 167–9. <https://doi.org/10.1096/fj.03-0402fje>
- Macri, A., Scanarotti, C., Bassi, A.M., Giuffrida, S., Sangalli, G., Traverso, C.E., Iester, M., 2015. Evaluation of oxidative stress levels in the conjunctival epithelium of patients with or without dry eye, and dry eye patients treated with preservative-free hyaluronic acid 0.15 % and vitamin B12 eye drops. *Graefe's Arch. Clin. Exp. Ophthalmol.* 253, 425–30. <https://doi.org/10.1007/s00417-014-2853-6>
- Mamer, O.A., Choinière, L., Treacy, E.P., 1999. Measurement of trimethylamine and trimethylamine N-oxide independently in urine by fast atom bombardment mass spectrometry. *Anal. Biochem.* 276, 144–149. <https://doi.org/10.1006/abio.1999.4351>
- Manach, C., Morand, C., Texier, O., Favier, M.L., Agullo, G., Demigne, C., Regeat, F., Remesy, C., 1995. Quercetin metabolites in plasma of rats fed diets containing rutin or quercetin. *J. Nutr.* 125, 1911–1922. <https://doi.org/10.1093/jn/125.7.1911>
- Manach, C., Scalbert, A., Morand, C., Rémésy, C., Jiménez, L., 2004. Polyphenols: Food sources and bioavailability. *Am. J. Clin. Nutr.* 79, 727–747. <https://doi.org/10.1093/ajcn/79.5.727>

- Mancini, M., Ordovas, J.M., Riccardi, G., Rubba, P., Strazzullo, P., 2011. Nutritional and metabolic bases of cardiovascular disease. Wiley-Blackwell.
- Mancini, S., Mariani, F., Sena, P., Benincasa, M., Roncucci, L., 2017. Myeloperoxidase expression in human colonic mucosa is related to systemic oxidative balance in healthy subjects. *Redox Rep.* 22, 399–407. <https://doi.org/10.1080/13510002.2016.1277049>
- Marseglia, L., Manti, S., D'Angelo, G., Nicotera, A., Parisi, E., Di Rosa, G., Gitto, E., Arrigo, T., 2015. Oxidative stress in obesity: A critical component in human diseases. *Int. J. Mol. Sci.* 16, 378–400. <https://doi.org/10.3390/ijms16010378>
- Martelli, A., Flori, L., Gorica, E., Piragine, E., Saviano, A., Annunziata, G., Di Minno, M.N.D., Ciampaglia, R., Calcaterra, I., Maione, F., Tenore, G.C., Novellino, E., Calderone, V., 2021. Vascular Effects of the Polyphenolic Nutraceutical Supplement Taurisolo®: Focus on the Protection of the Endothelial Function. *Nutrients* 13, 1540. <https://doi.org/10.3390/nu13051540>
- Martelli, A., Piragine, E., Citi, V., Testai, L., Pagnotta, E., Ugolini, L., Lazzeri, L., Di Cesare Mannelli, L., Manzo, O.L., Bucci, M., 2020. Erucin exhibits vasorelaxing effects and antihypertensive activity by H₂S-releasing properties. *Br. J. Pharmacol.* 177, 824–835.
- Martelli, A., Testai, L., Anzini, M., Cappelli, A., Di Capua, A., Biava, M., Poce, G., Consalvi, S., Giordani, A., Caselli, G., 2013. The novel anti-inflammatory agent VA694, endowed with both NO-releasing and COX2-selective inhibiting properties, exhibits NO-mediated positive effects on blood pressure, coronary flow and endothelium in an experimental model of hypertension and endotheli. *Pharmacol. Res.* 78, 1–9.
- Marzetti, E., Calvani, R., Cesari, M., Buford, T.W., Lorenzi, M., Behnke, B.J., Leeuwenburgh, C., 2013. Mitochondrial dysfunction and sarcopenia of aging: From signaling pathways to clinical trials. *Int. J. Biochem. Cell Biol.* <https://doi.org/10.1016/j.biocel.2013.06.024>
- Marzocchi, A., Magnani, B., 1986. Malattie vascolari, in: Zanussi, C. (Ed.), *Medicina Interna*. UTET, pp. 719–764.
- Mastromarino, P., Capobianco, D., Cannata, F., Nardis, C., Mattia, E., De Leo, A., Restignoli, R., Francioso, A., Mosca, L., 2015. Resveratrol inhibits rhinovirus replication and expression of inflammatory mediators in nasal epithelia. *Antiviral Res.* 123, 15–21. <https://doi.org/10.1016/j.antiviral.2015.08.010>
- Matos, L., Gouveia, A.M., Almeida, H., 2017. Resveratrol Attenuates Copper-Induced Senescence by Improving Cellular Proteostasis. *Oxid. Med. Cell. Longev.* 2017. <https://doi.org/10.1155/2017/3793817>

- Matsumura, N., Takahara, S., Maayah, Z.H., Parajuli, N., Byrne, N.J., Shoieb, S.M., Soltys, C.L.M., Beker, D.L., Masson, G., El-Kadi, A.O.S., Dyck, J.R.B., 2018. Resveratrol improves cardiac function and exercise performance in MI-induced heart failure through the inhibition of cardiotoxic HETE metabolites. *J. Mol. Cell. Cardiol.* 125, 162–173. <https://doi.org/10.1016/j.yjmcc.2018.10.023>
- Mattarei, A., Azzolini, M., Carraro, M., Sassi, N., Zoratti, M., Paradisi, C., Biasutto, L., 2013. Acetal derivatives as prodrugs of resveratrol. *Mol. Pharm.* 10, 2781–2792. <https://doi.org/10.1021/mp400226p>
- McCord, J.M., Fridovich, I., 1969. Superoxide dismutase. An enzymic function for erythrocyte (hemocuprein). *J. Biol. Chem.* 244, 6049–6055.
- McGrath, J.C., Lilley, E., 2015. Implementing guidelines on reporting research using animals (ARRIVE etc.): new requirements for publication in *BJP*. *Br. J. Pharmacol.* 172, 3189–3493.
- McMurray, F., Patten, D.A., Harper, M.E., 2016. Reactive Oxygen Species and Oxidative Stress in Obesity – Recent Findings and Empirical Approaches. *Obesity (Silver Spring)*. 24, 2301–2310. <https://doi.org/10.1002/oby.21654>
- Melo, P.S., Massarioli, A.P., Denny, C., Dos Santos, L.F., Franchin, M., Pereira, G.E., Vieira, T.M.F.D.S., Rosalen, P.L., De Alencar, S.M., 2015. Winery by-products: Extraction optimization, phenolic composition and cytotoxic evaluation to act as a new source of scavenging of reactive oxygen species. *Food Chem.* 181, 160–9. <https://doi.org/10.1016/j.foodchem.2015.02.087>
- Menotti, A., 1987. Epidemiologia dell'arteriosclerosi, in: Beretta Anguissola, A. (Ed.), *Trattato Delle Malattie Cardiovascolari*. UTET, pp. 83–116.
- Mente, A., Chalcraft, K., Ak, H., Davis, A.D., Lonn, E., Miller, R., Potter, M.A., Yusuf, S., Anand, S.S., McQueen, M.J., 2015. The Relationship Between Trimethylamine-N-Oxide and Prevalent Cardiovascular Disease in a Multiethnic Population Living in Canada. *Can. J. Cardiol.* 31, 1189–1194. <https://doi.org/10.1016/j.cjca.2015.06.016>
- Mills, G.A., Walker, V., Mughal, H., 1999. Quantitative determination of trimethylamine in urine by solid-phase microextraction and gas chromatography-mass spectrometry. *J. Chromatogr. B Biomed. Sci. Appl.* 723, 281–285. [https://doi.org/10.1016/S0378-4347\(98\)00542-8](https://doi.org/10.1016/S0378-4347(98)00542-8)
- Min, Y.D., Choi, C.H., Bark, H., Son, H.Y., Park, H.H., Lee, S., Park, J.W., Park, E.K., Shin, H.I., Kim, S.H., 2007. Quercetin inhibits expression of inflammatory cytokines through attenuation of NF- κ B and p38 MAPK in HMC-1 human mast cell line. *Inflamm. Res.* 56, 210–5. <https://doi.org/10.1007/s00011-007-6172-9>

- Mizushima, N., Komatsu, M., 2011. Autophagy: renovation of cells and tissues. *Cell* 147, 728–741.
- Mohammadi, A., Najari, A.G., Yaghoobi, M.M., Jahani, Y., Vahabzadeh, Z., 2016. Trimethylamine-N-Oxide Treatment Induces Changes in the ATP-Binding Cassette Transporter A1 and Scavenger Receptor A1 in Murine Macrophage J774A.1 cells. *Inflammation* 39, 393–404. <https://doi.org/10.1007/s10753-015-0261-7>
- Molins, B., Romero-Vázquez, S., Fuentes-Prior, P., Adan, A., Dick, A.D., 2018. C-reactive protein as a therapeutic target in age-related macular degeneration. *Front. Immunol.* 9, 808. <https://doi.org/10.3389/fimmu.2018.00808>
- Moranta, D., Barceló, P., Aparicio, S., Garau, C., Sarubbo, F., Ramis, M., Nicolau, C., Esteban, S., 2014. Intake of melatonin increases tryptophan hydroxylase type 1 activity in aged rats: Preliminary study. *Exp. Gerontol.* <https://doi.org/10.1016/j.exger.2013.10.012>
- Murphy, H.C., Dolphin, C.T., Janmohamed, A., Holmes, H.C., Michelakakis, H., Shephard, E.A., Chalmers, R.A., Phillips, I.R., Iles, R.A., 2000. A novel mutation in the flavin-containing monooxygenase 3 gene, FMO3, that causes fish-odour syndrome: Activity of the mutant enzyme assessed by proton NMR spectroscopy. *Pharmacogenetics* 10, 439–451. <https://doi.org/10.1097/00008571-200007000-00007>
- Nam, H.S., 2019. Gut microbiota and ischemic stroke: The role of trimethylamine N-oxide. *J. Stroke* 21, 151–159. <https://doi.org/10.5853/jos.2019.00472>
- Narayanan, N.K., Nargi, D., Randolph, C., Narayanan, B.A., 2009. Liposome encapsulation of curcumin and resveratrol in combination reduces prostate cancer incidence in PTEN knockout mice. *Int. J. Cancer.* <https://doi.org/10.1002/ijc.24336>
- Nazzaro, F., Orlando, P., Fratianni, F., Coppola, R., 2012. Microencapsulation in food science and biotechnology. *Curr. Opin. Biotechnol.* <https://doi.org/10.1016/j.copbio.2011.10.001>
- Negre-Salvayre, A., Coatrieux, C., Ingueneau, C., Salvayre, R., 2008. Advanced lipid peroxidation end products in oxidative damage to proteins. Potential role in diseases and therapeutic prospects for the inhibitors. *Br. J. Pharmacol.* 153, 6–20. <https://doi.org/10.1038/sj.bjp.0707395>
- Nencini, C., Giorgi, G., Micheli, L., 2007. No TitlProtective effect of silymarin on oxidative stress in rat brain. *Phytomedicine Int. J. Phyther. Phytopharm.* 14, 129–135.
- Newby, A.C., 2008. Metalloproteinase expression in monocytes and macrophages and its relationship to atherosclerotic plaque instability. *Arterioscler. Thromb. Vasc. Biol.* 28, 2108–14. <https://doi.org/10.1161/ATVBAHA.108.173898>

- Nie, J., Xie, L., Zhao, B.X., Li, Y., Qiu, B., Zhu, F., Li, G.F., He, M., Wang, Y., Wang, B., Liu, S., Zhang, H., Guo, H., Cai, Y., Huo, Y., Hou, F.F., Xu, X., Qin, X., 2018. Serum trimethylamine N-oxide concentration is positively associated with first stroke in hypertensive patients. *Stroke* 49, 2021–2028. <https://doi.org/10.1161/STROKEAHA.118.021997>
- Niemann, B., Chen, Y., Teschner, M., Al, E., 2011. Obesity induces signs of premature cardiac aging in younger patients: The role of mitochondria. *J. Am. Coll. Cardiol.* 57, 577–585.
- Niwa, Y., Ozaki, Y., Kanoh, T., Akamatsu, H., Kurisaka, M., 1996. Role of cytokines, tyrosine kinase, and protein kinase C on production of superoxide and induction of scavenging enzymes in human leukocytes. *Clin. Immunol. Immunopathol.* 79, 303–13.
- Olas, B., Nowak, P., Kolodziejczyk, J., Ponczek, M., Wachowicz, B., 2006. Protective effects of resveratrol against oxidative/nitrative modifications of plasma proteins and lipids exposed to peroxynitrite. *J. Nutr. Biochem.* 17, 96–102. <https://doi.org/10.1016/j.jnutbio.2005.05.010>
- Oldoni, T.L.C., Melo, P.S., Massarioli, A.P., Moreno, I.A.M., Bezerra, R.M.N., Rosalen, P.L., Da Silva, G.V.J., Nascimento, A.M., Alencar, S.M., 2016. Bioassay-guided isolation of proanthocyanidins with antioxidant activity from peanut (*Arachis hypogaea*) skin by combination of chromatography techniques. *Food Chem.* 192, 306–12. <https://doi.org/10.1016/j.foodchem.2015.07.004>
- Ozkan, G., Franco, P., De Marco, I., Xiao, J., Capanoglu, E., 2019. A review of microencapsulation methods for food antioxidants: Principles, advantages, drawbacks and applications. *Food Chem.* <https://doi.org/10.1016/j.foodchem.2018.07.205>
- Pahwa, R., Jialal, I., 2020. Atherosclerosis - StatPearls - NCBI Bookshelf [WWW Document]. URL <https://www.ncbi.nlm.nih.gov/books/NBK507799/> (accessed 4.23.21).
- Pandareesh, M.D., Mythri, R.B., Srinivas Bharath, M.M., 2015. Bioavailability of dietary polyphenols: Factors contributing to their clinical application in CNS diseases. *Neurochem. Int.* <https://doi.org/10.1016/j.neuint.2015.07.003>
- Pandey, K.B., Mehdi, M.M., Maurya, P.K., Rizvi, S.I., 2010. Plasma protein oxidation and its correlation with antioxidant potential during human aging. *Dis. Markers* 29, 31–36. <https://doi.org/10.3233/DMA-2010-0723>
- Paniker, N., Srivastava, S., Beutler, E., 1970. Glutathione metabolism of the red cells. Effect of glutathione reductase deficiency on the stimulation of hexose monophosphate shunt under oxidative stress. *Biochim. Biophys* 215, 456–460.

- Papamichael, C., Karatzis, E., Karatzi, K., Aznaouridis, K., Papaioannou, T., Protopogerou, A., Stamatelopoulos, K., Zam-pelas, A., Lekakis, J., Mavrikakis, M., 2004. Red wine's antioxidants counteract acute endothelial dysfunction caused by cigarette smoking in healthy nonsmokers. *Am. Heart J.* 147, 274.
- Papillo, V.A., Vitaglione, P., Graziani, G., Gokmen, V., Fogliano, V., 2014. Release of antioxidant capacity from five plant foods during a multistep enzymatic digestion protocol. *J. Agric. Food Chem.* 62, 4119–4126. <https://doi.org/10.1021/jf500695a>
- Park, S.J., Ahmad, F., Philp, A., Baar, K., Williams, T., Luo, H., Ke, H., Rehmann, H., Taussig, R., Brown, A.L., Kim, M.K., Beaven, M.A., Burgin, A.B., Manganiello, V., Chung, J.H., 2012. Resveratrol ameliorates aging-related metabolic phenotypes by inhibiting cAMP phosphodiesterases. *Cell* 148, 421–433. <https://doi.org/10.1016/j.cell.2012.01.017>
- Pawlowska, E., Szczepanska, J., Koskela, A., Kaarniranta, K., Blasiak, J., 2019. Dietary polyphenols in age-related macular degeneration: Protection against oxidative stress and beyond. *Oxid. Med. Cell. Longev.* 2019, 9682318. <https://doi.org/10.1155/2019/9682318>
- Petersen, K.S., Smith, C., 2016. Ageing-associated oxidative stress and inflammation are alleviated by products from grapes. *Oxid. Med. Cell. Longev.* 2016, 6236309. <https://doi.org/10.1155/2016/6236309>
- Pieta Dias, C., Martins de Lima, M.N., Presti-Torres, J., Dornelles, A., Garcia, V.A., Siciliani Scalco, F., Rewsaat Guimaraes, M., Constantino, L., Budni, P., Dal-Pizzol, F., Al., E., 2007. Memantine reduces oxidative damage and enhances long-term recognition memory in aged rats. *Neuroscience* 146, 1719–1725.
- Pignatelli, P., Menichelli, D., Pastori, D., Violi, F., 2018. Oxidative stress and cardiovascular disease: New insights. *Kardiol. Pol.* 76, 713–722. <https://doi.org/10.5603/KP.a2018.0071>
- Piskula, M.K., Yamakoshi, J., Iwai, Y., 1999. Daidzein and genistein but not their glucosides are absorbed from the rat stomach. *FEBS Lett.* 447, 287–291. [https://doi.org/10.1016/S0014-5793\(99\)00307-5](https://doi.org/10.1016/S0014-5793(99)00307-5)
- Podadera, P., Arêas, J.A.G., Lanfer-Marquez, U.M., 2005. Diagnosis of suspected trimethylaminuria by NMR spectroscopy. *Clin. Chim. Acta* 351, 149–154. <https://doi.org/10.1016/j.cccn.2004.09.006>
- Puato, M., Faggin, E., Pauletto, P., Pessina, A., 2002. La malattia aterosclerotica, in: Crepaldi, G., Baritussio, A. (Eds.), *Malattie Del Cuore e Dei Vasi. Estratto Da: Trattato Di Medicina Interna*. PICCIN, pp. 621–649.
- Raiola, A., Meca, G., Mañes, J., Ritieni, A., 2012. Bioaccessibility of Deoxynivalenol and its natural co-

occurrence with Ochratoxin A and Aflatoxin B 1 in Italian commercial pasta. *Food Chem. Toxicol.* 50, 280–287. <https://doi.org/10.1016/j.fct.2011.09.031>

Ramis, M.R., Sarubbo, F., Terrasa, J.L., Moranta, D., Aparicio, S., Miralles, A., Esteban, S., 2016. Chronic α -tocopherol increases central monoamines synthesis and improves cognitive and motor abilities in old rats. *Rejuvenation Res.* <https://doi.org/10.1089/rej.2015.1685>

Randrianarisoa, E., Lehn-Stefan, A., Wang, X., Hoene, M., Peter, A., Heinzmann, S.S., Zhao, X., Königsrainer, I., Königsrainer, A., Balletshofer, B., Machann, J., Schick, F., Fritsche, A., Hring, H.U., Xu, G., Lehmann, R., Stefan, N., 2016. Relationship of serum trimethylamine N-oxide (TMAO) levels with early atherosclerosis in humans. *Sci. Rep.* 6, 26745. <https://doi.org/10.1038/srep26745>

Ranney, A., Petro, M.S., 2009. Resveratrol protects spatial learning in middle-aged C57BL/6 mice from effects of ethanol. *Behav. Pharmacol.* 20, 330–336.

Rath, S., Heidrich, B., Pieper, D.H., Vital, M., 2017. Uncovering the trimethylamine-producing bacteria of the human gut microbiota. *Microbiome* 5, 54. <https://doi.org/10.1186/S40168-017-0271-9>

Reagan-Shaw, S., Nihal, M., Ahmad, N., 2008. Dose translation from animal to human studies revisited. *FASEB J.* 14, 3.

Rice-Evans, C.A., Miller, N.J., Paganga, G., 1996. Structure-antioxidant activity relationships of flavonoids and phenolic acids. *Free Radic. Biol. Med.* 20, 933–956.

Romanello, V., Sandri, M., 2016. Mitochondrial quality control and muscle mass maintenance. *Front. Physiol.* <https://doi.org/10.3389/fphys.2015.00422>

Romano, K.A., Vivas, E.I., Amador-Noguez, D., Rey, F.E., 2015. Intestinal microbiota composition modulates choline bioavailability from diet and accumulation of the proatherogenic metabolite trimethylamine-N-oxide. *MBio* 6. <https://doi.org/10.1128/mBio.02481-14>

Ronchetti, D., Borghi, V., Gaitan, G., Herrero, J., Impagnatiello, F., 2009. NCX 2057, a novel NO-releasing derivative of ferulic acid, suppresses inflammatory and nociceptive responses in in vitro and in vivo models. *Br. J. Pharmacol.* 158, 569–579.

Rosa, F.T., Zulet, M.Á., Marchini, J.S., Martínez, J.A., 2012. Bioactive compounds with effects on inflammation markers in humans. *Int. J. Food Sci. Nutr.* 63, 749–65. <https://doi.org/10.3109/09637486.2011.649250>

Rose, K.M., Parmar, M.S., Cavanaugh, J.E., 2014. Dietary supplementation with resveratrol protects against

striatal dopaminergic deficits produced by in utero LPS exposure. *Brain Res.* 1573, 37–43.

Roseno, S.L., Davis, P.R., Bollinger, L.M., Powell, J.J.S., Witczak, C.A., Brault, J.J., 2015. Short-term, high-fat diet accelerates disuse atrophy and protein degradation in a muscle-specific manner in mice. *Nutr. Metab.* 12. <https://doi.org/10.1186/s12986-015-0037-y>

Rotches-Ribalta, M., Andres-Lacueva, C., Estruch, R., Escribano, E., Urpi-Sarda, M., 2012. Pharmacokinetics of resveratrol metabolic profile in healthy humans after moderate consumption of red wine and grape extract tablets. *Pharmacol. Res.* <https://doi.org/10.1016/j.phrs.2012.08.001>

Rowan, S., Jiang, S., Korem, T., Szymanski, J., Chang, M.L., Szelog, J., Cassalman, C., Dasuri, K., McGuire, C., Nagai, R., Du, X.L., Brownlee, M., Rabbani, N., Thornalley, P.J., Baleja, J.D., Deik, A.A., Pierce, K.A., Scott, J.M., Clish, C.B., Smith, D.E., Weinberger, A., Avnit-Sagi, T., Lotan-Pompan, M., Segal, E., Taylor, A., 2017. Involvement of a gut-retina axis in protection against dietary glycemia-induced age-related macular degeneration. *Proc. Natl. Acad. Sci. U. S. A.* 114, E4472-4481. <https://doi.org/10.1073/pnas.1702302114>

Rueda-Orozco, P.E., Soria-Gomez, E., Montes-Rodriguez, C.J., Martinez-Vargas, M., Galicia, O., Navarro, L., Prospero-Garcia, O., 2008. A potential function of endocannabinoids in the selection of a navigation strategy by rats. *Psychopharmacology (Berl)*. 198, 565–576.

Rufino, M. do S.M., Alves, R.E., de Brito, E.S., Pérez-Jiménez, J., Saura-Calixto, F., Mancini-Filho, J., 2010. Bioactive compounds and antioxidant capacities of 18 non-traditional tropical fruits from Brazil. *Food Chem.* 121, 996–1002. <https://doi.org/10.1016/j.foodchem.2010.01.037>

Sack, M.N., Fyhrquist, F.Y., Saijonmaa, O.J., Fuster, V., Kovacic, J.C., 2017. Basic Biology of Oxidative Stress and the Cardiovascular System: Part 1 of a 3-Part Series. *J. Am. Coll. Cardiol.* 70, 196–211.

Salminen, A., Kaarniranta, K., Kauppinen, A., 2016. AMPK and HIF signaling pathways regulate both longevity and cancer growth: the good news and the bad news about survival mechanisms. *Biogerontology* 17, 655–680.

Salminen, A., Ojala, J., Huuskonen, J., Kauppinen, A., Suuronen, T., Kaarniranta, K., 2008. Interaction of aging-associated signaling cascades: Inhibition of NF- κ B signaling by longevity factors FoxOs and SIRT1. *Cell. Mol. Life Sci.* <https://doi.org/10.1007/s00018-008-7461-3>

Salucci, S., Falcieri, E., 2020. Polyphenols and their potential role in preventing skeletal muscle atrophy. *Nutr. Res* 74, 10–22. <https://doi.org/10.1016/j.nutres.2019.11.004>

San Cheang, W., Wong, W.T., Wang, L., Cheng, C.K., Lau, C.W., Ma, R.C.W., Xu, A., Wang, N., Huang, Y.,

- Tian, X., 2019. Resveratrol ameliorates endothelial dysfunction in diabetic and obese mice through sirtuin 1 and peroxisome proliferator-activated receptor. *Pharmacol. Res.* 139, 384–394.
- Sandoval-Acuña, C., Ferreira, J., Speisky, H., 2014. Polyphenols and mitochondria: An update on their increasingly emerging ROS-scavenging independent actions. *Arch. Biochem. Biophys.* 559, 75–90. <https://doi.org/10.1016/j.abb.2014.05.017>
- Sanna, V., Siddiqui, I.A., Sechi, M., Mukhtar, H., 2013. Resveratrol-loaded nanoparticles based on poly(epsilon-caprolactone) and poly(D,L-lactic-co-glycolic acid)-poly(ethylene glycol) blend for prostate cancer treatment. *Mol. Pharm.* <https://doi.org/10.1021/mp400342f>
- Santangelo, C., Vari, R., Scazzocchio, B., Di Benedetto, R., Filesi, C., Masella, R., 2007. Polyphenols, intracellular signalling and inflammation. *Ann. Ist. Super. Sanita* 43, 394–405.
- Santillo, M., Colantuoni, A., Mondola, P., Guida, B., Damiano, S., 2015. NOX signaling in molecular cardiovascular mechanisms involved in the blood pressure homeostasis. *Front. Physiol.* <https://doi.org/10.3389/fphys.2015.00194>
- Santini, A., Novellino, E., 2014. Nutraceuticals: Beyond the Diet Before the Drugs. *Curr. Bioact. Compd.* 10, 1–12. <https://doi.org/10.2174/157340721001140724145924>
- Santucci, L., Mencarelli, A., Renga, B., Al., E., 2006. Nitric oxide modulates proapoptotic and antiapoptotic properties of chemotherapy agents: the case of NO-pegylated epirubicin. *FASEB J.* 20, 765–767.
- Sarubbo, F., Esteban, S., Miralles, A., Moranta, D., 2018a. Effects of Resveratrol and other Polyphenols on Sirt1: Relevance to Brain Function During Aging. *Curr. Neuropharmacol.* 16, 126–136.
- Sarubbo, F., Moranta, D., Pani, G., 2018b. Dietary polyphenols and neurogenesis: Molecular interactions and implication for brain ageing and cognition. *Neurosci. Biobehav. Rev.* <https://doi.org/10.1016/j.neubiorev.2018.05.011>
- Sarubbo, F., Moranta, D., Pani, G., 2018c. Dietary polyphenols and neurogenesis: Molecular interactions and implication for brain ageing and cognition. *Neurosci. Biobehav. Rev.* <https://doi.org/10.1016/j.neubiorev.2018.05.011>
- Sarubbo, F., Ramis, M.R., Aparicio, S., Ruiz, L., Esteban, S., Miralles, A., Moranta, D., 2015. Improving effect of chronic resveratrol treatment on central monoamine synthesis and cognition in aged rats. *Age (Omaha)*. <https://doi.org/10.1007/s11357-015-9777-x>
- Sarubbo, F., Ramis, M.R., Kienzer, C., Aparicio, S., Esteban, S., Miralles, A., Moranta, D., 2018d. Chronic

Silymarin, Quercetin and Naringenin Treatments Increase Monoamines Synthesis and Hippocampal Sirt1 Levels Improving Cognition in Aged Rats. *J. Neuroimmune Pharmacol.* 13, 24–38.
<https://doi.org/10.1007/s11481-017-9759-0>

Scalbert, A., Johnson, I.T., Saltmarsh, M., 2005. Polyphenols: antioxidants and beyond. *Am. J. Clin. Nutr.* 81, 215S–217S.

Scalbert, Augustin, Manach, C., Morand, C., Rémésy, C., Jiménez, L., 2005. Dietary polyphenols and the prevention of diseases. *Crit. Rev. Food Sci. Nutr.* <https://doi.org/10.1080/1040869059096>

Scherz-Shouval, R., Elazar, Z., 2011. Regulation of autophagy by ROS: Physiology and pathology. *Trends Biochem. Sci.* 36, 30–8. <https://doi.org/10.1016/j.tibs.2010.07.007>

Schiano, E., Annunziata, G., Ciampaglia, R., Iannuzzo, F., Maisto, M., Tenore, G.C., Novellino, E., 2020. Bioactive Compounds for the Management of Hypertriglyceridemia: Evidence From Clinical Trials and Putative Action Targets. *Front. Nutr.* 7. <https://doi.org/10.3389/fnut.2020.586178>

Schiattarella, G.G., Sannino, A., Toscano, E., Giugliano, G., Gargiulo, G., Franzone, A., Trimarco, B., Esposito, G., Perrino, C., 2017. Gut microbe-generated metabolite trimethylamine-N-oxide as cardiovascular risk biomarker: A systematic review and dose-response meta-analysis. *Eur. Heart J.* 38, 2948–2956.
<https://doi.org/10.1093/eurheartj/ehx342>

Schramm, D.D., Collins, H.E., German, J.B., 1999. Flavonoid transport by mammalian endothelial cells. *J. Nutr. Biochem.* [https://doi.org/10.1016/S0955-2863\(98\)00104-1](https://doi.org/10.1016/S0955-2863(98)00104-1)

Scioli, M.G., Storti, G., D'Amico, F., Rodríguez Guzmán, R., Centofanti, F., Doldo, E., Céspedes Miranda, E.M., Orlandi, A., 2020. Oxidative Stress and New Pathogenetic Mechanisms in Endothelial Dysfunction: Potential Diagnostic Biomarkers and Therapeutic Targets. *J. Clin. Med.* 9, 1995.
<https://doi.org/10.3390/jcm9061995>

Seldin, M.M., Meng, Y., Qi, H., Zhu, W.F., Wang, Z., Hazen, S.L., Lusis, A.J., Shih, D.M., 2016. Trimethylamine N-oxide promotes vascular inflammation through signaling of mitogen-activated protein kinase and nuclear factor- κ B. *J. Am. Heart Assoc.* 5, e002767.
<https://doi.org/10.1161/JAHA.115.002767>

Selma, M. V., Espín, J.C., Tomás-Barberán, F.A., 2009. Interaction between phenolics and gut microbiota: Role in human health. *J. Agric. Food Chem.* 57, 6485–501. <https://doi.org/10.1021/jf902107d>

Selye, H., 1976. Forty years of stress research: principal remaining problems and misconceptions. *Can. Med. Assoc.* 115, 53–56.

- Selye, H., 1936. A syndrome produced by diverse nocuous agents. *Nature* 138, 32.
- Senthong, V., Wang, Z., Fan, Y., Wu, Y., Hazen, S.L., Tang, W.H.W., 2016. Trimethylamine N-oxide and mortality risk in patients with peripheral artery disease. *J. Am. Heart Assoc.* 5, e004237. <https://doi.org/10.1161/JAHA.116.004237>
- Setchell, K.D.R., Brown, N.M., Desai, P., Zimmer-Nechemias, L., Wolfe, B.E., Brashear, W.T., Kirschner, A.S., Cassidy, A., Heubi, J.E., 2001. Bioavailability of pure isoflavones in healthy humans and analysis of commercial soy isoflavone supplements, in: *Journal of Nutrition*. American Institute of Nutrition. <https://doi.org/10.1093/jn/131.4.1362s>
- Shadfar, S., Couch, M.E., McKinney, K.A., Weinstein, L.J., Yin, X., Rodriguez, J.E., Guttridge, D.C., Willis, M., 2011. Oral resveratrol therapy inhibits cancer-induced skeletal muscle and cardiac atrophy in vivo. *Nutr. Cancer* 63, 749–762. <https://doi.org/10.1080/01635581.2011.563032>
- Sharples, A.P., Hughes, D.C., Deane, C.S., Saini, A., Selman, C., Stewart, C.E., 2015. Longevity and skeletal muscle mass: The role of IGF signalling, the sirtuins, dietary restriction and protein intake. *Aging Cell* 14, 511–523. <https://doi.org/10.1111/accel.12342>
- Shirane, M., Hatakeyama, S., Hattori, K., Nakayama, K., Nakayama, K.I., 1999. Common pathway for the ubiquitination of $\text{I}\kappa\text{B}\alpha$, $\text{I}\kappa\text{B}\beta$, and $\text{I}\kappa\text{B}\epsilon$ mediated by the F-box protein FWD1. *J. Biol. Chem.* 274, 28169–74. <https://doi.org/10.1074/jbc.274.40.28169>
- Sies, H., Berndt, C., Jones, D.P., 2017. Oxidative Stress: Annual Review of Biochemistry. *Annu. Rev. Biochem.* 86, 715–748. <https://doi.org/10.1146/annurev-biochem-061516-045037>
- Singh, G., Pai, R.S., 2014. Optimized PLGA nanoparticle platform for orally dosed trans-resveratrol with enhanced bioavailability potential. *Expert Opin. Drug Deliv.* <https://doi.org/10.1517/17425247.2014.890588>
- Siti, H.N., Kamisah, Y., Kamsiah, J., 2015. The role of oxidative stress, antioxidants and vascular inflammation in cardiovascular disease (a review). *Vascul. Pharmacol.* <https://doi.org/10.1016/j.vph.2015.03.005>
- Sliwka, W., 1975. Microencapsulation. *Angew. Chemie Int. Ed. English.* <https://doi.org/10.1002/anie.197505391>
- Smith, J.L., Wishnok, J.S., Deen, W.M., 1994. Metabolism and excretion of methylamines in rats. *Toxicol. Appl. Pharmacol.* 125, 296–308. <https://doi.org/10.1006/taap.1994.1076>

- Sobrin, L., Seddon, J.M., 2014. Nature and nurture- genes and environment- predict onset and progression of macular degeneration. *Prog. Retin. Eye Res.* 40, 1–15. <https://doi.org/10.1016/j.preteyeres.2013.12.004>
- Sohal, R.S., Weindruch, R., 1996. Oxidative stress, caloric restriction, and aging. *Science* (80-.). 273, 59–63. <https://doi.org/10.1126/science.273.5271.59>
- Spencer, J.P., 2010. The impact of fruit flavonoids on memory and cognition. *Br. J. Nutr.* 104 Suppl, S40–S47.
- Spencer, J.P., 2009a. Flavonoids and brain health: multiple effects underpinned by common mechanisms. *Genes Nutr.* 4, 243–250.
- Spencer, J.P., 2009b. The impact of flavonoids on memory: physiological and molecular considerations. *Chem. Soc. Rev.* 38, 1152–1161.
- Spiegel, S., Milstien, S., 2000. Sphingosine-1-phosphate: signaling inside and out. *FEBS Lett.* 476, 55–57.
- Sridharan, S., Jain, K., Basu, A., 2011. Regulation of autophagy by kinases. *Cancers (Basel).* 3, 2630–2654.
- St-Pierre, J., Drori, S., Uldry, M., Silvaggi, J.M., Rhee, J., Jäger, S., Handschin, C., Zheng, K., Lin, J., Yang, W., Simon, D.K., Bachoo, R., Spiegelman, B.M., 2006. Suppression of Reactive Oxygen Species and Neurodegeneration by the PGC-1 Transcriptional Coactivators. *Cell* 127, 397–408. <https://doi.org/10.1016/j.cell.2006.09.024>
- Stallone, T., Capurso, S., Galiazzo, V., 2017. Comunicazione e compliance in nutraceutica, in: *Trattato Italiano Di Nutraceutica Clinica*. Scripta Manent Edizioni, pp. 37–44.
- Steinberg, S., 2013. Oxidative stress and sarcomeric proteins. *Circ. Res* 112, 393–405.
- Stojanović, S., Sprinz, H., Brede, O., 2001. Efficiency and mechanism of the antioxidant action of trans-resveratrol and its analogues in the radical liposome oxidation. *Arch. Biochem. Biophys.* 391, 79–89. <https://doi.org/10.1006/abbi.2001.2388>
- Subramaniam, S., Fletcher, C., 2018. Trimethylamine N-oxide: breathe new life. *Br. J. Pharmacol.* 175, 1344–1353. <https://doi.org/10.1111/bph.13959>
- Sullards, M., Liu, Y., Chem, Y., Merrill, Ahj., 2011. Analysis of mammalian sphingolipids by liquid chromatography tan_dem mass spectrometry (LC-MS/MS) and tissue imaging mass spectrometry (TIMS). *Biochim. Biophys. Acta - Biomembr.* 1811, 838–853.
- Sun, L.J., Sun, Y.N., Chen, S.J., Liu, S., Jiang, G.R., 2017. Resveratrol attenuates skeletal muscle atrophy induced by chronic kidney disease via MuRF1 signaling pathway. *Biochem. Biophys. Res. Commun.* 487, 83–89. <https://doi.org/10.1016/j.bbrc.2017.04.022>

- Suzuki-Sugihara, N., Kishimoto, Y., Saita, E., Taguchi, C., Kobayashi, M., Ichitani, M., Ukawa, Y., Sagesaka, Y.M., Suzuki, E., Kondo, K., 2016. Green tea catechins prevent low-density lipoprotein oxidation via their accumulation in low-density lipoprotein particles in humans. *Nutr. Res.* 36, 16–23.
<https://doi.org/10.1016/j.nutres.2015.10.012>
- Suzuki, T., Yazaki, Y., Voors, A.A., Jones, D.J.L., Chan, D.C.S., Anker, S.D., Cleland, J.G., Dickstein, K., Filippatos, G., Hillege, H.L., Lang, C.C., Ponikowski, P., Samani, N.J., van Veldhuisen, D.J., Zannad, F., Zwinderman, A.H., Metra, M., Ng, L.L., 2019. Association with outcomes and response to treatment of trimethylamine N-oxide in heart failure: results from BIOSTAT-CHF. *Eur. J. Heart Fail.* 21, 877–886.
<https://doi.org/10.1002/ehf.1338>
- Sverdlov, A.L., Elezaby, A., Qin, F., Al, E., 2016. Mitochondrial reactive oxygen species mediate cardiac structural, functional, and mitochondrial consequences of diet-induced metabolic heart disease. *J. Am. Hear. Assoc* 5, e002555.
- Tang, W.H.W., Wang, Z., Fan, Y., Levison, B., Hazen, J.E., Donahue, L.M., Wu, Y., Hazen, S.L., 2014. Prognostic value of elevated levels of intestinal microbe-generated metabolite trimethylamine-N-oxide in patients with heart failure: Refining the gut hypothesis. *J. Am. Coll. Cardiol.* 64, 1908–1914.
<https://doi.org/10.1016/j.jacc.2014.02.617>
- Tang, W.H.W., Wang, Z., Levison, B.S., Koeth, R.A., Britt, E.B., Fu, X., Wu, Y., Hazen, S.L., 2013. Intestinal microbial metabolism of phosphatidylcholine and cardiovascular risk. *N. Engl. J. Med.* 368, 1575–84.
<https://doi.org/10.1056/NEJMoa1109400>
- Teixeira, A., Baenas, N., Dominguez-Perles, R., Barros, A., Rosa, E., Moreno, D.A., Garcia-Viguera, C., 2014. Natural bioactive compounds from winery by-products as health promoters: A review. *Int. J. Mol. Sci.*
<https://doi.org/10.3390/ijms150915638>
- Tenore, G., Manfra, M., Stiuso, P., Al, E., 2012. Antioxidant profile and in vitro cardiac radical-scavenging versus pro-oxidant effects of commercial red grape juices (*Vitis vinifera* L. cv. Aglianico N.). *J. Agric. Food Chem.* 60, 9680–9687.
- Tenore, G., Pagano, E., Lama, S., Al, E., 2019. Intestinal anti_inflammatory effect of a peptide derived from gastrointestinal digestion of buffalo (*Bubalus bubalis*) mozzarella cheese. *Nutrients* 11, 610.
- Tenore, G.C., Campiglia, P., Giannetti, D., Novellino, E., 2015. Simulated gastrointestinal digestion, intestinal permeation and plasma protein interaction of white, green, and black tea polyphenols. *Food Chem.* 169, 320–326. <https://doi.org/10.1016/j.foodchem.2014.08.006>

- Tenore, G.C., Campiglia, P., Ritieni, A., Novellino, E., 2013. In vitro bioaccessibility, bioavailability and plasma protein interaction of polyphenols from Annurca apple (*M. pumila* Miller cv Annurca). *Food Chem.* 141, 3519–3524. <https://doi.org/10.1016/j.foodchem.2013.06.051>
- Tenore, G.C., Caruso, D., D'avino, M., Buonomo, G., Caruso, G., Ciampaglia, R., Schiano, E., Maisto, M., Annunziata, G., Novellino, E., 2020. A pilot screening of agro-food waste products as sources of nutraceutical formulations to improve simulated postprandial glycaemia and insulinaemia in healthy subjects. *Nutrients* 12, 1292. <https://doi.org/10.3390/nu12051292>
- Tenori, L., Hu, X., Pantaleo, P., Alterini, B., Castelli, G., Olivotto, I., Bertini, I., Luchinat, C., Gensini, G.F., 2013. Metabolomic fingerprint of heart failure in humans: A nuclear magnetic resonance spectroscopy analysis. *Int. J. Cardiol.* 168. <https://doi.org/10.1016/j.ijcard.2013.08.042>
- Trøseid, M., Ueland, T., Hov, J.R., Svardal, A., Gregersen, I., Dahl, C.P., Aakhus, S., Gude, E., Bjørndal, B., Halvorsen, B., Karlsen, T.H., Aukrust, P., Gullestad, L., Berge, R.K., Yndestad, A., 2015. Microbiota-dependent metabolite trimethylamine-N-oxide is associated with disease severity and survival of patients with chronic heart failure. *J. Intern. Med.* 277, 717–726. <https://doi.org/10.1111/joim.12328>
- Trotti, R., Carratelli, M., Barbieri, M., Micieli, G., Bosone, D., Rondanelli, M., Bo, P., 2001. Oxidative stress and a thrombophilic condition alcoholics without severe liver disease. *Haematologica* 86, 85–91.
- Truelsen, T., Thudium, D., Grønbaek, M., 2002. Amount and type of alcohol and risk of dementia: The Copenhagen City Heart Study. *Neurology*. <https://doi.org/10.1212/01.WNL.0000031421.50369.E7>
- Truong, V.-L., Jun, M., Jeong, W.-S., 2018. Role of resveratrol in regulation of cellular defense systems against oxidative stress. *BioFactors* 44, 36–49. <https://doi.org/10.1002/biof.1399>
- Tsao, R., 2010. Chemistry and biochemistry of dietary polyphenols. *Nutrients*. <https://doi.org/10.3390/nu2121231>
- Tsopmo, A., Awah, F.M., Kuete, V., 2013. Lignans and Stilbenes from African Medicinal Plants, in: *Medicinal Plant Research in Africa: Pharmacology and Chemistry*. Elsevier Inc., pp. 435–478. <https://doi.org/10.1016/B978-0-12-405927-6.00012-6>
- Tsuji, P.A., Stephenson, K.K., Wade, K.L., Liu, H., Fahey, J.W., 2013. Structure-activity analysis of flavonoids: Direct and indirect antioxidant, and antiinflammatory potencies and toxicities. *Nutr. Cancer* 65, 1014–25. <https://doi.org/10.1080/01635581.2013.809127>
- Tucker, K.L., Sage, T., Gibbins, J.M., 2012. Clot retraction, in: *Platelets and Megakaryocytes*. Springer, pp. 101–107.

- Turnbaugh, P.J., Hamady, M., Yatsunenko, T., Cantarel, B.L., Duncan, A., Ley, R.E., Sogin, M.L., Jones, W.J., Roe, B.A., Affourtit, J.P., Egholm, M., Henrissat, B., Heath, A.C., Knight, R., Gordon, J.I., 2009. A core gut microbiome in obese and lean twins. *Nature*. <https://doi.org/10.1038/nature07540>
- Ufnal, M., Zadło, A., Ostaszewski, R., 2015. TMAO: A small molecule of great expectations. *Nutrition* 31, 1317–1323. <https://doi.org/10.1016/j.nut.2015.05.006>
- Umar, S., Van Der Laarse, A., 2010. Nitric oxide and nitric oxide synthase isoforms in the normal, hypertrophic, and failing heart. *Mol. Cell. Biochem.* <https://doi.org/10.1007/s11010-009-0219-x>
- Urquiaga, I., D'Acuña, S., Pérez, D., Dicenta, S., Echeverría, G., Rigotti, A., Leighton, F., 2015. Wine grape pomace flour improves blood pressure, fasting glucose and protein damage in humans: A randomized controlled trial. *Biol. Res.* 48. <https://doi.org/10.1186/s40659-015-0040-9>
- Valko, M., Leibfritz, D., Moncol, J., Cronin, M.T.D., Mazur, M., Telser, J., 2007. Free radicals and antioxidants in normal physiological functions and human disease. *Int. J. Biochem. Cell Biol.* 39, 44–84. <https://doi.org/10.1016/j.biocel.2006.07.001>
- Vanacore, D., Messina, G., Lama, S., Al, E., 2018. Effect of restriction vegan diet's on muscle mass, oxidative status, and myocytes differentiation: a pilot study. *J. Cell. Physiol.* 233, 9345–9353.
- Velasquez, M.T., Ramezani, A., Manal, A., Raj, D.S., 2016. Trimethylamine N-oxide: The good, the bad and the unknown. *Toxins (Basel)*. 8, 326. <https://doi.org/10.3390/toxins8110326>
- Venigalla, M., Gyengesi, E., Münch, G., 2015. Curcumin and apigenin – Novel and promising therapeutics against chronic neuroinflammation in Alzheimer's disease. *Neural Regen. Res.* <https://doi.org/10.4103/1673-5374.162686>
- Venkataraman, K., Khurana, S., Tai, T.C., 2013. Oxidative stress in aging-matters of the heart and mind. *Int. J. Mol. Sci.* <https://doi.org/10.3390/ijms140917897>
- Vingerling, J.R., Dielemans, I., Bots, M.L., Hofman, A., Grobbee, D.E., De Jong, P.T.V.M., 1995. Age-related macular degeneration is associated with atherosclerosis: The rotterdam study. *Am. J. Epidemiol.* 142, 404–9. <https://doi.org/10.1093/oxfordjournals.aje.a117648>
- Virmani, R., Kolodgie, F.D., Burke, A.P., Finn, A. V., Gold, H.K., Tulenko, T.N., Wrenn, S.P., Narula, J., 2005. Atherosclerotic plaque progression and vulnerability to rupture: Angiogenesis as a source of intraplaque hemorrhage. *Arterioscler. Thromb. Vasc. Biol.* 25, 2054–61. <https://doi.org/10.1161/01.ATV.0000178991.71605.18>

- Walle, T., 2011. Bioavailability of resveratrol. *Ann. N. Y. Acad. Sci.* <https://doi.org/10.1111/j.1749-6632.2010.05842.x>
- Wang, B., Yang, Q., Sun, Y., Al., E., 2014. Resveratrol-enhanced autophagic flux ameliorates myocardial oxidative stress injury in diabetic mice. *J. Cell. Mol. Med.* 18, 1599–1611.
- Wang, D., Sun, H., Song, G., Yang, Y., Zou, X., Han, P., Li, S., 2018. Resveratrol Improves Muscle Atrophy by Modulating Mitochondrial Quality Control in STZ-Induced Diabetic Mice. *Mol. Nutr. Food Res.* 62. <https://doi.org/10.1002/mnfr.201700941>
- Wang, S., Chen, Yuying, Liang, H., Chen, Yiming, Shi, M., Wu, J., Liu, X., Li, Z., Liu, B., Yuan, Q., Li, Y., 2015. Intestine-Specific Delivery of Hydrophobic Bioactives from Oxidized Starch Microspheres with an Enhanced Stability. *J. Agric. Food Chem.* <https://doi.org/10.1021/acs.jafc.5b03575>
- Wang, Y., Xu, H., Fu, Q., Ma, R., Xiang, J., 2011. Protective effect of resveratrol derived from *Polygonum cuspidatum* and its liposomal form on nigral cells in parkinsonian rats. *J. Neurol. Sci.* 304, 29–34.
- Wang, Z., Klipfell, E., Bennett, B.J., Koeth, R., Levison, B.S., Dugar, B., Feldstein, A.E., Britt, E.B., Fu, X., Chung, Y.M., Wu, Y., Schauer, P., Smith, J.D., Allayee, H., Tang, W.H.W., Didonato, J.A., Lusis, A.J., Hazen, S.L., 2011. Gut flora metabolism of phosphatidylcholine promotes cardiovascular disease. *Nature* 472, 57–65. <https://doi.org/10.1038/nature09922>
- Wang, Z., Roberts, A.B., Buffa, J.A., Levison, B.S., Zhu, W., Org, E., Gu, X., Huang, Y., Zamanian-Daryoush, M., Culley, M.K., Didonato, A.J., Fu, X., Hazen, J.E., Krajcik, D., Didonato, J.A., Lusis, A.J., Hazen, S.L., 2015. Non-lethal Inhibition of Gut Microbial Trimethylamine Production for the Treatment of Atherosclerosis. *Cell* 163, 1585–1595. <https://doi.org/10.1016/j.cell.2015.11.055>
- Warwick, A., Lotery, A., 2018. Genetics and genetic testing for age-related macular degeneration review-article. *Eye* 32, 849–857. <https://doi.org/10.1038/eye.2017.245>
- Wheeler, D.S., Catravas, J.D., Odoms, K., Denenberg, A., Malhotra, V., Wong, H.R., 2004. Epigallocatechin-3-gallate, a Green Tea-Derived Polyphenol, Inhibits IL-1 β -Dependent Proinflammatory Signal Transduction in Cultured Respiratory Epithelial Cells. *J. Nutr.* 134, 1039–44. <https://doi.org/10.1093/jn/134.5.1039>
- Wong, R.H., Berry, N.M., Coates, A.M., Buckley, J.D., Bryan, J., Kunz, I., Howe, P.R., 2013. Chronic resveratrol consumption improves brachial flow-mediated dilatation in healthy obese adults. *J. Hypertens.* 31, 1819–1827.
- Wu, C., Li, C., Zhao, W., Xie, N., Yan, F., Lian, Y., Zhou, L., Xu, X., Liang, Y., Wang, L., Ren, M., Li, S., Cheng,

- X., Zhang, L., Ma, Q., Song, H., Meng, R., Ji, X., 2018. Elevated trimethylamine n-oxide related to ischemic brain lesions after carotid artery stenting. *Neurology* 90, e1283–e1290.
<https://doi.org/10.1212/WNL.0000000000005298>
- Xia, N., Förstermann, U., Li, H., 2014. Resveratrol and endothelial nitric oxide. *Molecules* 19, 16102–16121.
- Xiao, J., Kai, G., 2012. A review of dietary polyphenol-plasma protein interactions: Characterization, influence on the bioactivity, and structure-affinity relationship. *Crit. Rev. Food Sci. Nutr.*
<https://doi.org/10.1080/10408398.2010.499017>
- Yanez, M., Fraiz, N., Cano, E., Orallo, F., 2006. Inhibitory effects of cis- and trans-resveratrol on noradrenaline and 5-hydroxytryptamine uptake and on monoamine oxidase activity. *Biochem. Biophys. Res. Commun.* 344, 688–695.
- Yang, F., Oz, H.S., Barve, S., De Villiers, W.J.S., McClain, C.J., Varilek, G.W., 2001. The green tea polyphenol (-)-epigallocatechin-3-gallate blocks nuclear factor- κ B activation by inhibiting I κ B kinase activity in the intestinal epithelial cell line IEC-6. *Mol. Pharmacol.* 60, 528–33. [https://doi.org/10.1016/s0016-5085\(08\)80931-6](https://doi.org/10.1016/s0016-5085(08)80931-6)
- Yi, C., Fu, M., Cao, X., Tong, S., Zheng, Q., Firempong, C.K., Jiang, X., Xu, X., Yu, J., 2013. Enhanced oral bioavailability and tissue distribution of a new potential anticancer agent, Flammulina velutipes sterols, through liposomal encapsulation. *J. Agric. Food Chem.* <https://doi.org/10.1021/jf3055278>
- Yiu, C.Y., Chen, S.Y., Chang, L.K., Chiu, Y.F., Lin, T.P., 2010. Inhibitory effects of resveratrol on the Epstein-Barr virus lytic cycle. *Molecules* 15, 7115–7124. <https://doi.org/10.3390/molecules15107115>
- Yoshida, Y., Tsutaki, A., Tamura, Y., Kouzaki, K., Sashihara, K., Nakashima, S., Tagashira, M., Tatsumi, R., Nakazato, K., 2018. Dietary apple polyphenols increase skeletal muscle capillaries in Wistar rats. *Physiol. Rep.* 6. <https://doi.org/10.14814/phy2.13866>
- Yu, H., Huang, Q., 2011. Investigation of the absorption mechanism of solubilized curcumin using caco-2 cell monolayers. *J. Agric. Food Chem.* <https://doi.org/10.1021/jf201451m>
- Zhang, A.Q., Mitchell, S., Smith, R., 1995. Fish odour syndrome: Verification of carrier detection test. *J. Inherit. Metab. Dis.* 18, 669–674. <https://doi.org/10.1007/BF02436755>
- Zhang, A.Q., Mitchell, S.C., Smith, R.L., 1999. Dietary precursors of trimethylamine in man: A pilot study. *Food Chem. Toxicol.* 37, 515–520. [https://doi.org/10.1016/S0278-6915\(99\)00028-9](https://doi.org/10.1016/S0278-6915(99)00028-9)
- Zhang, Li, Li, Y., Gu, Z., Wang, Y., Shi, M., Ji, Y., Sun, J., Xu, X., Zhang, Lirong, Jiang, J., Shi, W., 2015.

Resveratrol inhibits enterovirus 71 replication and pro-inflammatory cytokine secretion in rhabdomyosarcoma cells through blocking IKKs/NF- κ B signaling pathway. *PLoS One* 10. <https://doi.org/10.1371/journal.pone.0116879>

Zhao, X., Zeisel, S.H., Zhang, S., 2015. Rapid LC-MRM-MS assay for simultaneous quantification of choline, betaine, trimethylamine, trimethylamine N-oxide, and creatinine in human plasma and urine. *Electrophoresis* 36, 2207–2214. <https://doi.org/10.1002/elps.201500055>

Zhao, Y., Chen, B., Shen, J., Wan, L., Zhu, Y., Yi, T., Xiao, Z., 2017. The Beneficial Effects of Quercetin, Curcumin, and Resveratrol in Obesity. *Oxid. Med. Cell. Longev.* 2017, 1459497. <https://doi.org/10.1155/2017/1459497>

Zhu, Q.Y., Huang, Y., Tsang, D., Chen, Z.Y., 1999. Regeneration of α -tocopherol in human low-density lipoprotein by green tea catechin. *J. Agric. Food Chem.* 47, 2020–5. <https://doi.org/10.1021/jf9809941>

Zhu, W., Gregory, J.C., Org, E., Buffa, J.A., Gupta, N., Wang, Z., Li, L., Fu, X., Wu, Y., Mehrabian, M., Sartor, R.B., McIntyre, T.M., Silverstein, R.L., Tang, W.H.W., Didonato, J.A., Brown, J.M., Lusic, A.J., Hazen, S.L., 2016. Gut Microbial Metabolite TMAO Enhances Platelet Hyperreactivity and Thrombosis Risk. *Cell* 165, 111–124. <https://doi.org/10.1016/j.cell.2016.02.011>

Zhu, Y., Li, Q., Jiang, H., 2020. Gut microbiota in atherosclerosis: focus on trimethylamine N-oxide. *APMIS* 128, 353–366. <https://doi.org/10.1111/apm.13038>

Zientara-Rytter, K., Subramani, S., 2016. Autophagic degradation of peroxisomes in mammals. *Biochem. Soc. Trans.* 44, 431–440.

Zinkernagel, M.S., Zysset-Burri, D.C., Keller, I., Berger, L.E., Leichtle, A.B., Largiadèr, C.R., Fiedler, G.M., Wolf, S., 2017. Association of the intestinal microbiome with the development of neovascular age-related macular degeneration. *Sci. Rep.* 7, 40826. <https://doi.org/10.1038/srep40826>

Zu, Y., Zhang, Y., Wang, W., Zhao, X., Han, X., Wang, K., Ge, Y., 2016. Preparation and in vitro / in vivo evaluation of resveratrol-loaded carboxymethyl chitosan nanoparticles. *Drug Deliv.* <https://doi.org/10.3109/10717544.2014.924167>

Zysset-Burri, D.C., Keller, I., Berger, L.E., Neyer, P.J., Steuer, C., Wolf, S., Zinkernagel, M.S., 2019. Retinal artery occlusion is associated with compositional and functional shifts in the gut microbiome and altered trimethylamine-N-oxide levels. *Sci. Rep.* 9, 15303. <https://doi.org/10.1038/s41598-019-51698-5>

Appendix A – Detailed materials and methods of *in vitro* studies and instrumental analyses

General materials and methods

HPLC method for characterisation of Taurisolo® chemical profile

HPLC/DAD studies were performed using a Hewlett Packard (Palo Alto, CA, USA) HP-1090 Series II, fitted with an auto sampler, a binary solvent pump, and a diode-array detector (DAD). The separation was achieved on a Synergy Polar-RP C18 column (150x4.6 mm I.D., 4µm particle size) preceded by a Polar RPsecurity guard cartridge (4x3 mm I.D.). The column temperature was set at 40°C. The mobile phase consisted of 0.1% formic acid in water (v/v) (A) and acetonitrile (B). Injection volume was 5µL and flow rate was kept at 0.9 mL/min for a total run time of 30 min. The gradient program was: 0 min 90% (A), 0–17 min 40%(A), 17–22 min 40% (A), 22–28 min 90% (A), and kept at 90% (A) until the end of the run at 30 min. HPLC/DAD analyses were performed monitoring six different wavelengths: 265 nm for rutin and kaempferol-3-glucoside, 275 nm for gallic acid, catechin, epi-catechin and syringic acid, 310 nm for p-coumaric acid, 325 nm for chlorogenic acid, caffeic acid and ferulic acid, 350 nm for quercetin and 520 nm for delphinidin 3,5-diglucoside and cyanidin 3-glucoside. Phenolic compounds were identified by comparing retention time and UV absorption spectra with available standards. Quantification was performed with standard curves of external standards generated by plotting HPLC peak areas against the concentrations (mg/l) ($r^2 > 0.99$).

In vitro simulated gastrointestinal digestion

The *in vitro* digestion experiments were performed according to the procedure described by Raiola et al. (Raiola et al., 2012) and by Tenore et al. (Tenore et al., 2013), with few modifications. For GI digestion, samples were mixed with 6 mL of artificial saliva composed of KCl (89.6 g/L), KSCN (20 g/L), NaH₂PO₄ (88.8 g/L), Na₂SO₄ (57.0 g/L), NaCl (175.3 g/L), NaHCO₃ (84.7 g/L), urea (25.0 g/L) and 290 mg of α -amylase. The pH of the solution was adjusted to 6.8 with HCl 0.1 N. The mixture was introduced in a plastic bag containing 40 mL of water and homogenized in a Stomacher 80 Microbiomaster (Seward, Worthing, UK) for 3 min. Immediately, 0.5 g of pepsin (14,800 U) dissolved in HCl 0.1 N was added, the pH was adjusted to 2.0 with HCl 6 N, and the solution was incubated at 37 °C in a Polymax 1040 orbital shaker (250 rpm) (Heidolph, Schwabach, Germany) for 2 h. Then the pH was increased to 6.5 with NaHCO₃ 0.5 N and 5 mL of a mixture of pancreatin (8.0 mg/mL) and bile salts (50.0 mg/ mL) (1:1; v/v), dissolved in 20 mL of water, was added and incubated at 37 °C in an orbital shaker (250 rpm) for 2 h. Finally, the mixture was centrifuged at 6000 rpm and the remaining pellets were treated first with 5 mL of 1 mg/mL Pronase E solution (pH 8 for 1 h), and then, with 150 µL of Viscozyme L (pH 4 for 16 h), in order to simulate the colon digestion process, as

previously described by Papillo et al. (Papillo et al., 2014). Each of the supernatants collected during the different digestion phases simulated were lyophilized, and then dissolved in methanol for the analysis.

DPPH assay

The antioxidant activity of tea samples was measured with respect to the radical scavenging ability of the antioxidants present in the sample using the stable radical 2,2-diphenyl-1-picrylhydrazyl (DPPH) (Sigma-Aldrich St. Louis, MO, USA). The analysis was performed by adding 100 μL of each sample to 1000 μL of a methanol solution of DPPH (153 mmol L^{-1}). The decrease in absorbance was determined with a UV-visible spectrophotometer (Beckman, Los Angeles, CA, USA). The absorbance of DPPH radical without antioxidant, i.e., the control, was measured as basis. All determinations were in triplicate. Inhibition was calculated according to the formula:

$$[(A_i - A_f)/A_c] \times 100,$$

where A_i is absorbance of sample at $t = 0$, A_f is the absorbance after 6 min, and A_c is the absorbance of the control at time zero (Brand-Williams et al., 1995). Trolox was used as standard antioxidant. Results were expressed in $\text{mmol Trolox Equivalent (TE)}$.

ABTS assay

The ABTS assay was performed according to the method described by Rufino et al. (Rufino et al., 2010) with slight modifications. ABTS solution was prepared [2,20 -azinobis(3-ethylbenzotiazoline-6- sulfonate)] by mixing 5 mL of ABTS 7.0 mM solution and 88 μL of potassium persulfate 2.45 mM solution, which was left to react for 12 h, at 5 $^\circ\text{C}$ in the dark. Then, ethanol water was added to the solution until an absorbance value of 0.700 (0.05) at 754 nm (Beckman, Los Angeles, CA, USA). The determination of sample absorbance was accomplished at room temperature and after 6 min of reaction. All determinations were in triplicate. Inhibition was calculated according to the formula:

$$[(A_i - A_f)/A_c] \times 100,$$

where A_i is absorbance of sample at $t = 0$, A_f is the absorbance after 6 min, and A_c is the absorbance of the control at time zero (Rufino et al., 2010). Trolox was used as standard antioxidant. Results were expressed in $\text{mmol Trolox Equivalent (TE)}$.

TMAO Quantification

A High-Performance Liquid Chromatography-mass spectrometry (HPLC/MS) method was performed for quantification of TMAO serum levels as described by Annunziata et al. (Annunziata et al., 2019b) and

reported in previous studies (Annunziata et al., 2019c; Barrea et al., 2019b, 2019d, 2018). Briefly, serum proteins were precipitated adding 160 μ L of methanol to 80 μ L of serum, vortex-mixing for 2 min and centrifuging at 12,000 rpm for 10 min (4 °C); the supernatants were used for the HPLC-MS analysis. The HPLC system Jasco Extrema LC-4000 system (Jasco Inc., Ithaca, NY) was coupled to an Advion Expression mass spectrometer (Advion Inc., Ithaca, NY) equipped with an ESI source, operating in positive ion mode. The separation of the analytes was performed using a Luna Hilic (5 μ particle size, 150x3mm) and security guard colon both supplied by Phenomenex (Torrance, CA, USA) were used. The column temperature was maintained at 60 °C during analysis. Mobile phase A composition: 0.15% formic acid in water containing a final concentration of 10 mM ammonium acetate; mobile phase B composition: methanol. Mobile phases ratio was 80:20 (A:B), run isocratically at a flow rate of 0.35 mL/min for 6 min, with a 5 μ l injection volume.

Circulating Oxidative Stress-Related Biomarkers Analysis

Serum levels of reactive oxygen metabolites (D-ROMs) and oxidized low-density lipoproteins (oxLDL) as oxidative stress-related biomarkers were monitored. Both D-ROMs and oxLDL analyses were carried out on an automated analyzer (Free Carpe Diem, Diacron International, Grosseto, Italy) using relative commercial kits (Diacron International) according to the manufacturer's instructions, as previously reported (Annunziata et al., 2019b; Barrea et al., 2019c).

- D-ROMs test (Free Carpe Diem, Diacron International, Grosseto, Italy) - 10 μ l of serum were transferred into 1cm cuvettes containing 1ml of R2 reagent (acetate buffer, pH4.8). The sample-containing mixture was gently mixed and 20 μ l of R1 reagent (a chromogenic mixture consisting of aromatic alkyl-amine, A-NH₂) were added. Cuvettes were mixed by inversion and samples were read at 546nm (5 min, 37°C) on an automated analyzer.
- LP-CHOLOX test (Free Carpe Diem, Diacron International, Grosseto, Italy) - 10 μ l of serum were added in a plastic tube containing 1ml of R1 reagent (indicators mixture) and two drops of R2 reagent (reduced iron) were transferred. The mixture was mixed by shaking, incubated at 37°C for 2 min and centrifuged at 1,400 g for 2 min. Supernatants were transferred into 1cm cuvettes and read at 505nm (37°C) on an automated analyzer. Blank was prepared following the same procedure, without the addition of sample.

Study-specific materials and methods

- Study: "Antioxidant activity of Taurisol[®] on human peripheral blood cells" (Annunziata et al., 2021)

Cell isolation and cell viability test

Venous blood samples were obtained from the antecubital vein of adults with MetS, in suitable vacutainers with EDTA as an anticoagulant. Blood samples were obtained at 08:00 after 12 h overnight fasting. Neutrophil fraction was purified following an adaptation of the method described by Bøyum (Bøyum, 1964). Blood was carefully introduced on Ficoll in a proportion of 1.5 : 1 and was then centrifuged at 900 g, at 4° C for 30 min. The precipitate containing the erythrocytes and neutrophils was incubated at 4° C with 0.15 M ammonium chloride to haemolyse erythrocytes. The suspension was centrifuged at 750 g, at 4° C for 15 min, and the supernatant was then discarded. The neutrophil phase at the bottom was washed first with ammonium chloride and then with phosphate buffer saline (PBS), pH 7.4. Cell viability was evaluated by a crystal violet nuclear staining assay, as previously described (Busquets-Cortés et al., 2018). Violet dye binds to proteins and DNA of living cells. Cells that undergo cell death lose their adherence to culture surface and are subsequently lost from the population of cells, reducing the amount of crystal violet staining in a culture. Briefly, cell suspension (500 µL) was incubated with 0.5% crystal violet solution (20 µL) in 30% acetic acid for 10 min at RT. Cells were then centrifuged at 1000rpm for 10 min and washed three times with PBS, until the dye stopped coming off. 100 µL of ethanol were added and all the volume was then transferred in a 96-well microplate and absorbance at 570 nm was recorded in a microplate reader (Bio-Tek Instruments, Inc., Winooski, VT, USA).

Total antioxidant capacity (FRAP)

The total antioxidant capacity was measured using the ferric reducing antioxidant power (FRAP) assay, following the method described by Benzie and Strain (Benzie and Strain, 1996).

Cell treatment and experimental design

Purified neutrophils from each study participants (n = 14) were cultured with RPMI 1640 culture medium containing 2 mM L-glutamine and divided into four aliquots: (i) control group (Ctr; neutrophils treated only with culture medium), (ii) control+Taurisolol[®] group (Taurisolol[®]; neutrophils treated with culture medium in addition to 1 mg/ml Taurisolol[®]), (iii) PMA group (PMA; neutrophils treated with culture medium in addition to 5 µg/ml PMA) and (iv) PMA+ Taurisolol[®] group (PMA+Taurisolol[®]; neutrophils treated with culture medium in addition to 5 µg/ml PMA and 1 mg/ml Taurisolol[®]). All neutrophil groups were incubated in polypropylene tubes at 37° C for 2 hours. Subsequently, the cells were pelleted by centrifugation (900 ×g, 5 min, 4° C) and cell-free supernatants were stored at -80° C until biochemical determinations; the determinations made in the cell-free supernatants will be considered as determinations in the extracellular media. Neutrophils were resuspended with 2 mL of PBS and one aliquot (1 mL) was centrifuged 900 ×g, 5 min, 4° C, and the precipitate containing the neutrophils was lysed with distilled water and stored at -80° C; determinations performed in the neutrophils lysates will be considered as determinations in the intracellular media.

Hydrogen peroxide production

H₂O₂ production in neutrophils was measured before and after stimulation with PMA using 2,7-dichlorofluorescein-diacetate (DCFH-DA) as indicator. A stock solution of DCFHDA (1 mg/mL) in ethanol was prepared and stored at 20 °C until analysis. DCFH-DA (30 µg/mL) in PBS was added to a 96-well microplate containing 150 µL of neutrophil suspension from each one of the six groups. The fluorescence (Ex, 480 nm; Em 530 nm) was recorded at 37° C for 1 h in FL 9800 Microplate Fluorescence Reader (Bio-tek Instruments, Inc.).

Antioxidant enzyme activity

The activities of CAT and MPO were determined both in extracellular and intracellular media. Both enzyme activities were determined with a Shimadzu UV-2100 spectrophotometer at 37°C. MPO activity was measured by guaiacol oxidation (Capeillère-Blandin, 1998). The reaction mixture contained sodium phosphate buffer pH7 and 13.5 mM guaiacol. The reaction was initiated by adding 300 mM H₂O₂, and changes at 470nm were monitored. CAT activity was measured by the spectrophotometric method of Aebi based on the decomposition of H₂O₂ (Aebi, 1984).

Malondialdehyde assay

Malondialdehyde (MDA) as a marker of lipid peroxidation was analyzed in gastrocnemius muscle homogenate by a colourimetric assay based on the reaction of MDA with a chromogenic reagent to yield a stable chromophore with maximal absorbance at 586 nm. Briefly, samples or standards were placed in glass tubes containing n-methyl-2-phenylindole (10.3 mM) in acetonitrile:methanol (3:1). HCl 12 N was added, and the samples were incubated for 1 h at 45° C. Absorbance was measured at 586 nm.

- Study: “Effects of Taurisol[®] on cardiomyoblast” (Lama et al., 2020)

Cell Culture

Rat cardiomyocytes (H9c2) (ATCC, Manassas, VA) cells were cultured in DMEM, at two different glucose concentration 5.5 mM (NH-H9c2) and 44 mM (HG-H9c2), supplemented with 10% fetal bovine serum, 100 U/mL of penicillin, and 100 lg/mL of streptomycin in 150 cm² tissue culture flasks at 37° C in a humidified atmosphere of 5% CO₂. The cells were fed every 2–3 days and subcultured once they reached 70–80% of confluence. After 4 hr incubation, cells were washed with 1% PBS to remove unattached dead cells and treated with Taurisol[®] (0,5 µg/µL), TMAO (50 µM), and TMAO/ Taurisol[®] combination.

Cell Proliferation Assay

The evaluation of cell proliferation was performed on NG-H9c2 and HG-H9c2 cell line after 24 and 72 hr incubation with Taurisolo[®], TMAO, and TMAO/ Taurisolo[®] combination. The cells were seeded in 96-well plates in a number of 30×10^2 per well. The growth was assessed by MTT viability assay as previously described (Gomez-Monterrey et al., 2011). Then, MTT assay was carried out by triplicate determination on at least three separate experiments. All data were expressed as mean \pm SD. We have determined also the cell number and proliferation by TC10 automated cell counter (Bio-Rad, Milan, Italy).

Morphological Evaluation of Cardiomyocytes by Confocal Microscopy

After 72 hr incubation with Taurisolo[®], TMAO, and TMAO/ Taurisolo[®] combination, the HG-H9c2 cells were fixed for 20 min with a 3% (w/v) paraformaldehyde (PFA) solution and permeabilized for 10 min with 0.1% (w/v) Triton X-100 in phosphate-buffered saline (PBS) at room temperature. To prevent nonspecific interactions of antibodies, cells were treated for 2 hr in 5% fetal bovine serum (FBS) in PBS; then, cells were incubated with a specific mouse monoclonal antibody raised against actin (1:500 Alexa Fluor[®], BD Pharmingen[™]) for 24 hr at 37° C. The slides were mounted on microscope slides by Mowiol. The analyses were performed with a Zeiss LSM 510 microscope equipped with a planapochromat objective X 63 (NA 1.4) in oil immersion. Actin fluorescence was collected in a multitrack mode. The nuclei were stained with 4',6-diamidino-2-phenylindole (DAPI) (Tenore et al., 2019).

Nitrite Levels

Nitrite was measured by the Griess reaction. Briefly, 50 μ L of medium was mixed with an equal volume of the Griess reagent (0.5% sulfanilamide, 2.5% H₃PO₄, and 0.05% naphthylethylene diamine in H₂O) and incubated for 10 min at room temperature. Absorbance was assayed at 550 nm and compared with a standard curve obtained using sodium nitrite (Tenore et al., 2012).

Thiobarbituric Acid-Reactive Species (TBARS) Assay

Samples were incubated with 0.5 mL of 20% acetic acid, pH 3.5, and 0.5 mL of 0.78% aqueous solution of thiobarbituric acid. After heating at 95° C for 45 min, samples were centrifuged at 4000 rpm for 5 min. The TBARS were quantified by spectrophotometry at 532 nm. Results were expressed as TBARS μ M/g of proteins. Each data point is the average of triplicate measurements, with each experiment performed in triplicate.

2.8. AST and LDH Assay. NG-H9c2 and HG-H9c2 cardiomyocytes (1×10^5 cells/well) after 24 and 72 hr incubation with Taurisolo[®], TMAO, and TMAO/ Taurisolo[®] combination were cultured in 6-well plates. The medium was collected for the measurement of the Aspartate transaminase (AST) and Lactate dehydrogenase (LDH) enzymes, including isoform 1 and 2 release. The enzyme activity was measured using

an Abbott Aeroset fully automatic biochemical analyzer (Abbott Laboratories, USA). The levels of enzymes were assayed according to the instructions provided with the corresponding enzymatic kits.

Western Blots

We followed the methods of Vanacore et al. 2018 (Vanacore et al., 2018) for evaluation the protein expression by Western blot. Briefly, the cells were cultured at different condition for 72 hr, and then, cell pellets were lysed with 1 mL of lysis buffer (1% Triton, 0.5% sodium deoxycholate, 0.1 M NaCl, 1 mM Ethylenediamine tetra-acetic acid (EDTA), pH 7.5, 10 mM Na₂HPO₄, pH 7.4, 10 mM Phenylmethyl sulfonyl fluoride, 25 mM benzamidine, 1 mM leupeptin, and 0.025 units/mL aprotinin). The lysates were centrifuged at 12,000 rpm for 10 min at 4° C. Equal amounts of protein extracts were separated by SDS-PAGE, electrotransferred to nitrocellulose, and reacted with the different antibodies (ERK, pERK, LC3II, and Mn-SOD). All Western blots were repeated for three times. GAPDH was used as internal control. To quantify the results, the relative amount of each protein was determined.

Mass Spectrometry

LIPID MAPS Lipidomics Gateway and Human Metabolome Database queries were used to assign putative identities to mass features using based on mass accuracy within ± 1 Da. (<http://www.lipidmaps.org/data/structure/index.html>.)

- Study: “Effects of Taurisolo[®] on endothelial function” (Martelli et al., 2021)

Cell cultures

Human aortic smooth muscle cells, HASMCs (Life Technologies, Carlsbad, CA, USA), were cultured in Medium 231 (Life Technologies, Carlsbad, CA, USA) supplemented with Smooth Muscle Growth Supplement (Life Technologies, Carlsbad, CA, USA), 1% of 100 units·ml⁻¹penicillin and 100 mg·ml⁻¹ streptomycin (Merck KGaA, Darmstadt, Germany). Human umbilical vein endothelial cells, HUVECs (Life Technologies, Carlsbad, CA, USA) were cultured in Medium 131 (Life Technologies, Carlsbad, CA, USA) supplemented with 10% Fetal Bovine Serum, 1% of 100 units·ml⁻¹penicillin and 100 mg·ml⁻¹ streptomycin, 1% L-Glutamine, heparin 10U/ml, epidermal growth factor (EGF, 10ng/ml), and basic fibroblast growth factor (bFGF, 5ng/ml) (Merck KGaA, Darmstadt, Germany). Both cell lines were cultured in T75 red cap tissue culture flasks at 37 °C in a humidified atmosphere of 5% CO₂. Cells were split 1:2 once a week and used until passage 20 for HASMCs and 13 for HUVECs.

Evaluation of the cell viability preservation against H₂O₂-induced cell damage in HASMCs and HUVECs

Cells were cultured up to 90% confluence and 24 h before the experiments they were plated into a 96-well cell culture transparent plate (at a density of 10^4 cells per well for HASMCs and 2×10^4 cells per well for HUVECs). After 24h, to allow cell attachment, the medium was replaced by fresh culture medium, and cells were treated with Taurisolo® (TAU 10, 30, and 100µg/ml) or vehicle for 1h. After 1h, cells were challenged with the oxidant stimulus, represented by H₂O₂ (200 µM for HASMCs and 100 µM for HUVECs). At the end of the 2h of H₂O₂ incubation, the cell viability was assessed using an aqueous solution of the cell proliferation reagent WST-1 (Roche, Basilea, Switzerland). It was added at a ratio of 1:10 of the total volume of the wells and incubated for 1h at 37 °C in a humidified atmosphere of 5% CO₂, and the absorbance was measured at $\lambda=495$ nm by a multiplate reader (EnSpire, Perkin-Elmer, Waltham, MA, USA).

Evaluation of cell viability preservation against H₂O₂-induced cell damage in HASMCs and HUVECs in the presence of Sirtuin and AMPK inhibitors

Cells were cultured up to 90% confluence and 24 h before the experiments, they were plated into a 96-well cell culture transparent plate (at a density of 10^4 cells per well for HASMCs and 2×10^4 cells per well for HUVECs). After 24h to allow cell attachment, the medium was replaced and both the cell lines were incubated for 1h with Sirtinol (a sirtuin inhibitor, Tocris Bio-Techne, Minneapolis, MN, USA) or Compound C (also known as dorsomorphin, an AMPK inhibitor, Merck KGaA, Darmstadt, Germany) at the concentration of 10µM, or both, or their vehicle. After 1h of incubation, Taurisolo® (TAU, 100µg/ml) or vehicle (culture medium) was added and incubated for 1h. After 1h, the cells were incubated for 2h with the pro-oxidant agent represented by H₂O₂ (200µM for HASMCs, and 100 µM for HUVECs). Cell viability was assessed using an aqueous solution of the cell proliferation reagent WST-1 (Roche, Basilea, Switzerland). It was added at a ratio of 1:10 of the total volume of the wells and incubated for 1h at 37 °C in a humidified atmosphere of 5% CO₂, and then the absorbance was measured at $\lambda=495$ nm by a multiplate reader (EnSpire, Perkin-Elmer, Waltham, MA, USA).

Measurement of intracellular H₂O₂-induced ROS production in HUVECs and HASMCs in the presence of Sirtuin and AMPK inhibitors

Cells were treated as reported in paragraph 2.2.2 and, at the end of the treatment, intracellular levels of reactive oxygen species (ROS) were measured. In particular, the ROS production was measured using an aqueous solution of the fluorescent probe dihydroethidium (DHE 10µM; Merck KGaA, Darmstadt, Germany) incubated at 37°C for 30 min in the dark and in a humidified atmosphere of 5% CO₂. Fluorescence values corresponding to intracellular ROS production were measured at $\lambda_{ex}=500$ nm and $\lambda_{em}=580$ nm by a multiplate reader (EnSpire, Perkin-Elmer, Waltham, MA, USA).

Cell experiments data analysis

The experiments were carried out in triplicate and repeated at least three times (n=9), and the values obtained were expressed as a mean \pm standard error (SEM). The data were analyzed by using the ANOVA one way test followed by Bonferroni's Multiple Comparison *post hoc* test; a level of $P < 0.05$ was considered to be a statistical significance limit (* $p < 0.05$; ** $p < 0.01$; *** $p < 0.001$).

Brachial artery flow-mediated dilation (FMD) and reactive hyperemia index (RHI)

All assessments were performed by the same expert operator, blinded for ongoing treatment. FMD and RHI were measured by ultrasound imaging, as described in the guidelines of the International Brachial Artery Reactivity Task Force (Corretti et al., 2002).

FMD and RHI of the brachial artery were evaluated according to a standardized ultrasound protocol (M. N. D. Di Minno et al., 2020) using an automatic edge detection software (Cardiovascular Suite®, FMD studio, QUIPU Srl, Pisa, Italy). Briefly, brachial artery was visualized on the longitudinal plane with ultrasound (10 MHz linear transducer, Esaote®, MyLab 25 Gold, Pisa, Italy). Brachial artery diameter (BAD) and the flow velocity were recorded at rest for 60 seconds and for 240 seconds during reactive hyperemia following 300 seconds of induced ischemia of the forearm (blood pressure cuff placed on the forearm and inflated up to 70 mmHg above the systolic blood pressure). FMD was calculated as (Max post-ischemic BAD – Basal BAD)/Basal BAD \times 100. The reactive hyperemia index (RHI) was calculated as (average flow velocity after cuff deflation/flow velocity measured at the baseline) (A. Di Minno et al., 2020).

- Study: "Effects of Taurisol® on AMD" (**article in press**)

Ophthalmic Outcomes Evaluation

CFT was monitored using an Optical Coherence Tomographer (Model Cirrus Zeiss HD-5000, Carl Zeiss, Wetzlar, Germany) to assess retinal structure and measure CFT after pupillary dilation. Twelve 6-mm radial scans spaced 15° were recorded. CFT was measured as the distance between the high-reflectance vitreoretinal interface and the retinal pigment epithelium/choriocapillaris complex based on the vertical and horizontal B-scans of the Stratus or based on the central B-scan of the Cirrus.

Visual acuity was assessed monocularly with the right eye tested first unless otherwise clinically indicated using a distance Snellen chart to determine the power that yielded best-corrected visual acuity.

- Study: "Effects of Taurisol® on muscle quality in aged rats" (Annunziata et al., 2020b)

Gastrocnemius muscle homogenate

Gastrocnemius muscle portions (100 mg) were homogenized in a relationship 1:5 in a solubilization buffer (250mM sucrose, 20mM Tris-HCl, 40mM KCl, and 2mM EGTA, pH 7.4), using a disperser (IKA T10 basic ULTRA-TURAX). The homogenates were sonicated at 20W and centrifuged (at 5000g, 4°C, for 15min) and supernatants were stored at -80°C until their utilization. Total protein content was measured by Bradford's protein-dye-binding assay (Bradford, 1976).

Total antioxidant capacity (FRAP)

The total antioxidant capacity was measured using the ferric reducing antioxidant power (FRAP) assay, following the method described by Benzie and Strain (Benzie and Strain, 1996).

Antioxidant activities determination

The activities of antioxidant enzymes (CAT, SOD, GRd and GPx) were determined in gastrocnemius muscle homogenates. All activities were determined with a Shimadzu UV-2100 spectrophotometer at 37°C. CAT activity was measured by the spectrophotometric method of Aebi based on the decomposition of H₂O₂ (Aebi, 1984). SOD activity was measured by an adaptation of the method of McCord and Fridovich (McCord and Fridovich, 1969). GRd activity was measured by a modification of the Goldberg and Spooner spectrophotometric method (Goldberg and Spooner, 1984). GPx activity was measured using an adaptation of the spectrophotometric method of Flohe and Gunzler (Flohe and Gunzler, 1984). Results were normalized with protein concentration.

Malondialdehyde assay

Malondialdehyde (MDA) as a marker of lipid peroxidation was analyzed in gastrocnemius muscle homogenate by a colourimetric assay based on the reaction of MDA with a chromogenic reagent to yield a stable chromophore with maximal absorbance at 586 nm. Briefly, samples or standards were placed in glass tubes containing n-methyl-2-phenylindole (10.3 mM) in acetonitrile:methanol (3:1). HCl 12 N was added, and the samples were incubated for 1 h at 45°C. Absorbance was measured at 586 nm.

N-Tyrosine determination

Nitrotyrosine (N-Tyr) were determined by immunological method OxiSelect™ Nitrotyrosine Immunoblot Kit (Cell Biolabs, INC) following the manufacturer's instructions. Total protein concentrations were measured by the method of Bradford. 10 µg of protein from samples homogenate were transferred onto a nitrocellulose membrane by the dot blot method. Nitrocellulose membranes were incubated with rabbit anti-N-Tyr antibody. This step was followed by incubation with a horseradish peroxidase antibody (goat anti-rabbit IgG) conjugate directed against the primary antibody. The membrane was then treated with luminol, which is converted to a

light-emitting form at wavelength 428 nm by the antigen/primary antibody/ secondary antibody/peroxidase complex. The light was visualized and detected by short exposure to a Chemidoc XRS densitometer (Bio-Rad Laboratories). Image analysis was performed using Quantity One-1D analysis software (Bio-Rad Laboratories). The coefficient of variation has been calculated to be 12% for N-Tyr index.

Gene expression

Total RNA was obtained from 0.1g from gastrocnemius muscle using TriPure Isolation Reagent (Roche Diagnostics) following the manufacturer's instructions. Total RNA was quantified using the Take3 Microplate in a PowerwaveXS spectrophotometer (BioTek, Winooski, VT, USA). A 1µg sample of total RNA was reverse transcribed to cDNA using 25U MuLV reverse transcriptase in 5µl retrotranscription mixture (10mM Tris-HCl pH 9.0, 50mM KCl, 0.1, 2.5mM MgCl₂, 2.5µM random hexamers, 10U RNase inhibitor, and 500µM of each dNTP) for 60min at 42°C in a Gene Amp 9700 thermal cycler (Applied Biosystems). cDNA solutions were diluted 1/10, and aliquots were frozen (-20°C) until analyzed. Real-time PCR was carried out using SYBR Green technology in a LightCycler rapid thermal cycler (Roche Diagnostics). The amplification program consisted of a preincubation step for denaturation of template cDNA (95°C, 10min) followed by 45 cycles consisting of a denaturation, an annealing, and an extension step under the conditions given in **Table X**. After each cycle, fluorescence was measured at 72°C.

Table X. Primers sequences and Real-Time PCR conditions

Gene	Sequence	Temperature (°C)	
B-Actin	Fw: 5'-AGG GAAATCGTGCGTGAC-3'	95°C	15 Seg
	Rev: 5'-CGCTCATTGCCGATAGTC-3'	60°C	30 Seg
		72°C	30 Seg
Mn-SOD	Fw: 5'-GGCCAAGGGAGATGTTACAA -3'	95°C	15 Seg
	Rev: 5'- GCTTGATAGCCTCCAGCAAC-3'	60°C	30 Seg
		72°C	30 Seg
IL-10	Fw: 5'-GGCTCAGCACTGCTATGTTGCC-3'	95°C	15 Seg
	Rev:5'-AGCATGTGGGTCTGGCTGACT -3'	60°C	30 Seg
		72°C	30 Seg
IL-6	Fw: 5'-GCCACTGCCTTCCCTACTTCA-3'	95°C	15 Seg
	Rev:5'- GACAGTGCATCGCTGTTCA-3'	60°C	30 Seg
		72°C	30 Seg
GPx	Fw: 5'-GCTCATGACCGACCCCAAGT-3'	95°C	15 Seg
	Rev:5'-GCCAGCCATCACCAAGCCAATA -3'	65°C	30 Seg

		72°C	30 Seg
Catalase	Fw: 5'-TGGCCTCCGAGATCTTTCAATG-3'	95°C	15 Seg
	Rev:5'-GCGCTGAAGCTGTTGGGGTAGTA-3'	63°C	30 Seg
		72°C	30 Seg
Sirt-1	Fw: 5'-TGGAGCAGGTTGCAGGAATCCA -3'	95°C	15 Seg
	Rev:5'-TGGCTTCATGATGGCAAGTGGC -3'	60°C	30 Seg
		72°C	30 Seg

Abbreviations: Mn-SOD, mitochondrial superoxide dismutase; IL-10, interleukin-10; IL-6, interleukin-6;

GPx, glutathione peroxidase; Sirt-1, sirtuin 1

Appendix B – Detailed materials and methods of animal-based studies

- Study: “Effects of Taurisol[®] on endothelial function” (Martelli et al., 2021)

All experimental procedures were carried out according to the Code of Ethics of the World Medical Association (Declaration of Helsinki, EU, Directive 2010/63/EU for animal experiments) and following the guidelines of the European Community Council Directive 86-609. The experiments were authorized by the Ethical Committee of the University of Pisa (Protocol number: 0037321/2013) and by the Italian Ministry of Health (authorization number 487/2020-PR). Animal studies were carried out in compliance with the ARRIVE guidelines and the Basel Declaration including the 3Rs concept (Kilkenny et al., 2010; McGrath and Lilley, 2015). All procedures were carried out to minimize the number of animals used and their suffering.

Evaluation of the vasorelaxing effect of Taurisol[®] on rat aorta rings in the presence and absence of endothelium

3-month-old male Wistar rats (280-350g) housed in cages with free access to food and water, were sacrificed with an overdose of Sodium Thiopental 100 mg/kg (MSD Animal Health, Milan, Italy), and thoracic descending aorta segment was excised, divided into 5mm-rings and set up on 20 mL organ baths, containing Tyrode solution (saline composition: NaCl 136,8; KCl 2,95; CaCl₂·2H₂O 1,80; MgSO₄·7H₂O 1,05; NaH₂PO₄·H₂O 0,41; NaHCO₃ 11,9; Glucose 5,5 mM), thermostated at 37°C and saturated with Clixocarb (95% O₂ and 5% CO₂). Each aortic ring was maintained under a preload of 2 g and, after a period of 30 min of stabilization, KCl 25 mM (CARLO ERBA Reagents S.r.l., Milan, Italy) was added to induce a vasoconstricting effect. After reaching a stable plateau, a test with Acetylcholine (Ach) 10⁻⁵M (Merck KGaA, Darmstadt, Germany), was performed to assess the presence of endothelium. As concerns the endothelium-intact aortic rings, a relaxation ≥70% of the KCl-evoked contraction was considered representative of a functional endothelium; on the other hand, the aortic rings exhibiting a relaxation <70% were discarded. As regards the endothelium-removed aortic rings, a relaxation <10% of the KCl-evoked contraction was considered representative of an acceptable lack of the endothelial layer; conversely the rings exhibiting a relaxation ≥10%, were discarded. This procedure was followed by washes to remove Ach and a stabilization period of 20 min (Bertini et al., 2010; Calderone et al., 2006).

At the end of the stabilization period, the aortic rings were challenged again with KCl 25mM to induce vasoconstriction and, once reached a stable plateau, increasing cumulative concentrations of Taurisol[®] (0,003; 0,01; 0,03; 0,1; 0,3; 1; 3 mg/mL) were administered in aortic rings with and without endothelium. To verify the involvement of endogenous nitric oxide (NO) in the endothelium-dependent vasorelaxation induced by Taurisol[®], the aortic rings with intact endothelium were pre-incubated with the inhibitor of NO biosynthesis L-NAME 100 μM (Merck KGaA, Darmstadt, Germany) for 20 min, before the administration of increasing cumulative concentrations of Taurisol[®]. The vasorelaxing effect promoted by Taurisol[®] was

expressed as a percentage of the maximum contraction induced by KCl 25 mM. The maximal vasorelaxant efficacy (E_{max}) represented the maximal vasorelaxing response achieved by the highest concentration of Taurisololo[®] and it is expressed as a percentage (%) of the contractile tone induced by KCl 25 mM. The potency parameter (pEC_{50}) is expressed as the negative logarithm of the molar concentration of Taurisololo[®] evoking an effect = 50% of E_{max} . Both the parameters for efficacy and potency are expressed as mean \pm SEM, from aortae of six animals ($n = 6$) for each different treatment (Calderone et al., 2007; Martelli et al., 2020).

Evaluation of the involvement of Sirtuins and AMPK pathways in the vasorelaxing activity of Taurisololo[®]

The potential mechanisms of action, accounting for the vasorelaxing effect exhibited by Taurisololo[®] on the endothelium-intact aortic rings, were investigated through the pre-incubation of the vessels, for 1h, with Sirtinol (a sirtuin inhibitor) 100 μ M (Tocris Bio-Techne, Minneapolis, MN, USA) or Compound C (also known as dorsomorphin, an AMPK inhibitor) 100 μ M (Merck KGaA, Darmstadt, Germany) or both at the concentration of 100 μ M. Therefore, after reaching a stable plateau obtained by administration of KCl 25 mM, increasing concentrations of Taurisololo[®] (0,003; 0,01; 0,03; 0,1; 0,3; 1; 3 mg/mL) were administered to each aortic ring. The vasorelaxing effect, observed after the administration of each concentration of Taurisololo[®], was expressed as a percentage of the maximum contraction induced by KCl 25 mM. The maximal vasorelaxant efficacy (E_{max}) represented the maximal vasorelaxing response achieved with the highest concentration of Taurisololo[®] and it is expressed as a percentage (%) of the contractile tone induced by KCl 25 mM. The potency parameter (pEC_{50}) is expressed as the negative logarithm of the molar concentration of Taurisololo[®] evoking an effect = 50% of E_{max} . Both the parameters for efficacy and potency are expressed as mean \pm SEM, from aortae of six animals ($n = 6$) for each different treatment.

Evaluation of the efficacy of Taurisololo[®] to restrain Noradrenaline (NA)-induced vasoconstriction

Three different concentrations of Taurisololo[®] (10, 30, 100 μ g/mL) or the corresponding vehicle (deionized water) were pre-incubated for 20 min on different isolated endothelium-intact aortic rings. Then, increasing concentrations of Noradrenaline (NA) (Merck KGaA, Darmstadt, Germany) (10^{-9} M; 3×10^{-9} M; 10^{-8} M; 3×10^{-8} M; 10^{-7} M; 3×10^{-7} M; 10^{-6} M) were added in each aortic ring. Finally, after the NA-cumulative concentration-response curve, the aortic rings were washed and, after a stabilization period of 20 minutes, KCl 60 mM was administered to obtain a maximal contraction (100%). The vasoconstricting effect of each NA concentration was expressed as a percentage of the vasoconstriction induced by KCl 60 mM. The maximal vasoconstricting efficacy (E_{max}) represented the maximal vasoconstricting response achieved with the highest concentration of NA and it is expressed as a percentage (%) of the contractile tone induced by KCl 60 mM. The potency parameter (pEC_{50}) is expressed as the negative logarithm of the molar concentration of NA evoking an effect = 50% of E_{max} (Martelli et al., 2020).

In vitro experiments statistical analysis

Experimental data were analyzed by a computer fitting procedure (software: GraphPad Prism 6.0). The experiments were conducted in triplicate and repeated at least three times (n=9). The statistical significance was obtained by the Two-Way ANOVA statistical analysis followed by Bonferroni post-test. Values were considered statistically different when $p < 0.05$.

Anti-hypertensive effects of Taurisol[®] in spontaneously hypertensive rats (SHRs) in vivo model

Twenty spontaneously hypertensive rats (SHRs; Charles River Laboratories, Calco, Italy) of 6 weeks of age (starting mean weight: 181 ± 3 g and systolic blood pressure: 186 ± 3 mmHg), were housed in cages with food and water *ad libitum* and were exposed to a 12h dark/light cycle. Although not yet affected by a condition of fully established hypertension, 6-week-old SHR rats were selected because they show a progressive increase in blood pressure up to maximum values around the 10th week of age. After a period of 2 weeks, during which animals were daily conditioned to be handled for measurement of blood pressure according to the "tail-cuff" method, by a BP recorder (BP-2000 Blood Pressure Analysis System, Series II, Visitech System, Apex, NC, USA), they were randomized into 4 groups (5 animals for each group). The 4 groups daily received (*per os*, dissolved in the drinking water) 4 different treatments for 4 weeks: 1) Tap water (control group), 2) Taurisol[®] 10mg/kg, 3) Taurisol[®] 20 mg/kg, and 4) Captopril 20mg/kg (Merck KGaA, Darmstadt, Germany) used as reference anti-hypertensive drug. Both Taurisol[®] and Captopril solutions were daily freshly prepared. During the 4 weeks of treatment, animals were weekly weighed to monitor health status and consider any dose adjustments. Systolic blood pressure was measured three times per week (on alternate days): specifically, conscious animals were placed into containment cages on a 37°C heated platform for 10 min and then systolic blood pressure values were recorded (Breschi et al., 2006, 2004). The statistical significance was obtained by the Two-Way ANOVA statistical analysis followed by Bonferroni post-test. Statistical significance was set at $p < 0.05$.

Evaluation of Taurisol[®] protection against endothelial dysfunction in SHRs

At the end of the chronic *in vivo* treatment, SHRs were sacrificed by an overdose of Sodium Thiopental (100 mg/kg, i.p.), their thoracic aortas were removed, and rings were set up as previously described, to assess the possible protection of Taurisol[®] against endothelial dysfunction. After setting up the aortic rings, they were pre-contracted with NA 1 μ M and, upon reaching the vasoconstriction plateau, Ach was administered at increasing cumulative concentrations (10^{-9} M; 3×10^{-9} M; 10^{-8} M; 3×10^{-8} M; 10^{-7} M; 3×10^{-7} M; 10^{-6} M) to assess the response of the endothelial component in each treatment group. Some aortic rings were used to verify that vasodilation was due to endothelial deficiency and not to damage of the smooth muscle component. For this purpose, Sodium Nitroprusside (SNP) (CARLO ERBA Reagents S.r.l., Milan, Italy), a NO-donor agent,

was administered at the same increasing cumulative concentrations used for Ach (Martelli et al., 2013). The maximal vasorelaxant efficacy (E_{max}) represented the maximal vasorelaxing response achieved with the highest concentration of Ach and it is expressed as a percentage (%) of the contractile tone induced by NA $1\mu\text{M}$.

The experiments were conducted in fivefold and derived from aortas of 5 different animals ($n=5$). The statistical significance was obtained by the Two-Way ANOVA statistical analysis followed by Bonferroni post-test. Statistical significance was set at $p<0.05$.

Effect of Taurisolo® on glycemic and lipid parameters in SHR

At the end of the 4-week of chronic *in vivo* treatment, the lipid (total cholesterol, HDL, LDL, triglycerides) and glycemic profiles were also investigated. After an 18-hour fasting, blood glucose measurement was carried out collecting blood from the tail of conscious animals, while the lipid panel was analyzed from blood collected from the heart of rats previously anesthetized with Sodium Thiopental (100mg/kg, i.p.). The instruments used were Glucocard™ blood glucose meter (Menarini, Florence, Italy) and Cobas b 101 (Roche Diagnostics, Basilea, Switzerland), respectively.

Preventive effects of Taurisolo® against cardiac hypertrophy in SHR

At the end of the chronic treatment, the heart of each animal was removed, washed, dried, dissected, and finally weighed to assess the preventive effects of Taurisolo® against the development of cardiac hypertrophy in SHR. Data were expressed as a ratio between heart weight and animal body weight (g/kg) (Breschi et al., 2006). Significance was obtained with One-Way ANOVA statistical analysis followed by Bonferroni post-test. Data were considered statistically different when $p<0.05$.

Measurement of coagulation factors and fibrinogen

Mice were randomly separated into four experimental groups of six animals of each, balancing body weight variation across groups. Taurisolo® (TAU®) at a dose of 1, 10 and 20 mg/kg and distilled water (TAU vehicle; Ctrl group) were administered orally (p.o.; 200 μl /mouse) for 4 weeks. Thereafter, blood was collected via intracardiac puncture in citrated blood samples to perform haematological investigations of coagulation factors, including prothrombin time (PT; expressed as seconds), partial thromboplastin time (PTT; expressed as seconds) and fibrinogen (expressed as mg/dl) (Feng et al., 2018). Blood biochemical examinations were performed by CELL-DYN Sapphire purchased from Abbott SRL (Milan, Italy). Standard laboratory procedures were used for blood sampling and measurements (Kim et al., 2018) and all procedures were conducted under strictly aseptic conditions.

Clot retraction assay

For clot retraction assay, we adopted the protocol proposed by Law and coll. with slight modifications (Law et al., 1999). Briefly, not-anticoagulated blood samples, obtained by intracardiac puncture (300 μ l) were transferred into Microvette® 300 Z (Sarstedt, Verona, Italy) containing clotting activator and incubated at room temperature for 2h in order to get clots formation. Thereafter, clots were collected and weighed (g), and residual serum volumes (μ l) were pipetted as an indirect value of clot reaction (Tucker et al., 2012).

The data and statistical analysis in 2.5 experimental procedures comply with the international recommendations on experimental design and analysis in pharmacology (Curtis et al., 2018) and data sharing and presentation in preclinical pharmacology (Alexander et al., 2018; George et al., 2017). The results obtained were expressed as the mean \pm SD. Statistical analysis were performed by using One-Way ANOVA followed by Bonferroni's for multiple comparisons. GraphPad Prism 8.0 software (San Diego, CA, USA) was used for analysis. Data were considered statistically significant when a value of $p \leq 0.05$ was achieved.

- Animal-based study: “Effects of Taurisol® on aged brain-associated cognitive decline” (**article in press**)

Animals

Young (3 months, $n=8$) and old (20 months, $n=24$) male Wistar rats (Harlan, Barcelona, Spain) were individually housed with free access to standard food (Panlab A04) and tap water, under controlled environmental conditions (20 ± 2 °C; 70 % humidity), in a sound-attenuated chamber, and maintained at 12-h light/dark photoperiod (lights on at 08:00 h daily) with an average of 300 lux of indirect light provided from fluorescent lamps. Animals were daily handled for several days prior to starting tests to reduce stress during testing. Every 3–4 days during treatments, animals were weighed. All procedures were in accordance with the European Convention for the Protection of Vertebrate Animals used for Experimental and other Scientific Purposes and in agreement with the Bioethical Committee of the University of Balearic Islands (Exp: 2019/14/AEXP).

Treatment

Old animals were randomly allocated into three intervention groups: control (Ctr; 50 mg/kg maltodextrins daily; $n=8$), active group 1 (100; 100 mg/kg Taurisol® daily; $n=8$) and active group 2 (200; 200 mg/kg Taurisol® daily; $n=8$); young animals were treated with 50 mg/kg maltodextrins (positive Ctr). Both treatments (maltodextrins and Taurisol®) were orally administered for 30 days. All animals also received NSD 1015 (100 mg/kg, i.p. at 0730 h) 30 min before being sacrificed by decapitation. This administration was performed to measure the *in vivo* activity of TPH and TH, through the accumulation of 5-HTP and DOPA

respectively during these 30 min. Brains were quickly removed and dissected on an ice-cold plate to separate pineal gland (1.2–1.3 mg), hippocampus (60–65 mg), and striatum (caudate-putamen) (15–20 mg), which were immediately frozen in liquid nitrogen and stored at –80 °C until assays.

Visuospatial Learning in Barnes Maze Test

The maze consists on a circular disk (130 cm diameter) elevated above the floor with 18 holes equidistantly located around the perimeter. Under one of these holes, there is a black box or target not visually discriminated from the centre of the maze. The maze was set in an experimental room with several visual cues to serve as reference points for locating the target. The bright light was used as a stimulus to find the target, accentuating the natural agoraphobia of rats (Barrett et al., 2009). Previous studies indicated that performance on this task requires spatial stimuli recognition mediated by the hippocampus (Deacon and Rawlins, 2002). Animals were habituated to the maze, allowing them to freely explore the maze the day before the test in one session (familiarization phase). Each rat was placed in the middle of the platform, the light was switched on and the animal had 3 min to escape by hiding in the target. If the rat did not escape, it was manually placed in the target box, where it remained for 1 min. Once the animal is inside the box the light was turned off. Between tests and trials, the whole apparatus was cleaned with ethanol 90%, to avoid the presence of olfactory or solid traces between animals. The day of the test, each rat performed four trials separated by 10 min. The trial finished when the animal entered the target or after 3 min when the animal was manually placed into the target box and remained there for 1 min. The time spent exploring the maze until reaching the target was denominated latency. Exploration of the non-target hole was counted as an error. Three different strategies to search the target were considered (Rueda-Orozco et al., 2008): direct (rats go directly to the target), serial (rats explore holes in sequence), or random (any other pattern to reach the target).

Motor Coordination in Rotarod Test

Motor ability and balance were evaluated on the rotarod treadmill (Panlab®). Animals were submitted to training sessions during 4 days prior to the test (one session/day) on a rotarod at a constant speed of 4 rpm until their performance was stabilized. In the test phase, the rats were placed on the rotarod in acceleration mode (from 4 to 40 rpm over a period of 60 s) for recording the latency to fall. Each rat repeated the test five times, leaving a 10 minutes for recovery.

- Animal-based study: “Effects of Taurisol® on muscle quality in aged rats” (Annunziata et al., 2020b)

Animals Ethics approval

Old male Sprague-Dawley rats (20 months; 580 ± 11.8 g weight; $n = 32$; Charles River, Spain) were housed individually in standard cages under controlled environmental conditions ($20 \pm 2^\circ\text{C}$; 70% humidity, and 12-h light/dark cycle, lights on at 08:00) with free access to standard food (Panlab A04, Spain) and tap water. All procedures were performed during the light period and in accordance with the European Convention for the Protection of Vertebrate Animals used for Experimental and other Scientific Purposes (Directive 86/609/EEC) and approved by the Bioethical Committee of the University (approval file number 2019/14/AEPX).

Experimental design

The animals were chronically treated once daily for 30 days. The aged placebo group ($n=8$) and the young control group ($n=8$) orally received 50 mg/kg of maltodextrin (Sigma–Aldrich, Madrid, Spain) as a vehicle, and the aged rats ($n=8$) were orally treated with 100 mg/kg of Taurisolo[®]. For the treatments, both Taurisolo[®] or maltodextrin were separately dissolved in water obtaining 100 mg/ml solutions that were orally administered, on the base of the animal body weights, in order to reach the treatment doses. Before starting the treatments, all the animals were accustomed to both the solution flavour and the mode of administration with 1-2 ml of maltodextrin solution for a week. This preventive procedure allowed high animal compliance for the 30-day treatment. All rats were sacrificed by decapitation 30 days after the treatment beginning at 08:00 (during dark/light change). Gastrocnemius muscles were quickly removed and immediately frozen in liquid nitrogen, and stored at -80°C until analysis.

Motor coordination in Rotarod test

Motor function and balance were evaluated by means of a rotarod (Panlab[®]). Animals performed training sessions during 5 days prior to the test (one session/day) on the rotarod at a constant speed (4 rpm) until they attained a stable performance. In the test day, the rats were placed on the rotarod in an acceleration mode (from 4 to 40 rpm over a period of 60 s) in order to evaluate the latency to fall down. Each rat repeated the test five times, leaving some minutes for recovery between tests. The mean measured was used as the motor coordination value. The rotarod design was performed at the beginning of the treatments (t_0) and after the 30 days of the treatments (t_{30}).

Appendix C – Detailed study populations and methods of RCTs

- RCT: “Effects of Taurisolo® on TMAO serum levels in healthy subjects” (Annunziata et al., 2019c)

Study design, setting and population

Healthy subjects, aged 25-35 years were enrolled in July 2018 from personnel and students of our Department. All subjects gave their informed consent for inclusion before they participated in the study. The study was conducted in accordance with the Declaration of Helsinki, and the protocol was approved by the Ethics Committee of AO Rummo Hospital (Benevento, Italy) (protocol n. 123512 of 18/06/2018).

This is a 70-day randomised, double-blind, single-centre, placebo-controlled, crossover trial. The subjects were randomly divided into two groups. They were followed by a crossover design consisted of run-in period (7 days), washout period (7 days) and intervention period (28 days). During the intervention period, each subject was given 300 mg Taurisolo® in acid-resistant capsules or placebo (identically appearing capsules containing only maltodextrin) twice daily, in correspondence of the two main meals. Subjects were instructed to annotate their dietary habits on a food diary and to maintain their habitual physical activity patterns for the entire duration of the study. In order to verify the compliance and increase protocol adherence, qualified personnel performed standardised and periodic telephone interviews, reminding patients to complete their daily reports, as previously described. During clinic visits, self-administered questionnaires on quality of life aspects were completed by each patient, and diaries were checked for data completeness and quality of documentation to ensure patient comprehension of the diary items.

Blood samples were collected after 12 h of fasting at days 8, 35, 42 and 70 in 10-mL EDTA-coated tubes (Becton–Dickinson, Plymouth, UK) and plasma was isolated by centrifugation (20 min, 2,200 rpm, 4 °C). All samples were stored at –80 °C until analysis. Subjects were instructed to abstain from alcohol consumption and practice of hard physical activity 48 h prior to blood sampling.

Exclusion criteria were: smoking, obesity (BMI > 30 kg/m²), diabetes, hepatic disease, renal disease, heart disease, family history of chronic diseases, drug therapy or supplement intake for hypercholesterolemia, drug therapy or supplement intake containing grape polyphenols, heavy physical exercise (> 10 h/week), pregnant women, women suspected of being pregnant, women who hoped to become pregnant, breastfeeding, birch pollen allergy, use of vitamin/mineral supplements 2 weeks prior to entry into the study, and donation of blood less than 3 months before the study.

Randomization, concealment, and blinding

A total of 20 eligible patients (10 men and 10 women, 25–35 years of age) were randomly assigned to two sub-groups (each one of 10 subjects). In the case of dropping out before the intervention period, the patient was replaced by the next eligible patient enrolled. The concealed allocation was performed using an internet-based randomization schedule, stratified by study site. An independent investigator, not clinically involved in the trial, generated the random number list. Patients, clinicians, core laboratories, and trial staff (data analysts statisticians) were blind to treatment allocation.

Study outcomes and data collection

Primary endpoints measured were the variations of Trimethylamine N-oxide (TMAO) serum levels. All raw patient ratings were evaluated in a blinded manner at the site of the principal investigator. The decision process was performed according to a consensus document (unpublished standard operating procedure) before unblinding in order to define conclusive primary efficacy data from a clinical perspective.

Safety

Safety was assessed using reports of adverse events provided by study participants as well as laboratory parameters concerning the hepatic and renal function, vital signs (blood pressure, pulse, height, weight, and body mass index), and physical or neurological examinations. These data regarding the safety were collected at days 8, 35, 42, and 70, including adverse events occurring in the first three weeks after cessation of treatments.

Statistics

Methodology

During the trial, it became apparent that dropouts and incomplete diary documentation created missing data that could not be adequately handled by the intended robust comparison.

To deal with the missing data structure, we used a negative binomial, generalized linear mixed effects model (NB GLMM) that not only yields unbiased parameter estimates when missing observations are missing at random (MAR), but also provides reasonably stable results even when the assumption of MAR is violated. Patients who did not provide any diary data (leading to zero evaluable days) were excluded from the MAR-based primary efficacy analysis, according to an “all observed data approach” as proposed by White and colleagues. This approach is statistically efficient without using multiple imputation techniques.

Data retrieved after withdrawal of randomized study treatment were also included in the analysis. Unless otherwise stated, all of the experimental results were expressed as mean \pm standard deviation (SD) of at least three replications. Statistical analysis of data was performed by the Student’s t-test or two-way ANOVA

followed by the Tukey-Kramer multiple comparison test to evaluate significant differences between a pair of means. Cochran's test ($P < 0.1$) were used to assess the statistic heterogeneity. The I² statistic was also calculated, and I² > 50% was considered as significant heterogeneity across studies. A random-effects model was used if significant heterogeneity was shown among the trials. Otherwise, results were obtained from a fixed-effects model. Percent change in mean and SD values were excluded when extracting SD values for an outcome. SD values were calculated from standard errors, 95% CIs, p-values, or t if they were not available directly.

Previously defined subgroup analyses were performed to examine the possible sources of heterogeneity within these studies and included health status, study design, type of intervention, duration, total polyphenols dose, and Jadad score. Treatment effects were analyzed using PROC MIXED with treatment and period as fixed factors, subject as a random factor and baseline measurements as covariates, and defined as weighted mean differences and 95% CIs calculated for net changes in parameters evaluated. Data that could not meet the criteria of variance homogeneity (Levene's test) and normal distribution (determined by residual plot examination and Shapiro–Wilks test) even after log transformation were analyzed by a nonparametric test (Friedman). The level of significance (α -value) was 95% in all cases ($P < 0.05$).

Analysis sets

The full analysis set population included all randomized patients, and patients who did not fail to satisfy a major entry criterion. Patients who did not provide primary efficacy data from efficacy analyses were excluded. The per protocol set consisted of all patients who did not substantially deviate from the protocol; they had two characteristics. Firstly, this group included patients for whom no major protocol violations were detected (for example, poor compliance, errors in treatment assignment). Secondly, they had to have been on treatment for at least 50 days counting from the day of first intake (completion of a certain prespecified minimal exposure to the treatment regimen). Hence, patients who prematurely discontinued the study or treatment were excluded from the per protocol sample.

Patient involvement

No patients were involved in setting the research question or the outcome measures, nor were they involved in developing plans for participant recruitment, or the design and implementation of the study. There are no plans to explicitly involve patients in dissemination. Final results will be sent to all participating sites.

Safety issues

Although no specific toxicity studies have been performed herein, the safety of polyphenol content of grapes has been widely demonstrated by mutagenicity tests, acute/subacute toxicity studies both in mice and

human. In particular, the Commission Regulation (EC) No. 258/1997 established 1000 mg as maximum polyphenolic extract daily intake in humans. Accordingly, the Taurisolo® dose adopted for the trial (600 mg/day) was compatible with that regarded as safe in humans. All results from laboratory analysis concerning the hepatic and renal function, indeed, did not indicate alteration of values after the Taurisolo® treatment period. Other safety assessments, such as vital signs, were all periodically monitored and baseline values did not change substantially during and at the end of the trial.

- RCT: “Effects of Taurisolo® on oxLDL and TMAO serum levels in overweight/obese subjects” (Annunziata et al., 2019b)

Study participants were overweight/obese subjects aged from 18 to 83 years, enrolled in September 2018. Smokers and subjects with hepatic disease, renal disease, heart disease, family history of chronic diseases, in drug therapy or supplement intake containing grape polyphenols, practicing heavy physical exercise (over 10 hours per week), pregnant, suspected of being pregnant or hoping to become pregnant, breastfeeding, birch pollen allergy, using vitamin or mineral supplements 2 weeks prior to entry into the study and donating of blood less than 3 months prior to the study were excluded. All subjects gave their informed consent for inclusion before they participated in the study. The study was conducted in accordance with the Declaration of Helsinki, and the protocol was approved by the Ethics Committee of AO Rummo Hospital (Benevento, Italy) (protocol 106 n. 123512 of 18/06/2018). This study is listed on the ISRCTN registry (www.isrctn.com) with ID ISRCTN10794277 (doi: 10.1186/ISRCTN10794277). This study was designed as a 16-week monocentric, double-blind, randomized, placebo-controlled, 2-arm parallel-group trial. Subjects were randomly allocated in two intervention groups: group A (300 mg Taurisolo® twice daily) and group B (300 mg Taurisolo®+300 mg pectin twice daily). The study consisted of 4-week run-in period, 8-week intervention period and a 4-week follow-up period. During the run-in period, subjects were given placebo (maltodextrins). Participants were asked to maintain their usual lifestyle habits throughout the entire study duration. Standardized and periodic telephone interviews were performed by qualified personnel in order to verify and increase the protocol compliance, and self-administered life quality questionnaires were completed by subjects during the clinic visits. Blood samples were collected after 12 h of fasting at weeks 0, 4, 8, 12 and 16 in 10-mL EDTA-coated tubes (Becton–Dickinson, Plymouth, UK) and plasma was isolated by centrifugation (20 min, 2,200g, 4 °C). All samples were stored at –80 °C until analysis. Subjects were asked to abstain from alcohol consumption and practice of hard physical activity 48 h prior to blood sampling.

- RCT: “Effects of Taurisolo® on oxLDL, DROMs and TMAO serum levels in subjects with CVD risk factors” (**article in press**)

Study population and protocol

Study participants were recruited by the Cardarelli Hospital (Naples, Italy). Subjects were enrolled in January–April 2019. All subjects underwent a standardised physical examination, assessment of medical history (for up to five years before enrolment), laboratory examination, measurement of blood pressure and heart rate, and evaluation of BMI. Body mass index (BMI) was calculated from body height and body weight. Body fat percentage was measured using a body composition analyzer (TBF-310, Tanita Corp., Tokyo, Japan) and systolic blood pressure, diastolic blood pressure, and heart rate, were measured using a HBP-9020 (OMRON COLIN Corp., Tokyo, Japan). At each clinic visit, subjects had to complete three self-administered questionnaires on quality of life aspects, and their diaries were checked for data completeness and quality of documentation to ensure subject comprehension of the diary items. Subjects aged 18–75 years with body mass index (BMI) ≥ 18.5 kg/m² were eligible for enrolment.

The subjects received oral and written information concerning the study before they gave their written consent. Protocol, letter of intent of volunteers, and synoptic document about the study were submitted to the Scientific Ethics Committee of AO Rummo Hospital (Benevento, Italy). The study was approved by the committee (protocol 106 n. 123512 of 18/06/2018), and carried out in accordance with the Helsinki declaration of 1964 (as revised in 2000). The subjects were asked to make records in an intake-checking table for the intervention study and side effects in daily reports.

Subjects were informed not to drink alcohol or perform hard physical activity 48 h prior to blood sampling. Participants maintained their usual dietary and lifestyle patterns throughout the study.

Study procedures

Participants arrived at the research centre in the morning after 12 h of fasting. All blood samples were taken in the morning and immediately after measurement of heart rate and blood pressure. Blood samples were collected from each participant before administration of the reference glucose solutions and the treatment beverages, in 3-mL EDTA-coated tubes (Becton–Dickinson, Plymouth, UK). Plasma was immediately isolated by centrifugation (20 min, 2,200 g, 4 °C). All biochemical analyses including fasting plasma glucose, total cholesterol, fasting plasma TG were performed with a Roche Modular Analytics System in the Central Biochemistry Laboratory of our Institution. Low-Density Lipoprotein (LDL) cholesterol and HDL cholesterol were determined by a direct method (homogeneous enzymatic assay for the direct quantitative determination of LDL and HDL cholesterol).

Statistics

Methodology

Unless otherwise stated, all of the experimental results were expressed as mean \pm SEM. Statistical analysis of data was performed by the Student's t test or Pearson correlation. The statistic heterogeneity was assessed by using Cochran's test ($p < 0.1$). The I² statistic was also calculated, and I² > 50% was considered as significant heterogeneity across studies. A random-effects model was used if significant heterogeneity was shown among the trials. Otherwise, results were obtained from a fixed-effects model. SD values were calculated from standard errors, 95% CIs, p-values, or t if they were not available directly. Previously defined subgroup analyses were performed to examine the possible sources of heterogeneity within these studies and included health status, study design, type of intervention, duration, total nutraceutical dose, and Jadad score. Treatment effects were analysed using PROC MIXED with treatment and period as fixed factors, subject as random factor and baseline measurements as covariates, and defined as weighted mean difference and 95% CIs calculated for net changes in fecal and serum parameters, and blood pressure values. Data that could not meet the criteria of variance homogeneity (Levenes test) and normal distribution (determined by residual plot examination and Shapiro–Wilks test) even after log transformation were analysed by a nonparametric test (Friedman). The level of significance (α -value) was 95% in all cases ($P < 0.05$).

Analysis set

The full analysis set population included all randomised subjects, and subjects who did not fail to satisfy a major entry criterion. The per protocol set consisted of all subjects who did not substantially deviate from the protocol. This group included subjects for whom no major protocol violations were detected (for example, poor compliance, errors in treatment assignment).

Statistics

All of the experimental data were expressed as mean \pm SEM. Statistical analysis of data was carried out by the Student's t test or Pearson correlation. The level of significance (α -value) was 95% in all cases ($P < 0.05$). The degree of linear relationship between two variables was measured using the Pearson product moment correlation coefficient (R). Correlation coefficients (R) were calculated using Microsoft Office Excel.

- RCT: "Effects of Taurisolo® on AMD" (**article in press**)

Study population and protocol

Study participants were recruited by the Cardarelli Hospital (Naples, Italy). Subjects were enrolled in January 2019. All subjects underwent a standardised physical examination, assessment of medical history (for up to five years before enrolment), laboratory examination, measurement of blood pressure and heart rate, and evaluation of BMI. Body mass index (BMI) was calculated from body height and body weight. Body fat percentage was measured using a body composition analyzer (TBF-310, Tanita Corp., Tokyo, Japan) and

systolic blood pressure, diastolic blood pressure, and heart rate, were measured using a HBP-9020 (OMRON COLIN Corp., Tokyo, Japan). At each clinic visit, subjects had to complete three self-administered questionnaires on quality of life aspects, and their diaries were checked for data completeness and quality of documentation to ensure subject comprehension of the diary items. Subjects aged 18-70 years with diagnosis of AMD were eligible for enrolment.

The subjects received oral and written information concerning the study before they gave their written consent. Protocol, letter of intent of volunteers, and synoptic document about the study were submitted to the Scientific Ethics Committee of AO Rummo Hospital (Benevento, Italy). The study was approved by the committee (protocol 106 n. 123512 of 18/06/2018), and carried out in accordance with the Helsinki declaration of 1964 (as revised in 2000). The subjects were asked to make records in an intake-checking table for the intervention study and side effects in daily reports.

Subjects were informed not to drink alcohol or perform hard physical activity 48 h prior to blood sampling. Participants maintained their usual dietary and lifestyle patterns throughout the study.

Study procedures

Participants arrived at the research centre in the morning after 12 h of fasting. All blood samples were taken in the morning and immediately after measurement of heart rate and blood pressure. Blood samples were collected from each participant before administration of the reference glucose solutions and the treatment beverages, in 3-mL EDTA-coated tubes (Becton–Dickinson, Plymouth, UK). Plasma was immediately isolated by centrifugation (20 min, 2,200 g, 4 °C). All biochemical analyses including fasting plasma glucose, total cholesterol, fasting plasma TG were performed with a Roche Modular Analytics System in the Central Biochemistry Laboratory of our Institution. Low-Density Lipoprotein (LDL) cholesterol and HDL cholesterol were determined by a direct method (homogeneous enzymatic assay for the direct quantitative determination of LDL and HDL cholesterol). Plasma insulin concentrations were measured using an enzyme linked immunosorbent (ELISA) assay commercial kit (InterMedical srl, Italy).

Statistics

Methodology

Unless otherwise stated, all of the experimental results were expressed as mean \pm SEM. Statistical analysis of data was performed by the Student's t test or Pearson correlation. The statistic heterogeneity was assessed by using Cochran's test ($p < 0.1$). The I² statistic was also calculated, and I² > 50% was considered as significant heterogeneity across studies. A random-effects model was used if significant heterogeneity was shown among the trials. Otherwise, results were obtained from a fixed-effects model. SD values were calculated from

standard errors, 95% CIs, p-values, or t if they were not available directly. Previously defined subgroup analyses were performed to examine the possible sources of heterogeneity within these studies and included health status, study design, type of intervention, duration, total nutraceutical dose, and Jadad score. Treatment effects were analysed using PROC MIXED with treatment and period as fixed factors, subject as random factor and baseline measurements as covariates, and defined as weighted mean difference and 95% CIs calculated for net changes in fecal and serum parameters, and blood pressure values. Data that could not meet the criteria of variance homogeneity (Levenes test) and normal distribution (determined by residual plot examination and Shapiro–Wilks test) even after log transformation were analysed by a nonparametric test (Friedman). The level of significance (α -value) was 95% in all cases ($P < 0.05$).

Analysis set

The full analysis set population included all randomised subjects, and subjects who did not fail to satisfy a major entry criterion. The per protocol set consisted of all subjects who did not substantially deviate from the protocol. This group included subjects for whom no major protocol violations were detected (for example, poor compliance, errors in treatment assignment).

Statistics

All of the experimental data were expressed as mean \pm SEM. Statistical analysis of data was carried out by the Student's t test or Pearson correlation. The level of significance (α -value) was 95% in all cases ($P < 0.05$). The degree of linear relationship between two variables was measured using the Pearson product moment correlation coefficient (R). Correlation coefficients (R) were calculated using Microsoft Office Excel.

- RCT: “Effects of Taurisolo® on endothelial function in healthy subjects” (Martelli et al., 2021)

Study population and protocol

Study participants were recruited from personnel and students of the Department of Pharmacy, University of Naples Federico II (Naples, Italy). Subjects were enrolled in February–April 2019. All subjects underwent a standardised physical examination, assessment of medical history (for up to five years before enrolment), laboratory examination, measurement of blood pressure and heart rate, and evaluation of BMI. Body mass index (BMI) was calculated from body height and body weight. Body fat percentage was measured using a body composition analyzer (TBF-310, Tanita Corp., Tokyo, Japan) and systolic blood pressure, diastolic blood pressure, and heart rate, were measured using a HBP-9020 (OMRON COLIN Corp., Tokyo, Japan). At each clinic visit, subjects had to complete three self-administered questionnaires on quality of life aspects, and their diaries were checked for data completeness and quality of documentation to ensure subject

comprehension of the diary items. Subjects aged 18–75 years with body mass index (BMI) ≥ 18.5 kg/m² were eligible for enrolment.

The subjects received oral and written information concerning the study before they gave their written consent. Protocol, letter of intent of volunteers, and synoptic document about the study were submitted to the Scientific Ethics Committee of AO Rummo Hospital (Benevento, Italy). The study was approved by the committee (protocol 106 n. 123512 of 18/06/2018), and carried out in accordance with the Helsinki declaration of 1964 (as revised in 2000). The subjects were asked to make records in an intake-checking table for the intervention study and side effects in daily reports.

Subjects were informed not to drink alcohol or perform hard physical activity 48 h prior to blood sampling. Participants maintained their usual dietary and lifestyle patterns throughout the study.

Study procedures

Participants arrived at the research centre in the morning after 12 h of fasting. All blood samples were taken in the morning and immediately after measurement of heart rate and blood pressure. Blood samples were collected from each participant before administration of the reference glucose solutions and the treatment beverages, in 3-mL EDTA-coated tubes (Becton–Dickinson, Plymouth, UK). Plasma was immediately isolated by centrifugation (20 min, 2,200 g, 4 °C). All biochemical analyses including fasting plasma glucose, total cholesterol, fasting plasma TG were performed with a Roche Modular Analytics System in the Central Biochemistry Laboratory of our Institution. Low-Density Lipoprotein (LDL) cholesterol and HDL cholesterol were determined by a direct method (homogeneous enzymatic assay for the direct quantitative determination of LDL and HDL cholesterol).

Statistics

Methodology

Unless otherwise stated, all of the experimental results were expressed as mean \pm SEM. Statistical analysis of data was performed by the Student's t test or Pearson correlation. The statistic heterogeneity was assessed by using Cochran's test ($p < 0.1$). The I² statistic was also calculated, and I² $> 50\%$ was considered as significant heterogeneity across studies. A random-effects model was used if significant heterogeneity was shown among the trials. Otherwise, results were obtained from a fixed-effects model. SD values were calculated from standard errors, 95% CIs, p-values, or t if they were not available directly. Previously defined subgroup analyses were performed to examine the possible sources of heterogeneity within these studies and included health status, study design, type of intervention, duration, total nutraceutical dose, and Jadad score. Treatment effects were analysed using PROC MIXED with treatment and period as fixed factors, subject as random factor

and baseline measurements as covariates, and defined as weighted mean difference and 95% CIs calculated for net changes in fecal and serum parameters, and blood pressure values. Data that could not meet the criteria of variance homogeneity (Levenes test) and normal distribution (determined by residual plot examination and Shapiro–Wilks test) even after log transformation were analysed by a nonparametric test (Friedman). The level of significance (α -value) was 95% in all cases ($P < 0.05$).

Analysis set

The full analysis set population included all randomised subjects, and subjects who did not fail to satisfy a major entry criterion. The per protocol set consisted of all subjects who did not substantially deviate from the protocol. This group included subjects for whom no major protocol violations were detected (for example, poor compliance, errors in treatment assignment).

Statistics

All of the experimental data were expressed as mean \pm SEM. Statistical analysis of data was carried out by the Student's t test or Pearson correlation. The level of significance (α -value) was 95% in all cases ($P < 0.05$). The degree of linear relationship between two variables was measured using the Pearson product moment correlation coefficient (R). Correlation coefficients (R) were calculated using Microsoft Office Excel.